



## **EMULSION-BASED ENCAPSULATION SYSTEMS STABILIZED WITH INSECT PROTEINS: PRODUCTION WITH PREMIX MICROPOROUS EMULSIFICATION**

**Junjing Wang**

**ADVERTIMENT.** L'accés als continguts d'aquesta tesi doctoral i la seva utilització ha de respectar els drets de la persona autora. Pot ser utilitzada per a consulta o estudi personal, així com en activitats o materials d'investigació i docència en els termes establerts a l'art. 32 del Text Refós de la Llei de Propietat Intel·lectual (RDL 1/1996). Per altres utilitzacions es requereix l'autorització prèvia i expressa de la persona autora. En qualsevol cas, en la utilització dels seus continguts caldrà indicar de forma clara el nom i cognoms de la persona autora i el títol de la tesi doctoral. No s'autoritza la seva reproducció o altres formes d'explotació efectuades amb finalitats de lucre ni la seva comunicació pública des d'un lloc aliè al servei TDX. Tampoc s'autoritza la presentació del seu contingut en una finestra o marc aliè a TDX (framing). Aquesta reserva de drets afecta tant als continguts de la tesi com als seus resums i índexs.

**ADVERTENCIA.** El acceso a los contenidos de esta tesis doctoral y su utilización debe respetar los derechos de la persona autora. Puede ser utilizada para consulta o estudio personal, así como en actividades o materiales de investigación y docencia en los términos establecidos en el art. 32 del Texto Refundido de la Ley de Propiedad Intelectual (RDL 1/1996). Para otros usos se requiere la autorización previa y expresa de la persona autora. En cualquier caso, en la utilización de sus contenidos se deberá indicar de forma clara el nombre y apellidos de la persona autora y el título de la tesis doctoral. No se autoriza su reproducción u otras formas de explotación efectuadas con fines lucrativos ni su comunicación pública desde un sitio ajeno al servicio TDR. Tampoco se autoriza la presentación de su contenido en una ventana o marco ajeno a TDR (framing). Esta reserva de derechos afecta tanto al contenido de la tesis como a sus resúmenes e índices.

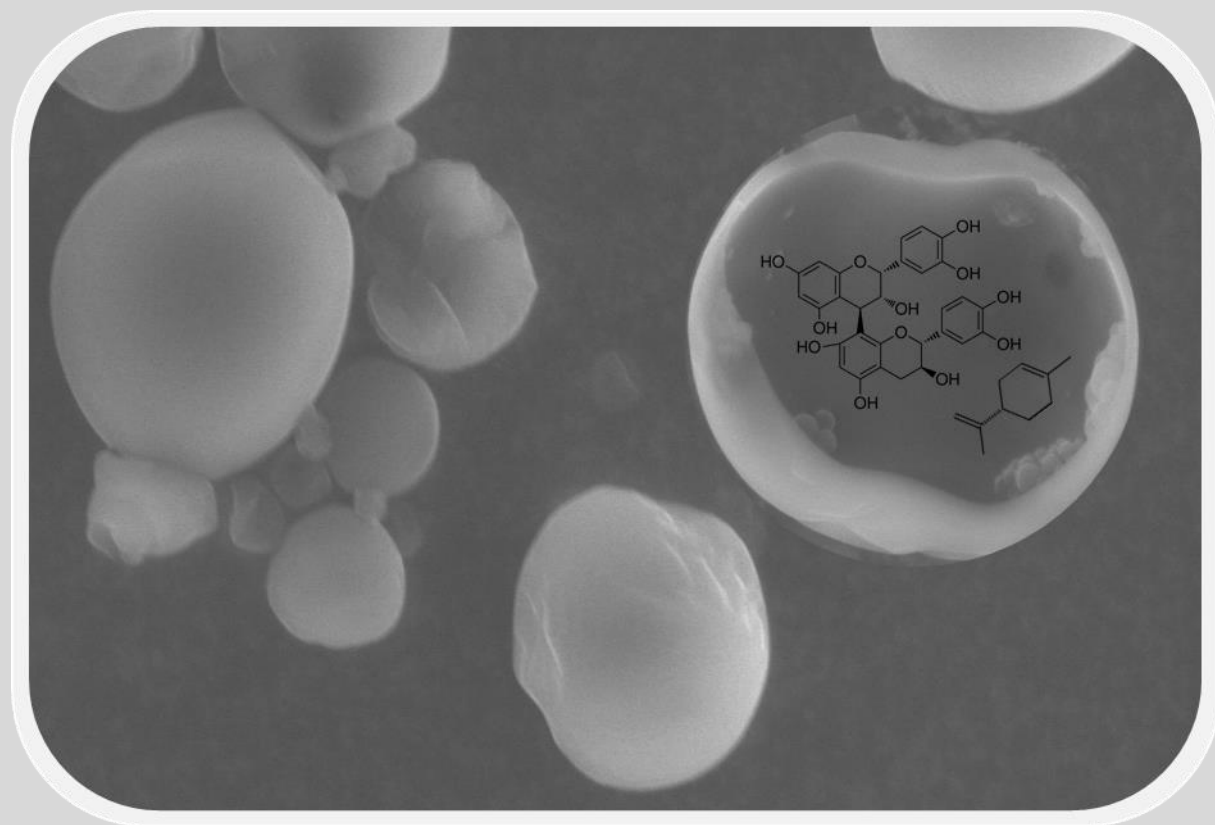
**WARNING.** Access to the contents of this doctoral thesis and its use must respect the rights of the author. It can be used for reference or private study, as well as research and learning activities or materials in the terms established by the 32nd article of the Spanish Consolidated Copyright Act (RDL 1/1996). Express and previous authorization of the author is required for any other uses. In any case, when using its content, full name of the author and title of the thesis must be clearly indicated. Reproduction or other forms of for profit use or public communication from outside TDX service is not allowed. Presentation of its content in a window or frame external to TDX (framing) is not authorized either. These rights affect both the content of the thesis and its abstracts and indexes.



# Emulsion-based encapsulation systems stabilized with insect proteins: Production with premix microporous emulsification

Junjing Wang

Universitat Rovira i Virgili



DOCTORAL THESIS  
2021

UNIVERSITAT ROVIRA I VIRGILI  
EMULSION-BASED ENCAPSULATION SYSTEMS STABILIZED WITH INSECT PROTEINS: PRODUCTION WITH  
PREMIX MICROPOROUS EMULSIFICATION  
Junjing Wang

UNIVERSITAT ROVIRA I VIRGILI  
EMULSION-BASED ENCAPSULATION SYSTEMS STABILIZED WITH INSECT PROTEINS: PRODUCTION WITH  
PREMIX MICROPOROUS EMULSIFICATION  
Junjing Wang

UNIVERSITAT ROVIRA I VIRGILI  
EMULSION-BASED ENCAPSULATION SYSTEMS STABILIZED WITH INSECT PROTEINS: PRODUCTION WITH  
PREMIX MICROPOROUS EMULSIFICATION  
Junjing Wang

Junjing Wang

**Emulsion-based encapsulation systems  
stabilized with insect proteins: Production with  
premix microporous emulsification**

Doctoral Thesis

Supervised by  
Dr. Carme Güell Saperas

Co-supervised by  
Dr. Montserrat Ferrando Cogollos



UNIVERSITAT ROVIRA I VIRGILI

Universitat Rovira i Virgili  
Department of Chemical Engineering

Tarragona 2021

UNIVERSITAT ROVIRA I VIRGILI  
EMULSION-BASED ENCAPSULATION SYSTEMS STABILIZED WITH INSECT PROTEINS: PRODUCTION WITH  
PREMIX MICROPOROUS EMULSIFICATION  
Junjing Wang



UNIVERSITAT  
ROVIRA I VIRGILI

Departament d'Enginyeria Química, ETSEQ

Campus Sescelades

Avinguda Països Catalans 26, 43007 Tarragona, Spain

I STATE that the present study, entitled "Emulsion-based encapsulation systems stabilized with insect proteins: Production with premix microporous emulsification", presented by Junjing Wang for the award of the degree of Doctor, has been carried out under my supervision at the *Departament d'Enginyeria Química* of Universitat Rovira i Virgili and that it fulfils all the requirements to obtain the doctoral degree.

Tarragona, September 30, 2021

Doctoral Thesis Supervisors

Dr. Carme Güell Saperas

Maria Montserrat Ferrando Cogollos  
- DNI 22699740M (AUT)  
Firmado digitalmente por Maria Montserrat Ferrando Cogollos -  
DNI 22699740M (AUT)  
Fecha: 2021.10.05  
16:20:36 +02'00'

Dr. Montserrat Ferrando Cogollos

UNIVERSITAT ROVIRA I VIRGILI  
EMULSION-BASED ENCAPSULATION SYSTEMS STABILIZED WITH INSECT PROTEINS: PRODUCTION WITH  
PREMIX MICROPOROUS EMULSIFICATION  
Junjing Wang

## Acknowledgements

Firstly, I would like to express my sincere gratitude to my supervisors Prof. Carme Güell and Prof. Montserrat Ferrando for the guidance during my Ph.D study and related research. I am grateful to their great support, patience, motivation, and immense knowledge. The guidance will continuously influence positively in my future career.

Secondly, I would like to thank Prof. Sílvia de Lamo-Castellví for her inspiration and valuable discussion which inspired me and my interest in edible insects.

Besides, I would like to thank all the lab fellows now and then. I want to thank Dr. Wael Kaade for giving me helpful advice in my research work as well as being a good listener and companion, to Nerea and Jordi for their warm-hearted supports and for sharing thousands of joyful moments whenever at work or off work, to Aurélie, Andrea, Morane, Montie, Ariadna and Albert for dedicating her/his time and effort in the project and the great time we spent investigating together, to Jitesh, Carmen, Halima, Madushika, Olga, Miriam and Aida for their support and helps. It is my great pleasure to join in the FoodIE family. Again I would like to thank all FoodIE members for creating a harmonious ambient and the fantastic time we have spent together, it values a lot to me.

Moreover, I would like to thank Josep Maria, Ana, Ángel, Tarama and Esther for supporting my research work especially in the technical aspect.

Also, I would like to thank Prof. M. Paz from Universidad de Lleida and Prof. Alejandro from Universidad de Granada for technical supports, and Prof. Karin from Wageningen University for the guidance and inspiring discussion during the project collaboration.

Many thanks to the European Union' s Horizon 2020 research and innovation programme under the Marie Skłodowska-Curie grant agreement (No. 713679) and the Universitat Rovira i Virgili (URV) for supplying research financial support.

An acknowledgement of gratitude is also made to safety management group in URV, I would be able to continue working on my project with appropriate protections during COVID period. I also thank the security staffs for their tolerance and acceptance to my enormous passion in my research work.

Last but not the least, I would like to thank my parents for their love and support.

UNIVERSITAT ROVIRA I VIRGILI  
EMULSION-BASED ENCAPSULATION SYSTEMS STABILIZED WITH INSECT PROTEINS: PRODUCTION WITH  
PREMIX MICROPOROUS EMULSIFICATION  
Junjing Wang

## Table of Contents

List of symbols and abbreviations

Abstract

Resumen

Chapter 1

Introduction & objectives .....	1
1.1 Emulsion-based encapsulation systems .....	3
1.1.1 Emulsions .....	4
1.1.2 Stabilization of emulsions .....	7
1.1.3 Emulsion-based solid microcapsules .....	9
1.2 Proteins as emulsifier.....	9
1.2.1 Dairy proteins.....	11
1.2.2 Plant proteins.....	12
1.2.3 Insect proteins .....	13
1.2.4 Others.....	18
1.2.5 Sustainability of insect proteins.....	18
1.3 Emulsion-based encapsulation technologies.....	22
1.3.1 Membrane/microporous emulsification technologies .....	22
1.3.2 Premix emulsification with dynamic membranes of tunable pore size (DMTS) .....	23
1.3.3 Production of emulsion-based solid microcapsules .....	30
1.4 Objectives.....	39

Chapter 2

Low-energy Membrane-based Processes to Concentrate and Encapsulate

Polyphenols from Carob Pulp .....	41
2.1. Introduction .....	43
2.2. Materials and Methods.....	46
2.2.1. Materials .....	46

2.2.2. Forward osmosis concentration .....	47
2.2.3 Production of $W_1/O/W_2$ emulsions using DMTS.....	49
2.2.4 Production of solid microcapsules by spray drying .....	51
2.2.5 Methods of analysis and characterization .....	51
2.3. Results and discussion .....	52
2.3.1. Forward osmosis concentration: effect of temperature on water flux and concentration.....	52
2.3.2. Encapsulation of polyphenols in $W_1/O/W_2$ double emulsions.....	55
2.3.3. Solid microcapsules production by spray drying .....	59
2.4. Conclusions .....	60
Chapter 3	
Black Soldier Fly ( <i>Hermetia illucens</i> ) Protein Concentrates as a Sustainable Source to Stabilize O/W Emulsions Produced by a Low-Energy High-Throughput Emulsification Technology .....	63
3.1 Introduction .....	65
3.2. Materials and Methods.....	67
3.2.1. Materials .....	67
3.2.2. Protein Extraction .....	67
3.2.3. Characterization of the BSF Powder and the BSFPC.....	68
3.2.4. Techno-Functional Properties of the BSFPC .....	68
3.2.5. Premix Membrane Emulsification.....	70
3.3. Results and Discussion .....	73
3.3.1. Chemical Composition of BSF Powder and BSFPC.....	73
3.3.2. Techno-Functional Properties.....	76
3.3.3. Dynamic Membrane of Tunable Pore Size (DMTS) Emulsification .....	80
3.4. Conclusions .....	87
Chapter 4	
Green solvents for lesser mealworm ( <i>Alphitobius diaperinus</i> ) powder defatting: effect on the lipidic profile and on the emulsifying properties of the resulting protein concentrates .....	89
4.1 Introduction .....	92
4.2 Materials and methods.....	94

4.2.1 Materials .....	94	
4.2.2 Lipid extraction .....	95	
4.2.3 Fourier transform infrared spectroscopy (FTIR) analysis.....	95	
4.2.4 Characterization of fatty acid methyl esters (FAMES) by gas chromatography.....	97	
4.2.5 Protein extraction .....	97	
4.2.6 Characterization of LMP and LMPC .....	98	
4.2.7 Production of oil-in-water (O/W) emulsions by DMTS .....	100	
4.2.8 Characterization of emulsion .....	101	
4.2.9 Production of solid microcapsules by spray drying .....	101	
4.2.10 Reconstitution of emulsion.....	102	
4.2.11 Statistical analysis .....	102	
4.3 Results and discussion .....	102	
4.3.1 Influence of solvent type on lipid extraction .....	102	
4.3.2 FAME analysis .....	104	
4.3.3 Amino acid profile and protein content.....	105	
4.3.4 Techno-functional properties of lesser mealworm protein concentrate (LMPC).....	106	
4.3.5 O/W emulsion production and stability.....	110	
4.3.6 Solid microcapsules.....	113	
4.4 Conclusion.....	114	
Chapter 5		
Emulsifying properties and emulsion stability of multiple emulsions stabilized with lesser mealworm ( <i>Alphitobius diaperinus</i> ) protein concentrate.....		115
5.1 Introduction .....	117	
5.2 Materials and methods.....	118	
5.2.1 Materials .....	118	
5.2.2 Preparation of lesser mealworm protein concentrate (LMPC) .....	120	
5.2.3 Osmolality of $W_1$ and $W_2$ .....	120	
5.2.4 $W_1/O/W_2$ emulsions production .....	120	
5.2.5 Environmental stress test .....	121	

5.2.6 Characterization of emulsions .....	122
5.2.7 Interaction of protein and polyphenols .....	124
5.3 Results and discussion .....	124
5.3.1. Production of $W_1/O/W_2$ emulsions stabilized with LMPC, WPI, and PPI .....	124
5.3.2. Influence of environmental factors .....	126
5.4 Conclusion .....	140
Chapter 6	
Polyphenol loaded microcapsules from W/O/W emulsions stabilized with lesser mealworm ( <i>Alphitobius diaperinus</i> ) protein concentrate .....	143
6.1 Introduction .....	145
6.2 Materials and methods .....	145
6.2.1 Materials .....	145
6.2.2 Preparation of lesser mealworm protein concentrate (LMPC) .....	146
6.2.3 $W_1/O/W_2$ emulsions production .....	147
6.2.4 Solid microcapsules production .....	147
6.2.5 Characterization of emulsions, solid microcapsules, and reconstituted emulsions .....	148
6.3 Results and discussion .....	149
6.3.1 Characterization .....	149
6.3.2 Reconstituted emulsions .....	152
6.4 Conclusion & future outlook .....	152
Chapter 7 Conclusion .....	155
7.1 General conclusions .....	157
7.2 Future work .....	159
References .....	161

## List of symbols

$\phi$	[kg h <sup>-1</sup> ]	Mass flow rate
$\rho_b$	[kg m <sup>-3</sup> ]	Bulk density
$\rho_e$	[kg m <sup>-3</sup> ]	Emulsion density
$\rho_f$	[kg m <sup>-3</sup> ]	Feed solution density
$\rho_p$	[kg m <sup>-3</sup> ]	Particle density
$\varepsilon$	[-]	Porosity
$\delta$	[-]	Span
$\eta_c$	[Pa·s]	Viscosity of continuous phase
$\eta_d$	[Pa·s]	Viscosity of dispersed phase
$\Pi_{W_1}$	[MPa]	Osmotic pressure of inner water phase
$\Pi_{W_2}$	[MPa]	Osmotic pressure of outer water phase
$A$	[m <sup>2</sup> ]	Effective surface area
$A_m$	[m <sup>2</sup> ]	Surface area of membrane
$C_{polyW_2}^n$	[gGAE L <sup>-1</sup> ]	Concentration of polyphenols in the outer water phase
$C_a$	[-]	Capillary number
$d_{10}$	[μm]	10% of droplets below this size
$d_{3,2}$	[μm]	Surface weighted mean diameter (Sauter mean diameter)
$d_{4,3}$	[μm]	Volume weighted mean diameter
$d_{50}$	[μm]	50% of droplets below this size
$d_{90}$	[μm]	90% of droplets below this size
$d_b$	[μm]	Glass microbead diameter
$d_i$	[μm]	Mean droplet diameter in $i$ class
$d_v$	[μm]	Interstitial void diameter

$H_{EL}$	[m]	Height of emulsified layer
$H_S$	[m]	Height of total solution
$H_t$	[m]	Height after foam generation
$H_0$	[m]	Initial height of solution
$H_0$	[-]	Protein surface hydrophobicity
$J_{FO}$	[m <sup>3</sup> m <sup>-2</sup> h <sup>-2</sup> ]	Transmembrane flux of forward osmosis
$J_{DMTS}$	[m <sup>3</sup> m <sup>-2</sup> h <sup>-2</sup> ]	Transmembrane flux of dynamic membrane of tunable pore size
$Kp$	[-]	Nitrogen to protein conversion factor
$m$	[kg]	Mass
$m_0$	[kg]	Initial mass of sample
$m_0$	[g]	Mass of empty flask
$m_1$	[kg]	Mass of sample after certain time
$m_{DM}$	[kg]	Dry matter of initial sample
$m_i$	[g]	Mass of input powder
$m_p$	[kg]	Mass of freeze-dried protein powder
$m_{polyPC}$	[kg]	Mass of carob polyphenols in the concentrated extract
$m_{polyPE}$	[kg]	Mass of carob polyphenols in the initial extract
$m_{polyW_1}^0$	[kg]	Initial polyphenol mass in the inner water phase
$m_t$	[g]	Mass of flask with sample after evaporation
$m_{W_1}^0$	[kg]	Initial mass of the inner water phase
$m_{W_2}^0$	[kg]	Initial mass of the outer water phase
$n_i$	[-]	Number of size classes
$Oh$	[-]	Ohnesorge number
$\acute{p}$	[-]	Pressure ratio
$pI$	[-]	Isoelectric point
$Re$	[-]	Reynold number

$T_g$	[°C]	Glass transition temperature
$\Delta t$	[h]	Time duration of the process
$We$	[-]	Weber number

## List of abbreviations

BCA	Bicinchoninic acid
BSAE	Bovine serum albumin equivalent
BSF	Black soldier fly
BSFP	Black soldier fly powder
BSFPC	Black soldier fly protein concentrate
cmc	Critical micelle concentration
CMC	Carboxyl methylcellulose
CTAB	Hexadecyltrimethylammonium bromide
DMTS	Dynamic membrane of tunable pore size
DS	Draw solution
EA	Emulsifying activity
EAI	Emulsifying activity index
EC	Emulsifying capacity
EE	Encapsulation efficiency [%]
EFSA	European Food Safety Authority
ESEM	Environmental scanning electron microscope
ETOH	Ethanol
FAME	Fatty acid methyl ester
FAO	Food and Agriculture Organization
FC	Foam capacity
FD	Freeze drying
FO	Forward osmosis
FS	Feed solution

FS	Foam stability
FTIR	Fourier transform mid infrared spectroscopy
GA	Gam Arabic
GAE	Gallic acid equivalent
GC	Gas chromatography
GHG	Greenhouse gas
HEX	Hexane
IPOH	Isopropanol
MD	Maltodextrin
MTHF	2-methyltetrahydrofuran
MUFA	Monounsaturated fatty acid
LBL	Layer-by-layer
LM	Lesser mealworm
LMP	Lesser mealworm powder
LMPC	Lesser mealworm protein concentrate
LO	Lemon oil
N	Nitrogen
O	Oil phase
OBC	Oil binding capacity
O/W	Oil-in-water emulsion
O/W/O	Oil-in-water-in-oil emulsion
PC	Polyphenol concentrate
PE	Polyphenol extract
PGPR	Polyglycerol polyricinoleate
PPI	Pea protein isolate
PR	Polyphenol re-concentrate

PS	Protein solubility
PUFA	Poly unsaturated fatty acid
RE	Retention efficiency
SD	Spray drying
SDS	Sodium Dodecyl Sulfate
SFA	Saturated fatty acid
SO	Sunflower oil
SPC	Surface polyphenol content [gGAE L <sup>-1</sup> ]
SPI	Soy protein isolate
TPC	Total polyphenol content [gGAE L <sup>-1</sup> ]
W <sub>1</sub>	Inner water phase
W <sub>1</sub> /O	Water-in-oil
W <sub>1</sub> /O/W <sub>2</sub>	Water-in-oil-in-water
O <sub>1</sub> /O <sub>2</sub> /O <sub>3</sub> /W	Oil-in-oil-in-oil-in-water
O <sub>1</sub> /W <sub>1</sub> /O <sub>2</sub> /W <sub>2</sub>	Oil-in-water-in-oil-in-water
W <sub>2</sub>	Outer water phase
WBC	Water binding capacity
WPC	Whey protein concentrate
WPI	Whey protein isolate

## Abstract

Encapsulation is a means of protection, preservation, and delivery of bioactive and/or sensitive compounds, such as antioxidants, aromas and flavours, which is widely applied in food, pharmaceutical, biomedicine, and cosmetic industries. Amongst the existing strategies, encapsulation of the target active compounds within the structure of single and multiple emulsions is chosen in this thesis on account of the high encapsulation efficiency and the good compatibility with different media.

The purpose of this thesis is to assess the use of both sustainable materials and technologies to produce emulsions and emulsion-based solid microcapsules as a means of encapsulation of ingredients for food applications. Specifically, single and double emulsions stabilised with sustainable protein sources have been produced by a low-energy high-throughput emulsification technology to encapsulate essential oils and polyphenols.

The low-energy high-throughput technology is based on the use of dynamic membranes of tunable pore size (DMTS), which consists of a layer of glass microbeads supported by a nickel metal microsieve. The thickness and interstitial void diameter of the DMTS system can be tuned by selecting the microbeads size and the amount of microbeads for the bed. Emulsions are produced by premix emulsification mode, where a coarse emulsion is refined by pressing it through DMTS system several times (cycles). The target droplet size distribution of the refined emulsions can be controlled mainly by tuning interstitial void diameter, thickness of the bed, applied pressure, number of cycles, and viscosity of the emulsion.

A case study on the valorisation of an agri-food by-product, carob pulp, has been implemented by coupling two low-energy membrane technologies: forward osmosis and membrane emulsification. A phenolic solution obtained through water extraction from carob pulp was concentrated via forward osmosis, and the polyphenol concentrate was encapsulated in the inner water phase ( $W_1$ ) of a water-in-oil-in-water ( $W_1/O/W_2$ ) emulsions stabilized with whey protein isolate (WPI) by premix emulsification with DMTS. The study combines for the first time both membrane techniques for food by-product valorisation, allowing to assess the basis for the production of  $W_1/O/W_2$  emulsions with the DTMS system. The research showed the importance of balancing the osmotic pressure between two aqueous phases which is a key of a successful encapsulation for this specific type of system. The polyphenol loaded  $W_1/O/W_2$  emulsions could be further processed by spray drying to produce solid microcapsules. After rehydrating the solid microcapsules, the structure of the  $W_1/O/W_2$  emulsion was partially recovered. The results of this study show the potential of combining membrane-based processes to concentrate and encapsulate bioactive compounds as a strategy to valorise agri-food products under mild process conditions.

Aiming for the use of more sustainable ingredients in the food industry in general and in encapsulation applications in particular, the techno-functional properties of proteins from edible insects are evaluated. Edible insects, an EU novel food, have nutritional, economic, and environmental benefits, therefore they are interesting replacers for animal proteins, such as dairy proteins, for feed and food applications.

Black soldier fly (BSF, *Hermetia illucens*) is one of the insects having higher organic to mass conversion rate. BSF protein concentrate (BSFPC) was obtained from aqueous extraction followed by acid precipitation at pH 4-4.3, and characterized on the amino acid profile, and nitrogen content. Techno-functional properties of the BSFPC including solubility, water binding capacity, oil binding capacity, foaming capacity, foam stability, emulsifying activity and interfacial tension were assessed, and compared to whey protein isolate (WPI). The BSFPC exhibited comparable or higher emulsifying activity values than WPI for the same concentrations, hence showing the potential for emulsion stabilisation. Sunflower oil and lemon oil emulsions with different oil fractions (20, 30, and 40%) stabilised with BSFPC or WPI were produced by the DMTS system. It was proved that BSFPC stabilises sunflower oil-water emulsions similarly to WPI, but with a slightly wider droplet size distribution. For lemon oil emulsions, BSFPC showed better emulsifying performance than WPI, specially for the highest oil fraction.

Lesser mealworm (*Alphitobius diaperinus*) is one of the high-profile edible insects. Fractionation of insect meals to obtain a lipid and a protein fraction involves several steps. Defatting is the first step of the fractionation process that is usually carried out by solvent extraction. To more sustainable extraction processes, hexane was compared with greener solvents such as ethanol, iso-propanol, and 2-methyltetrahydrofuran. The impact of the solvent on the extraction yield, the lipid profile, and the emulsifying activity of the resulting protein was assessed. It was proven that defatting is feasible with greener solvents and the emulsifying ability of the lesser mealworm protein concentrate (LMPC) remains the same regardless of the solvent used during defatting.

LMPC was further evaluated as emulsifier to stabilize  $W_1/O/W_2$  emulsions and compared to a plant protein (pea protein isolate, PPI) and WPI. It was found that LMPC is able to stabilize  $W_1/O/W_2$  emulsions comparably to whey protein and pea protein when using a premix emulsification with DMTS. Environmental stresses such as temperature (-20 °C, 4 °C, 25 °C, 37 °C, 65°C and 90 °C), pH (1.5, 4.0, 6.5-7.0 and 8.0), and osmotic pressure unbalance between  $W_1$  and  $W_2$  (10-fold water dilution of  $W_2$ , 50 mM and 250 mM NaCl added to  $W_2$ ) were applied to assess the stability of the emulsions, and the storage stability at certain conditions (25 and 4°C) were examined for 2 weeks. Under acidic conditions, LMPC shows similar performance as whey protein and outperforms pea protein. Under alkaline conditions the three proteins perform similarly, while the LMPC-stabilized emulsions are less able to withstand osmotic pressure differences. The LMPC stabilized emulsions are also more prone to droplet coalescence after a freeze-thaw cycle than the WPI-stabilized ones, but they are most stable when exposed to the highest temperatures tested (90 °C). From the results it is clear that LMPC has the ability to stabilise multiple emulsions and encapsulate a polyphenol.

As for enhancing the shelf-life of emulsions entrapping polyphenols and stabilised with LMPC, WPI or PPI, the thesis shows a first approach to the production of solid microcapsules from polyphenol loaded  $W_1/O/W_2$  emulsions by spray drying or freeze drying. Regardless of the drying technique and protein used as emulsifier, the produced solid microcapsules are able to retain the structure of  $W_1/O/W_2$  emulsions after rehydration.

The results of this work demonstrate the potential of insect proteins as a feasible alternative to animal proteins, and will contribute to further implementation of insect ingredients in food, feed, pharmaceutical, biomedicine, and cosmetic applications. In particular, the surface-active properties of insect proteins, able to stabilise different emulsion-based encapsulation systems, open the possibility to develop a new range of sustainable food-grade amphiphilic emulsifiers.

UNIVERSITAT ROVIRA I VIRGILI  
EMULSION-BASED ENCAPSULATION SYSTEMS STABILIZED WITH INSECT PROTEINS: PRODUCTION WITH  
PREMIX MICROPOROUS EMULSIFICATION  
Junjing Wang

## Resumen

La encapsulación es un medio de protección, preservación y liberación de compuestos bioactivos y/o sensibles, como antioxidantes, aromas y sabores, que se aplica ampliamente en la industria alimentaria, farmacéutica, biomédica y cosmética. Además, la encapsulación es un método útil y eficaz para enmascarar el olor o sabor desagradable de un ingrediente, así como para reducir el contenido en grasa cuando se emplea una emulsión múltiple. Entre las estrategias existentes, en esta tesis se ha seleccionado la encapsulación de compuestos activos en el interior de la estructura de emulsiones simples y múltiples debido a su alta eficiencia de encapsulación y elevado grado de compatibilidad con diferentes medios.

El objetivo de esta tesis es evaluar el uso de materiales y tecnologías sostenibles para producir emulsiones y microcápsulas sólidas basadas en emulsiones como medio de encapsulación de ingredientes alimentarios. Con el fin de encapsular aceites esenciales y polifenoles, se han elaborado emulsiones simples y dobles, estabilizadas con proteínas procedentes de fuentes de sostenibles, empleando una tecnología de emulsificación de alto rendimiento y bajas necesidades energéticas.

Esta tecnología, basada en el uso de membranas dinámicas de tamaño de poro ajustable (DMTS), consiste en una capa/lecho de microesferas de vidrio soportadas por un microsieve de metal de níquel. El diámetro del espacio intersticial y el grosor del sistema DMTS se pueden ajustar seleccionando el tamaño y la cantidad de microesferas en el lecho. Las emulsiones se producen mediante emulsificación premix, en la que se refina una emulsión polidispersa al presionarla a través del sistema DMTS varias veces (ciclos). La distribución del tamaño de gota de la emulsión refinada se puede controlar principalmente ajustando el diámetro del espacio intersticial, el espesor del lecho, la presión aplicada, el número de ciclos y la viscosidad de la emulsión.

A modo de estudio de caso se ha valorizado un subproducto agroalimentario, en concreto la pulpa de algarrobo, mediante la combinación de dos tecnologías de membrana de bajo consumo energético: ósmosis directa y emulsificación por membranas. Para ello, primero se concentró mediante ósmosis directa una solución fenólica procedente de una extracción con agua de pulpa de algarrobo y, a continuación, el concentrado de polifenoles se encapsuló en la fase acuosa interna ( $W_1$ ) de una emulsión agua-en-aceite-en-agua ( $W_1/O/W_2$ ) estabilizada con proteína de suero (WPI) y producida mediante emulsificación premix con DMTS. En este estudio se han aplicado, por primera vez, estas dos tecnologías de membrana a la valorización de subproductos alimentarios, lo que ha permitido establecer las bases para la producción de emulsiones  $W_1/O/W_2$  con el sistema DTMS. Esta investigación mostró la importancia de equilibrar la presión osmótica entre las dos fases acuosas, para conseguir una encapsulación exitosa en este tipo de emulsiones dobles. Posteriormente, mediante el secado por atomización de las emulsiones  $W_1/O/W_2$

con polifenoles se obtuvieron microcápsulas sólidas que, tras ser rehidratadas recuperaron parcialmente la estructura de una emulsión  $W_1/O/W_2$ . Los resultados de este estudio muestran el potencial de combinar procesos basados en membranas para concentrar y encapsular compuestos bioactivos como estrategia para valorizar productos agroalimentarios en condiciones de proceso suaves.

Con la finalidad de utilizar ingredientes más sostenibles en la industria alimentaria, en general, y en aplicaciones de encapsulación, en particular, se han evaluado las propiedades tecno-funcionales de proteínas de insectos comestibles. Los insectos comestibles, considerados *novel food* en la UE, tienen beneficios nutricionales, económicos y medioambientales, por lo que se proponen como sustituto de las proteínas animales, especialmente de las proteínas lácteas, tanto en alimentación animal como humana.

La mosca negra (BSF, *Hermetia illucens*) es uno de los insectos que tiene una mayor tasa de conversión orgánica a masa. El concentrado de proteína BSF (BSFPC) se obtuvo a partir de una extracción acuosa seguida de una precipitación ácida a pH 4-4,3 y se caracterizó a partir del perfil de aminoácidos y el contenido de nitrógeno. Se evaluaron las propiedades tecno-funcionales del BSFPC, incluida la solubilidad, la capacidad de retención de agua y de aceite, la capacidad espumante, la estabilidad de la espuma, la actividad emulsionante y la tensión interfacial, y se compararon con el aislado de proteína de suero (WPI). El BSFPC exhibió valores de actividad emulsionante comparables o más altos que el WPI para las mismas concentraciones, mostrando, por tanto, su elevado potencial como emulsificante. Mediante emulsificación premix con DMTS se obtuvieron emulsiones O/W de aceite de girasol y aceite esencial de limón, con fracciones del 20, 30 y 40%, estabilizadas con BSFPC o WPI. Se comprobó que BSFPC estabiliza las emulsiones O/W con aceite de girasol de manera similar a WPI, pero con una distribución de tamaño de gota ligeramente más amplia. Para las emulsiones de aceite de limón, BSFPC mostró una mayor capacidad como emulsionante que WPI, especialmente para la fracción de aceite más elevada.

El gusano de la harina *Alphitobius diaperinus* es un insecto comestible de elevado valor nutricional. El fraccionamiento de los molturados de este insecto para obtener una fracción lipídica y una fracción proteica incluye diferentes etapas. La primera consiste en un desgrasado mediante extracción con solventes orgánicos. En este caso, se substituyó el hexano por solventes más ecológicos como el etanol, el isopropanol y el 2-metiltetrahidrofurano para mejorar el proceso de extracción en términos de sostenibilidad. En concreto, se determinó el impacto del disolvente sobre el rendimiento de la extracción, el perfil lipídico y la actividad emulsionante de la proteína resultante. Los resultados permitieron concluir que cualquiera de los solventes alternativos es capaz de desgrasar sin comprometer la capacidad emulsionante del concentrado de proteína del gusano de la harina (LMPC), que no se vio modificada independientemente del disolvente.

Asimismo, se evaluó la capacidad de LMPC para estabilizar emulsiones  $W_1/O/W_2$  y se comparó con una proteína vegetal (aislado de proteína de guisante, PPI) y WPI. Se comprobó que LMPC es capaz de estabilizar emulsiones  $W_1/O/W_2$  de manera

comparable a WPI y PPI en emulsiones producidas mediante emulsificación premix con DMTS. Se determinó la estabilidad de estas emulsiones en diferentes condiciones de estrés ambiental tales como la temperatura (-20 °C, 4 °C, 25 °C, 37 °C, 65°C y 90 °C), pH (1,5, 4,0, 6,5-7,0 y 8,0) y el desequilibrio de presión osmótica entre W1 y W2 (reducción de la osmolalidad en W2 aplicando una dilución 1/10, incremento de la osmolalidad en W2 mediante adición de NaCl hasta conseguir una concentración de 50 mM y 250 mM ). Del mismo modo, se examinó la estabilidad de estas emulsiones durante el almacenamiento a 25°C y 4°C durante 2 semanas. En condiciones ácidas, LMPC mostró un rendimiento similar a WPI y superior a PPI. En condiciones alcalinas, las tres proteínas se comportaron de manera similar, mientras que las emulsiones estabilizadas con LMPC resultaron menos capaces de resistir las diferencias de presión osmótica. Las emulsiones estabilizadas con LMPC también fueron más propensas a la coalescencia tras un ciclo de congelación-descongelación que las estabilizadas con WPI, si bien fueron más estables cuando se expusieron a la temperatura más elevada (90 °C). Estos resultados permiten concluir que LMPC tiene la capacidad de estabilizar emulsiones múltiples y encapsular un extracto de polifenoles.

En cuanto a la mejora de la vida útil de emulsiones  $W_1/O/W_2$  estabilizadas con LMPC, WPI o PPI que contienen polifenoles, la tesis muestra una primera aproximación a la producción de microcápsulas sólidas empleando el secado por atomización o la liofilización de estas emulsiones. Independientemente de la técnica de secado y la fuente de proteína empleada como emulsificante, las microcápsulas sólidas obtenidas pudieron retener la estructura de las emulsiones  $W_1/O/W_2$  tras la rehidratación.

Los resultados de este trabajo muestran el potencial de las proteínas de insectos como alternativa viable a las proteínas de origen animal, contribuyendo a facilitar el empleo de los ingredientes de insectos en alimentación humana y animal o aplicaciones farmacéuticas, biomédicas y cosméticas. En particular, las propiedades tensoactivas de las proteínas de insectos, capaces de estabilizar diferentes sistemas de encapsulación basados en emulsiones, abren la posibilidad de desarrollar una nueva gama de emulsionantes sostenibles anfílicos de grado alimentario.

UNIVERSITAT ROVIRA I VIRGILI  
EMULSION-BASED ENCAPSULATION SYSTEMS STABILIZED WITH INSECT PROTEINS: PRODUCTION WITH  
PREMIX MICROPOROUS EMULSIFICATION  
Junjing Wang

# Chapter 1

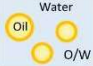




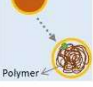



## Introduction & objectives



## 1.1 Emulsion-based encapsulation systems

Emulsion-based encapsulation systems have been primarily conceived to entrap, protect, and/or release active agents in pharmaceutical, food, feed, cosmetic, and agrochemical industries. The encapsulated active agents may include drugs, vitamins, nutraceuticals, nutrients, antimicrobials, antioxidants, flavours, and colours. The main reason for developing these encapsulation systems is to overcome challenges that normally limit the incorporation of these active agents into commercial products, such as poor solubility, susceptibility to chemical degradation, undesirable flavour profiles, low bioavailability, or limited bioactivity. As a result of the great progress made in emulsion-related research in recent years, more and more systems have been developed. Emulsion-based solid microcapsules, solid lipid particles, multilayer emulsions, high internal phase emulsions, gelled particles, polymeric particles, and Pickering emulsions are examples of multiphasic structures based on liquid-liquid dispersions of different complexity (Table 1.1)<sup>1-3</sup>.

Table 1.1. Description of the structure and main characteristics of conventional and some complex emulsion-based systems.

Type of emulsion	Structure	Characteristics
Conventional		Two immiscible phases, one dispersed as droplets in the other phase stabilized by emulsifier. e.g. oil-in-water “O/W” emulsion
Multiple		Emulsion in emulsion, three or more phases, involve both hydrophilic and lipophilic emulsifiers. e.g. water-in-oil-in-water “W/O/W” emulsion
Multilayer		Protection of more than two layers of stabilizers, disposed layer by layer.
High internal phase		High fraction of internal (dispersed) phase (typically >74%), droplets are closely packed.
Solid lipid particle		Emulsion formulated above melting point and later cooled down for lipids crystallization.
Polymeric particle		Lipophilic monomers dispersed in water phase stabilized by surfactant micelle. The polymerization of monomers within droplet begins once introduce the water soluble radical initiator.
Pickering		Stabilized by solid particles by partial wettability.
Gelling particle		Emulsion in a gel matrix.
Solid microcapsule		Dehydration of liquid emulsion with addition of wall material.

From the several types of encapsulation systems, emulsions and emulsion-based solid microcapsules are widely used in the food industry. Apart from their capacity to entrap, protect and release labile ingredients, emulsions also can<sup>4</sup>:

- Enhance the appearance of the product by keeping from phase separation.
- Improve organoleptic characteristics of food such as taste, colour, odour and mouthfeel.
- Reduce the fat content by replacing oil-in-water (O/W) emulsions with water-in-oil-in-water ( $W_1/O/W_2$ ) without affecting the physical characteristics of the product.

In the case of emulsion-based solid microcapsules, their convenience for dosing the entrapped active agent in industrial formulations and their high storage stability compared to emulsions have spread their applications.

In other fields, such as in biomedical applications, it is an effective form of drug delivery, cell therapy, anticancer treatment, and tissue engineering<sup>5-8</sup>, and in the cosmetics industry, it has been tested for skin hydration and protection<sup>9-11</sup>.

To select and design each of those systems, basic knowledge on the mechanisms controlling structure formation, the consequent processes responsible for the physicochemical properties (e.g., optical, rheological), and stability of the encapsulation system have to be considered in order to meet the needs of each particular application. The following sections will focus on the main properties of emulsions and emulsion-based solid microcapsules for food applications.

### 1.1.1 Emulsions

Emulsion, in a traditional sense, is a two immiscible liquid-phase system of one dispersed as droplets (dispersed phase) in the other one (continuous phase). The simplest example is oil dispersed within water, called oil-in-water (O/W) emulsion where oil is the dispersed phase and water is the continuous phase. Salad dressings, mayonnaise, and milk, etc. are the most common emulsion-based foods that can be found in daily life. When swapping the two phases, water-in-oil (W/O) emulsion is formed, examples of this are, margarine and low-fat spread.

According to the number and sequence of immiscible phases, multiple emulsions can be formulated such as double emulsions (water-in-oil-in-water,  $W_1/O/W_2$ , and oil-in-water-in-oil,  $O_1/W/O_2$ , water-in-water-in-water,  $W_1/W_2/W_3$ <sup>12</sup>) and four-phase emulsion ( $O_1/O_2/O_3/W$ )<sup>13</sup>. Minerals (e.g., iron and magnesium) and some water-soluble vitamins (e.g., vitamin C and B<sub>12</sub>) can be encapsulated in the inner water phase of  $W_1/O/W_2$  emulsions, and vitamin E can be loaded in the oil phase of  $W_1/O/W_2$  emulsions to enhance the nutritional properties of foods<sup>14-19</sup>. Phenolic compounds and probiotics (e.g., *Lactobacillus acidophilus*) can be encapsulated in  $W_1/O/W_2$  emulsions for functional foods<sup>20,21</sup>. Reduced-fat cheese and yogurt are also elaborated by using  $W_1/O/W_2$  emulsions<sup>22,23</sup>. Double emulsions are attracting the interests of research and industry due to their unique morphology, making them multifunctional carriers that are able to co-encapsulate both hydrophilic and lipophilic active molecules in the same particle.

Based on droplet size, emulsions are categorized as macroemulsions, nanoemulsions, and microemulsions (Table 1.2)<sup>8</sup>.

Table 1.2. Comparison of macroemulsions, nanoemulsions, and microemulsions.

	<b>Macroemulsion</b>	<b>Nanoemulsion</b>	<b>Microemulsion</b>
Droplet diameter	1-100 $\mu\text{m}$	20-500 nm	10-100 nm
Appearance	Opaque	Opaque or translucent	Translucent
Advantage	Low surfactant/oil ratio Natural macromolecular emulsifier, e.g. proteins Apt for multiple emulsion Common in food products	Kinetically stable Higher bioaccessibility Tunable rheology Apt for drug delivery, suitable in food, cosmetic,	Stable, long shelf-life Spontaneously formed Higher bioaccessibility Apt for cleaning formulations, chemical
Limit	Unstable	Thermodynamically unstable High surfactant/oil ratio	Cosurfactant required High surfactant (+cosurfactant)/oil ratio

Macroemulsions are the most common form of emulsions used in food industry that can be found in a variety of products, including milk, beverages, mayonnaise dips, sauces, and desserts<sup>24</sup>. The stability of thermodynamically unstable emulsions can be improved by reducing the density difference between the phases, decreasing the average droplet size or increasing the viscosity of the continuous phase<sup>25</sup>. Comparing with nanoemulsions, producing macroemulsions requires relatively lower shear, lower energy and results in higher productivity under the same type of techniques. The lower dosage of emulsifier in macroemulsions also reduces the toxicity level of the product. The term, emulsions, is used to refer to macroemulsions hereinafter.

Emulsions do not form spontaneously, hence an energy has to be supplied and it is necessary to incorporate a surface active agent to decrease the interfacial tension and prevent droplet coalescence. Conventional technologies to produce emulsions include rotor stator mixers, colloid mills, high-pressure homogenizers and ultrasonic homogenizers. The energy applied generates droplets of the dispersed phase within the continuous phase. The surface active agent, that is dissolved in the continuous phase, can adsorb onto the newly created interfaces and reduce the interfacial tension. In addition, a functional stabilizer can be integrated together in order to stabilize the produced emulsions against destabilizing factors including gravitational separation, flocculation, coalescence, Ostwald ripening, and phase separation<sup>26</sup> during the storage. Different destabilization effects are depicted in Figure 1.1.

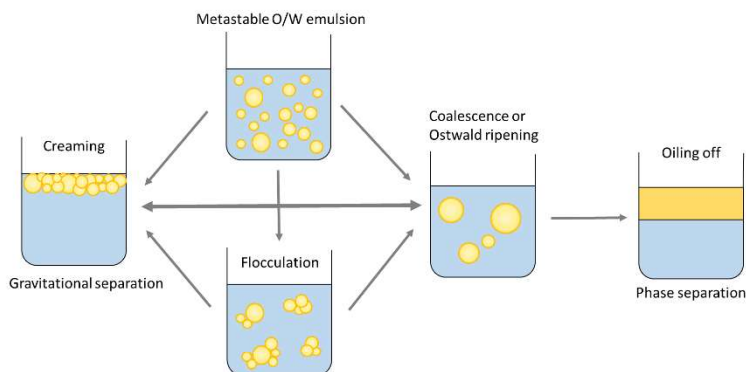


Figure 1.1 Schematic diagram of the physical destabilization mechanisms of emulsions.

Gravitational separation is driven by the difference of density between the two phases. Creaming (as shown in Figure 1.1) takes place when the density of dispersed phase is lower than that of the continuous phase, and vice versa, sedimentation occurs when the density of dispersed phase is higher than that of the continuous phase. The colloidal interaction between the droplets determines two types of droplet accumulation named coalescence and flocculation. Flocculation is related to the droplets attaching together to form flocs, and coalescence is the union of several droplets to build larger ones. Coalescence and flocculation are the result of several attractive forces between droplets and between the interfacial layers, being the main factors van der Waals forces, hydrophobic interaction, covalent interaction, and Ostwald ripening. Ostwald ripening is due to the solubility of smaller droplets (large curvature) is higher than larger droplets

(small curvature), hence small droplets diffuse and merge with larger droplets leading to the growth of large droplets<sup>27</sup>.

### 1.1.2 Stabilization of emulsions

Surfactants, emulsifiers and stabilizers are the three mostly used names referring to the surface active agents used for emulsion stabilization. Sometimes they are used as synonyms because they have the same function, but differences among them should be highlighted.

Surfactants are relatively small molecules with a hydrophilic “head” or polar group and a lipophilic “tail” or non-polar group. The head group can be anionic, cationic, zwitterionic or nonionic. Take O/W emulsion as an example, surfactant can adsorb onto the oil-water interface with the lipophilic end located in the oil phase and the hydrophilic end in the water phase (as illustrated in the Figure 1.2). In this way, interfacial tension between oil-water interface is decreased and the formed droplets can be stabilized from repulsive forces (electrostatic repulsion and steric hinderance), but also influenced by colloidal interaction forces between the droplets.

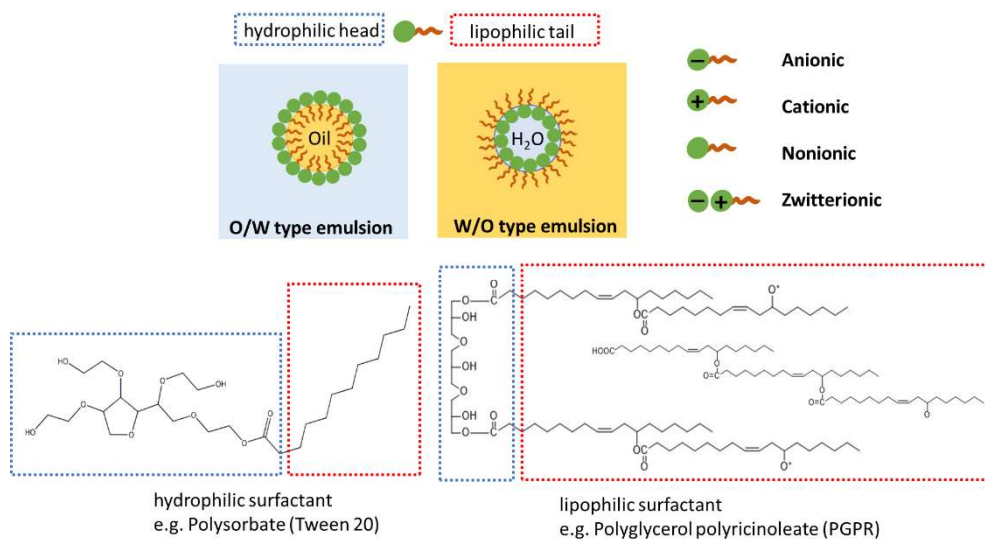


Figure 1.2. Schematic representation of different types of surfactants and how they stabilize a droplet. Chemical structures were given for a hydrophilic surfactant Tween 20 and a lipophilic surfactant PGPR.

Emulsifiers are usually defined as any surface active agent, from low molecular weight surfactants to biopolymers with amphiphilic nature, such as proteins, certain polysaccharides, and protein-polysaccharide complexes. Emulsifiers and stabilizers are defined in the article of European parliament and council directive No. 95/2/EC as:

- Emulsifiers—substances which make it possible to form or maintain a homogenous mixture of two or more immiscible phases such as oil and water in a foodstuff.

- Stabilizers – substances which make it possible to maintain the physico-chemical state of a foodstuff including substances which enable the maintenance of a homogenous dispersion of two or more immiscible substances in a foodstuff as well as which stabilize, retain or intensify an existing colour of a foodstuff.

Therefore, stabilizers include emulsifying agents as well as thickeners (e.g., carboxymethylcellulose), gelling agents (e.g., gelatin, agar, carrageenan, pectin), and weighting agents (e.g., sucrose acetate isobutyrate) (Figure 1.3).

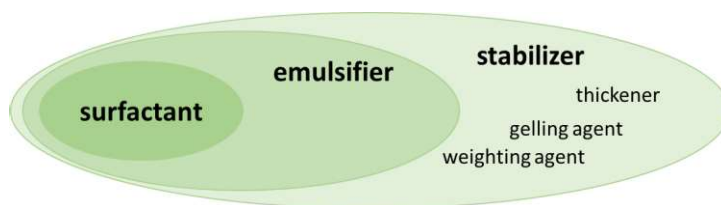


Figure 1.3. Classification of surfactant, emulsifier and stabilizer.

As for the selection of surfactants, in 1954, Griffin<sup>28</sup> laid down a method to classify them based on the relative proportions of the hydrophilic and lipophilic groups, named as the hydrophilie-lipophilie balance (HLB). The HLB values are set in a scale from 0 to 20 (Table 1.3) and are used to predict the functionality of a compound. Consequently, when multiple emulsions, such as  $W_1/O/W_2$  are produced, two surfactants are required, one with a low HLB value is needed to stabilize the  $W_1/O$  interphase, and one with a high HLB value for the  $O/W_2$  interphase.

Table 1.3. List of HLB values with different functions and some examples of small molecular surfactants<sup>29</sup>.

Category and examples	HLB
Antifoaming	2-3
Lipophilic emulsifier (stabilizing W/O emulsion)	3-6
e.g. Glycerol mono stearate	2.8
Sorbitan mono stearate	4.7
Wetting agent	7-9
Hydrophilic emulsifier (stabilizing O/W emulsion)	8-16
e.g. Sorbitan mono laurate	8.6
Poly(oxyethylene) sorbitan mono oleate	16
Detergent	13-15
Solubilizing agent	15-18

Surface active agents that have a hydrophilic and a lipophilic part often tend to aggregate in the form of micelles in solution. These aggregates have spherical shape with the lipophilic and the hydrophilic parts oriented depending on the polarity of the solvent. The critical micelle concentration (cmc) can be defined as the concentration of surfactants above which micelles are spontaneously formed. Upon reaching cmc, any further addition of surfactants will only increase the number of micelles and interfacial tension will not be reduced further on. Micelle formation can also enhance the solubility/transport of polar or non-polar components that are incorporated into their interior.

### 1.1.3 Emulsion-based solid microcapsules

The production of solid microcapsules from emulsions includes two steps which are the preparation of emulsions followed by water or continuous phase removal. To enhance the protection of the target component and build the solid microcapsules, a wall building material is often integrated. The selection of the wall material is of paramount importance for the success of the encapsulation, and it has to consider the nature of the core ingredients, the drying technique applied, the concentration of the wall material required, and the release mechanism. The most commonly used wall materials are maltodextrin, Arabic gum, chitosan, alginate and proteins<sup>30,31</sup>. The final shape of the microcapsules is influenced by the drying process and by the core and wall materials used. Several main structures of emulsion-based solid microcapsules are shown in Figure 1.4. For instance, solid microcapsules produced by spray drying have a typical sphere shape with multi core structure, which is discussed in detail in section 1.3.3.

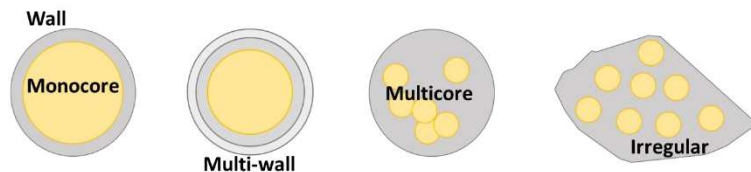


Figure 1.4 Schematic representation of emulsion-based solid microcapsules structures.

## 1.2 Proteins as emulsifier

Many proteins are surface active molecules that can be used as emulsifiers because of their ability to adsorb on to the oil-water interfacial layer and to form viscoelastic films to stabilize O/W type emulsions. As an example, HLB value of sodium caseinate is estimated at 14 due to high water solubility, which is suitable to stabilise O/W emulsions<sup>32</sup>. The protein functionality is attributed to its structure built up by chained amino acids. Amino acids are the basic building blocks that consist of an amino group, a carboxyl group, a hydrogen atom and a side chain group connected to the same carbon atom. Amino acids are linked into peptide chains by dehydration. Peptide chains go through four structure levels (primary, secondary, tertiary and quaternary) to configure the spatial structure driven by non-covalent interactions (such as hydrogen bonds, ionic bonds, van der Waals forces, and hydrophobic interactions) and covalent disulfide bonds. There are 20 amino acids (Figure 1.5) excluding selenocysteine and pyrrolysine (found only in a few bacteria).

The differences in polarities and charges of the amino acids make the protein molecule to have amphiphilic and zwitterionic natures. Proteins adsorb onto the surfaces of newly formed oil droplets created by homogenization of oil–water–protein mixtures, where they facilitate further droplet disruption by lowering the interfacial tension and retard droplet coalescence by forming protective membranes around the droplets. Proteins adsorb to the interface in three phases. First, the protein is transported to attach at the oil/water interface. In the second stage, the unfolding of the molecular chain is promoted by protein denaturation, and thus hydrophobic sites inherent in the core of the molecule are exposed and adsorbed on the surface of the oil droplet. Finally, adsorbed proteins produce a viscoelastic film around dispersed droplets for emulsion stabilization<sup>33,34</sup>. Electrostatic repulsion or steric hindrance are the main repulsive interactions between oil droplets, moreover the formation of an interfacial membrane that is resistant to rupture plays an important role in stabilizing the droplets against flocculation and coalescence during long-term storage.

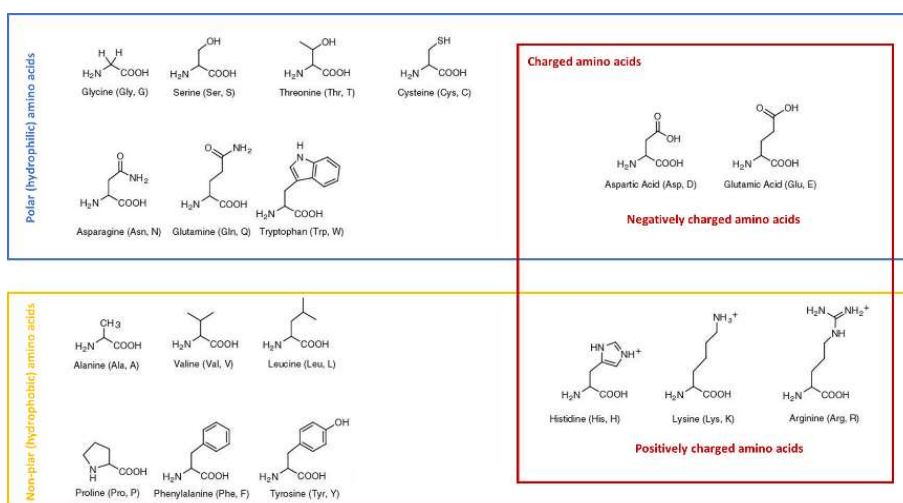


Figure 1.5. Classification of the 20 common amino acids.

Hydrolysis is one of the promising methods to break down protein molecules into short chain peptides. The hydrolysates obtained from controlled protein hydrolysis have enhanced techno-functional properties and/or become bioactive peptides. Enzymatic hydrolysis, under mild conditions, is mostly applied using proteases derived from plants and microorganisms such as the commercial enzymes Alcalase, Flavourzyme, and Protamex. The use of commercial enzymes allows to control the hydrolysis, to obtain a specific peptide bond cleavage, and ultimately results in improved nutritional and functional properties. Appearance, solubility, flavour, and biochemical safety of the hydrolysates vary with hydrolysis methods and the degree of hydrolysis. Protein hydrolysates are reported to have improved techno-functional properties including solubility, emulsifying, foaming and thermal stability, and the mineral binding. Moreover, it has been described that the resulting peptides have pain relieving, antihypertensive, antimicrobial, anti-inflammatory, antidiabetic, and anticancer properties. Therefore, it is a promising method to produce functional and nutritious foods.<sup>35–38</sup>

In food applications, proteins are widely employed to stabilise emulsion-based products, being the dairy ones the most commonly used. In recent years, the need of more sustainable ingredients has arisen interest in new sources of food grade proteins with emulsifying capacity. In the following sections, the properties as emulsifiers of dairy, plant and insect proteins will be reviewed.

### 1.2.1 Dairy proteins

Whey protein and casein are currently the most widely used dairy proteins in the food industry as stabilisers. They are hydrophilic emulsifiers suitable for the stabilization of O/W type emulsions. Whey protein, obtained from the liquid residue of cheese and casein production, is widely used for dairy products due to its unique functionality and nutritional properties. Whey proteins consist of  $\beta$ -lactoglobulin (50-55%),  $\alpha$ -lactalbumin (20-25%), and with small amount of bovine serum albumin (BSA), glycomacropeptide, and immunoglobulins.  $\beta$ -lactoglobulin (molecular weight of 18.4 kDa) is a globular protein having a spherical structure induced by tertiary structure, in which hydrophobic (lipophilic) sites are buried inward, and hydrophilic sites are located outward for dipole-dipole interactions with solvents.  $\alpha$ -lactalbumin (molecular weight of 14.2 kDa) has a bilobal structure established by intramolecular disulfide bonds, which can unfold and refold by itself depending on environmental circumstances<sup>34,39,40</sup>.

Casein is a mixture of phosphoproteins constituting 80% of the total protein content in bovine milk existing in the form of large aggregates/micelles. Casein aggregates consisting of four subunits:  $\alpha_{S1}$ -casein (23.6 kDa, 38%),  $\alpha_{S2}$ -casein (25.2 kDa, 10%),  $\beta$ -casein (24.0 kDa, 36%), and  $\kappa$ -casein (19.1 kDa, 12%).  $\alpha_{S1}$ - and  $\alpha_{S2}$ -caseins are naturally unfolded proteins with extended coil-like conformation, while  $\beta$ - and  $\kappa$ -caseins have molten globule-like proteins, which have a compact structure with a high degree of hydration and side-chain flexibility. Caseinate, the salt form of casein obtained by alkaline addition, is extensively used as emulsifier<sup>34</sup>. Casein is a more heat-resistant protein than whey protein, with a reported denaturation temperature above 80 °C, while whey protein starts to denature at 65 °C<sup>34,41</sup>.

Unstructured proteins, such as casein, are flexible which can go through rapid conformational changes and realignment once adsorbed at the oil-water interface. In the casein stabilized emulsion, with the prolonged storage, Available  $\beta$ -casein can replace other casein fractions at the oil-water interface due to its greater hydrophobicity. As for globular proteins, whey protein,  $\beta$ -lactoglobulin and  $\alpha$ -lactalbumin can stabilize at the oil-water interface rapidly by partially unfolding and tightly packing to form a rigid interfacial film<sup>34</sup>. Besides, O/W emulsions stabilized by lactoferrin (pI~8, separated from bovine milk) at near neutral pH (5~7) with the surface positively charged droplets that are stable against oil oxidation, that the droplets could repulse charged transition metal ions to catalyse oxidation<sup>42-45</sup>.

Emulsifying properties of dairy proteins have been tuned by producing protein-polysaccharide complexes and coacervates. Carboxymethylcellulose (CMC), Arabic gum, guar gum, xanthan gum, carrageenan, chitosan, alginate, and pectin are some of the polysaccharides used to form complexes with whey protein (including  $\beta$ -lactoglobulin

and  $\alpha$ -lactalbumin) and casein through electrostatic interactions<sup>33,46</sup>. The emulsion droplets stabilized by protein-polysaccharide complexes have a denser and more viscoelastic film layer that can enhance the emulsion stability by increasing the steric effect.

### 1.2.2 Plant proteins

Most plant-based proteins are complex storage globular proteins with molecular weight ranging from 10-400 kDa. Soy proteins mainly consist of  $\beta$ -conglycinin and glycinin, and pea proteins are composed mainly of vicilin and legumin. Various plant proteins have been assessed for their emulsifying properties, however, legume proteins such as soy and pea protein are extensively studied compared to cereal proteins (e.g., wheat and rice), and oilseed proteins (e.g., rapeseed/canola, sesame, hemp, sunflower seed and flaxseed)<sup>34</sup>. Cereal proteins including wheat, barley, and oat displayed relatively weaker emulsifying ability when compared to legume proteins<sup>47</sup>.

Due to their high molecular weight and solid protein structure, plant derived proteins have attracted attention to formulate Pickering emulsions. It is mentioned in several articles that the O/W emulsions prepared at acidic conditions (pH~3) with soy protein isolate (SPI) and pea protein isolate (PPI) presented a great stability against creaming due to the formation of a gel-like network or nano/submicron-size particles which acted as a Pickering stabilizer<sup>48-50</sup>. Nevertheless, more recent studies with PPI at pH 3 reported that protein molecules were the primary stabilizer for O/W instead of submicron-size particles<sup>51</sup>.

After a thermal treatment (90 °C for 10 min), legume protein (soy and pea proteins), excluding lupin, showed comparable results to  $\beta$ -lactoglobulin and the commercial emulsifier polysorbate 20 (Tween 20) as all of them could stabilize O/W emulsions with a similar droplet size (~0.4  $\mu\text{m}$ )<sup>52</sup>. Besides, not only enzymatic hydrolysis<sup>48,53</sup>, but also oxidation of PPI for 24h was reported to result in fragmentation and chemical changes that led to rapid formation of a thin and mobile interfacial film<sup>54</sup>.

The use of blended plant and dairy proteins to stabilise emulsions has been reported to have synergistic and antagonistic effects depending on the emulsion formulation<sup>55-57</sup>. For instance, a 10 wt% vegetable oil emulsion stabilised with 1 wt% protein blend of PPI and sodium caseinate (SC) at a ratio of 1:1, it was found to have a synergistic stabilization effect during 14 days of storage, compared to emulsions stabilized with either PPI or SC<sup>56</sup>. Conversely, another study using 0.5-0.7 wt% protein blends of SC and soy protein isolate (SPI) or PPI at a ratio of 1:1 to stabilize 10 wt% lycopene dissolved oil phase demonstrated antagonistic stabilizing effect with flocculation and coalescence after 14 days of storage<sup>57</sup>. The interfacial protein composition, the interfacial tension of the system, and the interfacial rheology properties were investigated to understand these results<sup>55,56</sup>. In all, plant proteins are likely to replace partially WPI as emulsifier in blends having the same stabilizing effect than WPI alone<sup>56</sup>. Moreover, plant protein-polysaccharide complexes can be also used as emulsifiers to enhance emulsion stability by increasing the steric effect, also a pea protein-proanthocyanidin (polyphenol) complex used as an “antioxidative” emulsifier, improved emulsion long-term storage stability<sup>58,59</sup>.

### 1.2.3 Insect proteins

Even though insects are a novel source of proteins from which research is still needed, there is a general agreement regarding their potential as a food ingredient because of the presented information about some of their properties, and their evident advantages in terms of sustainability. However, insect proteins have not been thoroughly studied, it still remains challenges to the researchers especially in the field of food science and technology.

In recent years, an increasing number of publications have reported the techno-functional and physico-chemical properties of insect proteins such as solubility, water and oil binding capacity, surface charge, rheology, gelling, coagulating, foaming and emulsifying properties, interfacial tension, surface hydrophobicity or antioxidant activity. Other characteristics/aspects, including *in vitro* digestibility and antibacterial activity have been initially investigated. The most widely studied insect species for feed and food applications are yellow mealworm (*T. molitor*), black soldier fly (*H. illucens*)<sup>60–62</sup>, lesser mealworm (*A. diaperinus*)<sup>63,64</sup>, two species of crickets (*G. sigillatus* and *A. domesticus*)<sup>63,65–67</sup> and edible grasshopper (*S. gregaria*)<sup>65,68</sup>.

Regarding protein extraction/isolation from the whole insect, several strategies are still being developed<sup>69–73</sup>. The most widely used method for extracting insect proteins is defatting followed by a selective precipitation with an alkaline extraction step and a subsequent acid precipitation. On that basis, additional treatments such as salting-in, salting-out and ultrasonication assisted extraction can improve the functionality of the protein obtained<sup>74,75</sup>. Moreover, the hydrolysate obtained by enzymatic hydrolysis, as mentioned previously, has shown improved solubility, emulsifying and foaming characteristics by several studies, making them suitable for a variety of food and feed applications<sup>35,66,76</sup>.

The emulsifying properties reported for some of the most promising insect species for industrial scale production of food and feed are summarised in Table 1.5. Before discussing the results on Table 1.5, it is important to mention that the emulsifying properties were measured using different methodologies depending on the reference, which impedes a direct comparison amongst all the results. Specifically, The methods to determine the emulsifying properties are emulsifying activity (EA in %, equation 1.4), emulsifying activity index (EAI in m<sup>2</sup>/g, equation 1.5), and emulsifying capacity (EC in mL/mg or %, equation 1.6 and equation 1.7, respectively) (Table 1.4).

Table 1.4. List of the methods to evaluate emulsifying property.

Property	Unit	Equation	
Emulsifying activity (EA)	%	$EA [\%] = \frac{H_e}{H_t} \times 100$	eq (1.4)
		Ratio of the height of emulsified layer ( $H_e$ ) and total height ( $H_t$ ). <sup>77</sup>	
Emulsifying activity index (EAI)	m <sup>2</sup> /g	$EAI [m^2/g] = \frac{2 \times 2.303 \times A \times D}{l \phi C}$	eq (1.5)
		Turbidity of produced emulsions (with sodium dodecyl sulfate dilution) at 500 nm. $A$ is absorbance, $D$ is dilution factor, $l$ is path length of light, $\phi$ is oil fraction in volume percentage, and $C$ is concentration of protein. <sup>78</sup>	
Emulsifying capacity (EC)	mL/mg	$EC [mL/mg] = \frac{V_{oil}}{m_{protein}}$	eq (1.6)
		Ratio of oil volume ( $V_{oil}$ ) added until the phase separation to the mass of protein powder used ( $m_{protein}$ ) to prepare protein solution. <sup>79</sup>	
Emulsifying capacity (EC)	%	$EC [\%] = \frac{V_e}{V_i} \times 100$	eq (1.7)
		Ratio of the volume of emulsified layer ( $V_e$ ) after holding for 10 min to the initial volume ( $V_i$ ). <sup>67</sup>	

As can be seen from Table 1.5, emulsifying activity (EA, calculated as eq 1.4) values vary in a wide range (0.3-73%) depending on the protein source and the concentration. In theory, EA above 50% indicates complete emulsification of all the oil introduced. Therefore, most of the insect proteins shown in Table 1.4 are suitable as emulsifiers at certain operation conditions. EA of several species of insect powders and enriched protein fractions are in the same range than those reported for plant sourced flours and their protein isolates such as corn gluten meal, chickpea, lentil, soy, kidney beans and peanut<sup>64</sup>. Furthermore, it is reported that EA of *L. migratoria* protein concentrate is similar to EA of egg white protein concentrate<sup>79</sup> when pH and salt concentration were adjusted (pH 5 and 3M NaCl). When comparing with dairy proteins, *S. gregaria* and *A. domesticus* protein extracts obtained from aqueous extraction at alkaline conditions or ultrasound assisted extraction displayed the same high emulsifying activity index (EAI, calculated as eq 1.5) as whey protein isolate (WPI)<sup>67</sup>. Whereas, emulsifying capacity (EC[m<sup>2</sup>/g], calculated as eq 1.6) reported from *T. molitor* protein isolate<sup>73</sup>, *G. sigillatus* protein hydrolysates<sup>65</sup> and protein extracts from *P. succincta* and *C. roseapbrunner*<sup>80</sup> are significantly lower than BSA (295 m<sup>2</sup>/g)<sup>80</sup>.

Gould and Wolf<sup>82</sup> focused on the emulsion stability of 20 wt% sunflower O/W emulsions stabilized with *T. molitor* protein extract, which was assessed under various

environmental stresses including temperature (-20 °C, 60-90 °C), pH (3-8) and salt concentration (NaCl 80-330 mM), and compared them to the emulsions stabilized by WPI. The emulsions stabilized with *T. molitor* protein extract had a droplet size slightly smaller than those stabilized with WPI (12 µm versus 14 µm), that was in agreement with the interfacial tension values at equilibrium of sunflower oil with *T. molitor* protein solution (11 mN/m) and sunflower oil with WPI solution (13 mN/m). *T. molitor* protein extract was also able to maintain the emulsion stability (without significant droplet coalescence) for a period of at least 2 months. The emulsions were also stable at NaCl concentration smaller than 330 mM as well as frozen (-20 °C) or heated up to 80 °C, while droplet flocculation was observed at pH (~4) close to the isoelectric point of protein. These results demonstrate the potential of insect proteins to replace whey protein in encapsulation and delivery system applications.

Table 1.5. Literature review on the emulsifying properties of insect proteins.

Insect species Scientific name	Protein concentration (w/v)	Protein solubility in water (~pH7)
Yellow mealworm	1%	5-97% (30%)
<i>Tenebrio molitor</i>	1%	30-95% (35-60%)
	1%	N/A <sup>e</sup>
	0.02-0.1%	20-55%
Tropical banded cricket	1%	5-96% (30%)
<i>Gryllodes Sigillatus</i>	0.5%	5-92% (10-90%)
	1%	35-50%
House cricket		
<i>Acheta domestica</i>	1%	N/A <sup>e</sup>
Large African cricket		
<i>Gryllidae sp</i>	7%	13-29% (29%)
Edible grasshopper	1%	0-70% (12-42%)
<i>Schistocerca gregaria</i>	1%	10-90% (25%)
Grasshopper	0.5%	45-90% (85%)
<i>Patanga succincta</i>		
Migratory locust	3.35 or 5%	10-55% (17-55%)
<i>Locusta Migratoria</i>		
Locust	0.5%	75-90% (85%)
<i>Chondracris roseapbrunner</i>		
Sudanese tree locust	7%	(23-27%)
<i>Anacridium melanorhodon</i>		
Honeybee	1%	5-100% (10-30%)
<i>Apis mellifera</i>		
Japanese rhinoceros beetle	1%	N/A <sup>e</sup>
<i>Allomyrina dichotoma</i>		
White-spotted flower chafer beetle	1%	N/A <sup>e</sup>
<i>Protaetia brevitarsis</i>		
Scorpion	5%	5-80% (10-25%)
<i>Buthus martensii Karsch</i>		
Silkworm	7%	N/A <sup>e</sup>
<i>Bombyx mori</i>		

<sup>a</sup> EA; <sup>b</sup> EAI; <sup>c</sup> EC [mL/mg]; <sup>d</sup> EC [%]; <sup>e</sup> N/A not applicable.

Oil	Emulsifying property	Ref.
Vegetable oil	67% <sup>a</sup>	65
Corn oil	22-56 m <sup>2</sup> /g <sup>b</sup>	74
Olive oil	70-80% <sup>d</sup>	83,84
Rapeseed oil	0.64-2.35 mL/mg <sup>c</sup>	85
Vegetable oil	62-73% <sup>a</sup>	65
Canola oil	7-32 m <sup>2</sup> /g <sup>b</sup>	66
Soybean oil	444-558 mL/g <sup>c</sup>	86
Corn oil	26.8-41.7% <sup>a</sup>	67
Soybean oil	46.8% <sup>a</sup>	87
Canola oil	39-100% <sup>d</sup>	68
Vegetable oil	69% <sup>a</sup>	65
Soybean oil	29 m <sup>2</sup> /g <sup>b</sup>	81
Sunflower oil	0.3-62.6% <sup>a</sup>	76,80
Soybean oil	37 m <sup>2</sup> /g <sup>b</sup>	81
Groundnut oil	46.6-55.5% <sup>a</sup> 1.4-2.7 mL/g <sup>c</sup>	88
Canola oil	21-100% <sup>d</sup>	68
Olive oil	70-80% <sup>d</sup>	83,84
Olive oil	70-100% <sup>d</sup>	83,84
Corn oil	40-46% <sup>a</sup>	75
Soybean oil	23-25% <sup>a</sup>	89

#### 1.2.4 Others

Fungi, microalgae and bacteria are also protein-rich sources with a protein content up to 92% as reported in literature<sup>89,90</sup>. They can be grouped as microbial protein source, which is the designation of protein derived from unicellular or multicellular microorganisms. It is not a novel concept to include microbial protein to supplement human and animal diets, since yeasts were already employed to supply protein requirements of human diets and animal feeding in the World War I<sup>90</sup>.

In general, the use of microbial proteins as an alternative emulsifier for food applications has been relatively more investigated than insect proteins. Proteins extracted from bacteria (*Aeribacillus pallidus*)<sup>92</sup> and yeasts (*Sccharomyces cerevisiae*)<sup>93,94</sup> showed comparable emulsifying activity and capacity to soy protein. For instance, the cell-free culture broth of filamentous fungus (*Curvularia lunata* IM 2901) showed a superior emulsifying ability to stabilize various oils, hydrocarbons, and organic solvents<sup>95</sup>. Recently, there is an increasing interest in microalgae as a novel source of food ingredients. The amount of several microalgae protein isolates required to produce stable O/W emulsions is found to be in the range of other protein sources such as dairy, egg, and legumes<sup>96</sup>. Other studies show that emulsions stabilized with protein hydrolysates from *Chlorella protothecoides* are prone to flocculate, however, they are stable against coalescence at protein concentration above 3% (w/w)<sup>76</sup>. Moreover, emulsions stabilized with proteins extracted from *Chlorella sorokiniana* and *Phaeodactylum tricornutum* remained stable at high salt concentration (up to 500 mM NaCl) and in addition to that the one stabilized with *Chlorella sorokiniana* showed high stability at pH>5<sup>77</sup>.

#### 1.2.5 Sustainability of insect proteins

According to the United Nations, the world population is rapidly increasing and is estimated to reach around 9.8 billion by 2050, while the food demand is expected to double<sup>97,98</sup>. This will inevitably lead to agricultural expansion and productivity growth, which in turn will over-pressure natural resources with increasing deforestation, greenhouse gas (GHG) emissions, and water consumption. Thus, alternative solutions to conventional livestock and feed sources are essential to cover the rise in protein and caloric food demands. Hence, it is necessary to pursue more sustainable production technologies for the conventional proteins and to start rebalancing the contributions between animal and plant proteins (or other alternatives), thus backing the sustainability of food systems, biodiversity, and eventually, a more efficient distribution of high-quality proteins for the entire world population.

Using edible insects as food has drawn great attention in the last decade. The Food and Agriculture Organization (FAO) department from the United Nation has claimed that edible insects are a good source of protein for dietary<sup>98</sup>. Likewise, other organizations such as the International Platform of Insects for Food and Feed (IPIFF), Insect Protein Association of Australia (IPAA), Asian Food and Feed Insect Association (AFFIA), and African Association of Insect Scientists (AAIS) are promoting the use of insects as food, feed and in other applications. However, insects are probably one of the most controversial alternatives to animal protein sources because it conflicts with cultural

habits in some populations. Most European and north American countries without entomophagy (habit of eating insects) tradition, are highly reluctant to consume edible insects as a result of distaste and disgust about their nature and appearance<sup>99-101</sup>. Conversely, it is reported that more than 2 billion of people worldwide are consuming edible insects, and entomophagy is a tradition in some countries in Africa (e.g., Cameroon, Congo, Kenya), southeast Asia (e.g., China, Thailand, Philippine) and Latin America (e.g., Mexico, Peru, Ecuador)<sup>98</sup>. It was suggested that incorporating insects in a masked way could enhance the consumer's acceptance<sup>102-104</sup>, which encouraged the application of edible insects in forms of milled powder and paste. Their use in pastas, tortilla chips, rusks, and breads were assessed in terms of nutritional value and structural and sensory features<sup>105-109</sup>, and several modern cookbooks with recipes using insects are also available<sup>110-112</sup>. The optimistic prospect of edible insects as a sustainable alternative lies on their values and contributions in nutritional, environmental, and economic aspects.

### Nutritional aspects

Chen et al.<sup>113</sup> summarized the chemical composition of nearly 100 insect species, they contain 20-70% of protein, 10-59% of lipids of which 26-82% are unsaturated fatty acids, and 2-10% of carbohydrate in dry matter weight. Among the reported values, insects from Orthoptera order such as cricket (*Grylodes sigillatus*) and grasshopper (*Schistocerca gregaria*) contain relatively high protein fraction (55-76%)<sup>65,67,114</sup> that is higher than wheat (11%), quinoa (12-18%), peas and beans (17-35%), soybean (52%), and it is comparable to those of beef and pork (40-75%), poultry (69%), and fish (71%) (Figure 1.6)<sup>114-116</sup>. Apart from macronutrients, insects are also a rich source of micronutrients such as minerals (iron, magnesium, calcium, and zinc) and vitamins (vitamin A, B<sub>2</sub>, and C)<sup>114,117</sup>.

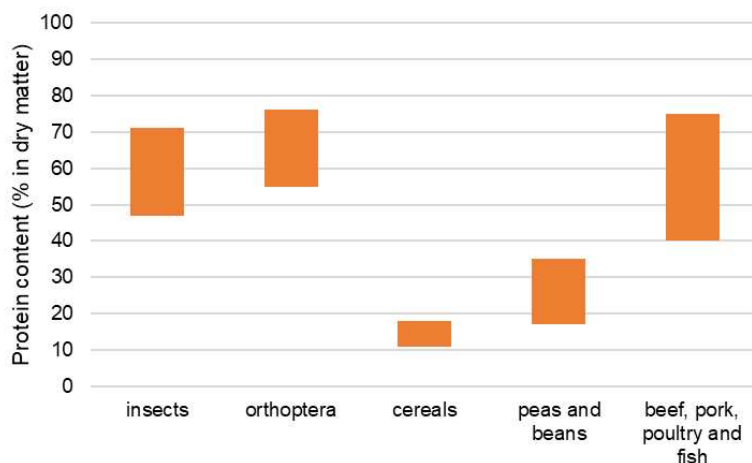


Figure 1.6. Protein content of insects (in general and from orthoptera order), compared to plants (cereals, peas and beans), and animal sources (beef, pork, poultry, and fish)<sup>90,113,114,116</sup>.

## Environmental aspects

As depicted in Figure 1.7, insect rearing has significant advantages over traditional livestock farming approaches in terms of the amount of land use, feed requirements, and water consumption. The reason why insects need less resources is because of their great feed conversion factor. The rapid growth rate and short closed life cycle make them to reproduce fast. In addition, it is not necessary to offer many land areas for their activities, and they can be easily reared in a vertically developed space. Therefore, insects have less impact on deforestation and soil fertility reduction, which may partially replace agriculture to alleviate the burden on ecosystem. The relatively less water footprint can help reducing water pollution.

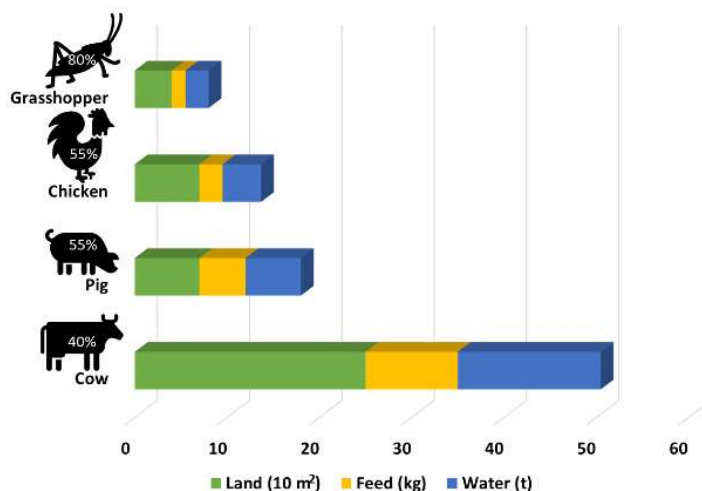


Figure 1.7. Required amount of land, feed and water for producing 1 kg of live animal weight<sup>119</sup>. The presented percentages are the corresponding edible portion.

Cutting back GHG emissions and reduce energy consumption are the fast approaches towards slowing down global warming. As can be seen from Figure 1.8, mealworm rearing has significantly less global warming potential than conventional animal husbandry as well the milk production<sup>120</sup>. In addition, it has been reported that ammonia and methane emissions were also much lower for insects than for breeding cows, pork, and poultry<sup>91,115</sup>. By contrast, on account of the poikilothermic nature of insects, a moderate amount of energy consumption is demanded for temperature control to optimize insects rearing<sup>115,120</sup>.

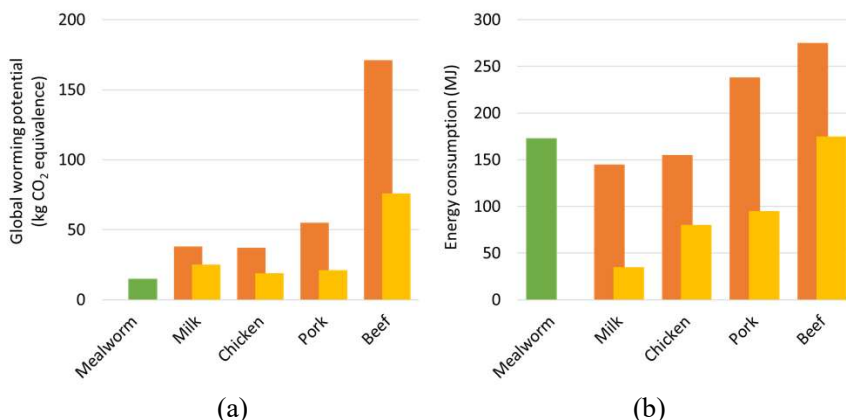


Figure 1.8. Global warming potential (GHG emission in CO<sub>2</sub> equivalence) (a), and energy used for producing one kg of edible protein (b)<sup>120</sup>. Orange and yellow bar indicates maximum and minimum values respectively.

### Economic aspects

The above-mentioned advantages of insect rearing associated to nutrition and environmental impact are reinforced by the economic aspects. On account of the high feed conversion factor exhibited by insects, a cost-effective and ecologic way of rearing insects is to transform organic waste into insect body mass. Using waste streams (e.g., kitchen waste, agricultural waste, agri-food by-products) as feed, insects can convert them into valuable macronutrients (e.g., proteins, unsaturated fatty acids, fibres) and micronutrients (e.g., minerals and vitamins). Hence, insect rearing is completely aligned with circular economy, as depicted in Figure 1.9.

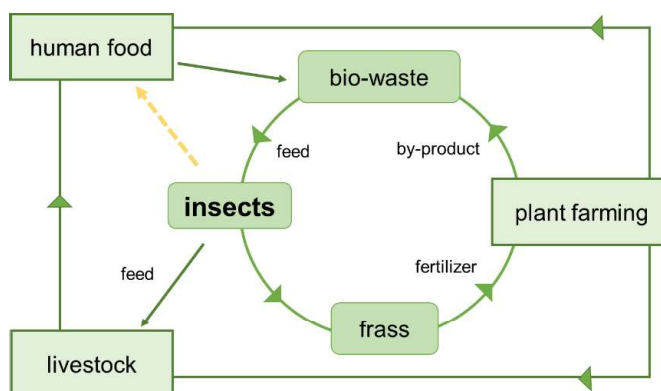


Figure 1.9. Circular economy involving insects rearing.

However, insect economy has not broadened up as expected due to the concerns in food safety. In the Codex Alimentarius, which represents international food standards, insects are only referred to as “impurities” at this stage. Regulations strongly differ from country to country and most western countries do not even specifically address insects.

This non-standardized legal status across the world represents the biggest hurdle for the edible insect industry since it hinders or slows the growth of a global edible insect market<sup>121</sup>. The microbiological contamination, toxicological hazards and allergenic reactions are supposed to be strictly revised in advance of introducing the legislation<sup>91,115</sup>. In Europe-wide, the novel food regulation came into effect since 2018 based on European Food Safety Authority (EFSA) which opened door for edible insects to be used in food applications, and the safety assessment on the dried yellow mealworm, frozen, dried and ground house cricket and migratory locust was reported in 2021 stating that there are no concerns on their stability and toxicity issue<sup>122–124</sup>.

### 1.3 Emulsion-based encapsulation technologies

#### 1.3.1 Membrane/microporous emulsification technologies

Conventional manufacturing processes to produce emulsions encompass high-pressure homogenizers, rotor-stator systems and colloid mills<sup>125</sup>. These techniques rely on high shear/inertia stress and/or cavitation to deform an interface and to generate droplets. Even though they can produce droplets with small particle size, they may have relatively wide droplet size distribution<sup>126</sup>. The drawbacks of conventional emulsification processes are the high energy consumption, damage of shear sensitive molecules, and decomposition of thermo labile ingredients. With the aim of producing emulsions with a narrow droplet size distribution applying a low energy input compared to that required by conventional technologies, membrane emulsification (ME) was firstly introduced in the early 1990s by Nakashima and coworkers<sup>127</sup>. In the late 1990s, Suzuki et al.<sup>128</sup> used premix ME to obtain higher production rates, while Nakashima and co-workers developed microchannel emulsification as an alternative to ME technology to better control droplet formation and, in turn, produce monodisperse emulsions<sup>129</sup>. Techniques for membrane emulsification may be classified into two groups (Figure 1.10): direct (or cross-flow) ME, in which a dispersed phase is injected through the membrane into the continuous phase where the formed droplets are collected, and premix ME, in which a coarse emulsion is pressed through the membrane to reduce the droplet size. In both systems, the membrane is the microporous structure responsible for droplet formation or further breakup. Importantly, the membrane has to be wetted by the continuous phase, hence to produce O/W emulsions a hydrophilic membrane it is required<sup>126,130–132</sup>.

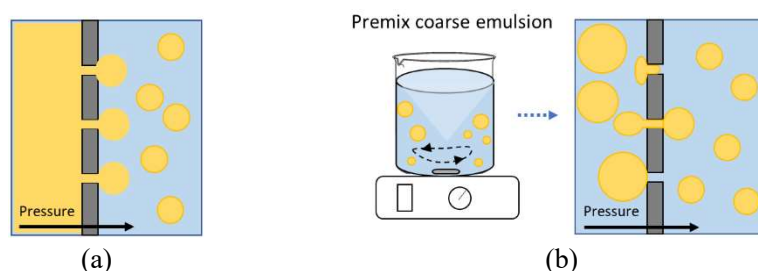


Figure 1.10. Schematic examples of (a) direct ME and (b) premix ME.

Membranes used for emulsification can be made of (i) glass materials, such as borosilicate, shirasu porous glass (SPG), microporous glass (MPG), and ceramic; (ii) polymers, such as polycarbonate, polyethersulfone (PES), cellulose mixed esters (MCE), cellulose acetate (CA), and nylon; (iii) metal, such as nickel sieve and stainless steel mesh; (iv) syringe filters composed of borosilicate glass fibres, polyethersulfone, nylon, cellulose acetate and cellulose ester<sup>131</sup>.

Direct ME is carried out by pushing the dispersed phase through membrane pores at a controlled injection rate. To detach the droplets which are formed at the membrane surface, some shear stress is applied. Usually, a flow of the continuous phase over the membrane surface provides a tangential shear that induces droplet snap-off. Droplet size can be controlled according to the characteristics of membrane, the cross-flow velocity, and the transmembrane pressure.

Premix ME is an emulsification process to refine coarse emulsions that are usually prepared by mechanical means and have a big droplet size and a wide size distribution. After the coarse emulsion is produced, refinement takes place by passing through the membrane by applying pressure. Usually 3-5 passes (cycles) are carried out in order to yield small droplet size and narrow size distribution. The process is widely used for high-throughput production of sized-controlled emulsion droplets and microparticles using low energy inputs<sup>131</sup>. Parameters such as membrane wettability, mean size of the membrane pores, oil-in-water interfacial tension, disperse phase viscosity, and hydraulic membrane resistance determine the transmembrane pressure required to successfully breakup droplets.

Both ME methods are low-energy compared to conventional methods, resulting in uniform droplet size using less surfactant, and they can be considered for scaling-up. Direct ME is limited by the relatively low flux of the dispersed phase, which might need to be recirculated to attain a high fraction of the dispersed phase in the emulsion. It also requires a large membrane area to increase the efficiency, which makes it relatively expensive to scale-up. Premix ME, in turn, can produce emulsions with higher disperse phase fraction and throughput than direct ME. However, membrane fouling can be of concern depending on the interaction between the emulsion components and the membrane, and membrane cleaning has to be considered.

### 1.3.2 Premix emulsification with dynamic membranes of tunable pore size (DMTS)

As an alternative to overcome membrane fouling and to increase productivity during premix ME, dynamic membranes of tunable pore size (DMTS), consisting of a layer or bed of micron-size silica beads supported by a nickel microsieve (Figure 1.11), was firstly developed by van der Zwan et al.<sup>133</sup>. It is called 'dynamic membrane' since it can be taken apart, easily cleaned and reused. Besides, this system can adjust the pore size of the membrane by placing silica microbeads of different sizes. Nazir and coworkers<sup>134</sup> stated that the layer of micron-size silica beads consists of interconnected interstitial voids that can be seen as organized asymmetric capillaries following an irregular path through the silica microbeads bed, which is comparable to conventional membranes pores.

In premix emulsification with DMTS, a coarse premix emulsion, produced by mechanical dispersion units, such as a magnetic stirrer and/or Ultra-Turrax, is subsequently transferred into the DMTS vessel and pressurized to pass through the dynamic membrane in the module. The droplets are disrupted while being pushed through the micro-channels within the bed. In this process, emulsion droplets are refined, and the new formed interfaces are stabilized by the emulsifiers present.

The main operating parameters to be controlled in premix emulsification with DMTS are microbead size and bed height (which determine the interstitial void diameter and the channel tortuosity), microbeads wettability, transmembrane pressure, and number of refining cycles. Besides, other properties related to the emulsion, such as viscosity ratio of the two emulsion phases or dynamic interfacial tension strongly affect the system performance.

The most commonly used silica microbead size in DMTS emulsification systems varies between 30  $\mu\text{m}$  and 99  $\mu\text{m}$ <sup>135,136</sup>. According to the microbead size and its porosity, the resulting interstitial void diameter is in the range of 13  $\mu\text{m}$  and 58  $\mu\text{m}$ . In addition, a dynamic membrane made of multilayers having different interstitial void diameters can be assembled by sequentially placing silica microbeads of different sizes. This arrangement, referred as 'layering' (Figure 1.11), was investigated for the first time by Kaade and coworkers<sup>136</sup>. The emulsions refined by the 'layering' setup take benefits from both sizes of microbeads, which leads to smaller droplet size with a narrower distribution.

Single emulsions (O/W) and double emulsions (W/O/W) with aqueous solution as continuous phase can be successfully refined using premix emulsification with DMTS, owing to the hydrophilic nature of the silica microbeads. However, it is also possible to prepare W/O emulsions once the microbeads are modified to have a hydrophobic surface by undergoing a hydrophobization process with organo-silane (mostly silane of C<sub>2</sub> to C<sub>20</sub>) coatings<sup>137</sup>.

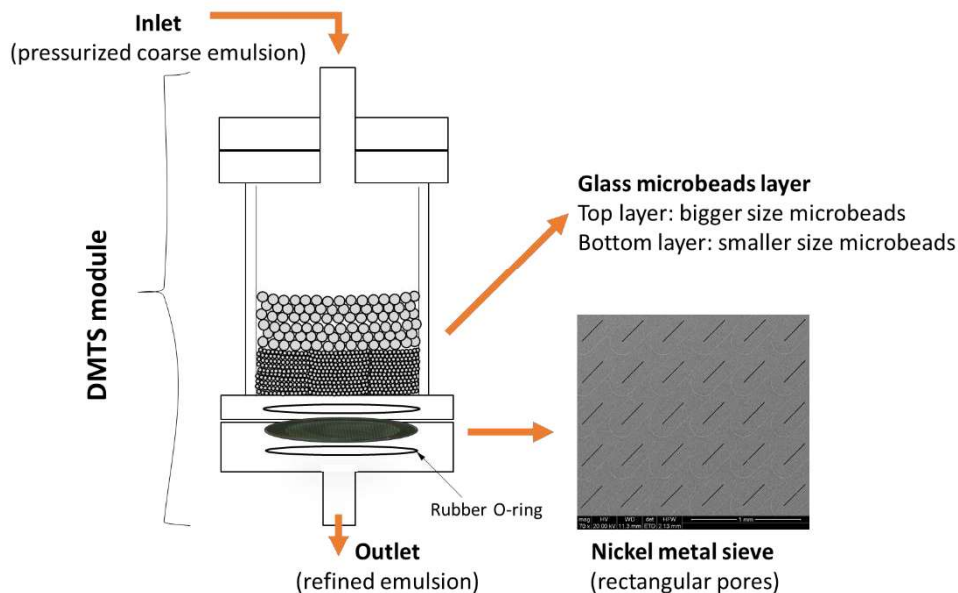


Figure 1.11. Schematic representation of the DMTS setup with the different microporous layers.

In addition to the advantages of disintegration and easy cleaning, the DMTS system is also capable to produce emulsions with controlled droplet size distribution with high productivity, enabling straightforward scaling up.

Droplet size and droplet size distribution are controlled by various operation parameters such as microbead size, height of bed layer, transmembrane pressure, number of emulsification cycles, and emulsion formulation. In general, when applying a low pressure (e.g., 200 kPa) in a thin bed layer (e.g., 2-2.5 mm), smaller droplet size is obtained from smaller beads due to a narrower interstitial void<sup>134,135</sup>. While when the applied pressure increases to 450 kPa, bigger beads are more efficient in breaking up droplets compared to smaller beads on account of higher shear stress, even though a narrower droplet size distribution is achieved with smaller beads<sup>136</sup>. By combining the benefits of using two different bead sizes ('layering'), the emulsion can be refined to have the target droplet size and a narrow size distribution<sup>136</sup>. As for the impact of the height of bed layer, it is more acute to tune the final droplet size distribution. In general, at a certain applied pressure and bead size, increasing the height of bed layer reduces the droplet size distribution, while there is an optimal height beyond which no more improvement is seen<sup>133,134</sup> since droplet coalescence might happen when the refined droplets are passing through a long channel (thicker bed), increasing droplet size distribution<sup>135,136</sup>. In premix ME in general and in DMTS systems in particular, transmembrane pressure is partially dedicated to droplet breakup and the other part to overcome the resistance from the bed layer of tortuous microchannels. Therefore, in a certain DMTS system, the higher pressure applied, the smaller droplet size is obtained attributed to the increased shear stress. In the most cases, 3-5 emulsification cycles are chosen, due to the main droplet breakup takes place during the first emulsification cycle, after which droplet size and

distribution are decreased limitedly, moreover, the further increase in the number of emulsification cycle may lead to droplet coalescence in the channel and a bigger span<sup>133</sup>. Besides, an enhanced processing temperature may result in a smaller droplet size due to the enhanced flow rate<sup>138</sup>.

The three major droplet breakup mechanisms observed by van der Zwan et al.<sup>139</sup> using direct visual observation are (Figure 1.12):

- **Snap-off due to localized shear forces.** It mainly occurs at pore inlets, pore outlets and pore junctions where large droplets breakup into small droplets by the shear of the continuous phase flow.
- **Breakup due to interfacial tension effects such as Laplace and Rayleigh instabilities.** Elongated and deformed droplets in a constriction or a channel are in a destabilized state at the interface due to Laplace and Rayleigh instabilities, which induce droplets breakup accompanied with the shear flow.
- **Breakup due to steric hindrance between droplets.** The accumulated droplets before the membrane or inside the channels can affect each other and induce droplet breakup.

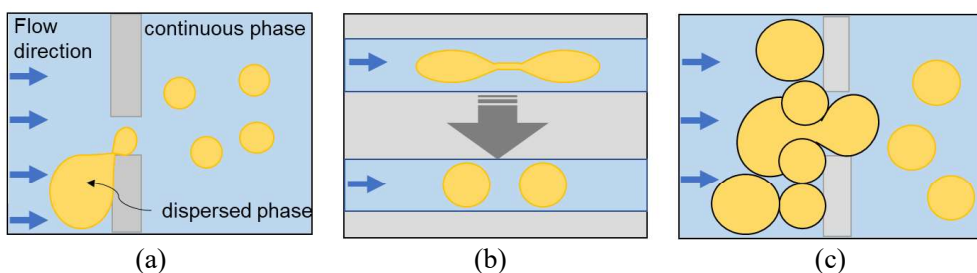


Figure 1.12. Schematic diagram of three main droplet breakup mechanism in premix emulsification. (a) Snap-off due to localized shear forces, (b) Breakup due to interfacial tension effects, and (c) Breakup due to steric hindrance between droplets.

One or several types of droplet breakup can take place simultaneously in the DMTS system. Due to a great variety of porous media (e.g., straight-through pores, tortuous interconnected pores and length of the channel) and the operating conditions (e.g., pressure and viscosity of emulsions). To model and characterise the process, several dimensionless numbers have been used to describe flow behaviour and droplet breakup as listed in table 1.6<sup>131</sup>. These parameters are also applied in the scaling relations of the system.

Table 1.6. List of dimensionless numbers used to describe flow and droplet breakup.

Dimensionless number	Expression	Description
Reynolds number	$Re = \frac{\rho_c u d_p}{\eta_c}$	A ratio of inertial to viscous forces in pores. Characterization of flow properties.
Weber number	$We = \frac{\rho_c u^2 d_d}{\sigma}$	A ratio of inertial to interfacial forces acting on a droplet. Identifying stable and unstable or disrupting droplet regime
Capillary number	$Ca = \frac{\eta_d u}{\sigma}$	A ratio of viscous to interfacial forces. Relating the viscous forces to deform droplets with the Laplace pressure that resist the deformation.
Ohnesorge number	$Oh = \frac{\sqrt{We}}{Re}$	Ohnesorge number relates all the major forces (i.e., inertial, viscous, interfacial) involved in droplet disruption.
Pressure ratio	$\hat{p} = \frac{\Delta p d_d}{\sigma}$	A ratio of transmembrane pressure to the droplet Laplace pressure. Relating the applied energy to the minimum amount of energy needed to deform the droplet.

Where  $\rho_c$  is the density of continuous (or emulsion) phase;  $u$  is the pore villosity;  $d_p$  is the particle size;  $d_d$  is the pore diameter;  $\eta_c$  is the viscosity of continuous (emulsion) phase;  $\eta_d$  is the viscosity of dispersed phase, and  $\sigma$  is interfacial tension.

Empirical scaling relations were developed by some researchers to predict the final droplet size based on the operational parameters (eq 1.8). The models are all based on the relationship established by taking into consideration of the effects of the bead size, the height of bed layer, and the energy density. It was demonstrated a good fit between experimental and estimated values<sup>133,134,140</sup>, which shows the potential to tune the DMTS parameters in order to obtain a desired droplet size.

$$d_{3,2} = \alpha E_v^{-\beta} N \gamma \left(\frac{H}{d_p}\right)^\delta \quad \text{eq (1.8)}$$

$d_{3,2}$  is the Sauter mean diameter predicted from the equation;  $E_v$  is the energy density, calculated from the ratio of power input to volumetric flow rate of emulsion;  $N$  is number of passes through the membrane;  $H$  is the height of bed layer;  $d_p$  is the particle size of the silica microbeads;  $\alpha, \beta, \gamma$ , and  $\delta$  are fitting parameters that depend on the type of premix ME system.

Table 1.7. Summary of DMTS emulsification results reported in the literature.

Emulsion type	Emulsifier	Oil	Pressure (kPa)
O/W	Tween 20	Hexadecane 5%	50-500
O/W	Tween 20 SDS CTAB	Hexadecane 5% (paraffin dissolved)	300
O/W	Tween 20	Precirol 6.5% with vitamin E 0.5%	50-500
O/W	Poly lactide	Decane	100-400
O/W	Tween 20	Lemon oil 20-40%	450
O/W	Pea protein chickpea protein lentil protein WPI	Sunflower oil 10%	300
G/W <sup>a</sup>	WPI	Nitrogen	100-500
W <sub>1</sub> /O/W <sub>2</sub>	PGPR <sup>b</sup> Tween 20	Sunflower oil 5.6%	200-600
W <sub>1</sub> /O/W <sub>2</sub>	PGPR <sup>b</sup> WPI	Sunflower oil 32%	200-500

a gas-in-water (foam).

b PGPR was used as lipophilic surfactant for stabilizing W<sub>1</sub>/O primary emulsion.

c computed values from reported data of  $d_{3,2}$  and  $d_v$ .

d values were displayed as mass flow rate.

Bead size ( $\mu\text{m}$ )	Height of bed layer (mm)	Ratio ( $d_{3,2}/d_v$ )	Flux ( $\text{m}^3\text{m}^{-2}\text{h}^{-1}$ )	Encapsulation efficiency	Ref.
55-90	1-20	0.2-0.6	30-768		133,134
55	2.5	0.05-0.35	0-500		140
30-90	1-5	0.05-1.15 <sup>c</sup>	3.1-32.2 g/s <sup>d</sup>		138
30-90	2-20	0.1-0.3	50-1000		135
42-99	2-9	0.03-0.1	200-1200		136
71	2		100		142
65	2.5		10-70		143
30-65	2-40	0.2-0.8	200-800	91-99% of NaCl	144
71	2		1-65	75-100% of beet root juice	141

The productivity of the emulsification process can be evaluated from the transmembrane flux, which depends on the operation conditions of the DMTS system (bead size, height of bed layer, transmembrane pressure, and emulsion formulation). In general, smaller beads and thicker bed layer lead to lower transmembrane flux due to more resistance produced by a narrower interstitial void and longer tortuous microchannels. Therefore, with a higher pressure, a higher flux is obtained on account of more energy invested in flowing the emulsions through the system. Apart from the dynamic membrane resistance, the formulation of the emulsion highly affects the transmembrane flux<sup>140</sup>. The more viscous the emulsion, the stronger resistance against deforming, which leads to a lower flux. Anionic and nonionic surfactants were suggested for DMTS systems to decrease the interaction between the negatively charged silica microbeads and the surfactant<sup>140</sup>. Tuning the operating conditions (2.2 mm height, 99  $\mu\text{m}$  beads, pressure of 450 kPa) a transmembrane flux of 1200  $\text{m}^3\text{m}^{-2}\text{h}^{-1}$  was reported during the production of 20 wt% lemon oil-in-water emulsions stabilized with Tween 20<sup>136</sup>. However, membrane fouling is a critical issue reducing the productivity of the system. It is considered that the use of high molecular weight emulsifiers, such as proteins, would tend to foul the membrane/microporous system. A decrease in transmembrane flux was observed during the emulsification of single and double emulsions stabilized with proteins as the number of emulsification cycles increased<sup>141,142</sup>. Even though fouling cannot be pointed out as the sole cause of flux reduction, since the physical properties of emulsion also change during refinement<sup>142</sup>. The DMTS system has been also used in a wide range of applications such as the formulation of solid lipid particles<sup>138</sup>, encapsulation of colorant<sup>141</sup> and even to produce nitrogen foams (gas-in-water emulsion)<sup>143</sup>.

Based on the above mentioned, the DMTS system has proven the robustness and versatility for producing emulsions with controlled droplet size distribution and high productivity, as well as it is a promising technique to scale up for industrial applications. In the lab-scale production, Laouini et al.<sup>137</sup> increased the production amount to 800 g of emulsions (O/W stabilized with 1.8 wt% Tween 80), successfully refining the emulsion and with no fouling during the process. Therefore, the scaling up of DMTS system can be achieved relatively easily compared to other conventional membranes (e.g. ceramic membranes) for which manufacturing bigger membranes with larger surface area is required. For the DMTS, scale-up can be operated by increasing the input emulsion volume and/or increase the membrane area by easily increasing the amount of silica microbeads and the diameter of the module. Table 1.7 summarizes the result from the reported literature employing premix ME with DMTS system to refine emulsions.

### 1.3.3 Production of emulsion-based solid microcapsules

Solid microcapsules can be produced from single and multiple emulsions by removing the water fraction. Since emulsions are thermodynamically unstable systems, preserving encapsulates in a solid matrix is a way to immobilize the encapsulates, to prolong the shelf-life, and to simplify the transportation, moreover, emulsions can be reconstituted easily after rehydration. Spray drying and freeze drying are the most common techniques applied for food and feed applications.

## Spray drying

Spray drying is the oldest and the most widely used technique to obtain emulsion-based microcapsules in food applications. The drying process is based on the atomization of a liquid feed that contacts with a hot drying air steam. The technique comprises of three steps: (i) atomization of the feed (ii) drying of the feed solution by a hot gas carrier to achieve the evaporation of the solvent, (iii) collection of dry particles by cyclones or a filter (Figure 1.13). In detail, the feed liquid is injected into the drying vessel through a nozzle or an atomizer in order to obtain small droplets followed by the evaporation of the solvent, then, these dried particles are separated from the drying gas by a cyclone or filter<sup>145,146</sup>.

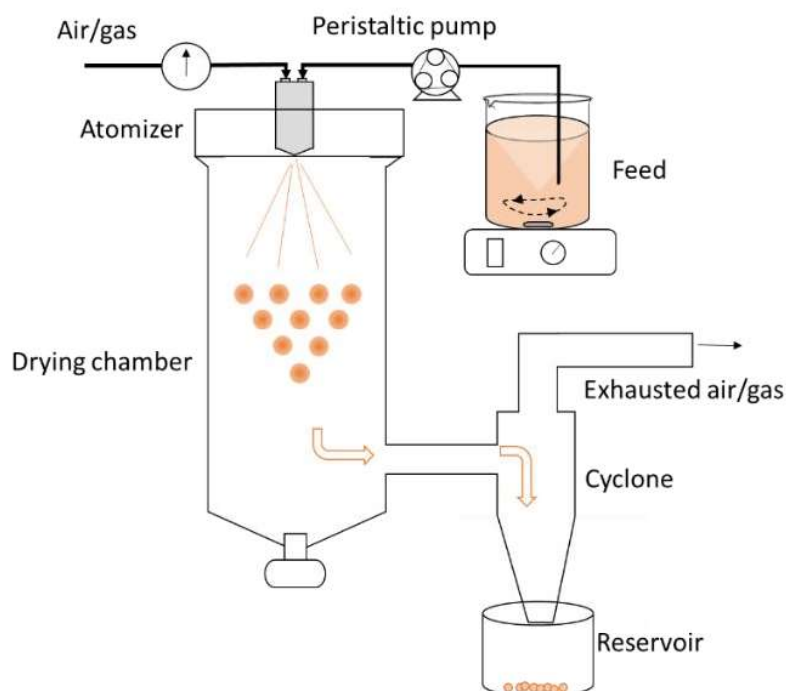


Figure 1.13. Schematic illustration of spray drying process.

As for the processing conditions, several critical parameters determine the quality of produced solid microcapsules and the production yield, they are inlet and outlet temperature, atomization pressure, feed flow rate, drying air flow rate and aspirator rate. The overall processing parameters depends on the composition, concentration and viscosity of the feed. The outlet temperature is tuned through the adjustment of other parameters. As for the inlet and outlet temperature, if it was too low, the water would not be evaporated completely in short time resulting in wet powders and low yield, if it was too high, the cracking of the microcapsules would occur<sup>146</sup>. Due to the presence of many variables, spray drying an emulsion-based system should be optimized in order to produce desired solid microcapsules with high quality and production yield.

Table 1.8. Summary of the microcapsules produced by spray drying from single or multiple emulsions reported in literature.

<b>Emulsion type</b>	<b>Encapsulated compound</b>	<b>Oil phase</b>
O/W	Carotenoids, Phenolics	Corn oil, Sunflower oil, Safflower oil
O/W	$\beta$ -carotene	Sunflower oil, Monoglyceride
O/W	$\beta$ -carotene	Vegetable oil
O/W	Citral	Citral
O/W	Fish oil	Fish oil
O/W	Fish oil	Fish oil
O/W	Rapeseed oil	Rapeseed oil
O/W	Annatto seed oil	Annatto seed oil
O/W	Drumstick oil	Drumstick oil
O/W	Corn oil	Corn oil
O/W	Krill oil	Krill oil
W <sub>1</sub> /O/W <sub>2</sub>	Procianidin	Sunflower oil
W <sub>1</sub> /O/W <sub>2</sub>	Anthocyanin extract	Rice bran oil
W <sub>1</sub> /O/W <sub>2</sub>	Phenolic extract	Soybean oil
W <sub>1</sub> /O/W <sub>2</sub>	Phenolic extract	Sunflower oil
W <sub>1</sub> /O/W <sub>2</sub>	Phenolic extract	Canola oil
W <sub>1</sub> /O/W <sub>2</sub>	Folic acid	Canola oil
W <sub>1</sub> /O/W <sub>2</sub>	Saffron	Sunflower oil
W <sub>1</sub> /O/W <sub>2</sub>	Carotenoids	Sunflower oil, Canolo cartamin oils
O <sub>1</sub> /W <sub>1</sub> /O <sub>2</sub> /W <sub>2</sub>	Orange oil (O <sub>1</sub> )	Vegetable oil (O <sub>2</sub> )

Wall material	Emulsification method	Temperature (inlet/outlet, °C)	Ref.
GA, MD	Rotor-stator	160/70	154
WPI, MD, Konjac glucomannan	Homogenizer	185/85	3
Casein, MD	Microfluidizer	100-120/60	155
Sucrose, Trehalose, MD, Modified starch	Blender	175/83	150
SPI	Rotor-stator Homogenizer	180/90	153
MD	Premix nylon and MCE membrane	190/90	151,152
PPI, Pea protein hydrolysate Glucose syrup	Homogenizer	180/70	53
GA	Ultrasound	170/--	157
MD, GA, WPC	Homogenizer	180/85	158
Brea gum, GA, Inulin	Ultrasound	150/60	159
WPC, MD, GA	Microfluidizer	130/71-75	160
WPI, MD, CMC, GA, Chitosan	Premix SPG membrane	170/80-90	149
Limed bone gelatin, CMC, MD Acacia hum, Chitosan	Rotor-stator	180/80-90	161
GA, MD, Alginate	Homogenizer	180/90	162
WPI, MD	Microfluidizer	175/90	163
WPI	Rotor-stator	160-180/70-80	156
Pectin, WPC, MD	Homogenizer	180/90	164
WPC, MD, Pectin	Homogenizer	140/90	165
GA, MD, Mesquite gum	Homogenizer	170/80	166
Lactose monohydrate Sodium caseinate	Rotor-stator	180/79-80	167

In general, the solid microcapsules fabricated via spray drying have a spherical shape with a smooth surface and a hollow structure. Vacuole formation originates from a shrinking process that occurs after the hardening of the outer surface is followed by expansion of air bubbles trapped inside the droplet<sup>146</sup>. Encapsulated compounds are incorporated inside of the shell matrix formed by wall materials or on the surface (inner and outer) of the particle. In other cases, the microcapsules may have irregular shape, dented surface or porous structure depending on the materials used and the processing parameters.

Emulsions can be reconstituted after dispersing the solid microcapsules in aqueous medium. In this way, the solid microcapsules fabricated by spray drying can not only protect the active compounds and extend the shelf-life, but also maintain the structure after rehydration which still keeps the role as an emulsion-based delivery carrier. However, the reconstituted emulsions were reported to have a bigger droplet size distribution compared to the original emulsions due to the heat during the spray drying process might rupture the interfacial layer, which led to some extent of droplet coalescence when redispersing them<sup>3,147,148</sup>. Hence, the impact of such a change in the reconstituted emulsions on the digestion and bioavailability of bioactive nutrients is worth evaluating based on individual formulation and application.

Table 1.8 listed some emulsion-based microcapsules produced by spray drying. As can be seen from Table 1.8, solid microcapsules were produced from single and multiple emulsions, including the encapsulation of essential oils such as citral<sup>150</sup> and fish oil<sup>151-153</sup>, and nutritional compounds such as  $\beta$ -carotene<sup>3,154,155</sup> were in O/W emulsions, and the encapsulation of water soluble bioactive compounds such as polyphenols in the inner water phase ( $W_1$ ) of double emulsions ( $W_1/O/W_2$ ). It worth highlighting that some studies also combined the premix membrane emulsification (premix ME) methods using nylon, mixed cellulose ester (MCE)<sup>151,152</sup> and SPG membranes<sup>149</sup> for the production of emulsions. As shown in Table 1.8, commonly used wall materials are polysaccharides such as maltodextrin (MD) with different dextrose equivalent values, Arabic gum (GA), and carboxyl methylcellulose (CMC). In some cases, the additional wall materials may be not required such as using high protein concentration, e.g., 10% whey protein isolate (WPI) was used as emulsifier as well as wall material<sup>156</sup>.

## Freeze drying

Freeze drying is also known as lyophilization which is a multi-stage process that consists of: (i) freezing, (ii) primary drying and (iii) secondary drying<sup>168</sup>. As a first step, the sample is frozen at a sufficient low temperature which can be achieved using liquid nitrogen, in a separate freezer or in the freeze-dryer itself. Next, as depicted in Figure 1.14, the primary drying begins when the pressure is lowered to values below the vapor pressure of ice and the temperature of the plate increases in order to supply the latent heat removed by ice sublimation. Thereafter, an open network of pores is formed due to the sublimation of the ice crystals, which provide a pathway for desorption of water from the sample during the secondary drying, when the shelf temperature is increased and the chamber pressure is reduced in order to remove liquid water.

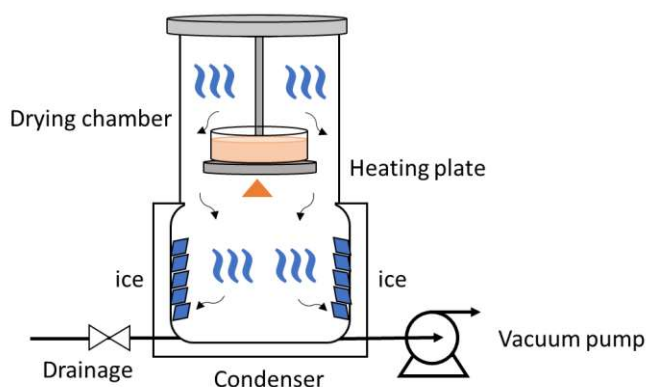


Figure 1.14 Schematic illustration of freeze drying process.

As listed in Table 1.9, essential oils such as cardamon oil<sup>169</sup> and limonene<sup>170</sup>, and nutritious vitamins such as  $\beta$ -carotene<sup>3,155,171</sup> and  $\alpha$ -tocopherol<sup>172</sup> were encapsulated in the O/W emulsions and polyphenols<sup>161,173</sup> were protected in  $W_1/O/W_2$  emulsions. The most applied emulsification methods paired with freeze drying are high pressure homogenization and ultrasound homogenization. As for freeze drying, not only wall materials are important for building the matrix, but also the use of cryoprotectant. As can be seen in Table 1.9, sucrose, trehalose, maltodextrin and gam arabic were mostly used as cryoprotectants to improve freeze-thaw stability of food emulsions. The presence of sugars can decrease the freezing temperature of water and increase the amount of unfrozen water available to disperse the oil droplets, as well as they can be a spacing matter between droplets which behaves as barrier to inhibit droplet merging. In concentrated sugar solutions, the emulsion droplets do not come into close contact with each other in the unfrozen glassy solution between ice crystals<sup>174</sup>.

Table 1.9. Summary of the microcapsules produced by freeze drying from single or multiple emulsions reported in literature.

<b>Emulsion type</b>	<b>Encapsulated compound</b>	<b>Oil phase</b>
O/W	$\alpha$ -tocopherol	Canola oil, Coconut oil
O/W	$\beta$ -carotene	Sunflower oil
O/W	$\beta$ -carotene	Soybean oil
O/W	$\beta$ -carotene	Vegetable oil
O/W	Capsaicinoids	Capsaicinoids
O/W	Limonene	Limonene
O/W	Cardamon essential oil	Cardamon essential oil
O/W	Curcumin	Olive oil
O/W	Krill oil	Krill oil
O/W	Flaxseed oil	Flaxseed oil
O/W	Annatto seed oil	Annatto seed oil
O/W	ID93 protein	Squalene
O/W	Calcein, 5-fluorouracil, Flurbiprofen	Phospholipids Cyclohexane
W <sub>1</sub> /O/W <sub>2</sub>	Anthocyanin extracts	Rice bran oil
W <sub>1</sub> /O/W <sub>2</sub>	Anthocyanins	Soybean oil
W <sub>1</sub> /O/W <sub>2</sub>	Black chokeberry pomace extract	Rapeseed oil
W <sub>1</sub> /O/W <sub>2</sub>	Topotecan	Cyclohexane, Chloroform
W <sub>1</sub> /O/W <sub>2</sub>	Xylitol	Corn oil, Menthol
W <sub>1</sub> /O/W <sub>2</sub>	not mentioned	Not mentioned

<b>Wall material/Cryoprotectant</b>	<b>Emulsification method</b>	<b>Ref.</b>
WPI, Ora-pro-nobis mucilage	Homogenizer	172
WPI, MD, Konjac glucomannan	Homogenizer	3
Sodium caseinate, MD, GA	Microfluidizer	171
MD, Casein	Microfluidizer	155
Modified starch	Ultrasound	175
GA, Gelatin, sucrose	Homogenizer	170
WPI, Guar gum, carrageen	Ultrasound	169
Sodium alginate, WPI	Ultrasound	176
WPC, MD, GA	Microfluidizer	160
WPI, MD, Sodium alginate	Sonication	177
GA	Ultrasound	157
Trehalose	Microfluidizer	178
Sucrose, Lactose, MD	Sonication	179
Limed bone gelatin, Acacia gum, Chitosan, CMC, MD	Rotor-stator Coacervation	161
Gelatin, GA	Rotor-stator, Coacervation	173
Milk protein concentrate	Homogenizer	180
Sucrose	Ultrasound	181
Gelatin, GA	Rotor-stator	182
Glucose, Trehalose, $\kappa$ -carrageenan, hydroxyethyl starch	Ethypharm's unique method	183

An acceptable freeze dried product should possess the same physical and chemical properties as the system before being submitted to the process, acceptable humidity, long-term stability and an elegant cake appearance<sup>168</sup>. Powders can be obtained after grinding. The freeze dried powder has a flake-like shape with smooth or folded surfaces depending on different formulas. Due to the sublimation of ice crystals, irregular and spongy porous microstructures can be observed. The encapsulates are immobilized in the matrix or exposed in the porous structure. Similar to the solid microcapsules fabricated by spray drying, freeze dried capsules can be rehydrated to reconstitute emulsions. The droplet size distribution may depend on the oil content, wall materials, and cryoprotectants used in the formulation. Smaller droplet size was observed in the reconstituted O/W emulsion encapsulating  $\beta$ -carotene<sup>3</sup>, which may be the result of the break-down of some large oil droplets during freezing as the formation of ice crystals. Whereas, the increase of droplet size distribution was reported in the reconstituted  $W_1/O/W_2$  emulsions encapsulating black chokeberry pomace extract stabilized by 14% milk protein in the absence of wall material, which was ascribed to the coalescence of oil droplets<sup>180</sup>. Unlike spray drying, using dairy protein alone as the wall building material is not sufficient to build a matrix for immobilizing large oil droplets. The same result was also observed by No et al.<sup>171</sup>. In their work, they found a larger droplet size distribution in the reconstituted O/W emulsions encapsulating  $\beta$ -carotene stabilized only by sodium caseinate without additional wall material. While when MD and GA were added in the system, droplet size distribution was improved.

Based on the above description, spray drying is a rapid, continuous, simple, economic, reproducible, and easy to scale up in comparison with other drying processes. However, the production yield is lower compared to freeze drying due to the residues of non-sufficiently dried particles remaining in the drying chamber. Besides, relatively high drying temperatures will damage thermal sensitive compounds such as polyphenols, vitamin C, colours, and flavours. Some limitations of wall materials such as polysaccharides has low water solubility, and sugar rich materials have low glass transition temperature lead to stickiness behaviour<sup>145,184</sup>. Freeze drying can reach very high (almost 100%) production yield without any loss during the drying process. The most significant advantage of freeze drying is that it is a simple process carried out at low temperature in the absence of air, resulting in prolonged and superior quality of products by preventing deterioration from oxidation or chemical modification. Freeze drying is the most suitable technique for dehydration of almost all heat sensitive active compounds as previously mentioned. However, freeze drying still has some drawbacks such as porous structure of freeze dried powders due to the ice sublimation<sup>145,146,184</sup>, and long process time (more than 20 h), besides, the high invest and operating costs in comparison to other techniques.

## 1.4 Objectives

The purpose of this work is to assess the use of both sustainable materials and technologies to produce emulsions and emulsion-based solid microcapsules as a means of encapsulation of ingredients for food applications. A low-energy high-throughput microporous emulsification system was aimed for the production of single and multiple emulsions, and the ability of proteins extracted from edible insects as an alternative emulsifier to whey protein is studied. These general goals can be achieved by accomplishing the following specific objectives:

- To assess the use of membrane-based processes to concentrate and encapsulate a carob polyphenol extract as a case study of pairing sustainable technologies for valorisation of food by-products.
- To design and implement extraction and characterization methodologies able to provide enriched protein fractions from edible insects, such as black soldier fly (*Hermetia illucens*) and lesser mealworm (*Alphitobius diaperinus*), with enhanced techno-functional properties.
- To assess the techno-functional properties of insect protein extracts, including solubility, isoelectric point (pI), water and oil binding capacity, foaming ability, emulsifying ability, and interfacial tension.
- To evaluate the emulsifying ability of insect protein extracts to stabilise food grade O/W emulsions produced by premix emulsification with dynamic membranes of tunable pore size and compare with dairy proteins.
- To analyse the potential of insect protein extracts to stabilise  $W_1/O/W_2$  emulsions, produced by premix emulsification with dynamic membranes of tunable pore size, to withstand various environmental stress (temperature, pH, and osmotic pressure unbalance) similarly to whey protein and pea protein.
- To investigate the effect of green solvents for insect meal defatting in the fatty acid profile of the lipid fraction and on the emulsifying ability of the resulting protein fraction.
- To explore the feasibility of producing emulsion-based solid microcapsules from O/W and  $W_1/O/W_2$  emulsions by spray drying and freeze drying stabilised with insect proteins as a means to increase the stability of the target compounds.



## Chapter 2

# Low-energy Membrane-based Processes to Concentrate and Encapsulate Polyphenols from Carob Pulp

### Abstract:

Forward osmosis (FO) and emulsification with dynamic membranes of tunable pore size (DMTS) were assessed to concentrate and encapsulate polyphenol extracts from carob pulp. In the FO step, a feed solution temperature of 40 °C resulted in the fastest concentration and the highest polyphenol yield. Moreover, FO at 35 °C enabled to concentrate up to about 20 times in three hours using a pilot scale unit of 0.5 m<sup>2</sup> of membrane area. Phenolic compounds were subsequently encapsulated in the inner water phase (W<sub>1</sub>) of water-in-oil-in-water (W<sub>1</sub>/O/W<sub>2</sub>) emulsions produced with DMTS, which enabled to obtain emulsions with a monomodal droplet size distribution (span<1, d<sub>3,2</sub> ≤20µm), and polyphenol encapsulation efficiencies ranging between 87.0 ± 0.2 % and 77.4 ± 0.4 %. To extend the shelf-life of the encapsulated polyphenols, solid microcapsules were produced by spray drying. After rehydrating the solid microcapsules, the structure of the W<sub>1</sub>/O/W<sub>2</sub> emulsion was partially recovered.

This chapter has been published as:

Wang, J., Martínez-Hernández, A., de Lamo-Castellví, S., Romero, M. P., Kaade, W., Ferrando, M., & Güell, C. (2020). Low-energy membrane-based processes to concentrate and encapsulate polyphenols from carob pulp. *Journal of Food Engineering*, 281, 109996.



## 2.1. Introduction

The increasing attention towards sustainability in the food sector has led to progressive implementation of valorization strategies to yield value-added compounds, such as antioxidants, colorants, flavors and dietary fibers from agri-food wastes. This is the case of carob (*Ceratonia siliqua L.*) fruits grown in Mediterranean countries, which are pods consisting of seeds and pulp. The commercial value of the carob fruit comes from its seeds that contain a widely used food additive, locust bean gum (E-410). After removing the seeds, about 90% of the total weight of the fruit is the pulp, which is mainly used for animal feed and a few food preparations<sup>185,186</sup>. However, the carob pulp contains different valuable components such as sugars, dietary fibers, and a great diversity of polyphenols and other minor components<sup>187</sup>. Goulas et al.<sup>187</sup> have reviewed the health benefits of fibers and polyphenols from carob, reporting anti-proliferative and apoptotic activity against cancer cells, anti-diabetic effects, anti-diarrheal effects and anti-hyperlipidemia effects. The presence of fibers and polyphenols makes the carob pulp an attractive raw material to obtain extracts that can be used in gluten-free bakery products, fortified durum wheat pasta, carob spread, low lactose yoghurt, marmalades, cookies and candies<sup>188–192</sup>. A process strategy to recover the polyphenol fraction from carob pod should consist of extraction, concentration, and stabilization of the biomolecules of interest. To do so, environmentally friendly technologies have evolved to increase product quality while reducing energy consumption or thermal detrimental effects.

In the conventional solid-liquid extraction process of polyphenols, a prior removal of the sugars by water extraction at room temperature is followed by several steps of polyphenols solubilization<sup>193</sup>. As for the remaining polyphenol fraction in the low-sugar-content carob pulp, it can be extracted using hot water, resulting in a water-soluble polyphenol fraction. The solid-liquid extraction process can produce high volumes of a diluted aqueous polyphenol extract that needs to be concentrated to reduce handling, storage and transportation costs and to obtain a suitable polyphenol content for its further uses. Concentration can be performed by several methods, such as evaporation, reverse osmosis and forward (or direct) osmosis. Forward osmosis (FO) is a low-energy membrane-based separation technology based on osmotic pressure difference between two solutions<sup>194,195</sup>. A draw solution (DS) with very high osmotic pressure circulates on one side of a water permeable membrane and on the other side of the membrane circulates a feed solution (FS) that has lower osmotic pressure. Under this configuration, water is driven from the FS to the DS because of osmotic pressure difference. This method prevents from applying high pressure to the solutions, since pressure is only required to circulate the draw and feed solutions, and it can be operated at mild temperatures<sup>196</sup>. Therefore, FO is a non-thermal concentration technology very promising for the food industry since it has a minimal impact on nutritional and organoleptic quality of the products. FO can concentrate to higher soluble solids values than reverse osmosis, which is usually limited to 22-23 °Brix<sup>197</sup> and it has a low irreversible fouling which decreases the costs of membrane cleaning and replacement. Food applications of FO range from

water desalination, fruit and vegetable juices concentration, including the enrichment of natural antioxidants and colorants to protein concentration in fish by-products, dewatering of whey in cheese manufacturing, concentration of acid whey from Greek yoghurt and concentration of artificial sugar solutions<sup>198–201</sup>.

To preserve the chemical stability of polyphenols in the concentrated extract, they should be further stabilized by encapsulation in liquid or solid systems. Encapsulation in water-in-oil-in-water ( $W_1/O/W_2$ ) emulsions, where the water-continuous system ( $W_2$ ) contains oil droplets that have smaller water droplets ( $W_1$ ) dispersed within, has been described as a successful system to protect and encapsulate sensitive hydrophilic compounds, such as polyphenols<sup>163,202–204</sup>.  $W_1/O/W_2$  emulsions involve the production of a  $W_1/O$  single emulsion and dispersion of the single emulsion in a  $W_2$  continuous phase. Several emulsification techniques, such as high-pressure homogenization, rotor-stator homogenization, ultrasonication, or membrane emulsification, are used to produce the inner  $W_1/O$  emulsion, although the secondary homogenization step is usually carried out using lower energy intensity than the in the primary step so as not to break the initial  $W_1/O$  emulsion<sup>205</sup>. Membrane emulsification, which uses low-shear stresses, has received increasing attention for producing multiple emulsions.

Membrane/microporous emulsification is carried out by pressing the dispersed phase into a continuous phase through the pores of a membrane or refining a coarse pre-emulsion by pushing through the membrane pores<sup>206</sup>. It is benefited by its low energy input and the possibility to obtain narrow droplet size distribution compared to other conventional process<sup>206</sup>. Dynamic membranes of tunable pore size (DMTS) (Figure 2.1), consisting of a bed of silica beads supported by a nickel microporous membrane, exhibit higher productivity than other membrane emulsification processes<sup>207</sup>, whilst maintaining its other advantages, such as a reduction of the mechanical stress and low energy consumption. Sodium chloride<sup>144</sup> and beet root juice<sup>141</sup> were successfully encapsulated in  $W_1/O/W_2$  emulsions produced with the DMTS system. The operation mode consists of producing a coarse  $W_1/O/W_2$  emulsion which is forced to pass through the micro-structured bed several times, decreasing the droplet size of the emulsion<sup>144</sup>. During emulsion refinement, release of the entrapped compound is unavoidable as a result of droplet break-up. Therefore, operation conditions such as applied pressure, bed height, interstitial void diameter and number of cycles must be adjusted to retain the entrapped compound while reducing the droplet size distribution. Moreover, the imbalance of osmotic pressure between inner and outer water phase in  $W_1/O/W_2$  emulsions is a primary source of instability during storage<sup>208</sup>.

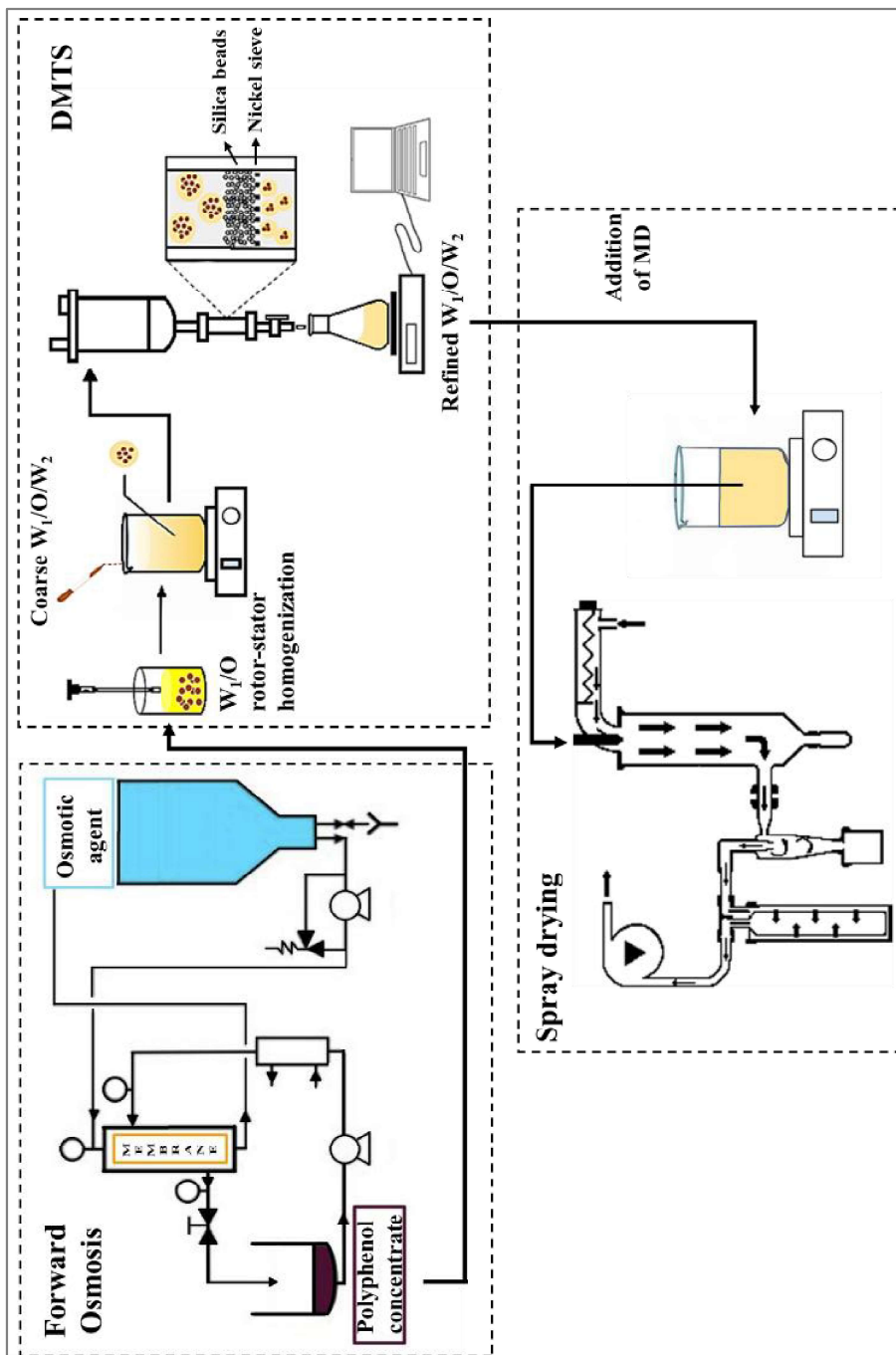


Figure 2.1 Schematic diagram of the concentration and encapsulation processes for the valorization of a carob polyphenol extract.

Even though  $W_1/O/W_2$  emulsions can protect the bioactive compounds, they have poor stability during storage, and dosage of liquid systems is more difficult to control in the production lines. Therefore, spray drying of the emulsions is a common strategy used by the food industry to produce solid microcapsules. The spray drying process requires the addition of wall-building materials, such as polysaccharides (e.g., maltodextrin), proteins (e.g., whey protein), and gums (e.g., Arabic gum), that are water soluble. Several authors have reported encapsulation of bioactive compounds by spray drying of  $W_1/O/W_2$  emulsions <sup>149,163,165,166</sup>.

The objective of the study was to assess the use of membrane-based processes to concentrate and encapsulate a carob polyphenol extract. Starting from a polyphenol diluted solution from carob pulp obtained by water extraction, concentration was performed using forward osmosis (FO) in a commercial pilot unit. The effect of temperature on water flux and polyphenol concentration was studied. Moreover, to increase the stability of the extracted polyphenols, encapsulation in liquid systems ( $W_1/O/W_2$  emulsions) and solid microcapsules was assessed.  $W_1/O/W_2$  emulsions were produced by DMTS, while solid microcapsules were obtained by spray drying the  $W_1/O/W_2$  emulsions. This study combines for the first-time concentration and encapsulation of a polyphenol extract by membrane-based processes, showing the potential of membrane technology to be implemented in bio-refinery of agri-food wastes.

## 2.2. Materials and Methods

### 2.2.1. Materials

Carob polyphenol extract, kindly provided by *Unió Corporació Alimentària* (Reus, Spain), had a total polyphenol content (TPC) of 1.13 g GAE L<sup>-1</sup> and 4.5 °Brix with sucrose, glucose and fructose as main soluble solids <sup>187,209,210</sup>. The draw solution (DS) used during FO was composed of potassium lactate 60 °Brix supplied by Ederna SAS (Toulouse, France). P3-ultrasil 112 (ECOLAB, Finland) and acetic acid (96%, Panreac, Spain) were used for cleaning and regeneration of FO membrane. As for preparation of emulsions, sunflower oil (bought at local supermarket) with 4 wt% polyglycerol polyricinoleate (PGPR, ref-4120 Palsgaard, Denmark) was the oil phase. Whey protein isolate (WPI) with a reported protein content of 98.1% on dry basis (BiPRO, lot no. JE 034-7-440-6, Davisco Foods International, Inc., Le Sueur, MN) was used as a hydrophilic emulsifier in  $W_2$  phase at a concentration of 1 wt%. In order to balance the osmotic pressure of two aqueous phases ( $W_1$  and  $W_2$ ), either NaCl (Panreac, Spain) or trehalose (Sosa Ingredients S.L., Spain) was added in the  $W_2$  phase as bulk agent. Sodium azide 0.02% (w/w) (Sigma-Aldrich, USA) was added to prevent bacterial growth. Food grade maltodextrin (lot no. 219425, MD, Pral, Barcelona) with a dextrose equivalent of 16.5-19.5 was added to the  $W_1/O/W_2$  emulsions as wall-building material for the microcapsules produced by spray drying. Sodium carbonate (Panreac, Spain), gallic acid monohydrate (Panreac, Spain) and Folin-Ciocalteu's reagent (Panreac, Spain) were used for total polyphenol content (TPC)

quantification. Sodium hydroxide, (Fisher Scientific, UK) and ethanol (96%, Scharlab S.L., Spain) were used to clean the DMTS system, that consists of a bed of silica beads (Unicorn Industrial Cleaning Solutions, the Netherlands) supported by a nickel micro-sieve (Stork Verco, Erbeek, the Netherlands).

### 2.2.2. Forward osmosis concentration

Concentration of carob polyphenol extract (PE) was carried out with FO pilot unit (EvapEOs® - Micro pilot unit) provided by Ederna SAS (Toulouse, France). The unit (Figure 2.1) was equipped with a cellulose triacetate membrane module that contains a spiral wound membrane of 0.5 m<sup>2</sup>, a feed solution (FS) reservoir, a draw solution (DS) reservoir and pumps for both solutions. The pressure inside the membrane module was controlled below 0.7 bar. A water bath was connected aside in order to control the temperature of the feed solution under 40 °C (maximum operating temperature of the membrane). For all experiments, 1 L of DS (osmotic agent) was placed initially and the transmembrane water flux ( $J_{FO}$ ) was measured every 30 min by measuring the time consumed to filtrate a fixed amount of FS and calculated with equation (2.1),

$$J_{FO} = \frac{m}{\rho_f A_m \Delta t} \quad \text{eq (2.1)}$$

where the  $m$  is the mass of FS added in kg;  $\rho_f$  is the density of FS in kg L<sup>-1</sup>;  $A_m$  is the surface area of membrane in m<sup>2</sup>;  $\Delta t$  is the time duration of the process.

When the flux dropped below 4 Lm<sup>-2</sup>h<sup>-1</sup>, 1 L fresh osmotic agent replaced the diluted osmotic agent to continue the process. PE was firstly concentrated to obtain polyphenol concentrate (PC) at different feed temperatures (25, 35 and 40 °C); several batches of PC were collected to continue the concentration process at 35°C to obtain a polyphenol re-concentrate (PR). The process parameters and initial and final polyphenol and sugar content during FO experiments are summarized in Table 2.1. The FO yield was obtained using equation (2.2).

$$Yield_{FO} [\%] = \frac{m_{polyPC}}{m_{polyPE}} \times 100 \quad \text{eq (2.2)}$$

Where  $m_{polyPC}$  is the amount of polyphenols in the concentrated extract and  $m_{polyPE}$  is the amount of polyphenol in the initial extract.

Table 2.1. Operating conditions and initial and final composition during FO concentration and re-concentration.

	FS	Product	T (°C)	V <sub>initial</sub> (L)	V <sub>initial</sub> (L)	TPC <sub>initial</sub> (gGAE L <sup>-1</sup> )	TPC <sub>final</sub> (gGAE L <sup>-1</sup> )	Sugar content	
								°Brix (initial)	°Brix (final)
Concentration			25				6.2±1.6		
	PE	PC	35	9.8±0.8	0.9±0.2	1.1±0.1	8.9±1.4	4.5	11.8
			40				8.2±0.8		
Re-concentration	PC	PR	35	2.8	0.9±0.1	8.2±0.1	18.4±1.7	11.8	24.5

Experiments were run at least in duplicate. Cleaning of the membrane was carried out after each FO concentration process following the manufacturer’s indications with 4%(v/v) ultrasil (pH 14) and acetic acid solution (pH 2). The water flux was measured after cleaning to ensure a minimum water flux value of 10 Lm<sup>-2</sup>h<sup>-1</sup> before reusing the membrane.

### 2.2.3 Production of W<sub>1</sub>/O/W<sub>2</sub> emulsions using DMTS

#### Production of coarse W<sub>1</sub>/O/W<sub>2</sub> emulsions

Composition of double emulsions is presented in Table 2.2. Initially, W<sub>1</sub>/O emulsion consisting of 15 g of W<sub>1</sub>, carob polyphenol re-concentrate (PR), and 35 g sunflower oil with 1.4 g PGPR dissolved (4 wt%) (O) were homogenized (Ultraturrax, IKA® T18 Digital, Germany) at 11000 rpm for 5 min (Figure 2.1). Then, 40 g of W<sub>1</sub>/O was added to 160 g of W<sub>2</sub> and mixed with a magnetic stirrer at 1600 rpm for 5 min. The high osmolality of W<sub>1</sub>, resulting from the high sugar and polyphenol concentration in PR, was balanced by adding NaCl (3.15 wt%) or trehalose (28.2 wt%) as bulk agent in W<sub>2</sub> to prevent emulsion instability<sup>211</sup>. Additionally, W<sub>2</sub> contained 1 wt% of whey protein isolate (WPI) as hydrophilic emulsifier. Osmolality of the carob polyphenol re-concentrate solution and the W<sub>2</sub> aqueous phase having different compositions (Table 2.2) was measured using vapor pressure osmometer (K-7000, KNAUER, Germany) at 39 °C. Calibration of the equipment was done with NaCl solution of 400 mOsmol kg<sup>-1</sup>.

Table 2.2. Composition of W<sub>1</sub>/O/W<sub>2</sub> emulsions and osmolality of the two aqueous phases.

Fraction	Phase	Composition	Bulk agent	Osmolality (mOsmol/L)
6 wt %	W <sub>1</sub>	PR	--	1200±2
14 wt %	O	4 wt% PGPR	--	--
			i) none	40
80 wt%	W <sub>2</sub>	1wt% WPI	ii) 3.15 wt% NaCl	1055±1
			iii) 28.2 wt% trehalose	1107±1

#### Refinement of W<sub>1</sub>/O/W<sub>2</sub> emulsions by DMTS

The setup of DMTS system is shown in Figure 2.1. Freshly prepared coarse emulsion was placed into the vessel of DMTS system, and it was forced to pass through the dynamic membrane consisting of a layer (4.35 mm height) of silica microbeads (101 µm diameter and 0.66 span) supported by a nickel microsieve of rectangular pores 300 µm x 25 µm (length x width) to refine the emulsions at 200 kPa by applying nitrogen gas (named as

emulsification cycle 1). A digital balance coupled with a laptop was placed under the recipient in order to record the collected mass during the emulsification. The emulsion was further refined by passing through the DMTS system the second time (cycle 2). The interstitial void diameter ( $d_v$ ) of the channels formed by the dynamic membrane made of silica microbeads was 59.3  $\mu\text{m}$ , calculated according to the equation (2.3),

$$d_v = \frac{4\varepsilon}{6/d_b(1-\varepsilon)} \quad \text{eq (2.3)}$$

where  $d_b$  is the bead diameter (101  $\mu\text{m}$ ) and  $\varepsilon$  is the bed porosity (0.47), which can be calculated by equation (2.4),

$$\varepsilon = 1 - \frac{\rho_b}{\rho_p} \quad \text{eq (2.4)}$$

where  $\rho_b$  and  $\rho_p$  are the densities of silica beads measured in the bulk (1301  $\text{kg m}^{-3}$ ) and in the air (2446  $\text{kg m}^{-3}$ ) respectively.

Transmembrane flux,  $J_{DMTS}$ , during each emulsification cycle in the DMTS system can be calculated using equation (2.5),

$$J_{DMTS} = \frac{\phi}{\rho_e A} \quad \text{eq (2.5)}$$

where  $\phi$  is the mass flow rate acquired by data recorded with the electronic balance,  $\rho_e$  is the emulsion density,  $A$  is the effective surface area of the DMTS.

The nickel sieve and silica beads were reused once they were cleaned and dried. The cleaning protocol for the nickel sieve was as described by Kaade et al.<sup>212</sup>. Briefly, the sieve was sonicated in the 4M NaOH solution bath for 5 min followed by rinsing under sonication in deionized water for 5 min with one replication. Silica beads were cleaned using soap and ethanol to remove the oil and dried in the oven at 100 °C.

In order to measure the polyphenol encapsulation efficiency in the emulsions, they were centrifuged for 10 min at 3000 rpm. Then, the  $W_2$  phase was collected and analyzed as described in section 2.2.5 for total polyphenol content. The mass of polyphenols that remained encapsulated in  $W_1$  was expressed as polyphenols encapsulation efficiency (EE) using equation (2.6)<sup>202</sup>,

$$EE [\%] = \frac{m_{polyW_1}^0 - C_{polyW_2}^n (m_{W_1}^0 + m_{W_2}^0)}{m_{polyW_1}^0 - C_{polyW_2}^n m_{W_1}^0} \times 100 \quad \text{eq (2.6)}$$

where  $m_{polyW_1}^0$  is the initial polyphenol mass in the inner water phase ( $W_1$ ),  $C_{polyW_2}^n$  is the concentration of polyphenols in the outer water phase ( $W_2$ ),  $m_{W_1}^0$  is the initial mass of the inner water phase, and  $m_{W_2}^0$  is the initial mass of the outer water phase.

## 2.2.4 Production of solid microcapsules by spray drying

Solid microcapsules from the  $W_1/O/W_2$  refined emulsions were obtained by spray drying. Freshly prepared  $W_1/O/W_2$  emulsions (cycle 1) were mixed with MD by adjusting oil to solids ratio (WPI, trehalose and MD) to 1:3 (w/w), followed by spray drying using a Büchi Mini Spray dryer B-290 (Flawil Switzerland) setting the inlet temperature at 170 °C, the outlet temperature was controlled at 100 °C, nozzle pressure of 4.5 bar, the feed flow rate of 4 mLmin<sup>-1</sup> and aspiration rate of 100% (35 m<sup>3</sup>h<sup>-1</sup>). Spray drying yield was calculated using equation (2.7),

$$Yield_{SD}[\%] = \frac{m_{capsules}}{m_{inlet\ solids}} \times 100 \quad \text{eq (2.7)}$$

where  $m_{capsules}$  is the amount of spray dried powders obtained, and  $m_{inlet\ solids}$  is the amount of solid compounds (trehalose, whey protein and maltodextrin) at the inlet of spray dryer.

## 2.2.5 Methods of analysis and characterization

### Polyphenol assay

The polyphenol concentration in the initial extracts, in samples taken during forward osmosis concentration, and in the final products (PC and PR) was analyzed based on Folin-Ciocalteu colorimetric method<sup>213</sup>. Briefly, 100 µL of diluted sample and 100 µL of Folin reagent were mixed with 2 mL of sodium carbonate solution (75 gL<sup>-1</sup>) and 2.8 mL of deionized water. After 1 h of incubation at room temperature in the dark, absorbance was measured at 750 nm by a UV-Vis spectrophotometer (Hach Lange DR5000, Hach Lange SLU, Spain). Calibration curve was made by taking gallic acid as standard, and the results were expressed as gram gallic acid equivalent per liter (gGAE L<sup>-1</sup>).

### Measurement of sugar content

The sugar content in PE, PC and PR were measured by refractometry (WAY-1S, Zuzi, Auxilab S.L., Spain). The results were given as Brix degrees (°Brix). Each sample was measured in triplicate.

### Droplet size and distribution

Droplet size distribution of  $W_1/O/W_2$  emulsions was measured after every emulsification cycle by laser diffraction using Mastersizer 2000 (Malvern Instruments). Sodium chloride solution (3.15 wt%), was used as the continuous phase in Mastersizer Hydro 2000G accessory in order to disperse the emulsion in a solution with similar osmotic pressure. Mean droplet size and droplet size distribution can be calculated, which were expressed as Sauter mean diameter  $d_{3,2}$  (equation 2.8) and the relative span factor (equation 2.9), respectively.

$$d_{4,3} = \frac{\sum n_i D_i^4}{\sum n_i D_i^3} \quad \text{eq (2.8)}$$

Where  $n_i$  is the number of droplets, and  $D_i$  is the diameter of the  $i^{\text{th}}$  droplet.

$$\delta = \frac{d_{90} - d_{10}}{d_{50}} \quad \text{eq (2.9)}$$

$d_x$  is the droplet diameter corresponding to  $x\%$  volume on a cumulative droplet size distribution curve.

### **Morphology of solid microcapsules**

Outer and inner morphology of the capsules was observed through FEI Quanta 600 Environmental scanning electron microscope (ESEM). Accelerating voltage was set to 20 kV. Rehydrated emulsion capsules in 3.15 wt% NaCl solution was observed under the optical microscope (Leica DM 2500) at 1000x.

### **Moisture content of solid microcapsules**

Moisture content of solid capsules was measured by titration method using Karl Fischer (TitroMatic 1S, Crison Instruments S.A., Spain) using solvent and titrant for Karl Fischer (Aquametric, Panreac Spain). Calibration was done using a water standard (Hydranal<sup>®</sup>- Water Standard 10.0, Fluka) and the results were expressed as mass per 100 g of powder (wet basis). Measurements were done in triplicate.

## **2.3. Results and discussion**

### **2.3.1. Forward osmosis concentration: effect of temperature on water flux and concentration**

Forward osmosis experiments were carried out using a carob polyphenol extract and a food grade osmotic agent as feed solution (FS) and draw solution (DS), respectively. The effect of feed temperature, 25 °C, 35 °C and 40 °C, on the transmembrane flux ( $J_{FO}$ ) and polyphenol concentration is shown in Figure 2.2.

Regardless the initial concentration of the carob polyphenol extract (PE) (Table 2.1), a high reproducibility and the same trend on transmembrane flux reduction can be observed from the seven experiments conducted at 35 °C (Figure 2.2-a). For clarity purposes, from this point on the results of FO will be shown as average values without the error bars. Figure 2.2-b shows that the overall processing time required for concentrating decreased by increasing the FS temperature. This was mainly attributed to the decrease of FS viscosity as temperature increases, which enhanced the mass transfer coefficient and, in turn, the water flux through the membrane<sup>214-216</sup>. The rise of water flux during the concentration at 25 °C (at around 130 min) in Figure 2.2-b (point A) was due to the replacement of the diluted DS by new osmotic agent to recover the flux which had dropped below 4 Lm<sup>-2</sup>h<sup>-1</sup>. Despite the replacement of the DS in the FO system, there was only a slight increase in the water flux on account of (1) the fouling of the membrane, since the FO system had been running for more than 2 h, and (2) by the increase in the polyphenol/sugar concentration of the FS. When the replacement of the DS was accompanied by the use of a clean membrane, as can be seen for the FO concentration at 35 °C (Figure 2.2-b, point B), water flux reached the same value as the one obtained after the initial 40 minutes of concentration. This is a clear indication that both membrane fouling and water activity gradient between FS and DS are key parameters controlling water flux.

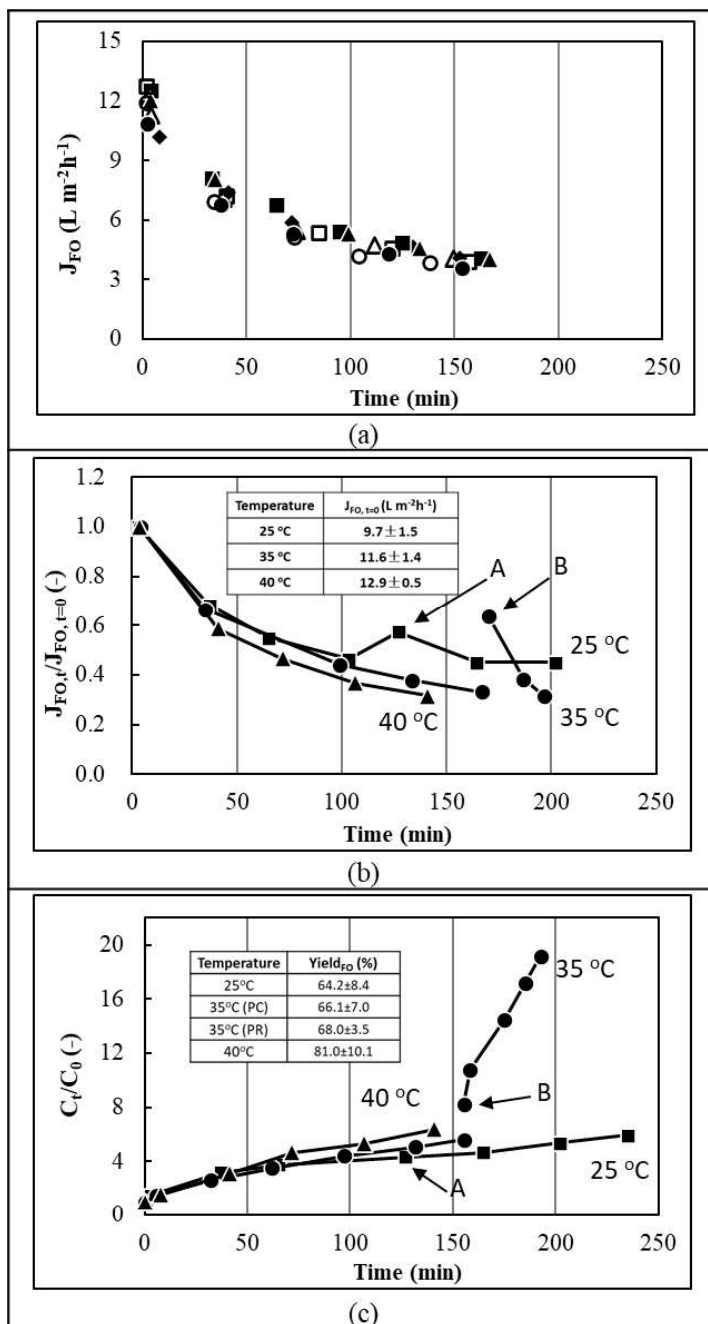


Figure 2. Effect of feed solution temperature on FO performance: (a) progress of water flux at 35 °C for 7 runs; (b) normalized flux ( $J_{FO,t} / J_{FO,t=0}$ ) to obtain PC at 25 °C, 35 °C and 40 °C; (c) normalized TPC ( $C_t / C_0$ ) in the feed solution. Arrow A is pointing the replacement of DS during FO, and arrow B indicates both the use of a clean membrane and new DS to continue concentration process.

The increase rate of polyphenol content (Figure 2.2-c) in PC showed no difference within the first hour at different FS temperature. From this point on, the increase rate was directly related to temperature. This is in agreement with higher water fluxes across the membrane obtained when the temperature of the FS increased, being an effective way in FO to accelerate the concentration process. As for obtaining the PR (FO of several PC batches) at 35 °C, the use of a clean membrane and new DS resulted in high water fluxes and consequently a fast increase in the polyphenol content. Significant loss of polyphenols during FO experiments was observed from the calculated yields (Figure 2.2-c). This loss could be caused either by polyphenols retention in the membrane or by their pass from the FS to the DS. The noticeable color change in DS was a clear indication that some phenolic compounds had diffused through the membrane. The higher yield of FO at 40 °C could be linked to a shorter operation time. In this study, 18-fold increase of carob polyphenol content (1.1 gL<sup>-1</sup> to 18.4 gL<sup>-1</sup>) was achieved by 3.3h of FO concentration at 35 °C. It has shown a higher efficiency compared to studies concentrating anthocyanins from red radish<sup>217</sup>, red cabbage<sup>218</sup> and grape<sup>219</sup> extracts. In these studies, they reported 6.8 to 14-fold increase in anthocyanin contents (from 0.22 gL<sup>-1</sup> to 8.19 gL<sup>-1</sup>) during 11 to 24 hours of FO concentration at temperatures ranging from 25 °C to 60 °C. Moreover, Nayak and Rastogi<sup>215</sup> achieved 54-fold increase in anthocyanin content (0.05 gL<sup>-1</sup> to 2.69 gL<sup>-1</sup>) concentrating a kokum extract during 18 hours at 25 °C. In the present case, the concentration process was fast at mild temperature conditions also because of the large membrane area (0.5 m<sup>2</sup>) of the pilot FO unit.

On the other hand, the fouling of the FO membrane must be considered. Even though high temperatures may trigger the increase of total polyphenol content by structural changes such as disruption, polymerization and re-synthesis of phenolic compounds<sup>213</sup>, studies on reverse osmosis have shown that there was no difference in polyphenol concentration and antioxidant properties at temperatures between 20 °C and 40 °C<sup>220</sup>. Moreover, Kim et al.<sup>221</sup> pointed out that FO membrane was less fouled with increasing the FS temperature due to the enhanced back diffusion of organic compounds from membrane surface, what would explain the higher polyphenol yield obtained at 40 °C. Despite these results, experiments to obtain PR extracts were run at 35 °C, because the maximum operating temperature of the membrane is 40 °C being not advisable for long-running processes.

### 2.3.2. Encapsulation of polyphenols in W<sub>1</sub>/O/W<sub>2</sub> double emulsions

For producing W<sub>1</sub>/O/W<sub>2</sub> emulsions able to entrap the carob polyphenol re-concentrate in W<sub>1</sub>, the formulation of the several phases had to be set up. In this kind of systems, the internal (W<sub>1</sub> in O) and external interfaces (W<sub>1</sub>/O in W<sub>2</sub>) require to be stabilized by surface active compounds. In this case, PGPR and WPI were used as lipophilic and hydrophilic emulsifiers, respectively<sup>141,144,202,211</sup>. Another important factor to maintain W<sub>1</sub>/O/W<sub>2</sub> emulsions stable is to prevent any significant imbalance of the osmotic pressure between W<sub>1</sub> and W<sub>2</sub>, that could induce any mass transport between the

two water phases. This phenomenon, facilitated by the inverse micelles formed by the lipophilic emulsifier, can end up in the transformation of  $W_1/O/W_2$  in a single emulsion or, further on, in phase separation.

In the current scenario,  $W_1$  phase, consisting of carob re-concentrate, exhibited an osmolality of  $1200 \text{ mOsmol kg}^{-1}$  which can be explained by its high solid soluble content which were mainly sugars (24.5 °Brix). The water extraction process produced a polyphenol extract containing sugars (4.5 °Brix) that was also concentrated during FO and possibly as well as low amount of soluble fibers such as pectin<sup>187,222</sup>. On account of the huge difference ( $1160 \text{ mOsmol kg}^{-1}$ ) of the osmolalities between the  $W_1$  and  $W_2$  phases (no bulk agent added) (Table 2.2), water from  $W_2$  phase can diffuse quickly to  $W_1$  phase which leads to the swelling of the inner water droplets ( $W_1$ ) and eventually they burst and release the compounds to  $W_2$  phase. This phenomenon was observed in the pre-trial of  $W_1/O/W_2$  emulsions formulated without bulk agent in  $W_2$  phase, which resulted in a polyphenol EE of 35% and 30% after first and second emulsification cycle, respectively in the DMTS system.

As reviewed by Muschiolik and Dickinson<sup>211</sup>, salt and sugars are most commonly used bulk agents added in the external aqueous phase in order to counter with the imbalance of osmotic pressure difference between two aqueous phases. Therefore, to balance the osmotic pressure of  $W_1$ , NaCl and trehalose were added to  $W_2$  to attain a concentration of 3.15 wt% and 28.2 wt%, respectively, leading to the osmolalities reported in Table 2.2, balancing the osmotic gradient. Osmolality in  $W_2$  phase was adjusted a little less than  $W_1$  phase referring to the study by Pawlik et al.<sup>223</sup>, whom observed lowest release of  $W_1$  fraction when the  $W_2$  phase was less than required for equilibrating the osmotic pressures.

The droplet size distribution of the coarse and refined emulsions (cycle 1 and 2) were measured right after emulsification. Figure 2.3 shows  $d_{3,2}$  evolution during DMTS emulsification which sustains the feasibility of using this emulsification system to refine  $W_1/O/W_2$  emulsions. As expected, a significant droplet reduction occurs during the first emulsification cycle followed by a minor decrease during the second emulsification cycle. After the first cycle, the span value was on the range of 0.8 to 0.9 which is an indication that the emulsions are in narrow size distribution. It is important to note that no significant effect of  $W_2$  composition was observed on the droplet size distribution during DMTS emulsification.

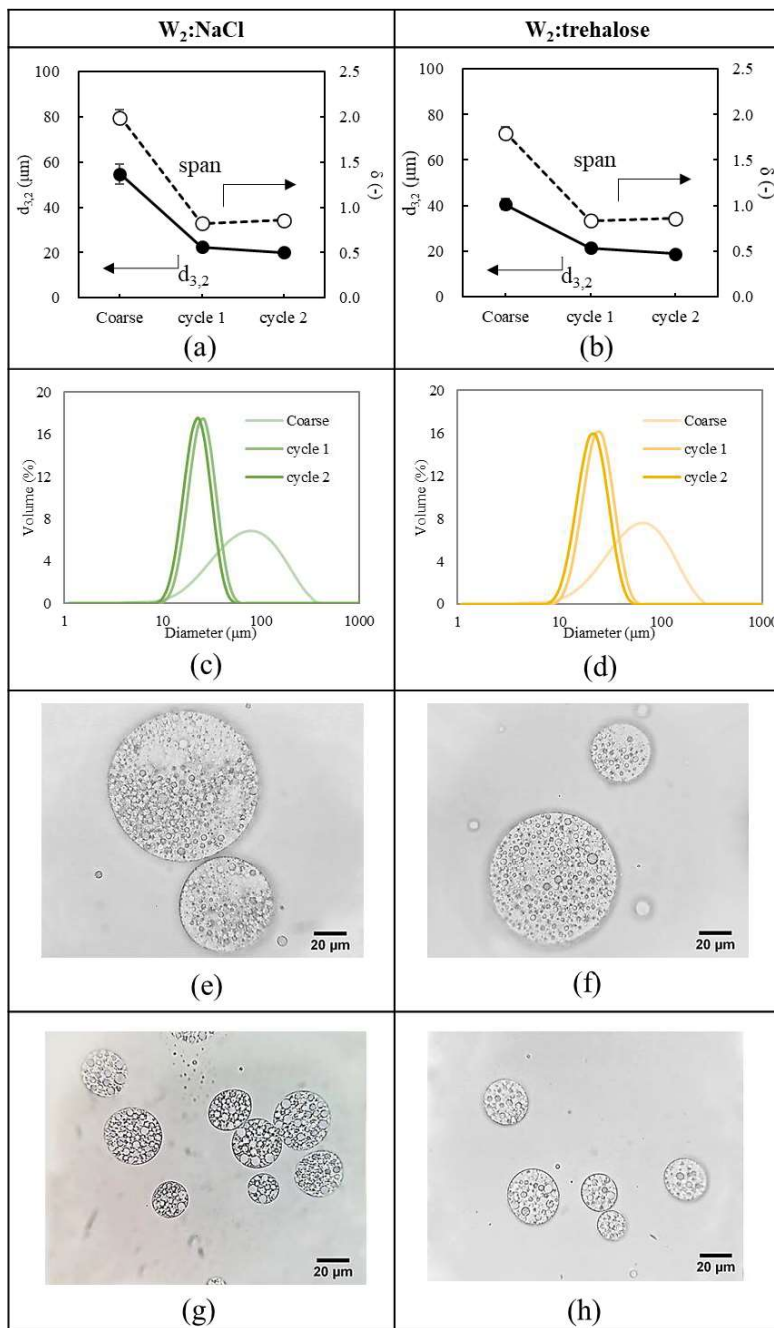


Figure 3. Results of W1/O/W2 coarse emulsion and refined emulsions formulated by adding NaCl or trehalose as bulk agent in W2: (a)(b) sauter mean diameter ( $d_{3,2}$ ) and span ( $\delta$ ) of W1/O/W2 as a function of emulsification cycle with error bars representing standard deviation ( $n=18$ ); (c)(d) droplet size distribution of W1/O/W2 as a function of emulsification cycle; (e)(f) optical microscope images of coarse W1/O/W2 emulsions;

(g)(h) optical microscope images of W<sub>1</sub>/O/W<sub>2</sub> emulsions after 2 cycles of emulsification in DMTS. Lines are guides to the eyes.

Regarding encapsulation efficiency (EE), a reduction with each emulsification cycle was observed (Table 2.3). Apparently, the release of the inner encapsulate was caused by droplet breakup during emulsification. Part of the inner aqueous fraction was released to W<sub>2</sub> phase when droplets were broken up in the microchannels of the DMTS system. These results agree with previous findings encapsulating anthocyanin in W<sub>1</sub>/O/W<sub>2</sub> by SPG membrane<sup>202</sup> and during encapsulation of concentrated beet root juice with a DMTS system<sup>141</sup>. In the present study, the composition of W<sub>2</sub> seems to influence the EE, obtaining values of 87.0 ± 0.2 % and 77.4 ± 0.4 % after two emulsification cycles for NaCl and trehalose, respectively. Moreover, the W<sub>1</sub>/O/W<sub>2</sub> emulsions maintained the EE above 50% for 14 days, with minor changes in d<sub>3,2</sub> (±1 μm) and span (± 0.1). This behavior agrees with previous results from Pawlik et al.<sup>223</sup> for the physical stability of W<sub>1</sub>/O/W<sub>2</sub> emulsions over 60 days with minor droplet size increase and 30% reduction of EE.

Table 2.3. Progress of droplet size, encapsulation efficiency and transmembrane flux of W<sub>1</sub>/O/W<sub>2</sub> emulsions prepared with NaCl and trehalose in W<sub>2</sub> before and after each emulsification cycle.

	W <sub>2</sub> : NaCl			W <sub>2</sub> : trehalose		
	d <sub>3,2</sub> (μm)	Flux (m <sup>3</sup> m <sup>-2</sup> h <sup>-1</sup> )	EE (%)	d <sub>3,2</sub> (μm)	Flux (m <sup>3</sup> m <sup>-2</sup> h <sup>-1</sup> )	EE (%)
Coarse	54.7±4.4	--	95.2±1.0	40.6±2.3	--	92.7±6.3
Cycle 1	22.4±0.4	135.9±24.9	87.3±0.7	21.3±0.1	148.2±8.6	79.4±0.1
Cycle 2	20.0±0.2	163.8±18.4	87.0±0.2	18.8±0.2	120.4±19.9	77.4±0.4

Considering the implementation of emulsification technology at industrial scale, both the emulsion properties (droplet size distribution and EE) and productivity are of importance. The results show that DMTS emulsification allows to produce monomodal and narrow droplet size distribution W<sub>1</sub>/O/W<sub>2</sub> emulsions with high EE (Table 2.3). As the flux during the process can be the indicator of productivity, results showed that the fluxes obtained at 250 kPa are well above 100 m<sup>3</sup>m<sup>-2</sup>h<sup>-1</sup>. These flux values are slightly higher or similar to the ones reported for W<sub>1</sub>/O/W<sub>2</sub> emulsification at lower pressures using SPG membranes<sup>224-226</sup>. Moreover, they were 30 times higher than the ones reported for a similar emulsification system to encapsulate concentrated beetroot juice in W<sub>1</sub>/O/W<sub>2</sub> emulsions, which had flux of 5 m<sup>3</sup>m<sup>-2</sup>h<sup>-1</sup> at second cycle<sup>141</sup>, and in the range (100-800 m<sup>3</sup>m<sup>-2</sup>h<sup>-1</sup>) reported by Sahin et al.<sup>144</sup> for the encapsulation of NaCl in W<sub>1</sub>/O/W<sub>2</sub> emulsions at pressure range of 200 kPa to 600 kPa and silica beads size of 30 to 90 μm.

It seems that the composition of the W<sub>2</sub> phase affects the flux progress during emulsification. For the W<sub>1</sub>/O/W<sub>2</sub> emulsions produced with trehalose in the W<sub>2</sub> phase, the

flux slightly decreases during emulsification, possibly due to the accumulation of droplets in or before the micro-structured silica bed. However, when NaCl was used to balance the osmotic pressure in the  $W_1/O/W_2$  emulsions, the flux slightly increased from cycle 1 to cycle 2. This trend has already been reported during the production of O/W emulsions by membrane emulsification which is attributed to both the lack of fouling and the endpoint of droplet breakup, that enables to use all the energy (pressure applied) in flowing the emulsion through the system<sup>130,227</sup>. The difference in viscosity of the  $W_2$  phase when it contains NaCl or trehalose is thought to be responsible of the different behavior in flux progress, even though there was no effect on droplet breakup with a minor impact in the EE.

### 2.3.3. Solid microcapsules production by spray drying

Although  $W_1/O/W_2$  emulsions are suitable systems to encapsulate and protect the carob polyphenols, solid microcapsules can extend the shelf-life of the product and facilitate its dosage for industrial applications. Spray drying has been selected to turn the emulsions into solid microcapsules, following the methodology described in section 2.2.2. Refined  $W_1/O/W_2$  emulsions by DMTS after cycle 1 were selected for spray drying since the main droplet size reduction happened during the first emulsification cycle, as explained in the section 2.3.2 (Figure 2.3). From the two different formulations, only the ones with trehalose in the  $W_2$  phase have been dried. This is mainly because the use of a 3% NaCl solution as outer water phase, even though balances the osmotic pressure and leads to high fluxes during emulsification, will affect the taste of the product. Besides, the emulsion with trehalose in  $W_2$  requires addition of lower amounts of wall-building materials such as maltodextrin.

In the selection process for a sugar to balance the osmotic pressure, due attention was paid to the glass transition temperature ( $T_g$ ) of several edible sugars. Materials with high  $T_g$  are easy to dry, whereas those with low  $T_g$  are impossible to dry since they remain in the fluid state under normal drying conditions. Trehalose with a  $T_g$  of 115°C is a much more suitable sugar than glucose ( $T_g=30$  °C) and sucrose ( $T_g=60$  °C)<sup>228</sup>. By adjusting the inlet and outlet temperatures at 170 and 100 °C, respectively, solid microcapsules were produced. The yield of the drying process (calculated using equation 8) was  $32.7 \pm 1.3$  % and the moisture content of the microcapsules  $3.9 \pm 0.5$  wt %. A freshly prepared  $W_1/O/W_2$  emulsion was analyzed by an optical microscope at 1000x magnification before spray drying (Figure 2.4-a). The inner aqueous droplets containing the carob polyphenols entrapped by big oil droplets can be clearly seen from the figure. Once dried, the morphology of the solid microcapsules was analyzed by ESEM. As can be seen in Figure 2.5, spray dried capsules are spherical with smooth surface that is related to a rapid drying velocity. The similar inner surface of the capsules can be noticed by breaking them (Figure 2.5-c). The structure of  $W_1/O/W_2$  emulsions was partially recovered after rehydration of the solid microcapsules, as can be seen in Figure 2.4-b. This figure shows

$W_1$  droplets within large oil droplets, as well as small oil droplets, suggesting that some entrapped polyphenols in the inner water phase were released.

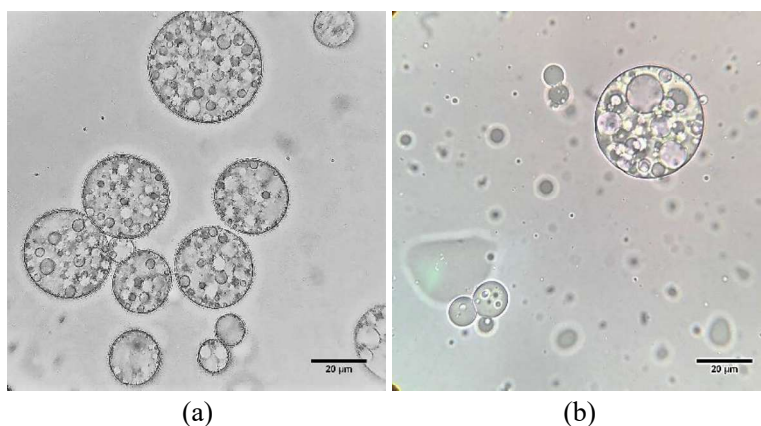


Figure 2.4. Microscopic images of  $W_1/O/W_2$  emulsions with 28.2 wt% trehalose in the external aqueous phase after one cycle of emulsification in DMTS: (a) freshly prepared and (b) rehydration of  $W_1/O/W_2$  spray dried capsules.

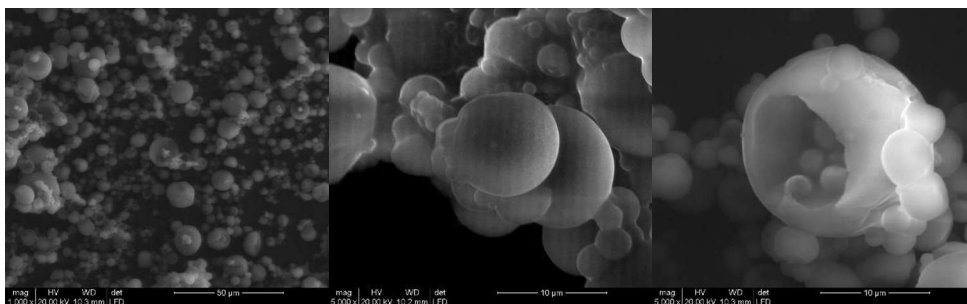


Figure 2.5. ESEM images of spray dried  $W_1/O/W_2$  emulsion capsules: (a) at magnification of 1000x; (b) at magnification of 5000x and (c) after mechanical break.

## 2.4. Conclusions

Forward osmosis is a suitable method to concentrate bioactive compounds such as polyphenols extracted from carob pulp. The highest feed solution temperature was more effective in terms of process time and polyphenol yield due to the increase in mass transfer coefficient. To protect the polyphenols obtained after FO, encapsulation in  $W_1/O/W_2$  emulsions was proven feasible using a low energy-high throughput emulsification system (DMTS), based on a microporous bed of silica beads. Regardless of the bulk agent (NaCl or trehalose) used to balance the osmotic pressure, encapsulation efficiency was between 77 and 87%, and emulsions showed a narrow droplet size distribution. In terms of productivity, the fluxes were significantly higher than the ones reported for different applications using DMTS. To extend the shelf-life of the encapsulated polyphenols, solid microcapsules were successfully produced by spray drying  $W_1/O/W_2$  emulsions containing a mixture of trehalose and maltodextrin as a wall material. After rehydrating

the solid microcapsules, the structure of the  $W_1/O/W_2$  emulsion was partially recovered. The results of this study show the potential of combining membrane-based processes to concentrate and encapsulate bioactive compounds as a strategy to valorize agri-food by-products under mild process conditions.



## Chapter 3

# Black Soldier Fly (*Hermetia illucens*) Protein Concentrates as a Sustainable Source to Stabilize O/W Emulsions Produced by a Low-Energy High-Throughput Emulsification Technology

### Abstract

There is a pressing need to extend the knowledge on the properties of insect protein fractions to boost their use in the food industry. In this study several techno-functional properties of a black soldier fly (*Hermetia illucens*) protein concentrate (BSFPC) obtained by solubilization and precipitation at pH 4.0–4.3 were investigated and compared with whey protein isolate (WPI), a conventional dairy protein used to stabilize food emulsions. The extraction method applied resulted in a BSFPC with a protein content of 62.44% (Kp factor 5.36) that exhibited comparable or higher values of emulsifying activity and foamability than WPI for the same concentrations, hence, showing the potential for emulsion and foam stabilization. As for the emulsifying properties, the BSFPC (1% and 2%) showed the capacity to stabilize sunflower and lemon oil-in-water emulsions (20%, 30%, and 40% oil fraction) produced by dynamic membranes of tunable pore size (DMTS). It was proved that BSFPC stabilizes sunflower oil-in-water emulsions similarly to WPI, but with a slightly wider droplet size distribution. As for time stability of the sunflower oil emulsions at 25 °C, it was seen that droplet size distribution was maintained for 1% WPI and 2% BSFPC, while for 1% BSFPC there was a slight increase. For lemon oil emulsions, BSFPC showed better emulsifying performance than WPI, which required to be prepared with a pH 7 buffer for lemon oil fractions of 40%, to balance the decrease in the pH caused by the lemon oil water soluble components. The stability of the emulsions was improved when maintained under refrigeration (4 °C) for both BSFPC and WPI. The results of this work point out the feasibility of using BSFPC to stabilize O/W emulsions using a low energy system.

This chapter has been published as:

Wang, J., Jousse, M., Jayakumar, J., Fernández-Arteaga, A., de Lamo-Castellví, S., Ferrando, M., & Güell, C. (2021). Black Soldier Fly (*Hermetia illucens*) Protein Concentrates as a Sustainable Source to Stabilize O/W Emulsions Produced by a Low-Energy High-Throughput Emulsification Technology. *Foods*, 10(5), 1048.



### 3.1 Introduction

The Food and Agriculture Organization (FAO) of the United Nations reports that the global population is likely to grow up to nine billion by 2050<sup>97,229</sup> inducing a dramatic increase of food demand. There is a general agreement that the conventional protein sources will not be able to provide the approximately 260 million tons of proteins required by 2050, hence, there is a need to explore alternative protein sources that are both sustainable and possess high nutritional value. Beans and legumes containing high protein content (e.g., beans 23.5%, lentils 36.7%, and soybean 41.1% in dry matter) involved in the human diet since ancient times can be a good alternative, and soy is nowadays the most valuable protein source for feed; however, to rely solely on plant proteins to fill the expected protein gap puts huge pressure on the already pressured agricultural fields and raises serious environmental concerns<sup>99,117,230–233</sup>.

Among the alternative protein sources, edible insects have drawn great attention in recent decades and FAO has claimed that edible insects are a good source of protein for dietary purposes<sup>99</sup>. Even though entomophagy, eating insects as foods, is being practiced by more than two billion people worldwide, most western developed countries have serious objections to consuming edible insects as a result of distaste and disgust about their nature and appearance<sup>99–103,234</sup>. Some studies showed that insect consumption was more acceptable in a masked way or when it was invisible in the food<sup>102,104,105</sup>, which encouraged the integration of edible insects as milled powders and/or pastes in food products, as well as using their different functional fractions such as proteins, fatty acids, and chitin<sup>66,82,85,235</sup>. Moreover, in January 2021, the EFSA Panel on nutrition has adopted a scientific opinion on the safety of yellow mealworm as a novel food pursuant to Regulation (EU) 2015/2283.

There are several applications of insect functional fractions, from a recent study on the production of nano-emulsions from insect oils with potential application as drug/bioactive delivery systems<sup>236</sup> to other studies that explore the antimicrobial activity of peptides purified from insect proteins<sup>61</sup>. There are several studies testing protocols for extracting/purifying the protein fraction from crude insect meal for black soldier fly (*Hermetia illucens*), mealworm (*Tenebrio molitor*), grasshopper (*Schistocerca gregaria*), honey bee (*Apis mellifera*), locust (*Locusta migratoria*), and cricket (*Gryllobes sigillatus*)<sup>65,68,76,80,82,85</sup>. Their procedures were based on the solubilization of protein in aqueous solution by adjusting pH values. Most of the studies on protein extraction/purification explore the potential functionality of the protein fractions. Gould and Wolf<sup>82</sup> used *T. molitor* protein as an emulsifier to stabilize sunflower oil-in-water emulsions produced by mechanical stirring; they obtained stable emulsions with droplet size smaller than emulsions stabilized with whey protein. Mishyna et al.<sup>68</sup> concluded that both *S. gregaria* and *A. mellifera* protein extracts have an emulsifying capacity comparable to whey protein; however, the insect source leads to some differences in the stability of the emulsions. Insect protein fractions have also been investigated with promising results as an ingredient in food formulations to replace meat in sausages<sup>237</sup> and meat batters<sup>238</sup>. Therefore, insect proteins, besides being used as a protein source, have the potential to be used in food and feed formulations to replace conventional proteins

(such as dairy proteins) as gelling and emulsifying agents. This potential and the variations in the properties depending on the insect species and the development stage deserve more research studies to better understand their techno-functional properties, which will be highly relevant for food/feed industry regarding the preparation, processing, and storage of their edible insect food products.

Black soldier fly (*Hermetia illucens*) is a true fly belonging to the family Stratiomyidae, whose larvae contain 42% crude protein and 29% fat on average in the dry matter<sup>239</sup>. Although the protein content in black soldier fly (BSF) larvae is lower than in insects from the orthoptera species such as adult locusts, grasshoppers, and crickets which were reported to have up to 77% protein content in the dry matter<sup>240</sup>, the advantage of BSF is the survival rate and the efficiency of converting organic materials into their own biomass<sup>231,232</sup>. Promising data on techno-functional properties of BSF protein fractions has been reported by Bußler et al.<sup>85</sup>, while Caligliani et al.<sup>235</sup> presented a systematic approach for BSF meal fractionation, and suggested the use of enzymatic treatment to tailor the properties of the protein fractions. Even though the data regarding the emulsifying activity of BSF protein extracts is scarce, its potential to replace conventional dairy proteins, such as whey protein, in food/feed formulations is worthy to study.

As for the emulsification process, membrane emulsification is a widely used technique with advantages such as reduced mechanical stress, low energy consumption, and uniform droplet formation<sup>130</sup>. One of the reported drawbacks of membrane emulsification is the low productivity, which can prevent widespread application in the industry. Dynamic membranes of tunable pore size (DMTS) have been applied to produce lemon oil emulsions<sup>136</sup> and double emulsions encapsulating pigments<sup>141</sup> in premix mode, that is, producing a coarse emulsion which is then refined by passing through the microstructured system. The DMTS system consists of a layer of glass microbeads supported by a nickel microsieve placed on the bottom of the membrane module. Because of this configuration, the DMTS system is easy to clean and re-use, and most importantly, requires low-energy input and yields high fluxes, showing its potential as a sustainable emulsification technology for industrial applications. This emulsification system has already been proved successful to produce sunflower oil-in-water emulsions stabilized with legume proteins<sup>142</sup>, but it has never been tested for insect proteins.

This research aimed to assess the potential of black soldier protein extracts to stabilize O/W emulsions produced by a low-energy high-throughput emulsification technology. To achieve this goal, first, a protocol for protein extraction was implemented to obtain BSF protein concentrate (BSFPC), second, relevant techno-functional properties (solubility, foaming capacity and foam stability, emulsifying activity, water/oil binding capacity, and interfacial tension) of BSFPC were obtained and compared to whey protein isolate, and third, sunflower and lemon oil emulsions were produced by the DMTS system and compared with whey protein. This study provides relevant data towards the use of more sustainable protein sources and technologies in food production.

## 3.2. Materials and Methods

### 3.2.1. Materials

Partially defatted black soldier fly powder (BSF powder) was kindly provided by Hexafly (County Meath, Ireland). Sodium hydroxide pellets (NaOH, Chem-Lab NV, Zedelgem, Belgium) and hydrochloric acid (37–38% HCl, J.T. Baker, Griesheim, Germany) were used for BSF protein extraction. Hexane ( $\geq 99\%$ , Sigma-Aldrich, Poznań, Poland) was used for removing lipid fraction. The BCA (bicinchoninic acid) assay kit (Pierce Biotechnology, Thermo Scientific, Rockford, IL, USA) was used for protein quantification giving the results in bovine serum albumin (BSA) equivalent value. Note that BSF concentrations that are BSA eq % are given hereinafter as % for simplicity. Phosphate buffer (pH 7) was prepared using sodium phosphate dibasic heptahydrate ( $\text{HNa}_2\text{O}_4\text{P}7\text{H}_2\text{O}$ , ACROS, Barcelona, Spain) and sodium phosphate monobasic monohydrate ( $\text{H}_2\text{NaO}_4\text{PH}_2\text{O}$ , ACROS, Barcelona, Spain). Acetic buffers (pH 3 and 5) were prepared with sodium acetate (Sigma-Aldrich, USA) and acetic acid (96%, Panreac, Barcelona, Spain). Buffers for pH 9 and 11 were prepared by sodium hydroxide (Chem-lab, Zedelgem, Belgium) and sodium tetraborate (ACROS, Spain). Whey protein isolate (WPI) was purchased from Davisco Foods International, Inc. (97.6%, Lot.JE151-4-420, Eden Prairie, MN, USA). Sunflower oil used as the oil phase for the O/W emulsions was purchased from a local supermarket (Borges S.A., Tarragona, Spain) and lemon oil (24L120 Limón Aroma) was ordered from Dallant S.A., Barcelona, Spain.

### 3.2.2. Protein Extraction

The protein extraction process was based on Zhao et al.<sup>73</sup> with some modifications. A total of 30 g of BSF powder was mixed with 150 mL of 0.25 M NaOH solution and the mixture was heated to 40 °C for one hour with constant agitation at 400 rpm on a magnetic stirrer (RCT ST, IKA, Staufen, Germany). The mixture was centrifuged (Meditronic 7000599, J.P. SELECTA, Barcelona, Spain) at 4490 rpm for 15 min and the lipid fraction on the top was carefully separated by pipets. The pellet was reserved for further extraction (twice more), while the pH of the supernatant was adjusted to 4.0–4.3 by adding 37% HCl and 1N HCl successively, followed by centrifugation (3750 rpm, 15 min) to obtain the precipitated proteins. After the centrifugation, the precipitated proteins were collected in plastic petri dishes and were kept at –60 °C until freeze drying. The precipitated proteins were freeze-dried (LYOQUEST-85 PLUS, Telstar, Barcelona, Spain) for 24 h at 0.2 mbar with the plates heated to 20 °C. Freeze-dried samples were combined, ground, and defatted. Defatting was carried out by stirring 50 g of freeze-dried powder and 250 mL of hexane for one hour, after which powders were settled down and the hexane layer was decanted. This procedure was repeated until no color was observed in the hexane layer. The remaining hexane in the powders was evaporated in the fume hood for 2 days. Next, samples were collected and were kept in a desiccator at 4 °C until being used.

The yield of the extraction process and the yield of the protein extraction in this study were defined as equations (3.1) and (3.2), respectively.

$$\% \text{Extraction yield} = \frac{\text{gram of BSFPC output}}{\text{gram of BSF powder input}} \times 100 \quad \text{eq (3.1)}$$

$$\%Protein\ yield = \frac{gram\ of\ protein\ in\ BSFPC\ output}{gram\ of\ protein\ in\ BSF\ powder\ input} \times 100 \quad eq\ (3.2)$$

### 3.2.3. Characterization of the BSF Powder and the BSFPC

#### Amino Acid Composition, Total Nitrogen, and Protein Content

Total nitrogen and amino acid contents were analyzed by AGROLAB Ibérica S.L.U (Tarragona, Spain) based on Kjeldahl and the European Union Commission Regulation REG(UE) 152/2009, III, F: 2009-02 methods, respectively. Nitrogen to protein conversion factor,  $K_p$ , was calculated from the ratio of the sum of amino acid residue weights to nitrogen content<sup>241</sup>. The calculated  $K_p$  factor was used to estimate the protein content in the samples.

#### Fourier Transform Mid Infrared Spectroscopy (FTIR)

The BSF powder and the BSFPC obtained after freeze drying and defatting were analyzed by following the protocol of Mellado-Carretero et al.<sup>242</sup> to qualitatively determine the efficiency of the defatting process. For the acquisition of the spectral profiles, 4 mg of each sample was taken randomly and placed onto the sample stage of a portable spectrometer Cary 630 (Agilent Technologies Spain SL, Madrid, Spain), equipped with a single bounce ATR diamond crystal accessory and a deuterated triglycine sulfate (DTGS) detector. A pressure clamp was used to ensure optimal contact between samples and the diamond crystal. A background scan was extracted from every sample scan to prevent the effect of environmental changes. Spectra were acquired from 4000 to 800  $cm^{-1}$  with 8  $cm^{-1}$  of resolution using MicroLab PC software (Agilent Technologies SL, Madrid, Spain).

### 3.2.4. Techno-Functional Properties of the BSFPC

#### Protein Solubility

Protein solubility was examined with the similar method as described in the literature<sup>68</sup>. As it is pH, temperature, and ionic strength dependent, the measurements were performed at room temperature and different pH buffers with the same molarity. A sample of BSFPC (0.2 g of powder) was dispersed into 10 mL of 0.2 M buffer (pH 3, 5, 7, 9, and 11) and stirred for 2 h. The mixtures were centrifuged (Biocen 22R, Orto Alresa, Madrid, Spain) at 3250 g for 20 min. The protein content in the supernatants was quantified using BCA assay kit. All the experiments were performed at least in duplicate. The protein solubility was calculated as equation (3.3).

$$\%PS = \frac{Soluble\ protein\ in\ the\ supernatant}{Total\ protein\ content\ in\ the\ powder} \times 100 \quad eq\ (3.3)$$

#### Isoelectric Point (pI) Determination

pI of soluble protein fraction from BSFPC was determined by zeta potential using Zetasizer Nano-ZS (Malvern Instruments, Worcestershire, UK). A total of 0.1% of BSFPC soluble protein solution was prepared at pH 7, and the pH was subsequently adjusted to 5.5, 5.0, 4.5, 4.0, and 3.5 by adding 1N HCl and 0.01N HCl gradually. Zeta

potential of supernatant after centrifugation at 3250 g for 20 min was measured and plotted against pH. The isoelectric point set to the pH region where the Zeta potential was close to 0.

### Water and Oil Binding Capacity

Water binding capacity (WBC) and oil binding capacity (OBC) were analyzed by the method as reported in the literature<sup>76</sup>. Briefly, for WBC, 0.5 g of powders were mixed with 2.5 mL of 0.2 M phosphate buffer (pH 7) and vortexed in a centrifugation tube for 60 s followed by centrifugation at 3250 g for 20 min at room temperature. The supernatant was decanted and the tube with the residual pellet was placed upside down on a filter paper for 60 min, to drain the residual non-bound water, before recording the weight. The WBC is calculated as shown in equation (3.4),

$$WBC \left[ \frac{g_{water}}{g_{DM}} \right] = \frac{m_1 - m_0}{m_{DM}} \times 100 \quad \text{eq (3.4)}$$

where  $m_0$  is the initial weight of the sample,  $m_1$  is the weight of residual after 60 min, and  $m_{DM}$  is the dry matter of the initial sample which can be calculated by measuring the weight changes of the fresh sample being kept in the oven (UN55, Memmert, Büchenbach, Germany) at 105 °C until no difference in weight is observed.

As for OBC, similarly, 0.5 g powders were mixed with 2.5 mL of commercial sunflower oil and vortexed for 60 s twice with 5 min of pause in between. The rest of the procedure is identical to WBC analysis using equation (3.5) for the calculation. Both WBC and OBC analyses were done in triplicate.

$$OBC \left[ \frac{g_{oil}}{g_{DM}} \right] = \frac{m_1 - m_0}{m_{DM}} \times 100 \quad \text{eq (3.5)}$$

### Foaming Capacity (FC) and Foam Stability (FS)

The foaming properties were analyzed following the literature<sup>68</sup> with minor modifications. A sample of 20 mL of 0.1% BSFPC solution prepared with 0.2 M pH 7 buffer was placed in a 50 mL plastic tube and subjected to vigorous rotor-stator homogenization (Ultra Turrax T18 digital, IKA, Staufen, Germany) at 1200 rpm for 2 min. The height of the foam layer after 10 s and 120 min was recorded. FC and FS (from experiments run in duplicate) were calculated using equations (3.6) and (3.7), respectively<sup>68</sup>,

$$\%FC = \frac{H_t}{H_0} \times 100 \quad \text{eq (3.6)}$$

$$\%FS = \frac{FC_{120}}{FC_0} \times 100 \quad \text{eq (3.7)}$$

where  $H_0$  is the initial height of protein solution in the tube,  $H_t$  is the height of generated foam after agitation,  $FC_0$  is the initial FC (after 10 s), and  $FC_{120}$  is the one obtained after 120 min.

### Emulsifying Activity (EA)

EA was evaluated at different protein concentrations (0.1%, 0.5%, and 1.0%) of both BSFPC and WPI using the method described by Purschke et al.<sup>76</sup>. Briefly, in a beaker 10 mL of protein solution and 10 mL of sunflower oil were homogenized using ULTRA TURRAX at 11,000 rpm for 30 s. An aliquot of 10 mL of the emulsion was transferred into a 15 mL scaled tube and centrifuged at 3250 g for 20 min at room temperature. Triplicates were performed for each sample. The height of the emulsified layer was noted, and the EA was calculated using equation (3.8)<sup>76</sup>,

$$\%EA = \frac{H_{EL}}{H_S} \times 100 \quad \text{eq (3.8)}$$

where  $H_{EL}$  is the height of emulsified layer and  $H_S$  is the total height of solution in the tube.

### Interfacial Tension Analysis

The pendant drop method was applied to monitor the interfacial tension changes of the interface of commercial sunflower oil and water phase by the tensiometer (CAM 200, KSV instrument, Espoo, Finland) coupled with the software CAM 2008. A capillary syringe filled up with water or protein solution (0.1% w/w) with a plastic cylindrical tip (diameter 0.71 mm) was fitted in the tensiometer. The tip was immersed in the sunflower oil in a quartz cuvette. A pendant drop was generated by a capillary syringe with a controlled volume of 15  $\mu\text{L}$  ( $\pm 2 \mu\text{L}$ ), and the interfacial tension was recorded immediately and every 5 min for 90 min or until it reached equilibrium. Reflective indices of 1.480 and 1.475 for sunflower oil and lemon oil were used for the calculation. Duplicates were performed for each water solution.

### 3.2.5. Premix Membrane Emulsification

#### Preparation of O/W coarse emulsion

A total of 150 g of O/W emulsion was prepared based on the formulation in Table 3.1. The whey protein solution was prepared by dissolving the desired amount of WPI in deionized water (or in 0.2 M phosphate buffer pH 7) and stirring for 2 h. The solution was kept in the fridge overnight for complete hydration. BSFPC solution was prepared by dissolving BSFPC powder and stirring for 1 h followed by the pH adjustment to 7 by 1 M NaOH. After further stirring for 2 h, the solution was kept overnight in the fridge. Protein concentration was quantified using the BCA assay kit after centrifugation twice at 3750 rpm for 15 min, and the required concentration of BSFPC solution was obtained by dilution with deionized water (or 0.2 M phosphate buffer pH7). The coarse emulsion was prepared by homogenizing the oil phase and water phase in a beaker using a rotor-stator homogenizer (Ultra Turrax T18 digital, IKA, Staufen, Germany) at 15,800 rpm for 2 min and at 15,400 rpm for 1 min with 30 s of pause every 1 min to avoid temperature rising.

Table 3.1. Composition of O/W emulsions.

Oil Phase	Oil Fraction	Emulsifier in Water Phase	Water Phase Medium
Sunflower oil or lemon oil	20 wt.%, 30 wt.%, or 40 wt.%	1% WPI 1% BSFPC 2% BSFPC	Deionized water or 0.2 M phosphate buffer pH7 <sup>1</sup>

<sup>1</sup> 0.2M phosphate buffer pH 7 was tested only for 20 and 40 wt.% lemon oil emulsions stabilized by 1% WPI, 1% BSFPC and 2%BSFPC.

### Emulsification with Dynamic Membranes of Tunable Pore Size (DMTS)

In a cylindric module, 2 g of 94.2  $\mu\text{m}$  glass microbeads (resulting in a height of 8.3 mm layer) were placed on top of a nickel sieve having a pore size of  $289 \times 13 \mu\text{m}$  (length  $\times$  width) with a thickness of 120  $\mu\text{m}$  as illustrated on Figure 1. A pressure vessel was connected to the DMTS module where the coarse emulsions were pressurized by nitrogen to pass through the micron-sized interstitial voids formed by the glass microbeads layer to achieve droplet breakup. The emulsions were collected in an Erlenmeyer placed above an electronic balance to record the mass gain over time. The same procedure was repeated four times (five emulsification cycles in total) to further refine the emulsions. The interstitial void diameter ( $d_v$ ) of the channels formed by glass microbeads was 78.4  $\mu\text{m}$ , calculated as equation (3.9),

$$d_v = \frac{4\varepsilon}{(1-\varepsilon)6/d_b} \quad \text{eq (3.9)}$$

where  $d_b$  is the microbeads diameter (94.2 $\mu\text{m}$ ) and  $\varepsilon$  is the porosity (0.55), which can be calculated using the particle ( $\rho_p$ ) and bulk ( $\rho_b$ ) densities of glass microbeads using equation (3.10).

$$\varepsilon = 1 - \frac{\rho_b}{\rho_p} \quad \text{eq (3.10)}$$

Transmembrane flux,  $J_{DMTS}$ , was calculated using equation (3.11),

$$J_{DMTS} = \frac{\phi}{\rho_e A} \quad \text{eq (3.11)}$$

where  $\phi$  is the mass flow rate acquired from the mass/time data recorded with the electronic balance,  $\rho_e$  is the emulsion density,  $A$  is the effective surface area of the DMTS.

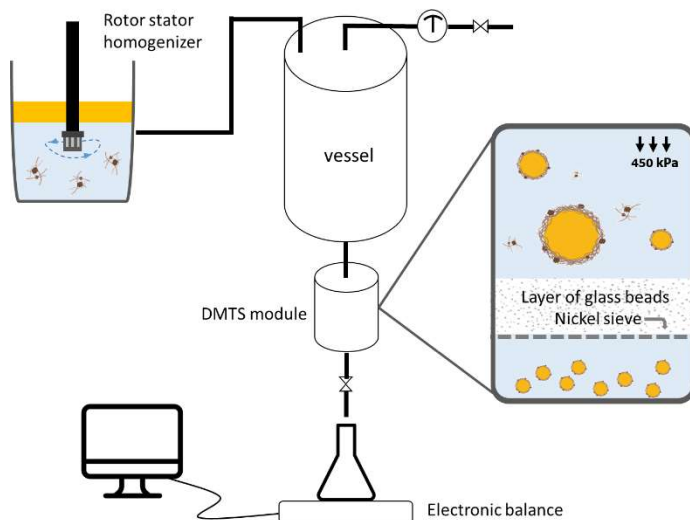


Figure 3.1. Premix emulsification and dynamic membrane of tunable pore size emulsification setup.

The dynamic membrane was disassembled once the emulsification was completed (5 cycles) and the nickel sieve and glass microbeads were reused after cleaning based on the protocol applied by Kaade et al.<sup>212</sup>. Dishwashing detergent and ethanol were used to clean glass microbeads.

### Particle Size and Distribution

The particle size distribution of O/W emulsions was measured after every emulsification cycle by laser diffraction using Mastersizer 2000 (Malvern Instruments, Worcestershire, UK). Particle reflective indices were set to 1.480 and 1.475 for sunflower oil and lemon oil, respectively, and the dispersant reflective index was set to 1.330. Mean droplet size and droplet size dispersion can be calculated, and expressed as Sauter mean diameter  $d_{3,2}$  (equation 3.12) and the span factor (equation (3.13)), respectively,

$$d_{3,2} = \frac{\sum n_i D_i^3}{\sum n_i D_i^2} \quad \text{eq (3.12)}$$

where  $n_i$  is the number of droplets, and  $D_i$  is the diameter of the  $i^{\text{th}}$  droplet,

$$\delta = \frac{d_{90} - d_{10}}{d_{50}} \quad \text{eq (3.13)}$$

where  $d_x$  is the droplet diameter corresponding to  $x\%$  volume on a cumulative droplet size distribution curve.

### Zeta Potential

Zeta potential of emulsions was measured using Zetasizer Nano-ZS (Malvern Instruments, Worcestershire, UK). Samples were diluted 100 times by deionized water. The same values of reflective indices for the particle (sunflower or lemon oil droplets)

and dispersant as those used in the measurement of particle size and distribution were also applied here.

### **Analysis of Emulsion Stability**

Several 10 mL aliquots were collected in tubes for every freshly produced emulsion. Emulsions were kept at room temperature (25 °C) and in refrigerator (4 °C) for 7 days. Droplet size distribution, as well as zeta potential were measured after 1, 3, and 7 days.

### **Statistical Analysis**

The data described are mean  $\pm$  standard deviation. Significant differences between the groups were determined using ANOVA and Tukey test ( $p < 0.05$ ).

## **3.3. Results and Discussion**

### **3.3.1. Chemical Composition of BSF Powder and BSFPC**

#### **Amino Acids, Total Nitrogen, and Protein Content**

The protein content in the BSFPC was determined based on the amino acids and total nitrogen contents and compared with the BSF powder. Nitrogen-to-protein conversion factor ( $K_p$ ) for insects is lower than the conventional value ( $K_p = 6.25$ ) due to the existence of non-protein nitrogen compounds such as chitin<sup>243</sup>. Therefore, it is necessary to recalculate the  $K_p$  from amino acids contents as described in Section 3.2.3. The  $K_p$  values calculated shown in Table 3.2 are slightly lower than the true values as they were calculated based on only 17 amino acids, which led to slightly lower amount of protein contents estimated. Most of the amino acid contents measured in BSFPC were higher than those in the BSF powder resulting in an increase of the  $K_p$  value from 4.71 to 5.36. It indicates that the extraction process effectively reduced non-protein nitrogen compounds<sup>235</sup>. Based on the calculated  $K_p$  values and the total nitrogen contents of the BSF powder and BSFPC, the protein contents were 39.00% and 62.44%, respectively, which are comparable to those (36.7% and 67.6%) reported by Janssen et al.<sup>243</sup> using pH 6 phosphate buffer in protein extraction.

Results showed the essential amino acid contents in BSFPC meet the FAO recommendation of protein quality. Some amino acids were two (histidine and threonine) and three times (phenylalanine and tyrosine) higher than the recommended values, except for undetermined content of tryptophan (Table 3.2). It also showed comparable protein quality to soybean, a plant sourced agriproduct. However, BSFPC contained slightly lower amount of leucine and lysine compared to casein protein. The protein extraction process resulted in a loss of total amount of sulphur amino acids (methionine and cysteine), which decreased from 35.4 mg/g protein in BSF powder to 28.2 mg/g protein in BSFPC, which is mainly due to the reduction of cysteine (from 0.43% DM in BSF powder to 0.36% DM in BSFPC). Even though cysteine is not classified as an essential amino acid, it is the key amino acid conforming disulphide bonds in high order protein structure<sup>244</sup>. The reduction of cysteine can be attributed to the strengthened protein's

tertiary and quaternary structure with multiple disulphide bridges of cysteines, which makes it difficult to extract out<sup>245</sup>.

Table 3.2. Amino acid composition, total nitrogen, and calculated Kp (nitrogen to protein conversion factor) value and protein content for BSF (black soldier fly) powder and BSFPC (black soldier fly protein concentrate), compared to soybean, casein, and FAO (Food and Agriculture Organization) recommendation for adults.

	<b>BSF Powder (% DM)</b>	<b>BSFPC (% DM)</b>	<b>BSF Powder (mg/g Protein)</b>	<b>BSFPC (mg/g Protein)</b>	<b>2013 FAO Soybean (mg/g Protein)</b>	<b>Casein (mg/g Protein)</b>	<b>Casein (mg/g Protein)</b> <sup>5</sup>
<b>Essential amino acid</b>							
His	1.71	2.60	43.8	41.6	16	25	32
Ile	2.12	3.68	54.4	58.9	30	47	54
Leu	3.36	5.80	86.9	92.9	61	85	95
Lys	3.06	5.12	78.5	82.0	48	63	85
Met+Cys <sup>3</sup>	1.38	1.76	35.4	28.2	23	24	35
Phe+Tyr <sup>4</sup>	5.23	9.43	134.1	151.1	41	97	111
Thr	1.96	3.21	50.3	51.4	25	38	42
Val	2.71	4.79	69.5	76.7	40	49	63
Trp	1.87 <sup>1</sup>	nd <sup>2</sup>	nd <sup>2</sup>	Nd <sup>2</sup>	6.6	11	14
<b>Non-essential amino acid</b>							
Asp	4.79	8.07	122.8	129.2			
Glu	6.17	8.53	158.2	136.6			
Ala	3.08	4.84	80.0	77.5			
Arg	2.52	3.92	64.6	62.8			
Gly	2.66	3.72	68.2	59.6			
Pro	2.74	4.10	70.3	65.7			
Ser	1.99	3.16	51.0	50.6			
Kp	4.71	5.36					
<b>Total</b>							
Nitrogen (%) <sup>3</sup>	8.28	11.65					
Protein content (%)	39.00	62.44					
Extraction yield (%)	35.8						
Protein yield (%)	59.3						

<sup>1</sup> value is referenced from Janssen et al.<sup>243</sup>; <sup>2</sup> not determined; <sup>3</sup> sum of sulphur amino acids (Cys and Met); <sup>4</sup> sum of aromatic amino acids (Phe and Try); <sup>5</sup> values from Young and Pellet<sup>248</sup>.

In this study, a 35.8% of extraction yield and a 59.3% of protein yield were obtained which was higher than the protein yield reported by Janssen et al.<sup>243</sup> (17.1%) and in the range (47% to 91%) of which obtained by Caligiani et al.<sup>235</sup> using three different extraction methods. As for the studies on other insect species, 17% to 30.8% of extraction

yields and 26.4% to 59.9% of protein yields were reported from *T. molitor*<sup>63,82,85,246</sup>, *Z. morio*, *A. diaperinus*<sup>247</sup>, *A. domesticus*, *B. dubia*<sup>63</sup>, *L. migratoria*<sup>80</sup>, *S. gregaria*, and *A. mellifera*<sup>68</sup>.

### Attenuated total Reflectance Fourier Transform Mid-Infrared Spectroscopy (ATR-FT-MIR)

Figure 3.2 shows the attenuated total reflectance FTIR raw spectra and Savitzky–Golay’s second derivatives (11 points) of BSF powder and BSFPC before and after defatting. Raw spectra and second derivatives of BSF powder and BSFPC before and after defatting show four important spectral regions: 2930–2850  $\text{cm}^{-1}$ , 1753  $\text{cm}^{-1}$ , 1630–1510  $\text{cm}^{-1}$ , and 1150–1020  $\text{cm}^{-1}$ . These spectral regions have also been reported by other authors that have analyzed different insect species, *P. succincta*, *C. roseapbrunner*<sup>81</sup>, *T. molitor*, *A. diaperinus*, *G. sigillatus*, *A. domesticus*, and *L. migratoria*<sup>242</sup>. Strong IR bands at 2924  $\text{cm}^{-1}$ , 2853  $\text{cm}^{-1}$ , and 1753  $\text{cm}^{-1}$  linked to  $\text{CH}_2$  asymmetric stretching,  $\text{CH}_2$  symmetric stretching, and  $\text{C}=\text{O}$  stretching of lipids, respectively<sup>249</sup>, are present in BSF powder and BSFPC before defatting spectra. In the spectrum of BSFPC after defatting, the IR band at 1753  $\text{cm}^{-1}$  disappeared and the absorbance of the IR bands at 2924  $\text{cm}^{-1}$ , 2853  $\text{cm}^{-1}$  significantly decreased.

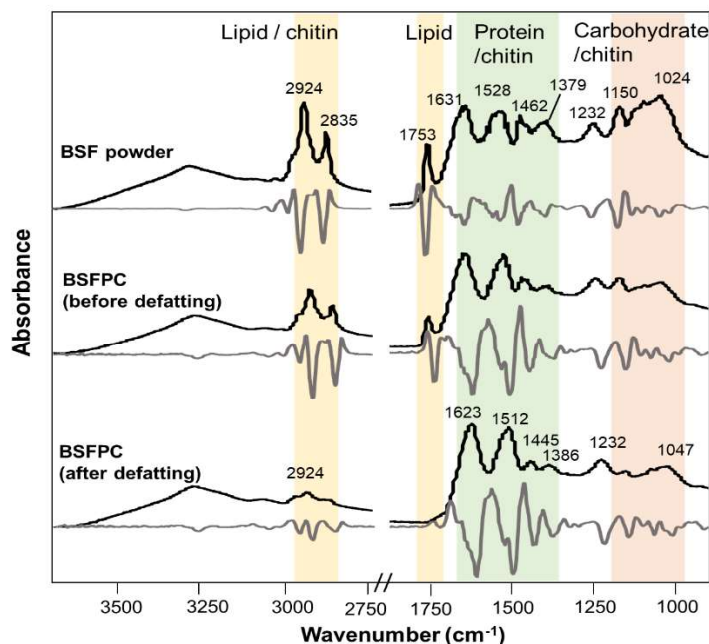


Figure 3.2. Attenuated total reflectance Fourier transform mid infrared spectroscopy (FTIR) raw spectra (black line) of BSF (black soldier fly) powder and BSFPC (black soldier fly protein concentrate) before and after defatting and the corresponding Savitzky–Golay’s second derivatives (grey line).

### 3.3.2. Techno-Functional Properties

To determine the techno-functional properties of BSFPC and assess its potential applications, solubility, WBC and OBC, FC and FS, EA and interfacial tension were analyzed and summarized in Figures 3.3 and 3.4.

#### Protein Solubility and Isoelectric Point (pI)

As for the protein application in aqueous media, solubility is of importance. Figure 3a shows that solubility of BSF powder and BSFPC depends largely on pH value, with the highest solubilities (19.1% and 38.0%) at pH 11, and lowest solubility (10.5 % and 12.4 %) at pH 5. Isoelectric point (pI) of BSFPC was determined to be in the range of pH 4.0 to 4.5 (Figure 3.3-a), which explained the lowest solubility observed at pH 5. This is in agreement with the range of protein pI (4–5) found in the literature of *T. molitor*<sup>65,85</sup>, *S. gregaria*<sup>65,68</sup>, *A. domesticus*<sup>65</sup>, *A. mellifera*<sup>68</sup>, and *H. illucens*<sup>85</sup>. Overall, the solubility values for BSF powder and BSFPC are comparatively lower than the ones reported for *T. molitor*<sup>85,246</sup>, and *S. gregaria* and *A. mellifera*<sup>68</sup>. Nevertheless, the BSFPC presented an improved protein solubility compared to the BSF powder shown by the two-fold increase of solubility at pH 7–11. Purschke et al.<sup>80</sup> also observed the synergic effect of ionic strength (1 % NaCl to 3 % NaCl) between pH 4 and pH 9 on protein solubility for *T. molitor* protein concentrate. Moreover, protein solubility can be improved after enzymatic hydrolysis of *A. domesticus* and *L. migratoria* powders<sup>66,76</sup>. None of these strategies were used in this study to increase the solubility of the BSFPC but they could be applied when solubility must be enhanced. Since some techno-functional properties such as foaming and emulsifying depend on the soluble protein fraction, based on the solubility results obtained, protein solutions at pH 7 were prepared to conduct foaming and emulsifying tests in the later sections.

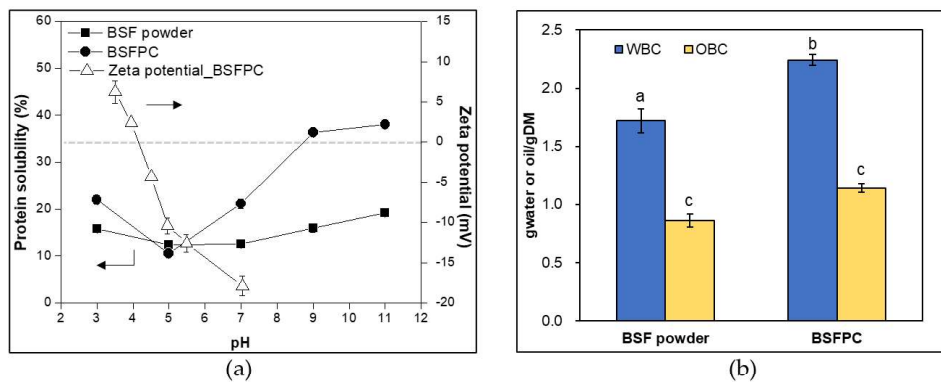


Figure 3.3. (a) Protein solubility at pH ranging from 3 to 11 and zeta potential at pH ranging from 3.5 to 7; (b) WBC (water binding capacity) and OBC (oil binding capacity) of BSF (black soldier fly) powder and BSFPC (black soldier fly protein concentrate). Different lowercase letters indicate significant differences at the  $p < 0.05$  level.

#### Water binding capacity (WBC) and oil binding capacity (OBC)

WBC and OBC are critical features of food ingredients in food processing and applications. They are related to the ability of taking up and retaining water and oil, respectively, which directly affect the texture and the flavor of the products, especially in meat and bakery<sup>250</sup>. As for foods with high protein content, protein molecule structure, amino acid composition, pH, hydrophilicity, and hydrophobicity on protein surface are determining factors of WBC and OBC<sup>65,250</sup>. BSFPC had WBC of 2.2 g water/g DM that is higher than the reported 0.4 g water/g DM and 1.5 g water/g DM for *T. molitor* protein extract and enzymatic hydrolysate of *L. migratoria* protein<sup>80,85</sup>, respectively, but lower than hexane defatted *T. molitor* powders (2.7 g water/g DM)<sup>251</sup> (Figure 3.3-b). As for the OBC, the value obtained for BSFPC (1.1 g oil/g DM) was higher than the reported one for *T. molitor* protein extract<sup>85</sup>, in the range of the ones for defatted *T. molitor*<sup>251</sup>, and lower than the one reported from enzymatic hydrolysate of *L. migratoria* protein<sup>80</sup>. The relatively higher WBC might be due to the higher protein content in the BSFPC which contains more hydrophilic groups to bind with water molecules. On the contrary, OBC can relate to the hydrophobic groups on the surface of protein molecules to bind with oil. Zielińska et al.<sup>65</sup> reported higher values of WBCs (2.18–3.95 g<sub>water</sub>/gDM) and OBCs (1.98–3.33 g<sub>oil</sub>/gDM) of protein extracts from *T. molitor*, *L. migratoria*, and *A. domesticus* than the ones found for BSFPC. The WBC and OBC of the BFS powder and BSFPC are comparable to plant-based flours such as wheat and rice, which were reported to have WBC from 1.4 to 1.9 g<sub>water</sub>/gDM, and OBC from 1.5 to 1.9 g<sub>oil</sub>/gDM, respectively<sup>252</sup>. Therefore, the BSFPC obtained in this study seems to be suitable in broad food applications entailing high protein content.

### **Foaming capacity (FC) and foam stability (FS)**

A total of 0.1 wt.% and 2 wt.% whey protein isolate (WPI) solutions and 0.1 wt.% soluble BSFPC solutions were compared in terms of FC and FS. As it is shown in Figure 3.4a, 0.1% BSFPC displayed higher FC (51%) than 0.1% WPI (21.4 %) and even than 2% WPI (41.7%). The mechanical agitation by Ultra Turrax introduced not only air bubbles but also energy into the whole system which can unfold the protein structure and change the protein conformation favoring the stabilization of air bubbles at the air-water interface. It is reported that protein extraction and enzymatic hydrolysis resulted in the generation of small peptides with surface-stabilizing residues which can rapidly diffuse onto the interface and rearrange the structure to improve FC<sup>65,66,68,80</sup>. Yi et al.<sup>63</sup> and Purschke et al.<sup>76</sup> discussed the impact of pH and ionic strength on foaming and found improved foaming behavior both at near protein pI and at increased NaCl concentration. Apart from the protein structure, the positive effect of carbohydrates on foaming was explained by Zielińska et al.<sup>65</sup> which might be also the case in this study due to the BSFPC contained 62.44% of protein and the remaining parts are possibly carbohydrates and soluble fibers.

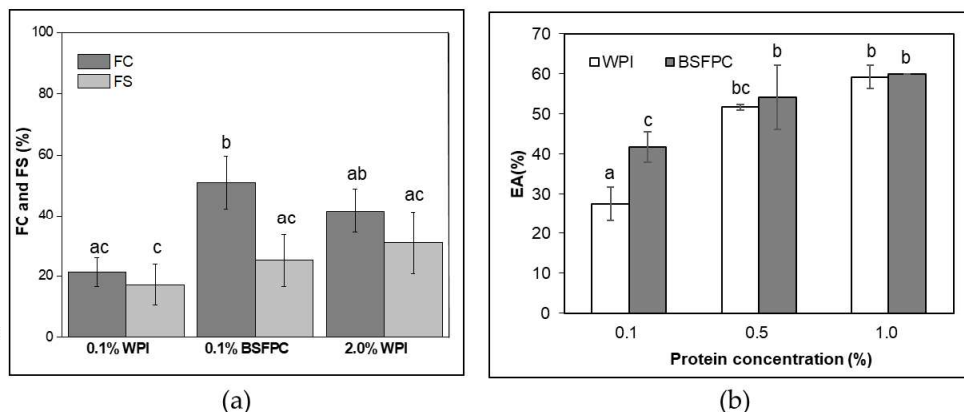


Figure 3.4. (a) FC (foaming capacity) and FS (foam stability) among different concentration of WPI (whey protein isolate) and BSFPC (black soldier fly protein concentrate); (b) EA (emulsifying activity) compared WPI with BSFPC. Different lowercase letters indicate significant differences at the  $p < 0.05$  level.

Regardless of the FC, 2% WPI solution showed the highest FS at 120 min after foam generation (31.1%), followed by 0.1% BSFPC (25.2%) and 0.1% WPI (17.3%). Due to the higher concentration of protein in the 2% WPI solution, the viscoelastic film formed at the air-water interface<sup>68,76</sup> was more durable. Nevertheless, BSFPC is considered to be suitable for preparing food products based on foams.

### Emulsifying activity (EA)

EAs of WPI and BSFPC at concentrations of 0.1%, 0.5%, and 1.0% were assessed as described at subsection 3.2.4. BSFPC at 0.1% presented higher EA than 0.1% WPI; however, both were not able to emulsify all oil. A visible top oil layer was observed after centrifugation, which was more significant for 0.1% WPI. When the protein concentration was raised to 0.5%, the gap in EA between WPI and BSFPC was reduced (51.7% and 54.2%, respectively) and the EA values were nearly equal (59.2% and 60.0%) at 1.0% protein concentration. It is worth mentioning that 0.5% BSFPC was able to emulsify all oil fraction, whereas 0.5% WPI was not competent to do so until further increased to 1%.

The results of EAs showed the same trend as the FC of WPI and BSFPC discussed in the previous section. As both properties are dependent on the functionality of hydrophobic groups on the protein surface and its molecular flexibility, it can be assumed that BSFPC can be used in emulsification as other conventional emulsifiers, such as WPI. This was also explained by Zielińska et al.<sup>65</sup> who reported improved EAs in insect protein extracts compared to their whole fraction powders, which was due to the increased protein contents in the protein extracts, especially with the amount of the hydrophobic amino acids. Purscke et al.<sup>76</sup> studied the effect of pH and ionic strength on the EA of *L. migratoria* protein concentrates concluding EA increased with the increase of ionic strength, and the highest EA was reached near the isoelectric point of the protein. However, regarding the functionality of a protein to be used as an emulsifier, there are

more factors to be considered, such as the stability of emulsions, droplet size distributions, and zeta-potential, which are explained in the later sections.

## Interfacial Tension

The effect of WPI and BSFPC on sunflower oil-water interfacial tension was analyzed as described in the subsection 3.2.4. As indicated in Figure 3.5, the interfacial tension of sunflower oil-water was around 25 mN/m and no significant reduction was observed due to the absence of surface-active compounds. The addition of WPI or BSFPC lowered the interfacial tension almost instantaneously to 13.7 and 8.4 mN/m, respectively. During the next 10 min, the interfacial tension decreased quickly, and from that point on the decrease was slower, reaching a plateau value of 10.3 mN/m and 3.4 mN/m for WPI and BSFPC, respectively. The dynamics of the interfacial tension is limited by the diffusion rate of emulsifiers and, subsequently, the time required to reach and adsorb at the interface. When analyzing the progress of interfacial tension in similar oil-water systems stabilized with food grade proteins<sup>142</sup> three different phases have been identified: (i) a lag-time controlled by the initial migration of protein molecules to the interface, (ii) a sharp decrease by absorption of protein molecules on interface, and (iii) a slow decrease to reach pseudo-equilibrium interfacial tension by rearrangement of protein molecules and multilayer-film formation. Results in Figure 3.5 show a two-phase process with no significant lag time, and a faster diffusion and adsorption of BSFPC resulted in lower interfacial values at time 0 than WPI. Differences in the molecular weight, protein composition, and structure may lead to differences in the performance of BSFPC to reduce the interfacial tension in the sunflower oil-water<sup>82,253</sup>.

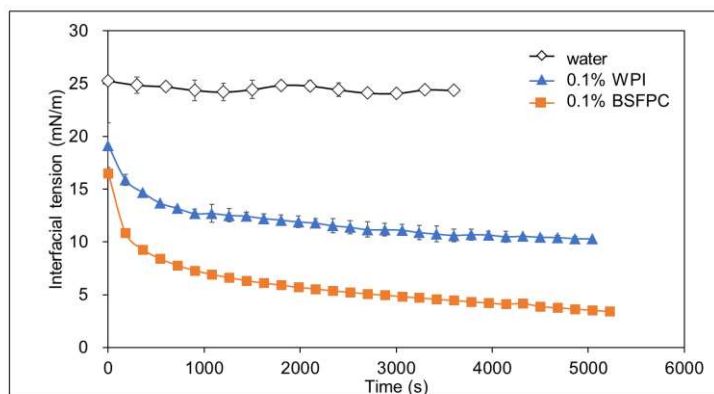


Figure 3.5. Interfacial tension between aqueous solutions of water, 0.1% WPI (whey protein isolate) and 0.1% BSFPC (black soldier fly protein concentrate), respectively, and sunflower oil (25 °C).

This finding agrees with the results reported by Gould and Wolf<sup>82</sup> who compared the effects of whey protein and *T. molitor* protein on the purified sunflower oil-water interface, and obtained equilibrium interfacial tensions of 13 mN/m and 12 mN/m for whey protein and *T. molitor* protein extract, respectively.

### 3.3.3. Dynamic Membrane of Tunable Pore Size (DMTS) Emulsification

After proving the emulsifying capacity of BSFPC at certain conditions of rotor-stator homogenization, we assessed their ability to stabilize emulsions produced with a low-energy membrane emulsification technique. Premix membrane emulsification with DMTS was used to obtain BSFPC and WPI-stabilized O/W emulsions formulated with sunflower (SO) or lemon oil (LO).

#### Droplet Size Distribution

Both oils are widely used in the food industry in the form of an emulsion, although they show important differences in composition and water solubility. SO, broadly used as a medium for delivering lipophilic micronutrients such as carotenoids and vitamin E<sup>254</sup>, is a complex mixture of fatty acids, totally immiscible in water, while LO, used as a flavoring and antimicrobial agent, is rich in terpenes and partially water soluble<sup>255,256</sup>.

As can be seen in Figure 3.6, BSFPC was able to stabilize O/W emulsions to a similar or even to a higher extent than WPI all along the emulsification process. Notice that all proteins were prepared with no buffering solution. Besides, the different nature of each oil strongly impacted the progress of droplet size and span, especially at the highest oil fraction. During DMTS emulsification, droplets break up as they go through the interstitial voids between the microbeads that make up the dynamic membrane, in this case with a mean diameter of 78.4  $\mu\text{m}$ . In most cases, droplet size reduction followed an analogous pattern: a large droplet size reduction took place at the first emulsification cycle, after which there were only minor reductions with a slight increase in span, which agrees with the studies using the same set-ups<sup>134,144</sup>.

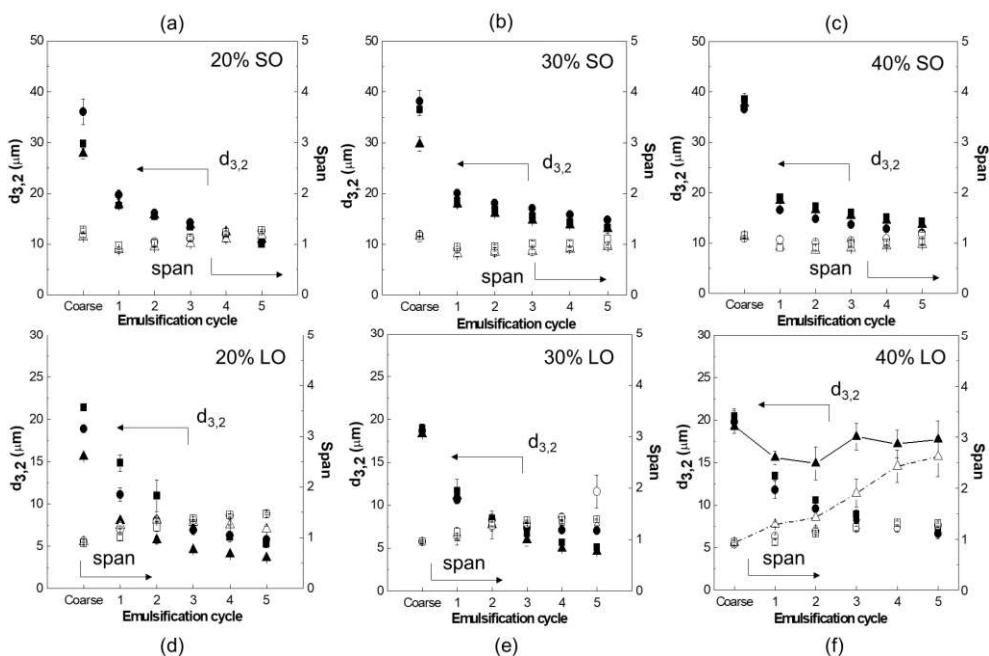


Figure 3.6. Sauter mean diameter ( $d_{3,2}$ , full symbols) and span (empty symbols) versus the number of emulsification cycles for emulsions at different oils and oil fractions: (a) 20% SO (sunflower oil); (b) 30% SO; (c) 40% SO; (d) 20% LO (lemon oil); (e) 30% LO; and (f) 40% LO. (▲  $d_{3,2}$ -1% WPI (whey protein isolate); ●  $d_{3,2}$ -1% BSFPC (black soldier fly protein concentrate); ■  $d_{3,2}$ -2% BSFPC; △ span-1%WPI; ○ span-1% BSFPC; □ span-2% BSFPC).

As for SO emulsions,  $d_{3,2}$  and span reached values of  $12.5 \pm 1.8 \mu\text{m}$  and  $1.1 \pm 0.1$ , respectively, after five cycles of DMTS emulsification regardless of the emulsifier and oil fraction, even though  $d_{3,2}$  of the coarse emulsion (cycle 0) ranged from  $28 \mu\text{m}$  to  $40 \mu\text{m}$  for emulsions with 20% and 40% oil fraction, respectively. Therefore, the surface-active properties of BSFPC and WPI were able to stabilize even the highest oil-in-water interface area created during emulsification of 40% oil fraction emulsions.

Compared to SO, LO emulsions showed smaller droplet size of the coarse emulsions with values ranging from  $18 \mu\text{m}$  to  $22 \mu\text{m}$  because of the lower interfacial tension of the LO-water system ( $12.9 \pm 0.2 \text{ mN/m}$ <sup>257</sup> and  $11.82 \text{ mN/m}$ <sup>258</sup>) compared to the SO-water system ( $25 \text{ mN/m}$ , Figure 5). After the refining process with DMTS,  $d_{3,2}$  decreased to values between  $4 \mu\text{m}$  and  $7 \mu\text{m}$  and span ranged from 1 to 2 when oil fraction was kept below 30% (Figure 6d–f). However, when the oil fraction increased to 40%, WPI stabilized emulsions could not further get refined in DMTS after three cycles what resulted in higher values of  $d_{3,2}$  and span than those obtained with BSFPC stabilized emulsions, which could be successfully refined over five emulsification cycles (Figure 6f). The poor performance of WPI as an emulsifier in the LO/W system could be linked to the chemical composition of LO, containing anhydrous acids and phenolic acids from the peel<sup>259,260</sup>, able to diffuse in the water phase and reduce pH below the WPI isoelectric point, in a range of 4.8–5.1. The water phase of LO/W emulsions containing 40% oil fraction showed a pH of 5.03 that may cause aggregation and precipitation of whey proteins and, in turn, a reduction of their surface-active capacity. At these conditions, the slightly lower isoelectric point of BSFPC (pH 4.0–4.5) was more favorable to stabilize LO/W emulsions with a 40% oil fraction.

To confirm the impact of pH on protein performance to stabilize LO/W emulsions, a set of experiments was carried out using 0.2 M phosphate buffer pH 7 as water phase. LO/W emulsions having 20% and 40% oil fraction were formulated with 1% WPI, 1% BSFPC, or 2% BSFPC. Figure 3.7 shows how, under these pH conditions, whey proteins were able to successfully stabilize LO/W emulsions during emulsification. After five emulsification cycles, emulsions with 20% oil fraction showed  $d_{3,2}$  of  $3.1 \mu\text{m}$  and span of 0.98, while those emulsions with 40% oil fraction had a  $d_{3,2}$  of  $3.6 \mu\text{m}$  and span of 1.15. Regarding BSFPC, although it also stabilized LO/W emulsions in the five cycles of DMTS emulsification, it was not able to maintain the span that increased over the process. The results obtained from WPI emulsified LO emulsions with 20% and 40% oil fractions were similar to what reported by Kaade et al.<sup>136</sup> which had slightly smaller  $d_{3,2}$  due to the smaller-size emulsifier Tween 20 was used.

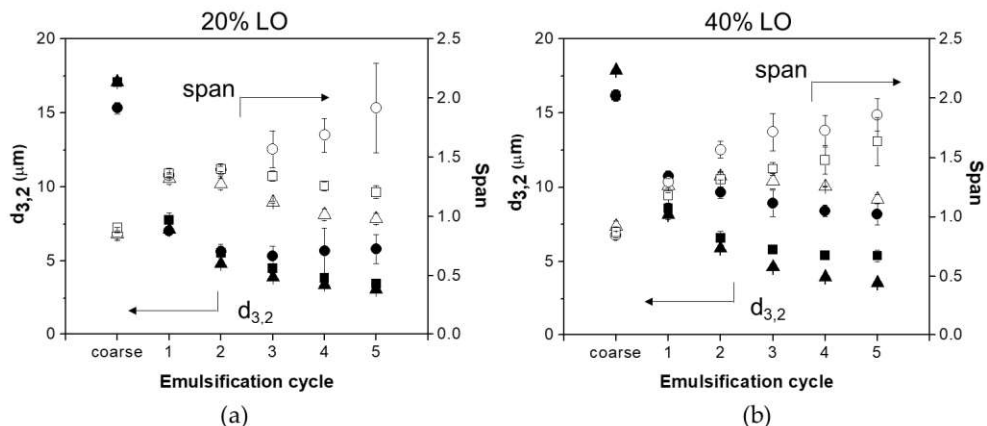


Figure 3.7. Sauter mean diameter ( $d_{3,2}$ , full symbols) and span (empty symbols) versus the number of emulsification cycles for produced LO (lemon oil) emulsions with 0.2 M phosphate buffer in the water phase at different oil fractions: (a) 20% LO and (b) 40% LO. ( $\blacktriangle$   $d_{3,2}$ -1 % WPI (whey protein isolate);  $\bullet$   $d_{3,2}$ -1 % BSFPC (black soldier fly protein concentrate);  $\blacksquare$   $d_{3,2}$ -2 % BSFPC;  $\triangle$  span-1%WPI;  $\circ$  span-1% BSFPC;  $\square$  span-2% BSFPC).

## Productivity

The productivity of the emulsification process, measured as flux during emulsification, is a key parameter for process scale-up. Fluxes obtained during the fifth emulsification cycle of SO emulsions ranged from  $206 \text{ m}^3\text{m}^{-2}\text{h}^{-1}$  to  $481 \text{ m}^3\text{m}^{-2}\text{h}^{-1}$  and the ones of LO emulsions were between  $231 \text{ m}^3\text{m}^{-2}\text{h}^{-1}$  and  $617 \text{ m}^3\text{m}^{-2}\text{h}^{-1}$ , depending on the oil fraction (Figure 8). The higher values obtained for LO emulsions can be attributed to the lower viscosity of this oil ( $1.41 \text{ mPa}\cdot\text{s}$  at  $25 \text{ }^\circ\text{C}$ )<sup>257</sup> compared to the one of SO ( $48.8 \text{ mPa}\cdot\text{s}$  at  $26 \text{ }^\circ\text{C}$ )<sup>261</sup> since as in any membrane system, flux is inversely proportional to the viscosity. Consequently, the lowest flux values always correspond to the emulsions with the highest oil fraction. As for the effect of the protein type and concentration, Figure 8 shows that regardless of the emulsion formulation, refining emulsions stabilized with WPI resulted in higher fluxes than the ones stabilized with BSFPC. Given that BSFPC had a protein content of 62.4% and the impurities can be carbohydrates and soluble fibers, it is thought that they contributed to increase the viscosity of the continuous phase. The effect of the viscosity of the continuous phase on the flux for the DMTS system has been previously seen by Kaade et al.<sup>136</sup>, who reported higher fluxes during the emulsification of LO emulsions stabilized with 2 wt.% Tween 20 than the ones obtained using 1% WPI. Moreover, proteins and other compounds in BSFPC stabilized emulsions can also result in fouling of the DMTS system, compared to emulsions stabilized with WPI as already observed during premix emulsification with several microstructured systems<sup>135,136,262,263</sup>.

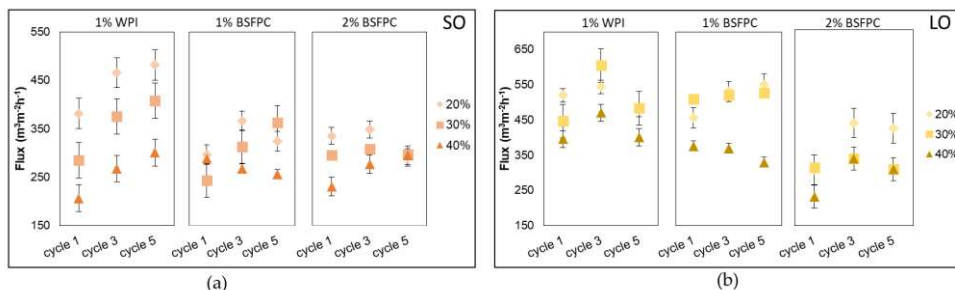


Figure 3.8. Transmembrane fluxes obtained at cycle 1, 3, and 5 during DMTS (dynamic membrane of tunable pore size) emulsifications of (a) SO (sunflower oil) emulsions and (b) LO (lemon oil) emulsions with different formulations.

### Stability of the Emulsions

SO emulsions stabilized with WPI (1%) and BSFPC (1 and 2%) with oil fractions of 20%, 30%, and 40% were kept at room temperature (25 °C) for seven days. Samples were measured on days 1, 3, and 7 of storage to follow changes in the droplet size distribution. Although all the emulsions had creaming after one day of storage, it can be seen from the droplet size distribution measurements (Figure 3.9) that SO emulsions, in general, can maintain its  $d_{3,2}$  and span during seven days of storage at 25 °C with a minor increase in  $d_{3,2}$  (<2  $\mu\text{m}$ ) and span (<0.5). There was a moderate increase in span for the emulsions stabilized with 1% BSFPC with 20% SO at day 7 which can be the aggregation of oil droplets due to the protein-protein interaction<sup>264</sup>. In agreement with droplet size distribution evolution in time, zeta potential of 1% BSFPC SO emulsions kept at 25 °C was below  $-30$  mV (Figure 3.10), the reference value for sufficient electrostatic repulsion to prevent droplet coalescence. SO emulsions stabilized by WPI showed a stronger surface repulsive effect (zeta potentials between  $-45$  mV and  $-40$  mV) than the ones stabilized by BSFPC ( $-40$  mV to  $-35$  mV).

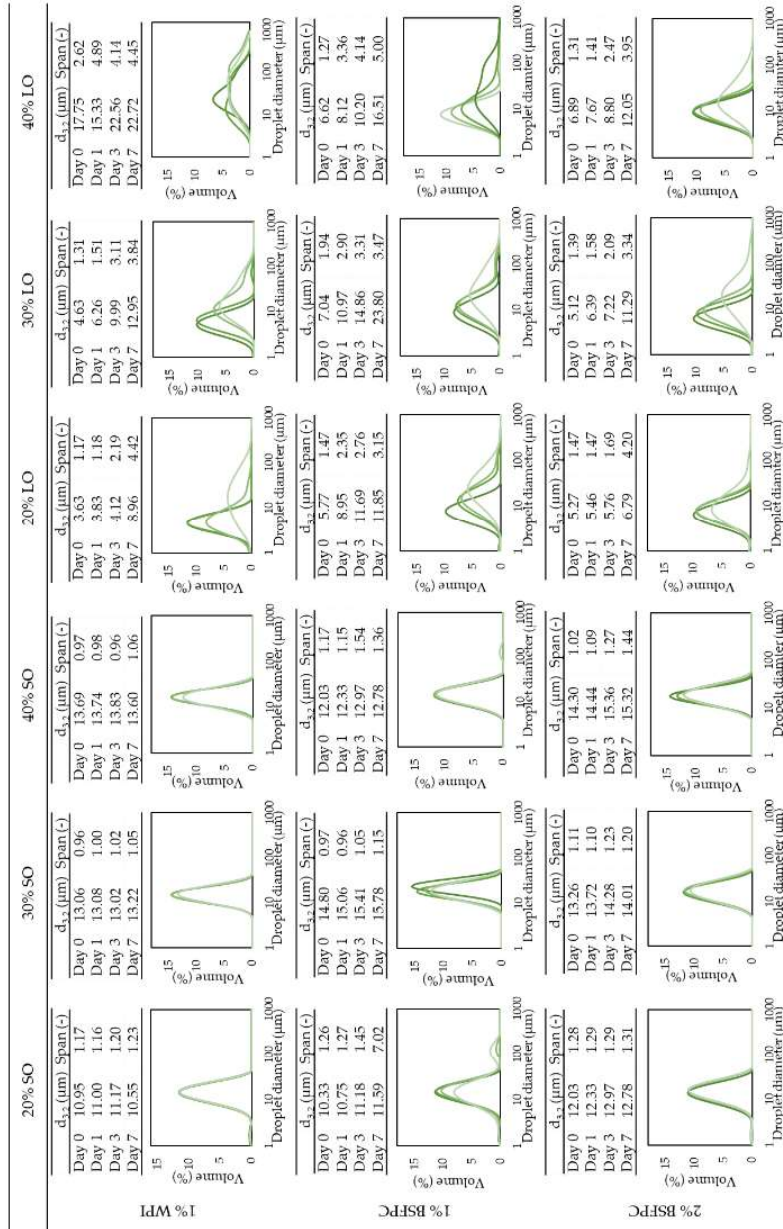


Figure 3.9. Particle size distribution of SO (sunflower oil) and LO (lemon oil) emulsions (no buffer added) stabilized by 1%WPI (whey protein isolate), 1% BSFPC (black soldier fly protein concentrate), and 2% BSFPC at day 0, day 1, day 3, and day 7 of storage at room temperature (25 °C). The color transparency scale indicates the length of storage time: from darkest to lightest refer fresh emulsion (day 0), day 1, day 3, and day 7.

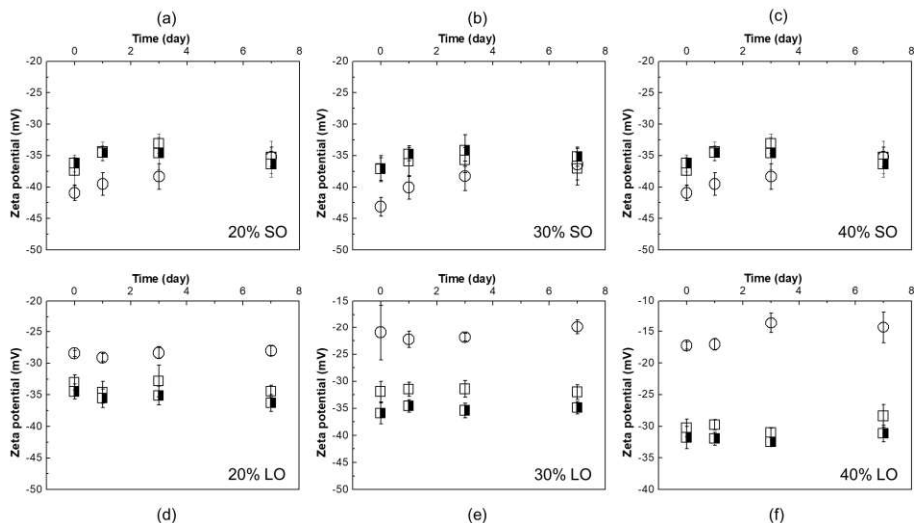


Figure 3.10. Zeta potential versus storage time at room temperature (25 °C) for produced emulsions (no buffer added) at different oils and oil fractions: (a) 20% SO (sunflower oil); (b) 30% SO; (c) 40% SO; (d) 20% LO (lemon oil); (e) 30 % LO; and (f) 40 % LO. (○) 1% WPI (whey protein isolate); (□) 1% BSFPC (black soldier fly protein concentrate); and (■) 2% BSFPC).

As for LO emulsions, the ones prepared with unbuffered proteins were kept at room temperature (Figure 3.9), while the emulsions prepared with buffered proteins were kept at both room temperature and refrigeration (Figure 3.11). The emulsions without buffer showed a significant increase in  $d_{3,2}$  and span after seven days of storage at 25 °C, regardless of the protein used. These changes agree with the zeta potential values (−28.4 mV to −17.3 mV, Figure 3.10d–f) of WPI stabilized emulsions, which indicate a tendency to droplet coalescence. In LO emulsions the pH decreases to values close to the pI of WPI, affecting the protein conformation and hence emulsion stability. Since the  $I_p$  of BSFPC used in this study is slightly lower than the one of WPI, the decrease of pH has a lower impact on the protein conformation. The emulsions showed a lower increase of  $d_{3,2}$  and span after seven days of storage at 25 °C than emulsions stabilized with WPI. For BSFPC the zeta potential values were maintained in the range of −35.9 mV to −30.3 mV for all the emulsions. As for the LO emulsions prepared with phosphate buffer, the ones with WPI showed a slight increase of  $d_{3,2}$  and span after seven days of storage at 25 °C and almost no changes when stored at 4 °C. The stability of these emulsions correlates well with their zeta potential values, −70 mV to −50 mV (Figure 3.12). However, when using a phosphate buffer to produce emulsions with BSFPC,  $d_{3,2}$  and span increased more than for the unbuffered emulsions at 25 °C. Decreasing the storage temperature had a positive effect on the emulsion stability, mainly for the lowest oil fraction. From these results, it seems that the BSFPC obtained in this work could be a better option for encapsulating lemon oil without the need of buffering the pH of the continuous phase.

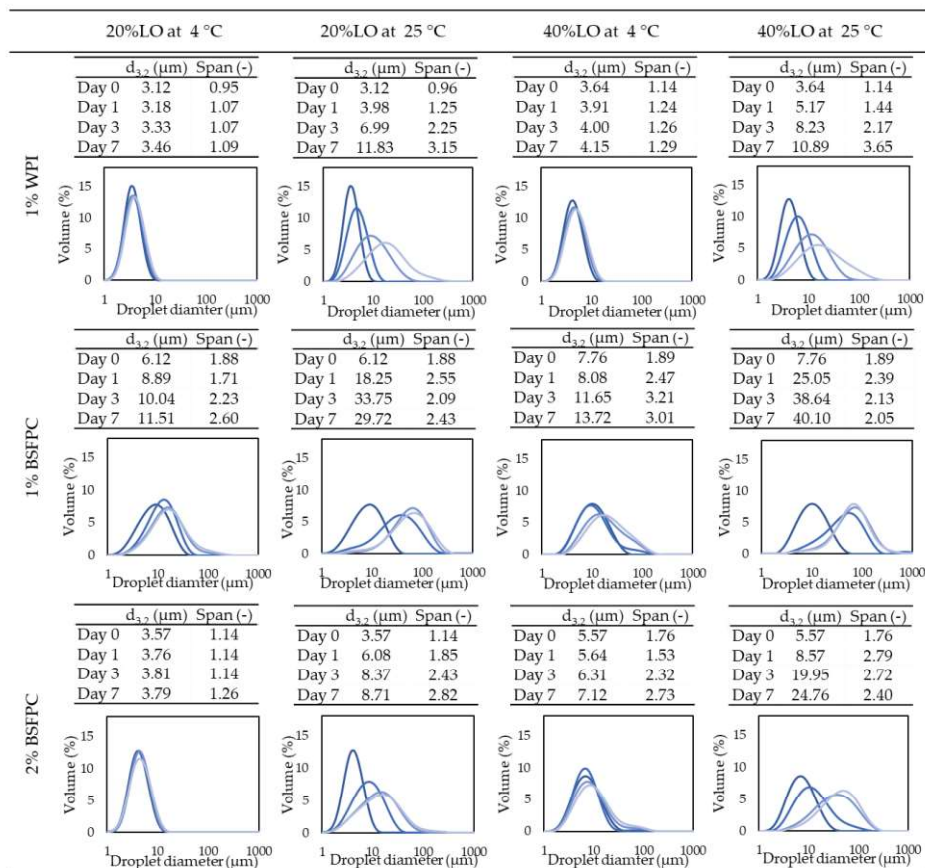


Figure 3.11. Particle size distribution of LO (lemon oil) emulsions stabilized by buffered 1% WPI (whey protein isolate), buffered 1% BSFPC (black soldier fly protein concentrate), and buffered 2% BSFPC after day 0 fresh emulsion, day 1, day 3, and day 7 of storage at room temperature (25 °C) and in fridge (4 °C). The color transparency scale indicates the length of storage time: from darkest to lightest refer fresh emulsion (day 0), day 1, day 3, and day 7.

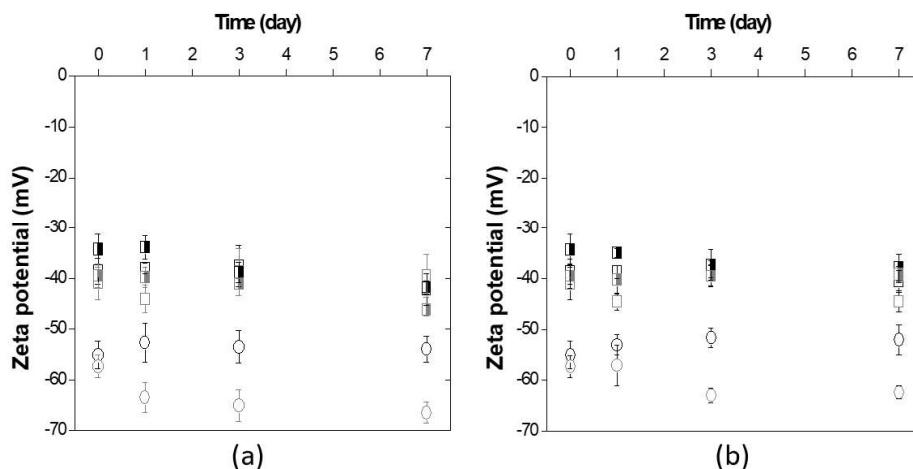


Figure 3.12. Zeta potential of LO emulsions (0.2 M phosphate buffer pH 7) versus storage time: (a) at room temperature (25 °C); (b) in fridge (4 °C). (○ 20%LO-1% WPI; □ 20%LO-1% BSFPC; ■ 20%LO-2% BSFPC; ○ 40%LO-1% WPI; □ 40%LO-1% BSFPC and ■ 40%LO-2% BSFPC;).

### 3.4. Conclusions

This study presents a holistic approach to the use of black soldier fly protein to stabilize food emulsions. The extraction process enabled enrichment of the protein content from 39% (original powder) to almost 63% thereby resulting in a protein concentrate (BSFPC). The essential amino acid profile of BSFPC is similar to soybean and casein and meets the FAO recommendation. As for the techno-functional properties of the BSFPC compared to WPI, it has been proven that BSFPC has higher FC and FS than WPI at low protein concentration (0.1%). Moreover, it was found that BSFPC has higher values of EA for low protein concentration (0.1%) than WPI and comparable values to WPI for 2% concentration. These results show the potential of BSFPC to be used in food formulations to replace totally or partially WPI. Moreover, the ability of BSFPC to lower the interfacial tension in the sunflower oil/water system as well as the values for WBC and OBC, point out the high potential of this protein to stabilize food emulsions. This has been proved using BSFPC to stabilize emulsions with two oils frequently used in the food industry, such as sunflower oil and lemon oil. The emulsions have been produced using a low-energy high-throughput system previously tested with conventional food emulsifiers. Droplet size distribution and fluxes obtained for sunflower oil emulsions stabilized with BSFPC are comparable to the ones obtained with emulsions stabilized with WPI. For lemon oil emulsions, however, BSFPC successfully reduced droplet size distribution of emulsions with 20% to 40% oil fraction, while the ones produced with WPI for 40% oil fraction showed an increase in the droplet size distribution from the third emulsification cycle onwards. It has been seen that since lemon oil is partially soluble in water when the emulsions have more than 30% oil fraction, there is a decrease in the pH of the emulsion. For WPI this pH decrease leads to a value close to pI of the protein, and therefore lowering its ability to stabilize the oil-water interface. Since the BSFPC has a lower pI, this phenomenon is not that important. As for the storage stability of the emulsions, the results point out that BSFPC has comparable results to WPI

for sunflower oil at 4 °C. For lemon oil, or at higher temperatures (25 °C) WPI can better maintain the droplet distribution if the pH can be controlled. Even though further research is required to improve the protein extraction process to improve its solubility, the results of this study show the potential of BSFPC to become a sustainable protein for the food industry.

## Chapter 4

# Green solvents for lesser mealworm (*Alphitobius diaperinus*) powder defatting: effect on the lipidic profile and on the emulsifying properties of the resulting protein concentrates

### **Abstract**

In view of the expected industrial bio-fractionation of insects, it is important to assess the impact of extraction methods and materials used on the techno-functional properties of specific fractions such as lipids and proteins. In this study, several kinds of organic solvents such as hexane, isopropanol, ethanol and 2-methyltetrahydrofuran (2-MeTHF) were selected for lipid extraction from lesser mealworm (*Alphitobius diaperinus*), and their effects were assessed on the extraction efficiency and the composition of extracted lipids. In addition, the lesser mealworm protein concentrate (LMPC) was produced from protein extraction of defatted powders by different solvents, and their emulsifying property was evaluated. The oil-in-water (O/W) emulsions were produced via premix emulsification coupled with a low-energy high-throughput dynamic membrane of tunable pore size (DMTS). Among the solvents used, the 2-MeTHF presented much higher extraction and recovery efficiency and with a second higher lipid yield. LMPC obtained from defatted powders by different solvents showed similar emulsifying properties and capacity to stabilize O/W emulsions over time, irrespective to the solvents used in the defatting step. Solid microcapsules were successfully produced from O/W emulsions stabilized with LMPC in the presence of maltodextrin, and the liquid emulsions could be reconstituted after rehydration.





## 4.1 Introduction

The use of protein fractions obtained from edible insects has drawn increasing attention in the recent decades to fill the gap of the expected protein demand by 2050<sup>63,65,82,99</sup>. However, there are still a small number of applications in the food and feed products, that are expected to increase after the EFSA favorable opinion about the safety of yellow mealworm (*T. molitor*) larvae<sup>122</sup>, migratory locust (*L. migratoria*)<sup>124</sup> and house cricket (*A. domesticus*)<sup>123</sup>. Insect powders have a variable lipid content between 10% and 30% on a wet weight basis<sup>247</sup>, and up to 75% based on dry weight basis<sup>265,266</sup>, depending on the species and the metamorphic stage. Lipids are a source of energy, and dietary fats are important macronutrients. In the lipid profile of edible insects, essential fatty acids including linoleic (18:2 $\omega$ 6) and linolenic (18:3 $\omega$ 3) and their respective derivatives are found, with the ratio of polyunsaturated to saturated fatty acids in the range of 0.22-1.75, and the ratio of  $\omega$ -6 to  $\omega$ -3 ranging from 0.33-204.15, which are highly dependent on species, feed, environmental conditions, and the stage of life<sup>247,266-268</sup>.

Aqueous extraction, three-phase partitioning, Soxhlet, Folch, and supercritical CO<sub>2</sub> are previously implied in lab scale for the study of defatting efficiency of insect powders and the lipid profile<sup>247,267</sup>. Different polarity of the solvent may result in slightly different lipid profile: for example, the several insect lipids extracted by Soxhlet method with petroleum ether as solvent and Folch methods using dichloromethane and methanol as solvent contained free fatty acids and glycerides, which are absent from the one extracted with demineralized water, which contained a higher amount of  $\omega$ -3 with a low ratio of  $\omega$ -6 to  $\omega$ -3 and less polar lipids<sup>267</sup>. Besides the lipid extraction yield is highly dependent on the extraction methods: for instance, the lipid extraction yield on *A. domesticus* using Soxhlet method with ethanol as a solvent was 22.7% w/w while it was reduced to 11.9% w/w when using supercritical CO<sub>2</sub><sup>247</sup>. However, a regular Soxhlet extraction normally requires a long processing time (~8h) with heating (40-70°C)<sup>269</sup>, which is energy-consuming and unsuitable for heat-sensitive compounds. Therefore, in most of the lab-scale research focused on the fractionation of proteins from insect powders, the pre-defatting step is carried out by solvent mixing and decantation process. Adámková et al. examined lipid profile on three different mealworm species, *Z. morio* (giant mealworm), *T. molitor*, and *A. diaperinus* (lesser mealworm/buffalo worm), among which *Z. morio* showed the highest lipid total amount of 390±4 g.kg<sup>-1</sup> in DM, while *T. molitor* contained higher concentration of polyunsaturated lipids compared to saturated lipids (ratio in weight>1)<sup>270</sup>.

In the commercial edible oil processing, such as oil extraction from oilseeds, hydraulic pressing, expeller pressing and solvent extraction using hexane are implied. Even though hexane is a widely used solvent in food extraction processes because of its excellent solubilizing ability on lipophilic compounds, easy oil recovery and narrow boiling point, it is known to be an air pollutant due to its toxicity and harmfulness<sup>271</sup>. 2-methyltetrahydrofuran (2-MeTHF), a biomass-derived eco-friendly solvent, has been introduced as an alternative sustainable solvent to replace hexane for green extraction of natural products<sup>269,272</sup>. Some researchers compared the hexane and 2-MeTHF in the lipid extraction of black soldier fly (*H. illucens*, BSF) larvae<sup>268,272</sup>, showing a better lipid

recovery and an enhanced bioactivity in BSF oils extracted with 2-MeTHF. Regarding the protein fraction, a relatively higher protein dispersibility and solubility in 0.2% KOH solution were observed in the insect powder defatted by 2-MeTHF compared to the one defatted by hexane<sup>268</sup>. Hence, 2-MeTHF is an effective and promising alternative solvent for extraction of lipids. Besides, C2-C4 alcohols are also organic solvents with good performances and wide applications, such as ethanol and isopropanol. There are several ways to produce C2-C4 alcohols, while the vast majority of ethanol is produced by microbial fermentation from sugars and starches, which is considered sustainable as renewable feedstocks are used<sup>273</sup>. Ethanol is used as a solvent for perfumes and paints, and also a key component in wine, spirits, and beer, while the abundant use is as automobile fuel either alone or as an additive to gasoline to increase the octane number. Isopropanol is directly used as solvents and chemicals which is produced mainly by the hydration of propylene with sulfuric acid<sup>273</sup>. While propylene is a by-product of petroleum refining, which requires high energy consumption and results in adverse environmental impact<sup>274</sup>.

As for the impact of defatting/lipid extraction using conventional solvents on the protein functionality in defatted powders and protein extracts, reported results don't show a clear trend. Akposan et al.<sup>275</sup> studied the functionality of caterpillar (*I. oyemens*) protein extracts obtained from full-fat powders and defatted (by hexane) powders, which displayed higher water solubility index, water and oil absorption capacity, foam capacity and stability while lower emulsion capacity and the stability of the protein extract from the defatted powder than from the full-fat powder. Similar studies with *T. molitor* larvae and silkworm pupae (*B. mori*) powder showed no big impact on the protein functionality as a result of the solvent defatting step<sup>237</sup>. On a study about the techno-functional properties of defatted cricket (*G. bimaculatus*) powders obtained with three different solvents (ethanol, hexane or acetone), water/oil binding capacity, foaming property, emulsifying capacity and gel formation ability were all affected to a different but significant extent ( $p < 0.05$ ) depending on the solvent used<sup>86</sup>. In a different work of *T. molitor* larvae powder, a defatting by hexane in combination with a protein extraction in alkaline aqueous solution led to a partial or complete proteolysis of the higher molecular weight proteins into smaller ones<sup>85</sup>.

Among various techno-functional properties of proteins, their capacities to decrease the interfacial tension and stabilize oil-in-water interfaces enhance their use as amphiphilic emulsifiers in a large range of emulsion-based food products and in encapsulation technology. Dairy proteins are conventionally used in the formulation of emulsions, while in recent years, in line with the need of new sustainable sources of food ingredients, the potential of insect proteins as emulsifiers is gaining interest<sup>82</sup>. In this context, the production of protein extracts from insects has to meet the standards of sustainable good practices. Accordingly, the use of green solvents, such as 2-MeTHF, should be prioritized and assessed in terms of lipid extraction, but also with respect to the functionality of the protein fraction obtained after the defatting step.

The aim of this study is to evaluate impact of a greener solvent 2-MeTHF on defatting *A. diaperinus* larvae powders and on its lipid profile, and on the emulsifying

property of the protein concentrate extracted from defatted powders. The evaluation was conducted by comparing with commonly used organic solvents including hexane, isopropanol, and ethanol. Defatted powders were subjected to protein extraction. The protein concentrates obtained were evaluated on the amino acid and protein content, water/oil binding capacity, foaming capacity, emulsifying activity, and surface hydrophobicity. Then, the protein concentrates were used as emulsifiers for stabilizing oil-in-water emulsions. The potential of producing solid microcapsules using the emulsions stabilized by insect protein was assessed in the end for extending the possibility of insect protein applications.

## 4.2 Materials and methods

### 4.2.1 Materials

Lesser mealworm powder (LMP) was purchased from Kreca (the Netherlands), with a composition (provided by the manufacturer) of 28.7% fat, 59.6% protein, 2.7% carbohydrates and 3.7% fiber on a wet weight basis. 95.6% of dry matter (DM) was obtained by gravimetric analysis, keeping 0.1-0.5 g samples in the 105 °C oven (UN55, Memmert, Germany) until no weight change. Organic solvents used for defatting were hexane (>99%, pesticide grade, Chem-Lab NV, Belgium), isopropanol (>99.8%, Chem-Lab, Belgium), ethanol (absolute, Scharlau, Spain) and 2- methyltetrahydrofuran (2-MeTHF, EMPLURA, USA). n-Hexane (>95%, HPLC grade, PanReac, Germany), methanol dry (PanReac, Germany), sulfuric acid (H<sub>2</sub>SO<sub>4</sub>, 99.999%, Sigma-Aldrich, USA), sodium chloride (NaCl, pharma grade, PanReac, Germany), sodium bicarbonate (NaHCO<sub>3</sub>, >99.7%, Sigma-Aldrich, USA) and FAME standard (Supelco® 37 component FAME mix, 10mg/mL in methylene chloride (varied), Sigma-Aldrich, USA) was used in lipid analysis. As for protein extraction, sodium hydroxide pellet (NaOH, Chem-Lab NV, Belgium) and hydrochloric acid (37-38% HCL, J. T. Baker, Germany) were used. BCA (bicinchoninic acid) assay kit (Pierce Biotechnology, Thermo Scientific, USA) was used for protein quantification, which was expressed as bovine serum albumin equivalent value (BSAE). For the simplicity, protein concentration was shown as % instead of BSAE%. Whey protein isolate (WPI) is purchased from Davisco Foods International with protein content of 98.1% on dry basis (BiPRO, lot no. JE 034-7-440-6, Davisco Foods International. Inc., Le Sueur, MN). Sunflower oil used for formulating O/W emulsions was purchased from a local supermarket, and it was used without further purification. Food grade maltodextrin (lot no. 219425, Pral, Spain) with a dextrose equivalent of 16.5–19.5 was used as wall material for solid microcapsules produced by spray drying.

Table 4.1 Some physical parameters of the solvents, values are adapted from the literature<sup>268,269</sup>.

Solvent	Boiling Point (°C)	Vapor pressure at 20 °C (kPa)	Energy required to evaporate per ton of solvent (kW.h)	log P*	Toxicity index**
Hexane	68	17	120.1	3.9	6
Iso-propanol	82.5	4.4	225.8	0.2	5
Ethanol	78.37	5.8	268.6	-0.2	5
2-MeTHF	80.2	13.6	126.1	1.8	4

\* The log P value for a compound is the logarithm (base 10) of the partition coefficient (P), which is defined as the concentration ratio of the compound between organic phase (octanol) and aqueous phase (water) at equilibrium.

\*\* Index was acquired from ACD lab software, taking into account AMES test, genotoxicity hazards, hERG inhibitors, LD50, toxicity category, aquatic toxicity, endocrine disruption, health effects and MRDD.

#### 4.2.2 Lipid extraction

Lipid extraction was carried out by mixing 50 g (on a wet basis) of LMP with 250 mL of organic solvent. Four different solvents (hexane, isopropanol, ethanol and 2-MeTHF) were assessed separately. The mixture was stirred at 400 rpm over a magnetic stirrer for 1 h and then was left to settle until complete phase separation. The solvent layer that contains the dissolved lipids was collected by decantation and reserved, while the remaining precipitate was mixed with 250 mL of clean solvent to continue with the lipid extraction (Figure 4.1). The process was repeated until no significant lipid bands (at wavelength 1700-1800 and 2800-3000  $\text{cm}^{-1}$ ) demonstrated in FTIR analysis as described in section 4.2.3. The final solid precipitate was dried in the fume hood to remove remaining solvent and stored in a desiccator until protein extraction.

The solvents collected during the extraction process were rotary evaporated (LABOROTA 4000-efficient, Heidolph, Germany) at the conditions listed in the figure 4.1. The lipid fraction remaining in the round-bottom flask was kept in the fume hood to remove trace solvents left in the samples, and the amount of lipids was measured gravimetrically until there was no more mass reduction. The lipid fraction obtained with each solvent was collected in a glass tube with cap and kept in fridge (4 °C) with an aluminum foil coverage until further analysis. The lipid yield/content extracted was calculated as equation (4.1),

$$Yield_{lipid}[\% DM] = \frac{m_l}{m_i} \times 100 \quad \text{eq (4.1)}$$

where  $m_i$  is the mass of LMP input in DM,  $m_l$  is the mass of lipids.

#### 4.2.3 Fourier transform infrared spectroscopy (FTIR) analysis

Solid powders after settling and solvent removal were maintained in the hood until it could be ascertained that they were solvent-free. The powders after each defatting cycle was analyzed by FTIR following the protocol of Mellado-Carretero et al.<sup>242</sup>. For the acquisition of the spectral profiles, 4 mg of powder sample was taken randomly after mixing and placed onto the sample stage of a portable spectrometer Cary 630 (Agilent Technologies Spain SL, Madrid, Spain), equipped with a single bounce ATR diamond crystal accessory and a deuterated triglycine sulfate (DTGS) detector. A pressure clamp was used to ensure optimal contact between samples and the diamond crystal. A background scan was extracted from every sample scan to prevent the effect of environmental changes. Spectra were acquired from 4000 to 800  $\text{cm}^{-1}$  with 8  $\text{cm}^{-1}$  of resolution using MicroLab PC software (Agilent Technologies SL, Madrid, Spain).

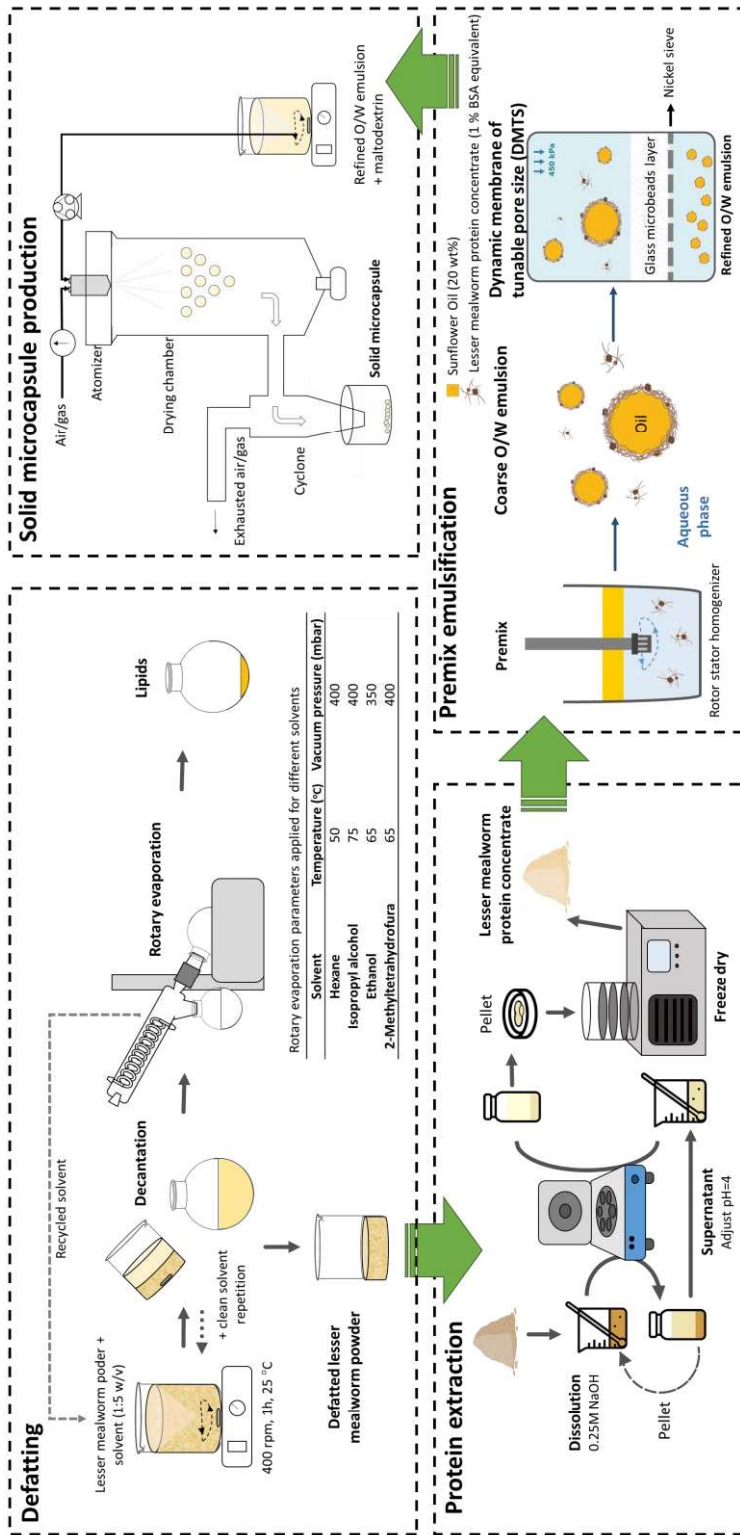


Figure 4.1. Schematic diagram of the entire experimental design starting from defatting to protein extraction, premix emulsification and ending up with solid microcapsule production.

#### 4.2.4 Characterization of fatty acid methyl esters (FAMES) by gas chromatography

Extracted lipids were converted to FAMES through acid catalysis esterification according to the method reported in the literature<sup>276</sup>. In a 20 mL screw cap glass tube, 20-50 mg of lipid sample was added with 1 mL n-hexane and 2 mL of 1% H<sub>2</sub>SO<sub>4</sub> in methanol. The reaction was carried out overnight (12 h) in a dry bath (FB15101, Fisher Scientific, UK) set at 50 °C, then, 5 mL of 5% NaCl solution was added. The extraction of FAMES was conducted by adding 5 mL hexane and vortex (Fisherbrand, Germany) at 3000 rpm vigorously. The tube was left to stand until complete phase separation, after which the hexane layer was removed completely using a glass Pasteur pipette (Fisherbrand, Germany) and transferred into a new tube. The extraction and separation processes were repeated by adding another 5 mL of hexane in the original tube. 4 mL of 2% NaHCO<sub>3</sub> solution was mixed with separated hexane and vortexed vigorously to wash out impurities. After settling down, hexane layer with the dissolved FAMES was transferred to an HPLC vial for further analysis by gas chromatography (GC).

The FAMES were analyzed by gas chromatography with a flame ionization detector (GC-FID) (6890N, Agilent Technologies, USA) coupled with an automatic injector (7683 series, Agilent Technologies), and a HP-INNOWax column (19091N-133) with helium as a carrier gas. For the calibration of the method, a 37 component FAME standard mixture was used. The injection volume of the sample was 1.5 µL with a split ratio 20:1. The oven temperature program began at 150 °C, holding for 1 min and increased by 2.9 °C min<sup>-1</sup> to 230 °C, and then holding for 1 min. The detector and injector temperature were set at 260 °C for the duration of the analysis.

#### 4.2.5 Protein extraction

Defatted LMP from each solvent was subsequently used for protein extraction following a method based on Zhao et al.<sup>73</sup> with some modifications. 30 g of defatted powder was mixed with 150 mL of 0.25 M NaOH solution (a ratio of 1:5 (w/v)) and the mixture was heated to 40 °C for one hour with constant agitation at 400 rpm on a magnetic stirrer. The mixture was centrifuged (Meditronic 7000599, J.P. SELECTA, Spain) at 4490 rpm for 15 min. Two more NaOH extraction was repeated on the pellet and the supernatant was combined. The pH (Accumet AE150, Fisher Scientific, Singapore) of the supernatant was adjusted to reach the value between 4.0-4.3 by adding 37% HCl and 1N HCl successively followed by a centrifugation at 3750 rpm for 15 min. After centrifugation, pellets were collected in plastic petri dishes and were kept at -60 °C until freeze drying. Freeze drying (LYOQUEST-85 PLUS, Telstar, Spain) was carried out for 24 h at 0.2 mbar with the plates heated to 20 °C. Freeze-dried samples were ground, collected separately according to different defatting solvent used, and stored in a desiccator at room temperature. The yield of protein extraction was expressed as equation (4.2),

$$Yield_{protein}[\% DM] = \frac{m_p \times C_p}{m_i \times C_i} \times 100 \quad \text{eq (4.2)}$$

where  $m_p$  is the mass of freeze-dried protein concentrate powder in DM,  $C_p$  is the protein content (%) in the protein concentrate powder,  $C_i$  is the protein content (%) in the lesser meal worm powder (untreated) in DM. Protein content (%) is calculated from the nitrogen content and nitrogen (N) to protein conversion factor ( $K_p$ ).

The lesser mealworm protein concentrate (LMPC) obtained from defatting by 4 different solvents followed by protein extraction was expressed as LMPC\_HEX (defatted by hexane), LMPC\_IPOH (defatted by iso-propanol), LMPC\_ETOH (defatted by ethanol) and LMPC\_METHF (defatted by 2-MeTHF).

#### 4.2.6 Characterization of LMP and LMPC

Amino acid and nitrogen contents of LMP and LMPC from the defatted powders by 4 solvents were analysed by AGROLAB Ibérica S.L.U (Tarragona, Spain) based on Kjeldahl and the European Union Commission Regulation REG(UE) 152/2009, III, F: 2009-02 methods, respectively. The protein content (%) on a wet matter basis can be expressed as eq (4.3),

$$\text{Protein content [\%, on a wet weight basis]} = N \times K_p \quad \text{eq (4.3)}$$

where N is nitrogen content in %, and  $K_p$  is nitrogen to protein conversion factor, which is calculated from the ratio of the sum of amino acid residue weights to nitrogen content<sup>243</sup>.

On account of the high protein content in the LMPC obtained from the defatted LMP by ethanol, techno-functional properties such as solubility, isoelectric point, water and oil binding capacity, foaming properties, emulsifying activity and surface hydrophobicity were analysed using LMPC\_ETOH and compared them with black soldier fly protein concentrate (BSFPC) obtained using the same protein extraction method and post defatted by hexane.

#### Isoelectric point (pI) determination

pI of soluble protein fraction from LMPC\_ETOH and BSFPC was determined by zeta potential using Zetasizer Nano-ZS (Malvern Instruments, U.K.). 0.1% of soluble protein solution was prepared at pH 7, and the pH was subsequently adjusted to 5.5, 5.0, 4.5, 4.0, and 3.5 by adding 1N HCl and 0.01N HCl gradually. Zeta potential of supernatant after centrifugation at 3250 g for 20 min was measured and plotted against pH. The isoelectric point set to the pH region where the Zeta potential was close to 0.

#### Water and oil binding capacity

Water binding capacity (WBC) and oil binding capacity (OBC) were analyzed by method as reported in the literature<sup>76</sup>. Briefly, for WBC, 0.5 g of LMPV\_ETOH or BSFPC powders were mixed with 2.5 mL of 0.2 M phosphate buffer (pH 7) and vortexed in a centrifugation tube for 60 s followed by centrifugation at 3250 g for 20 min at room temperature. The supernatant was decanted and the tube with the residual pellet was placed upside down on a filter paper for 60 min, to drain the residual non-bound water, before recording the weight. The WBC is calculated as shown in equation 4.4,

$$WBC \left[ \frac{g_{water}}{g_{DM}} \right] = \frac{m_1 - m_0}{m_{DM}} \times 100 \quad \text{eq (4.4)}$$

where  $m_0$  is the initial weight of the sample,  $m_1$  is the weight of residual after 60 min, and  $m_{DM}$  is the dry matter of the initial sample.

As for OBC, similarly, 0.5 g powders were mixed with 2.5 mL of commercial sunflower oil and vortexed for 60 s twice with 5 min of pause in between. The rest of the procedure is identical to WBC analysis using equation 4.5 for the calculation. Both WBC and OBC analyses were done in triplicate.

$$OBC \left[ \frac{g_{oil}}{g_{DM}} \right] = \frac{m_1 - m_0}{m_{DM}} \times 100 \quad \text{eq (4.5)}$$

### Foaming capacity and foam stability

The foaming properties were analyzed following the literature<sup>68</sup> with minor modifications. A sample of 20 mL of 0.1% LMPC\_ETOH, BSFPC or whey protein isolate (WPI) solution prepared with 0.2 M pH 7 buffer was placed in a 50 mL plastic tube and subjected to vigorous rotor-stator homogenization (Ultra Turrax T18 digital, IKA, Germany) at 1200 rpm for 2 min. The height of the foam layer after 10 s and 120 min was recorded. Foaming capacity (FC) and foam stability (FS) (from experiments run in duplicate) were calculated using equations 4.6 and 4.7, respectively<sup>68</sup>,

$$FC [\%] = \frac{H_t}{H_0} \times 100 \quad \text{eq (4.6)}$$

$$FS [\%] = \frac{FC_{120}}{FC_0} \times 100 \quad \text{eq (4.7)}$$

where  $H_0$  is the initial height of protein solution in the tube,  $H_t$  is the height of generated foam after agitation,  $FC_0$  is the initial foaming capacity (after 10 s) and  $FC_{120}$  is the one obtained after 120 min.

### Emulsifying activity (EA)

EA was evaluated at different protein concentrations (0.1%, 0.5%, and 1.0%) of LMPC\_ETOH, BSFPC and WPI using the method described by Purschke et al.<sup>76</sup>. Briefly, in a beaker 10 mL of protein solution and 10 mL of sunflower oil were homogenized using ULTRA TURRAX at 11000 rpm for 30 s. An aliquot of 10 mL of the emulsion was transferred into a 15 mL scaled tube and centrifuged at 3250 g for 20 min at room temperature. Triplicates were performed for each sample. The height of the emulsified layer was noted, and the emulsifying activity was calculated using equation 4.8<sup>76</sup>,

$$EA [\%] = \frac{H_{EL}}{H_S} \times 100 \quad \text{eq (4.8)}$$

where  $H_{EL}$  is the height of emulsified layer and  $H_S$  is the total height of solution in the tube.

## Surface hydrophobicity ( $H_o$ )

According to the method described by Nakai<sup>277</sup>,  $H_o$  was evaluated based on probe spectrofluorometry. In brief, LMPC\_ETOH, BSFPC or WPI solution prepared in 0.02M phosphate buffer pH 7 was diluted to following concentrations: 0, 0.0005, 0.0025, 0.005 and 0.01%. An aliquot of 4mL and 20 $\mu$ L of 8mM ANS (8-anilino-1-naphthalenesulfoate) were mixed with vortex and kept in the dark (with aluminum foil) for 15min. The fluorescence intensity was measured at an excitation wavelength of 390nm, emission wavelength of 470nm and with both excitation and emission slip width of 5 nm. The buffer with ANS was used as protein concentration of 0%.  $H_o$  is expressed as the slope of the linear regression of relative fluorescence intensity plotted versus protein concentration (%).

### 4.2.7 Production of oil-in-water (O/W) emulsions by DMTS

Sunflower O/W emulsions (120 g) were prepared in a premix mode with DMTS. LMPC obtained from different defatting solvents were assessed. The aqueous phase was prepared firstly starting from a stock insect protein solution that was prepared by dissolving 13 g of LMPC in 250 mL of deionized water, stirring at 400 rpm over a magnetic stirrer, and measuring the pH of the mixture every 30 min, adjusting to 7 with 1M NaOH. After 2 h of stirring, the mixture was kept in fridge overnight for a complete hydration. The pH of the solution was adjusted to 7 again the day after, and the protein concentration was quantified by the BCA assay kit on the supernatant obtained after two consecutive centrifugations at 3750 rpm for 15 min. A 1% LMPC solution was prepared by dilution of this stock LMPC solution. To prepare 20% sunflower O/W emulsions, 24 g of sunflower oil was added into 96 g of 1% LMPC solution. Premix coarse emulsion was produced by rotor-stator homogenization (Ultra Turrax T18 digital, IKA, Germany) at 15600 rpm for 3 min with a 30 s break every min.

The coarse emulsion was then refined by forcing the emulsion through a microporous DMTS system consisting of 2 g of 94  $\mu$ m glass microbeads (leading to a height of 4.3 mm of the glass microbeads layer with interstitial void diameter of 78.4  $\mu$ m) supported by a nickel microsieve having rectangular pores of 300  $\mu$ m x 30  $\mu$ m (length x width) at 450 kPa. Refined emulsions were collected in a flask placed above an electronic balance to record the mass flow rate during the emulsification. In this study the emulsion passed 5 times (cycles) through the DMTS systems.

Transmembrane flux during each emulsification cycle was calculated based on equation (4.9),

$$J_{DMTS} = \frac{\phi}{\rho_e A} \quad \text{eq (4.9)}$$

where  $\phi$  is the mass flow rate acquired from the mass/time data recorded with the electronic balance,  $\rho_e$  is the emulsion density which is 1.092 kg m<sup>-3</sup>,  $A$  is the effective surface area.

## 4.2.8 Characterization of emulsion

### Droplet size distribution

The particle size distribution of O/W emulsions was measured after every emulsification cycle by laser diffraction using Mastersizer 2000 (Malvern Instruments, U.K.). Particle reflective indices were set to 1.480 and the dispersant reflective index was set to 1.330. Mean droplet size and droplet size dispersion can be calculated, and expressed as Sauter mean diameter  $d_{3,2}$  (equation 4.10) and the span factor (equation 4.11), respectively,

$$d_{3,2} = \frac{\sum n_i D_i^3}{\sum n_i D_i^2} \quad \text{eq (4.10)}$$

where  $n_i$  is the number of droplets, and  $D_i$  is the diameter of the  $i^{\text{th}}$  droplet.

$$\delta = \frac{d_{90} - d_{10}}{d_{50}} \quad \text{eq (4.11)}$$

where  $d_x$  is the droplet diameter corresponding to x% volume on a cumulative droplet size distribution curve.

### Zeta potential

Zeta potential of emulsions was measured using Zetasizer Nano-ZS (Malvern Instruments, U.K.). Samples were diluted 100 times by deionized water. The same values of reflective indices for the particle and dispersant as those used in for droplet size analysis were also applied here.

### Stability

Emulsion aliquots (10 mL) were collected in tubes for every freshly produced emulsion. Emulsions were kept at room temperature (25 °C) for 7 days. Droplet size distribution, as well as zeta potential were measured after 1, 3 and 7 days.

## 4.2.9 Production of solid microcapsules by spray drying

Solid microcapsules were produced by spray drying of 100 g O/W emulsions stabilized by LMPC. As the very first trial, only the O/W emulsions stabilized by LMPC\_ETOH was assessed due to its relatively high protein content. Maltodextrin (MD) was added to the freshly produced emulsion at a ratio MD:oil=3:1 (w/w) and stirred for two hours. The spray dryer used is a co-current flow atomizer with a two-fluid nozzle (BÜCHI Mini Spray Dryer B-29, Switzerland). The tube used of the peristaltic pump is a standard silicon tube (inner diameter: 2.0mm). The aspirator rate was always fixed at 100% and the inlet temperature at 170 °C. The outlet temperature was about 90 °C by setting the spray flow at 40 mm (666.93 m<sup>3</sup>/h) and the peristaltic pump at 45%.

Microstructure of the solid microcapsules were observed using environmental scanning electron microscopy (ESEM, FEI Quanta 600, Thermo Scientific, Austria), and the images were taken at magnification between 300 and 17000.

#### 4.2.10 Reconstitution of emulsion

Solid microcapsules were redispersed into water to reconstitute O/W emulsions. Droplet size distribution was measured as described in the subsection 4.2.8. Microstructure of reconstituted emulsions was observed by optical microscope (Leica DM 2500) at x100 magnification lens with immersion oil.

#### 4.2.11 Statistical analysis

The data described are mean  $\pm$  standard errors of duplicate (n=2) or triplicate (n=3) observations. ANOVA with Tukey test was applied to determine variations between samples/mean scores at  $p < 0.05$ .

### 4.3 Results and discussion

#### 4.3.1 Influence of solvent type on lipid extraction

In order to determine the efficiency of each solvent on defatting the LMP, after one decantation, the powder was dried and measured with FTIR to validate the remaining composition. The extraction and the validation processes were repeated until no clear lipid bands shown. The results show that after 2 lipid extraction cycles, significant effect on removing lipid fraction was observed from the samples defatted by hexane, isopropanol and 2-MeTHF, which is validated from the absence of lipid representative bands at wavelength 1700-1800 and 2800-3000  $\text{cm}^{-1}$  (Figure 4.2). Whereas in case of using ethanol, it is demonstrated that at least 9 repetitions were required for achieving the same defatting effect (Figure 4.3). Therefore, hexane, isopropanol and 2-MeTHF are relatively effective in lipid extraction compared to ethanol in terms of the solvent consumption, processing time, and energy consumption (Table 4.2).

Table 4.2 Summary of solvent consumption for complete defatting and the according yield of lipid extraction. Different letters denote significant differences ( $p < 0.05$ ) between different defatting (n=2).

Solvent	Ratio of powder to solvent (g:mL)	Total number of extraction cycle	of Extraction duration (h)	Yield <sub>lipid</sub> (% DM)
Hexane	1:5	2	2	27.8 $\pm$ 0.3 <sup>a</sup>
Isopropanol	1:5	2	2	33.6 $\pm$ 0.5 <sup>ab</sup>
Ethanol	1:5	9	9	41.3 $\pm$ 4.6 <sup>b</sup>
2-MeTHF	1:5	2	2	34.2 $\pm$ 0.4 <sup>ab</sup>

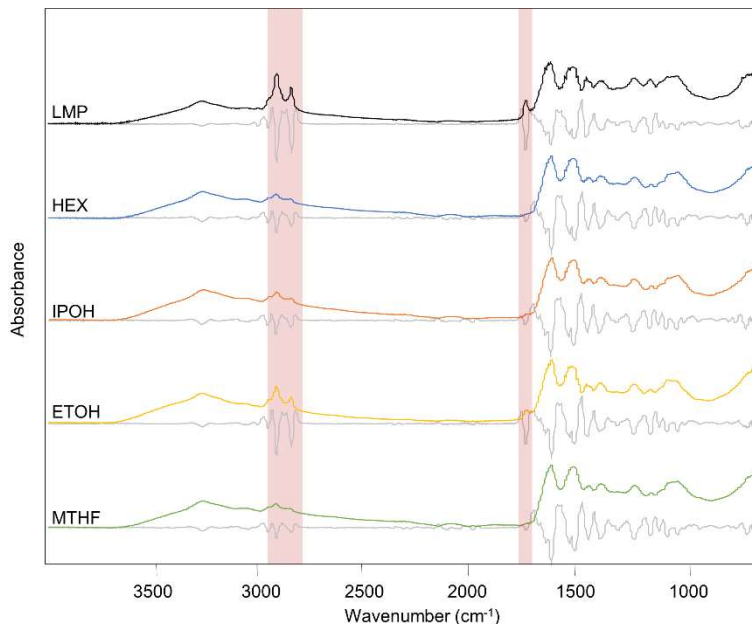


Figure 4.2 Attenuated total reflectance Fourier transform mid infrared spectroscopy (FTIR) raw spectra of lesser mealworm powder (LMP) and powders after twice of defatting using hexane (HEX), isopropanol (IPOH), ethanol (ETOH) and 2-MeTHF (MTHF), and the corresponding Savitzky–Golay’s second derivatives by taking 11 points of window (grey line).

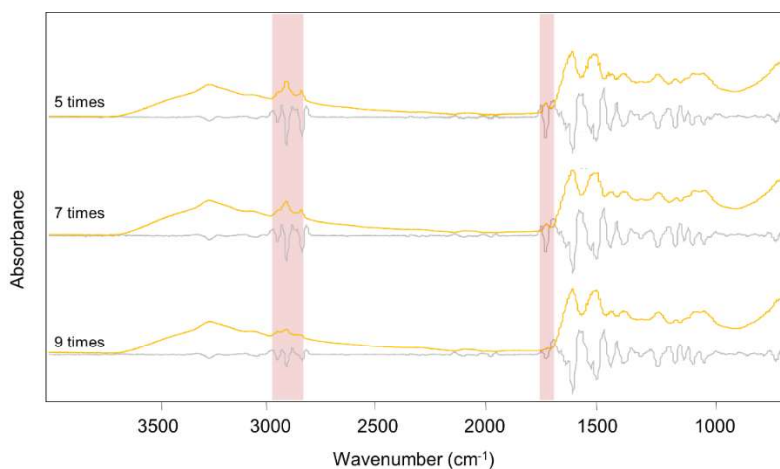


Figure 4.3 Attenuated total reflectance Fourier transform mid infrared spectroscopy (FTIR) raw spectra of powders after 5, 7, and 9 times of defatting using ethanol, and the corresponding Savitzky–Golay’s second derivatives by taking 11 points of window (grey line).

The extracted lipid was yielded at a range of 27.8 and 41.3% DM, in which the highest value was obtained with ethanol and the lowest with hexane (Table 4.2). Except for hexane, the lipid samples extracted in other solvents were higher than 30.0% DM. The significant difference was seen only between the lipid yields of using hexane and ethanol as the solvent. Likewise, the highest lipid extraction yield using ethanol as the solvent was reported by Soxhlet extraction<sup>247</sup> of *A. domesticus* (22.7% DM) and *T. molitor* (28.8% DM) powders compared to using hexane, petroleum ether, ethyl acetate, and also in the stirring extraction<sup>73</sup> using ethanol to defat *T. molitor* (33.1-34.8% DM) powder compared to using a blend of hexane:isopropanol (3:2, v/v). As ethanol is relatively polar (log *P* of -0.2, Table 4.1), it has a better partitioning ability/solubilizing with polar lipids during the lipid extraction, such as phospholipids<sup>247</sup>. Besides, ethanol can extract relatively higher amount of polysaturated fatty acids that are relatively polar compared to monosaturated fatty acids and long chain saturated fatty acids, which is elucidated with more information in the following section. Besides, alcohol solvent such as ethanol and isopropanol are commonly used for the extraction of phenolics<sup>278</sup> including phenolic acid, flavonoid, tannins and lignin. Although using ethanol can yield higher amount of lipid, 2-MeTHF is still considered to be more reasonable and suitable solvent for lipid extraction in present case, as ethanol extraction required more energy in lipid recovery and solvent recycling (Table 4.2 and Figure 4.1). The lipid extraction in *A. diaperinus* has been only reported for analytical methods at laboratory scale. Using Soxhlet extraction with petroleum ether or diethyl ether, the lipid content was of 14-29% DM<sup>71,270,279</sup>, which is comparable or lower than those extracted with alcohol or 2-MeTHF solvent in this study.

#### 4.3.2 FAME analysis

The fatty acids profile of the lipid fraction extracted from the different solvents (Table 4.3) demonstrated a ratio of unsaturated fatty acids (USFA) to saturated fatty acid (SFA) between 1.8 and 2.0, in accordance with the profiles found in previous studies<sup>267,270</sup>. Moreover, these values of USFA to SFA ratio are linked to a lipidic profile that is suitable for dietary intake<sup>280</sup>. Irrespective to the solvents, the three most abundant fatty acids were palmitic acid (C16:0), oleic acid (C18:1 cis+trans) and linoleic acid (C18:2 trans) which took up more than 85% of total fatty acids. The amount of stearic acid (C18) and linolenic acid (C18:3n3) contributed to around 10% and the rest of the fatty acids listed were all in trace amount (< 1%). The fatty acid profile is also similar to other insect species reported such as *T. molitor*, *A. domesticus*, *Z. morio* and *B. dubia*<sup>247,266,267,270</sup>, however, *H. illucens* presented higher amounts of SFA, especially 42% of lauric acid (C12), than of USFA<sup>268</sup>.

In relation to the highest lipid extraction yield obtained with ethanol, one can notice that ethanol is capable to extract slightly higher amount of relatively polar fatty acids that are PUFA such as C18:2 and C18:3, while slightly lower amount of relatively non-polar fatty acids that MUFA such as C18:1 and C16:1, and long chain SAF such as C16, compared to the lipid profiles of other solvents (hexane, isopropanol and 2-MeTHF) (Table 4.3). This is in agreement with the observation of the fatty acid profiles of *T. molitor* and *A. domesticus* lipids extracted using ethanol compared to using hexane, petroleum ether or ethyl acetate by Soxhlet extraction<sup>247</sup>.

Table 4.3 Relative percentage of fatty acid composition (%) in lipids (mean  $\pm$  SD, n=2) extracted from *A. diaperinus* using different solvents.

Fatty acid		Hexane	Isopropanol	Ethanol	2-MeTHF
SFA	C14	0.67 $\pm$ 0.00	0.67 $\pm$ 0.00	0.67 $\pm$ 0.00	0.66 $\pm$ 0.00
	C15	0.16 $\pm$ 0.01	0.15 $\pm$ 0.01	0.17 $\pm$ 0.00	0.16 $\pm$ 0.00
	C16	25.73 $\pm$ 0.27	24.90 $\pm$ 0.46	24.14 $\pm$ 0.24	25.06 $\pm$ 0.05
	C17	0.30 $\pm$ 0.01	0.30 $\pm$ 0.00	0.31 $\pm$ 0.01	0.31 $\pm$ 0.01
	C18	8.13 $\pm$ 0.12	7.77 $\pm$ 0.28	7.77 $\pm$ 0.10	8.03 $\pm$ 0.01
	C20	0.36 $\pm$ 0.02	0.38 $\pm$ 0.03	0.36 $\pm$ 0.00	0.36 $\pm$ 0.01
MUFA	C16:1	0.27 $\pm$ 0.04	0.11 $\pm$ 0.16	0.00 $\pm$ 0.00	0.46 $\pm$ 0.65
	C17:1	0.09 $\pm$ 0.00	0.17 $\pm$ 0.05	0.18 $\pm$ 0.01	0.19 $\pm$ 0.01
	C18:1 cis+trans	32.64 $\pm$ 0.05	31.91 $\pm$ 0.37	31.11 $\pm$ 0.01	31.23 $\pm$ 0.27
PUFA	C20:1	0.21 $\pm$ 0.02	0.22 $\pm$ 0.00	0.20 $\pm$ 0.01	0.22 $\pm$ 0.01
	C18:2 trans	28.45 $\pm$ 0.06	29.87 $\pm$ 0.25	31.50 $\pm$ 0.24	28.61 $\pm$ 0.07
	C18:3n3	1.68 $\pm$ 0.01	1.77 $\pm$ 0.00	1.87 $\pm$ 0.01	1.72 $\pm$ 0.00
	C18:3n6	0.04 $\pm$ 0.06	0.07 $\pm$ 0.00	0.08 $\pm$ 0.01	0.08 $\pm$ 0.01
	C20:2	0.46 $\pm$ 0.01	0.45 $\pm$ 0.00	0.45 $\pm$ 0.02	0.45 $\pm$ 0.00
	C20:3n6	0.00 $\pm$ 0.00	0.00 $\pm$ 0.00	0.00 $\pm$ 0.00	0.06 $\pm$ 0.08
	C20:4	0.19 $\pm$ 0.01	0.19 $\pm$ 0.00	0.19 $\pm$ 0.02	0.23 $\pm$ 0.01
Ratio USFA to SFA		1.81	1.90	1.96	1.83
Total unknown		0.61 $\pm$ 0.09	1.09 $\pm$ 0.27	1.00 $\pm$ 0.06	2.17 $\pm$ 0.76

#### 4.3.3 Amino acid profile and protein content

The defatted insect powders consist mainly of proteins and carbohydrates including chitin. To further purify the protein fraction, protein extraction using insect powders defatted from different solvents was carried out as described in section 4.2.5. As for the protein quantification in the extracts, nitrogen content 17 amino acids out of 20 were analyzed due to the limitations of the analytical method. Comparing the LMPC to LMP (see Table 4.4), the concentration of most of the amino acids was higher in LMPC except for cystine. Similar results were obtained in protein extracts from BSF powder as mentioned in Chapter 3, which can be attributed to the strengthened protein's tertiary and quaternary structure with multiple disulphide bridges of cysteines, which makes it difficult to extract out<sup>245</sup>. Table 4.4 also shows how nitrogen content increased from 9.23% in LMP to 12.69-13.61% in LMPC while Kp values ranged from 4.85 to 5.60-5.76 in LMP and LMPC, respectively. Besides, the significant raise of protein content observed in all LMPC, between 71.06 and 78.27% (on a wet basis), with respect the original value of 44.77% in LMP, proves that the protein was extracted out and separated from the non-protein nitrogen fraction (mainly chitin). The results are highly comparable to that reported by Janssen et al.<sup>243</sup> who found an average Kp value of 5.60  $\pm$  0.39 for the protein extracts from 3 insect (*T. molitor*, *A. diaperinus* and *H. illucens*) powders.

Table 4.4 The results of amino acid composition, nitrogen content and calculated Kp value and protein content for the LMPC (lesser mealworm protein concentrate) obtained from the LMP (lesser mealworm powder) defatted by different solvents. Results of protein extracts are shown as mean  $\pm$  SD from duplicated trials. Different letters denote significant differences (p < 0.05) between samples obtained with different defatting solvents for specific parameter (n=2).

Amino acid	LMP	LMPC_HEX	LMPC_IPOH	LMPC_ETOH	LMPC_MTHF
Asp	4.82	8.73 ± 0.10	8.85 ± 0.11	9.38 ± 0.15	8.43 ± 0.18
Glu	7.49	12.05 ± 0.05	12.10 ± 0.30	12.85 ± 0.05	11.70 ± 0.20
Ala	3.91	5.44 ± 0.06	5.64 ± 0.11	5.93 ± 0.02	5.43 ± 0.11
Arg	3.13	4.93 ± 0.09	5.02 ± 0.13	5.24 ± 0.06	4.83 ± 0.03
Cys	0.59	0.45 ± 0.01	0.46 ± 0.04	0.43 ± 0.01	0.46 ± 0.03
Phe	2.33	4.44 ± 0.03	4.57 ± 0.05	4.82 ± 0.18	4.28 ± 0.12
Gly	2.6	3.84 ± 0.02	3.91 ± 0.01	4.17 ± 0.07	3.76 ± 0.08
His	1.85	2.74 ± 0.01	2.94 ± 0.10	2.98 ± 0.21	2.69 ± 0.01
Ile	2.52	4.32 ± 0.02	4.39 ± 0.06	4.61 ± 0.035	4.18 ± 0.01
Leu	3.57	6.85 ± 0.02	6.86 ± 0.15	7.18 ± 0.10	6.62 ± 0.12
Lys	3.67	6.14 ± 0.07	6.17 ± 0.09	6.41 ± 0.02	5.95 ± 0.09
Met	0.83	1.40 ± 0.03	1.41 ± 0.05	1.33 ± 0.02	1.32 ± 0.02
Pro	3.22	4.04 ± 0.02	4.15 ± 0.04	4.25 ± 0.05	4.03 ± 0.11
Ser	2.38	3.67 ± 0.06	3.73 ± 0	3.95 ± 0.09	3.57 ± 0.10
Tyr	3.73	6.84 ± 0.05	7.42 ± 0.26	7.98 ± 0.44	6.83 ± 0.23
Thr	2.28	3.73 ± 0.06	3.85 ± 0.09	4.05 ± 0.02	3.67 ± 0.01
Val	3.22	4.95 ± 0.03	5.11 ± 0	5.40 ± 0.10	4.86 ± 0.09
N (%)	9.23	12.88 ± 0.01	12.95 ± 0.15	13.61 ± 0.01	12.69 ± 0.24
Kp	4.85	5.65 ± 0.02	5.76 ± 0.01	5.62 ± 0.04	5.60 ± 0
Protein content (%)	44.77	72.75 ± 0.73 <sup>a</sup>	74.51 ± 0.94 <sup>ab</sup>	78.27 ± 0.78 <sup>b</sup>	71.06 ± 1.82 <sup>a</sup>
Protein yield (% DM)	--	61.08 ± 16.13 <sup>a</sup>	65.73 ± 26.14 <sup>a</sup>	62.38 ± 23.79 <sup>a</sup>	70.48 ± 4.22 <sup>a</sup>

Analyzing the influence of the solvent used during defatting on the protein content of the final concentrates, it can be seen from the Table 4.4 that LMPC\_ETOH had the highest protein concentration, followed by LMPC\_IPOH > LMPC\_MTHF > LMPC\_HEX. As for protein extraction yield, LMPC\_MTHF showed a higher average value of 70.48% DM compared to other samples, while no significant difference was indicated due to the high deviation from experiments. Overall, using 2-MeTHF as defatting solvent resulted in a similar efficiency in lipid extraction, lipid profile, and also the efficiency in the later on protein extraction and protein content, hence it is a good option to replace hexane to be used in the defatting of insect powders as a green solvent. As for the obtained protein concentrate, it is worth evaluating the techno-functional properties to give more knowledge on its performance and to broaden up the applications.

#### 4.3.4 Techno-functional properties of lesser mealworm protein concentrate (LMPC)

In this section, several techno-functional properties of LMPC\_ETOH, black soldier fly protein concentrate (BSFPC) post-defatted by hexane (Chapter 3), and/or with whey protein isolate (WPI).

## Isoelectric point (pI)

As shown in the Figure 4.4, in the pH range 2.0-4.0, both proteins have a net surface positive charge, and in the pH range 4.5-7.0, a net surface negative charge. While at pI, protein molecules have zero net surface charge and undergo unfolding in structure and start to aggregate and precipitate on account of the increased protein-protein hydrophobic interaction. LMPC displayed pI at the same range pH 4.0-4.5 but somewhat lower than black soldier fly protein concentrate (BSFPC) extracted with the same method. It agrees with the acidic pH range (4.0-4.3) applied for precipitation of protein fraction during the last step of aqueous extraction process. Both values are in the reported range for insect proteins (pI 3.0-5.0)<sup>70,281</sup>. Figure 4.4 provides important information on the estimation of protein solubility at various pH range, but mostly for the functionality as stabilizer at different pH.

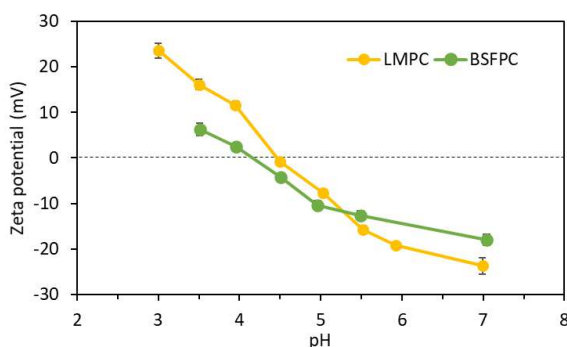


Figure 4.4 Zeta potential of LMPC and BSFPC at varied pH. Error bars correspond to standard deviation of the mean.

## Water binding capacity (WBC) and oil binding capacity (OBC)

Interactions of water and oil with flours are very important in food transformation because of their effects on the flavor and texture of foods. WBC and OBC demonstrate the capacity of the powder to bind with water and oil, respectively, which is related to protein contents include amino acid composition, protein conformation and surface polarity/hydrophobicity. The higher the number of hydrophilic units exposed on the solid surface, the higher WBC. Similarly, when more lipophilic units are placed on the surface, OBC increases. As Figure 4.5 shows, WBC in general is higher than OBC for the tested proteins which indicates the greater affinity to water and their hydrophilic nature. Moreover, protein extraction has significantly increased the WBC of both insect samples (2.16 to 3.13  $\text{g}_{\text{water}} \cdot \text{g}^{-1}$  DM from LMP to LMPC, and 1.72 to 2.24  $\text{g}_{\text{water}} \cdot \text{g}^{-1}$  DM from BSFP to BSFPC), while the OBC was significantly enhanced only for the BSF sample (0.86 to 1.14  $\text{g}_{\text{oil}} \cdot \text{g}^{-1}$  DM from BSFP to BSFPC). The increment is attributed to the increase in protein content after the protein extraction, which increased number of available functional sites that could bind with water and oil molecules. WBC was greater in lesser mealworm powder (LMP) than in black soldier fly powder (BSFP) and the same trend was observed when comparing lesser mealworm protein concentrate (LMPC) with black soldier fly protein concentrate (BSFPC). In all cases, OBC was smaller than WBC,

showing a higher hydrophilic nature of the powder surface before the defatting and after the protein extraction process. WBC and OBC of LMPC are in the range of the reported values of WBC (0.85-3.95  $\text{g}_{\text{water}}\cdot\text{g}^{-1}$  DM) and OBC (0.4-2.74  $\text{g}_{\text{oil}}\cdot\text{g}^{-1}$  DM) for yellow mealworm (*T.molitor*) protein extracts<sup>65,85</sup>.

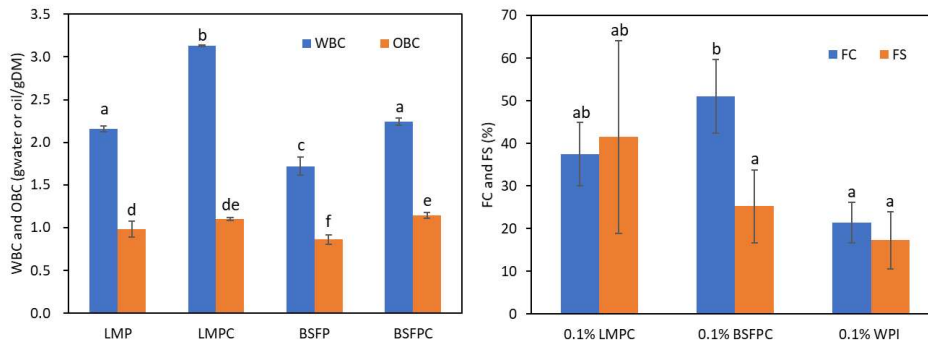


Figure 4.5 WBC and OBC (left) of LMP (lesser mealworm powder) and BSFP (black soldier fly powder) and their protein concentrates LMPC and BSFPC powders. FC and FS (right) of LMPC compared with BSFPC and WPI. Error bars correspond to standard deviation of the mean and the presence of different letters indicate a significant difference between samples at  $p < 0.05$  ( $n=3$ ).

### Foaming capacity (FC) and foam stability (FS)

Foam is a gas-in-water system, where air/gas bubble is stabilized in water by the presence of stabilizers. In food technology, foams are used to improve the texture, consistency, and appearance of foods. Protein on the air-water interface can arrange the structure to lower down the surface tension to stabilize air bubble. Foam formation and foam stability are a function of the type of protein, surface hydrophobicity, pH, ionic strength, processing methods, viscosity, and surface tension. In this case we compared the performance of LMPC and BSFPC with WPI, a well-known foaming and foam stabilizing agent. BSFPC exhibited a FC higher than 51.0% which is more than twice the FC of WPI (21.4%), followed by the FC of LMPC (37.5%) at protein concentration of 0.1%. The higher FC of BSFPC can be related to the slightly higher OBC of BSFPC than of LMPC, which indicates a relatively faster adsorption for BSFPC molecules on the air-water interface than LMPC. LMPC demonstrated the highest FS among other proteins, which indicates that LMPC molecules may be more flexible to undergo structural rearrangement on the air-water interface to strengthen the interfacial film, therefore the generated foams are relatively stable against defoaming compared to BSFPC and WPI. Similarly, the reported protein extract of *S. gregaria* (1% w/v) showed higher FC and FS as well as OBC (99%, 92% and 3.33  $\text{g}_{\text{oil}}\cdot\text{g}^{-1}$  DM respectively) than those of *T.molitor* (32.67%, 30.33% and 2.74  $\text{g}_{\text{oil}}\cdot\text{g}^{-1}$  DM respectively) and *G.sigillatus* (6.17%, 66.78% and 3.22  $\text{g}_{\text{oil}}\cdot\text{g}^{-1}$  DM respectively)<sup>65</sup>. Liya et al.<sup>63</sup> reported the 1.7% w/v *A. diaperinus* protein solution had a negligible foam ability, while protein solution prepared by other insect species such as *Z. morio* and *A. domesticus* could generate foam with certain stability,

however, it was not as stable as the foam formulated by albumin solution from chicken egg white.

### Emulsifying activity (EA) and Surface hydrophobicity ( $H_o$ )

Comparable to foaming property, emulsifying property is also related to a stabilization at interface, but on oil-water interface. It is also an important property as many food products are emulsions such milk and salad dressing. Not only the type of protein and its surface hydrophobicity, but also the pH, ionic strength and viscosity of the medium influence the formation and stability of an emulsion. As can be seen from Figure 4.6, LMPC displayed the greatest EA (52.3%) at the lowest protein concentration (0.1%) followed by BSFPC (41.7%) and WPI (27.5%). With the increase in protein concentration from 0.5% to 1.0%, LMPC maintained the highest EA (61%) while the differences with BSFPC and WPI were reduced to non-significant level, reaching a similar EA value with 1% of protein concentration. Higher EAs of protein extracts (1% w/v) from other insect species of *T.molitor* (66.6%), *G. sigillatus* (72.6%) and *S.gregaria* (67.8) were reported compared to plant seeds proteins (18-65%)<sup>65</sup>. Therefore, insect protein is a promising material to be used as a hydrophilic emulsifier in the stabilization of oil-in-water (O/W) type emulsion, which is studied in detail comparing the impact of pre-defatting solvents in the following section.

The superior EA of LMPC can be related to its higher protein surface hydrophobicity ( $H_o$ ) compared to BSFPC as it shows in Figure 4.6.  $H_o$  is related to the amount of hydrophobic units exposed on the molecule in the soluble protein fraction different from OBC which is the property of the whole powders of insect protein concentrate. Thus,  $H_o$  is highly relevant to the emulsifying properties as it affects the ability of the soluble protein molecules to adsorb to the oil-water interface<sup>33</sup>. However, it is not the only key parameter to assess the emulsifying properties. Protein molecular size, molecular flexibility, surface charge, and solubility also have great influences on the overall emulsifying properties<sup>82</sup>. As can be seen from Figure 4.6, WPI exhibited higher  $H_o$  than LMPC and BSFPC, while the EA at low protein concentration (0.1%), both insect protein concentrate performed better than WPI. Likewise, Mishyna et al.<sup>68</sup> observed a higher  $H_o$  of WPI compared to the ones of insect protein extracts from *S. gregaria* and *A. mellifera*<sup>68</sup>, while all of them displayed an identical emulsifying capacity.

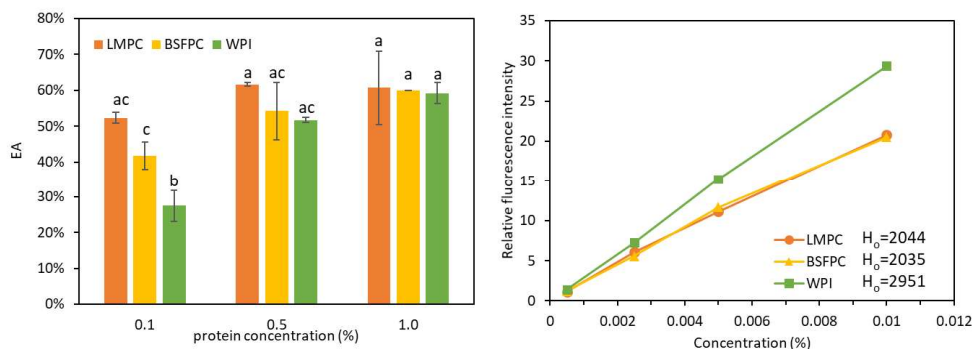


Figure 4.6 EA (left) and  $H_o$  (right) of LMPC compared with WPI and BSFPC. Error bars correspond to standard deviation of the mean and the presence of different letters indicate a significant difference between samples at  $p < 0.05$  ( $n=3$ ).

#### 4.3.5 O/W emulsion production and stability

In the previous section, LMPC\_ETOH showed some promising results on the techno-functional properties, especially on the emulsifying activity compared to WPI<sup>82</sup>. To further evaluate the impact of the defatting solvent on the emulsifying properties of the protein concentrates obtained thereafter, O/W emulsions stabilized with each of the LMPC (LMPC\_HEX, LMPC\_IPOH, LMPC\_ETOH and LMPC\_MTHF) were produced by premix membrane emulsification while emulsion stability was monitored during 1 week of storage at room temperature (25 °C). Emulsification with dynamic membranes of tunable pore size (DMTS) is a low-energy high-throughput technique that can be used in premix mode.

Sunflower O/W emulsions were produced as described in the section 4.2.7 using premix emulsification with DMTS. Coarse emulsions produced by rotor-stator homogenization displayed moderately similar values in  $d_{3,2}$  and span (Figure 4.7) regardless of the solvent used for defatting. At the end of the refinement process, 5 emulsification cycles, all emulsions showed a similar  $d_{3,2}$  of  $8.4 \pm 1.0 \mu\text{m}$  and span of  $1.42 \pm 0.6$ . Minor differences were found in the emulsion stabilized by LMPC\_MTHF which exhibited a relatively high reduction in the droplet size after 3 emulsification cycles, however, it presented a moderately higher span during cycle 1 to 5 compared to others. As it can be seen from the histograms of droplet size distribution (Figure 4.8), after one DMTS emulsification cycle, most of the emulsions had a narrow droplet size distribution with/without a small tail in the smaller size range. The presence of the detected smaller size droplets ( $< 4 \mu\text{m}$ ) was confirmed by microscopic images (Figure 4.9).

Transmembrane flux obtained during DMTS emulsification ranged from 100 to 300  $\text{m}^3\text{m}^{-2}\text{h}^{-1}$ . From the results shown in Figure 4.7, the emulsions stabilized by LMPC\_HEX, LMPC\_IPOH and LMPC\_ETOH showed an increase at the cycle 2 which is on account of the droplet break-up took place during the cycle 1 led to small size droplets which made it easier and faster to pass through the membrane. However, the later flux reduction for the emulsion stabilized by LMPC\_MTHF might be ascribed to the fouling of the membrane/microporous system. It has been well reported in literature that the use of proteins as emulsifiers can result in the fouling and blocking of membranes<sup>282,283</sup>. Nevertheless, all the formulations displayed fluxes above 100  $\text{m}^3\text{m}^{-2}\text{h}^{-1}$  overall, which indicates the DMTS is a productive technology for premix membrane emulsification as compared to other membranes such as membranes made of polycarbonate, Nylon, polyethersulfone and cellulose mixed esters<sup>262</sup>.

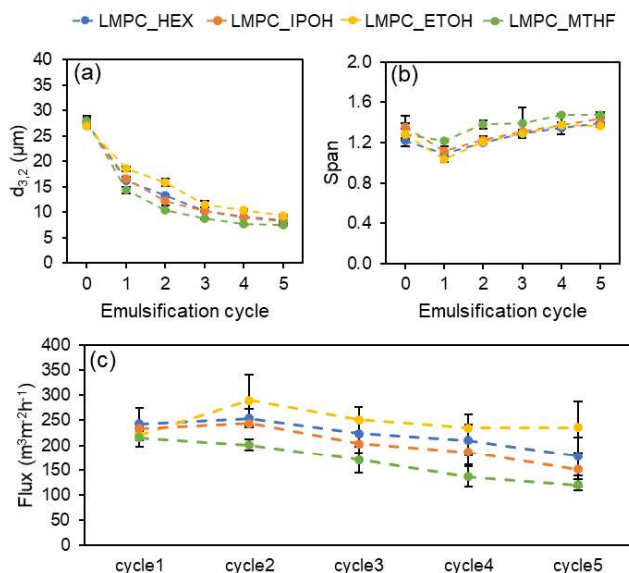


Figure 4.7 Droplet size distribution ( $d_{3,2}$  and span) of the emulsions stabilized with LMPC defatted in different solvents.

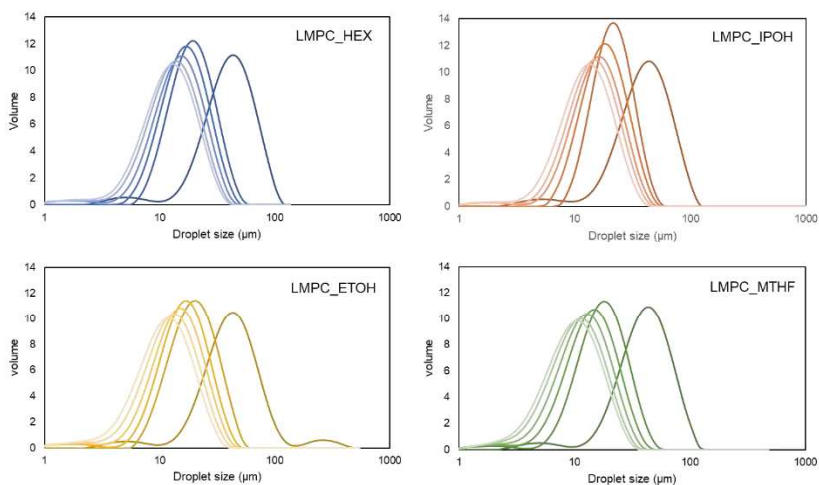


Figure 4.8 Histogram of droplet size distribution of emulsions stabilized by LMPC, the dark to light color indicates the emulsification cycle increased from 0 (coarse) to 5.

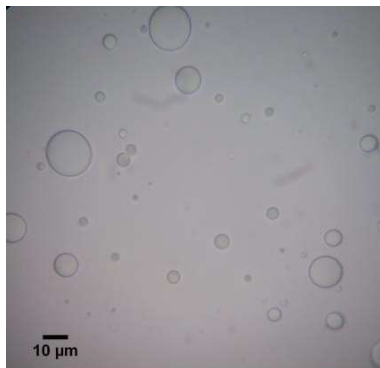


Figure 4.9 Microscopic image of O/W emulsions stabilized by LMPC (pre-defatted using ethanol) after 5 emulsification cycles at magnification of 100x.

As for the storage stability, most of the emulsions could maintain the droplet size distribution for a duration of 3 days at 25 °C except for the one stabilized by LMPC\_ETOH, which exhibited a fluctuation in span after 1 day of storage (Figure 4.10). After 7 days of storage, emulsions stabilized with LMPC\_HEX and LMPC\_ETOH reached a span of about 2.5, while for the ones stabilized by LMPC\_IPOH and LMPC\_MTHF span was around 2.0, whilst the mean droplet size displayed a minor increase ( $\leq 1\mu\text{m}$ ). The increase of span and  $d_{3,2}$  can be attributed to droplet coalescence. Although the zeta potential values maintained below -30 mV (which is considered to have sufficient electrostatic repulsion to stabilize droplets) over 7 days of storage (Figure 4.10), it is not always the only determining factor. Therefore, considering from the emulsification process in DMTS, droplet size distribution, emulsion stability and productivity, it can be concluded that the defatting solvent tested has no effect on the quality of emulsions produced in premix membrane emulsification in DMTS.

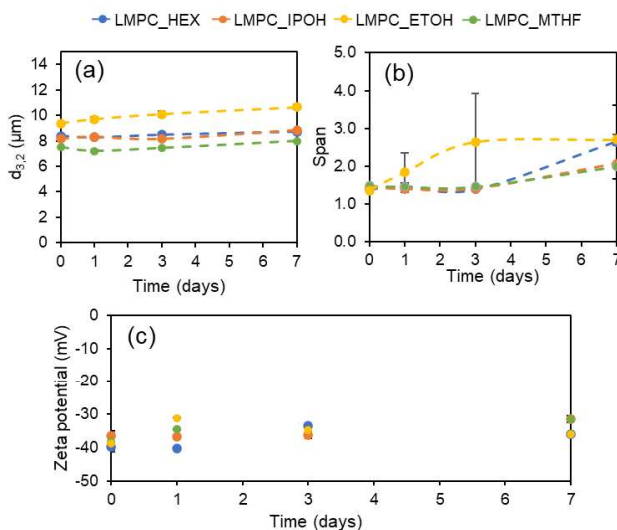


Figure 4.10 Variation of (a)  $d_{3,2}$ , (b) span and (c) zeta potential of emulsions stabilized with LMPC defatted by different solvents during 7 days of storage at 25 °C.

#### 4.3.6 Solid microcapsules

As emulsion is a thermodynamically unstable system, by removing the aqueous phase, it facilitates the shelf-life of the product by the protection from chemical deterioration and environmental factors, simplifies the handling, dosage and transportation. The advantage of the protection and the controlled release of the encapsulate is maintained due to the emulsion is able to reconstitute after rehydration. It worth pointing out that neither spray drying of insect protein nor dehydration of insect protein stabilized emulsions is reported at this moment. This first practice has followed the comparable method and processing conditions as other literatures<sup>151,158</sup>.

For the production of solid microcapsules, 150 mL of 20 wt% sunflower O/W emulsions stabilized by LMPC (pre-defatted by ethanol) was produced using premix emulsification in DMTS system. Spray drying was performed at the conditions described in section 4.2.9. As a wall-building material, maltodextrin, was previously added in the refined emulsion to facilitate a shell formation and, in turn, protect the encapsulate and the emulsions during the spray drying process. As shown in the Figure 4.11, the addition of maltodextrin did not affect the droplet size distribution the original emulsion. From the ESEM photos, it can be seen that the produced solid microcapsules have a typical smooth spherical shape, also with some dented surface and presented some degree of agglomeration. A similar morphology was also observed in the study of spray dried multiple emulsions stabilized by whey protein and MD<sup>163</sup>, and a direct encapsulation of cactus polyphenols with MD<sup>284</sup>. The agglomeration of the particles is dependent on the properties of the material, and may be reduced by modifying drying conditions<sup>284</sup>. The wall thickness of the capsules is about 400 nm as it can be seen in Figure 4.12. The reconstituted emulsion displayed a wider span value, which can be result of the droplet destabilization (coalescence) during the drying process. In all, it is a successful production of solid microcapsules from O/W emulsions stabilized by insect protein, which can be rebuild the O/W emulsion structure after rehydration.

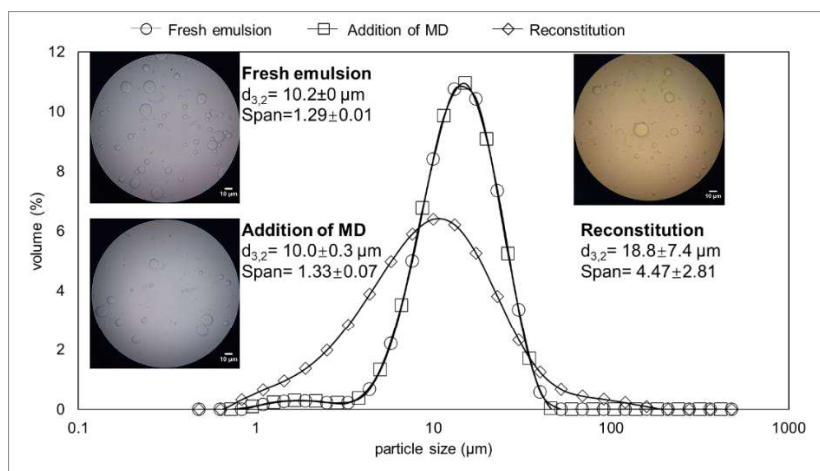


Figure 4.11 Droplet size distribution of fresh emulsion, with addition of MD and reconstituted emulsion with microscopic photos attached (scale bar indicates 10  $\mu\text{m}$ ).

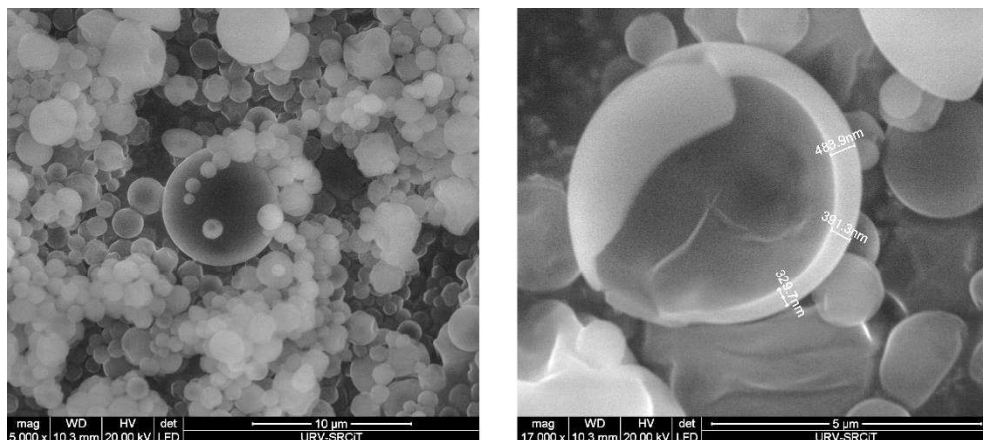


Figure 4.12 ESEM images of solid microcapsules overview at 5000x magnification (left) and an indication of wall thickness of a broken capsules at 17000x magnification.

#### 4.4 Conclusion

Among the solvents used, 2-MeTHF is the most suitable solvent for lipid extraction/defatting with the higher lipid yield and efficiency, besides it is a sustainable alternative as it is a biomass-derived ecofriendly solvent. Extracted lipids consist of three most abundant fatty acids C18:1 cis+trans, C18:2 trans and C16, irrespective to the solvent used. The protein concentration in the extracted LMPCs displayed at the range of 71.1 to 78.3%, with the higher value obtained from the 2-MeTHF defatted powders. Nevertheless, their emulsifying ability was highly similar irrespective to the defatting solvent used. Hence, the solvent did not affect the protein functionality. Furthermore, solid capsules produced from O/W emulsions stabilized by LMPC\_ETOH was successfully formulated with addition of maltodextrin, and the emulsions could be reconstituted after rehydration. To be noted that this is the first practice of using insect protein in the production of solid microcapsules. The cheerful results provide more opportunities for insect protein to be implemented in various complex systems such as in multiple emulsions (water-in-oil-in-water), and different drying methods to produce solid microcapsules such as freeze drying.

## Chapter 5

# Emulsifying properties and emulsion stability of multiple emulsions stabilized with lesser mealworm (*Alphitobius diaperinus*) protein concentrate

### Abstract

Water-in-oil-in-water ( $W_1/O/W_2$ ) emulsions are complex delivery systems for polyphenols amongst other bio-actives. To stabilize the oil-water interphase, dairy proteins are commonly employed, that ideally are replaced by other from more sustainable sources, such as insect proteins. In this study, lesser mealworm (*Alphitobius diaperinus*) protein concentrate (LMPC) is assessed and compared to whey protein (WPI) and pea protein (PPI), to stabilize  $W_1/O/W_2$  emulsions and encapsulate a commercial polyphenol. The results show that LMPC is able to stabilize  $W_1/O/W_2$  emulsions comparably to whey protein and pea protein when using a low-energy membrane emulsification system. The final droplet size ( $d_{4,3}$ ) is 7.4  $\mu\text{m}$  and encapsulation efficiency between 72-74%, regardless of the protein used. Under acidic conditions, the LMPC shows similar performance as whey protein and outperforms pea protein. Under alkaline conditions the three proteins perform similarly, while the LMPC-stabilized emulsions are less able to withstand osmotic pressure differences. The LMPC stabilized emulsions are also more prone to droplet coalescence after a freeze-thaw cycle than the WPI-stabilized ones, but they are most stable when exposed to the highest temperatures tested (90 °C). The results show the ability of LMPC to stabilize multiple emulsions and encapsulate a polyphenol, which opens the door for application in foods.

This chapter has been submitted as:

Wang, J., Ballon, A., Schroën, K., de Lamo-Castellví, S., Ferrando, M., & Güell, C. Emulsifying properties and emulsion stability of multiple emulsions stabilized with lesser mealworm (*Alphitobius diaperinus*) protein concentrate, *Food Research Internationa*.



## 5.1 Introduction

Multiple emulsion-based delivery systems, especially water-in-oil-in-water ( $W_1/O/W_2$ ) double emulsions can be applied to tune the bioactive profile of foods, pharma products, and cosmetics as they can encapsulate, protect and release bioactive lipids (such as vitamin E) and water-soluble compounds such as vitamins B and C, flavorings, polyphenols, and probiotics<sup>14,211,285</sup>. Polyphenols are well-known highly effective antioxidants that possess various health benefits such as prevention of cancer, inflammation, diabetes, and cardiovascular diseases<sup>30,286</sup>. They exist in a wide range of plants in nature, and they are a well-known target for by-product or food-waste valorization, such as grape seeds<sup>204</sup>, spent coffee grounds<sup>287</sup>, and olive leaves<sup>288</sup>. Due to their sensitivity to light, heat, oxidation, and to certain pH values, encapsulation of polyphenols has been carried out using several technologies. Amongst them, water-in-oil-in-water ( $W_1/O/W_2$ ) emulsions are a promising strategy based on the high encapsulation efficiency, chemical stability and increased bio-accessibility upon controlled release<sup>286,289–291</sup>. The incorporation of polyphenols encapsulated in  $W_1/O/W_2$  emulsions into several food matrices for instance yoghurt<sup>289,292</sup>, salad dressing<sup>288</sup>, and meat products<sup>293</sup> have been recently reported in the literature.

During the formation of emulsions, the emulsifier plays an important role in both decreasing the interfacial tension and preventing coalescence of the droplets, therefore, the selection of a suitable emulsifier is a key step in the formulation of a stable emulsion system.  $W_1/O/W_2$  emulsions commonly use lipophilic emulsifiers to stabilize the  $W_1/O$  primary emulsion, such as polyglycerol polyricinoleate (PGPR), Tween 80, and lecithin<sup>211</sup>. As for stabilizing  $W_1/O$  emulsion in the  $W_2$  phase, in general, natural food-grade ingredients such as dairy proteins, whey, and casein from milk, are widely used because of their amphiphilic structure. From the viewpoint of green and sustainable development, it is of great significance to replace proteins from dairy sources with feasible alternatives from a sustainable source that can alleviate global warming. Thus, plant and insect proteins are promising alternatives that have attracted attention for their techno-functional properties<sup>91</sup>.

Plant proteins such as protein isolated from peas (*Pisum sativum L.*, PPI) is nutritious, gluten-free, non-genetically modified, and presents low allergenicity<sup>294</sup>, has been characterized for its techno-functional properties, and to some extent for emulsifying properties to stabilize O/W emulsions and Pickering emulsions solely or as PPI-polysaccharides conjugates<sup>48,51,295,296</sup>. The incorporation of plant proteins in the formulation of  $W_1/O/W_2$  emulsions is scarcely reported. Xu et al.<sup>297</sup> evaluated the stability of pigment-encapsulated  $W_1/O/W_2$  emulsions stabilized by soy protein isolate under various temperatures and salt concentrations, which demonstrated great heat stability and a tolerance to  $< 5$  mM  $CaCl_2$ , and Tamnak et al.<sup>298</sup> reported that  $W_1/O/W_2$  emulsions stabilized by pectin-PPI conjugate resulted in higher emulsion stability and zeta potential, smaller droplet size and better encapsulation properties than the emulsions stabilized with native pectin and Tween 80.

Insect proteins have drawn attention in recent years as a sustainable alternative to more classic animal proteins in several world areas, mainly where insects are not habitually consumed. The Food and Agricultural Organization (FAO) promotes the consumption of insects due to their great nutritional value, less greenhouse gas emission during rearing, and a short life cycle with a great potential economic benefit<sup>99</sup>. In Europe, the first safety assessment on the use of dried yellow mealworm as novel food was reported in 2021 with encouraging results<sup>122</sup>. Edible insects have high protein content on a dry weight basis, e.g., 44.8-50.1% in yellow mealworm (*Tenebrio molitor*), 42.0-45.8% in cricket (*Acheta domestica*), 62.4-67.2% in grasshoppers (*Oedalium asiaticum*, *Angaracris rhodopa*, *Chorthippus dubius* and *C. fallax*), and 57.6% in lesser mealworm (*Alphitobius diaperinus*)<sup>115,299</sup>.

Investigations on techno-functional properties including solubility, water and oil binding capacity, foaming capacity, surface hydrophobicity, gelling properties, coagulation properties, and emulsifying ability of various insect powders, and their protein extracts have already shown promising outcomes<sup>65,68,74,85,246,300</sup>. In addition, enzymatic hydrolysis of the protein extracts could efficiently enhance their functionalities and obtain bioactive peptides with antioxidative, antihypertensive, antidiabetic, and antimicrobial properties<sup>64,66,76,281,301,302</sup>. As for the studies in emulsions stabilized with insect proteins, In the previous Chapter 3, a superior performance of black soldier fly (*Hermetia illucens*) protein concentrate on emulsifying high fraction (40 wt%) of lemon oil compared to whey protein isolate (WPI) was observed, and Gould and Wolf<sup>82</sup> found that sunflower oil emulsions stabilized with mealworm protein displayed smaller droplet size and less protein concentration was required compared to WPI; in addition, the produced emulsion also showed great stability under wide environmental stresses (temperature at -20 °C and 60-90 °C, pH 3-8 and ionic strength 80-330 mM). These results show the potential of insect proteins to stabilize emulsions and are a good starting point to broaden their use to more complex systems such as W<sub>1</sub>/O/W<sub>2</sub> emulsions.

The objective of this work is to study the ability of lesser mealworm protein concentrate (LMPC) to stabilize W<sub>1</sub>/O/W<sub>2</sub> emulsions designed to encapsulate and protect a commercial procyanidin-rich extract. The performance of the insect protein will be compared with a conventional dairy protein (whey protein) and a protein from another sustainable source (pea protein). The effect of several environmental stresses such as temperature, pH, and salt concentration on the emulsion stability will be assessed for LMPC and compared with the other two selected proteins. Special attention is paid to protein-polyphenol interactions. To the best of our knowledge, this is the first attempt to assess the use of an insect protein to stabilize W<sub>1</sub>/O/W<sub>2</sub> emulsions, providing relevant results regarding its feasibility and potential applications in food, pharmaceuticals, and cosmetics.

## 5.2 Materials and methods

### 5.2.1 Materials

The composition of double emulsions is listed in Table 5.1. Vitaflavan (DRT, France) is a red-violet-colored commercial white grape seed extract, with a reported total

polyphenol content above 96% and antioxidant activity (ORAC) of 19000 mmol TEQ g<sup>-1</sup> that will be referred to hereafter as procyanidin-rich extract. 10 wt% procyanidin-rich extract solution was vacuum filtered through 11 µm pores (grade 1 filter paper, Whatman, UK) before use. Polyglycerol polyricinoleate (PGPR, ref-4120 Palsgaard, Denmark) was used as a lipophilic emulsifier dissolved in commercial sunflower oil (Borges S.A., Spain). Proteins investigated in this study are whey protein isolate (WPI, BiPRO, lot no. JE 034-7-440-6, Davisco Foods International, Inc., USA) with a reported protein content of 98.1% on a dry basis, less mealworm protein concentrate (LMPC) was extracted from insect powder BUFFALO'S (Kreca Ento-Food BV, the Netherlands) on lab-scale, and pea protein isolate (PPI, Roquette, NUTRALYS, s85F, France) had a reported purity of 80-90%. To produce LMPC, 2-methyl tetrahydrofuran (2-MeO, EMPLURA, Germany) was used in pre-defatting, sodium hydroxide pellet (CHEM-LAB, Belgium) and hydrochloric acid (37-38% HCl, J.T. Baker, Germany) were used for extraction.

Table 5.1. Formulations of W<sub>1</sub>/O/W<sub>2</sub> emulsions and osmotic properties of aqueous phases.

Phase	Fraction (%)	Composition	Osmolality (mOsmol/kg)	Calculated osmotic pressure (MPa)
W <sub>1</sub>	6	10 wt% procyanidin-rich extract	105.65 ± 4.97	0.56 ± 0.03
O	14	6 wt% PGPR in sunflower oil	--	--
W <sub>2</sub>	80	i. 1 wt% WPI (0.4 wt% NaCl) in phosphate buffer pH 7, 0.02 wt% Na <sub>3</sub> N	107.83 ± 1.07	0.57 ± 0.01
		ii. 1% LMPC (0.06 wt% NaCl) in phosphate buffer pH 7, 0.02 wt% Na <sub>3</sub> N	110.03 ± 2.78	0.58 ± 0.01
		iii. 1% PPI (0.25 wt% NaCl) in phosphate buffer pH 7, 0.02 wt% Na <sub>3</sub> N	104.93 ± 1.24	0.55 ± 0.01

2 wt% WPI solution was prepared one day before by dissolving WPI powder in 5 mM phosphate buffer pH 7 prepared with di-sodium hydrogen phosphate dihydrogen, (Scharlau, Spain) and sodium phosphate monobasic monohydrate (ACROS, Spain) under magnetic stirring for 2 h at 400 rpm and kept in the fridge overnight for complete hydration. LMPC and PPI solutions were prepared similarly to WPI using buffer, and pH adjustment to 7.0 every 30 min using 4 M NaOH or 1N HCl. After two hours, the solutions were put in the fridge overnight. LMPC and PPI concentrations were quantified before use with the Pierce™ BCA protein assay kit (Thermoscientific, USA) and concentrations were expressed as bovine serum albumin equivalent value (BSAE%, w/w). The concentration of WPI and the BSAE% of LMPC and PPI was obtained by dilution

in buffer and the addition of sodium chloride (NaCl, Panreac, Spain), and antimicrobial agent sodium azide (Na<sub>3</sub>N, Sigma-Aldrich, USA) as indicated in Table 5.1. LMPC and PPI protein concentration is shown in % for simplicity reasons. Sodium carbonate (Panreac, Spain), gallic acid monohydrate (Panreac, Spain) and Folin-Ciocalteu's reagent (Panreac, Spain) were used for total polyphenol content (TPC) quantification.

In the emulsification module, glass micro-beads with a size of 38 µm (Microspheres-nanospheres, USA) were placed on top of a nickel sieve (Stork Verco, Erbeek, the Netherlands). Sodium hydroxide and ethanol (96%, Scharlab, Spain) were applied for cleaning of nickel sieve and silica beads respectively.

### 5.2.2 Preparation of lesser mealworm protein concentrate (LMPC)

Defatting of the original lesser mealworm powder was carried out using the organic solvent 2-MeO. Shortly, 50 g of lesser mealworm whole-fraction powder was mixed with 250 mL of 2-MeO in a covered beaker and stirred magnetically at 300 rpm for 1 h. Then decantation of the solvent layer was carried out after complete phase separation. The process was repeated 3 times in total by adding 250 mL of 2-MeO each time. The remaining solvent in the powder was evaporated in the fume hood over 3 days. Protein extraction was conducted based on the literature<sup>82</sup> with slight modifications. In brief, 30 g dried defatted powder and 150 mL of 0.25M NaOH solution were stirred at 400 rpm for 1 h at 40 °C. The mixture was centrifuged for 15 min at 3358 g. The supernatant was separated, and its pH was adjusted to 4.0-4.5 with HCl to precipitate protein; the remaining pellet was subsequently used for protein extraction repeating the process two more times. The precipitated protein from the 3 extractions was combined and centrifuged (15 min, 2343 g), then it was freeze-dried (LYOQUEST-85 PLUS, Telstar, Spain) for 24 h at 0.2 mbar vacuum and plate temperature at 20 °C. The collected freeze-dried protein powders were blended and stored in a desiccator with a water activity of 0.075.

### 5.2.3 Osmolality of W<sub>1</sub> and W<sub>2</sub>

Osmolality of water phases was measured using vapor pressure osmometer (K-7000, KNAUER, Germany) at 39±2 °C calibrated by 400 mOsmol/kg NaCl solution. To balance the relatively high osmolality of the 10 % procyanidin-rich extract solution (W<sub>1</sub>), NaCl was added to the protein solutions (W<sub>2</sub>) as shown in Table 5.1. Results are shown as mean ± standard deviation (n=5).

### 5.2.4 W<sub>1</sub>/O/W<sub>2</sub> emulsions production

#### **Coarse W<sub>1</sub>/O/W<sub>2</sub> emulsion**

The method for producing W<sub>1</sub>/O/W<sub>2</sub> emulsions was followed as described in Chapter 2. In brief, the primary emulsion (W<sub>1</sub>/O) was generated by adding W<sub>1</sub> phase solution into sunflower oil with 6% PGPR under rotor-stator homogenization (Ultra Turrax T18 digital, IKA, Germany) for 5 min at 11000 rpm. Then, the primary emulsion was introduced into W<sub>2</sub> phase, containing the dissolved protein, while being stirred at 1600 rpm for 5 min on a magnetic stirrer to produce the coarse W<sub>1</sub>/O/W<sub>2</sub> emulsions.

## Refinement of $W_1/O/W_2$ emulsions by dynamic membranes of tunable pore size (DMTS)

DMTS consists of a layer of glass microbeads placed on top of a nickel sieve (Figure 5.1). The nickel sieve had pores of  $284.7 \times 12.8 \mu\text{m}$  (length  $\times$  width) with a thickness of  $120 \mu\text{m}$ . Glass microbeads of  $38 \mu\text{m}$  ( $0.44 \text{ g}$ ) were placed in the module on top of the nickel sieve, which resulted in  $2 \text{ mm}$  layer with an interstitial void diameter of  $\sim 22 \mu\text{m}$ , as calculated in the Chapter 3. Coarse emulsions were placed in the vessel and immediately passed through the DMTS system pressurized to  $500 \text{ kPa}$  with  $\text{N}_2$ ; this process is called one emulsification cycle. Three emulsification cycles were conducted for  $W_1/O/W_2$  emulsions stabilized with the three proteins. Refined emulsions were collected separately in a flask placed on an electronic balance to record the mass gain every second, from which transmembrane flux can be calculated as:

$$J_{DMTS} = \frac{\phi}{\rho_e A} \quad \text{eq (5.1)}$$

where  $\phi$  is the mass flow rate as acquired from data recorded with the electronic balance,  $\rho_e$  is the emulsion density,  $A$  is the effective surface area of the DMTS.

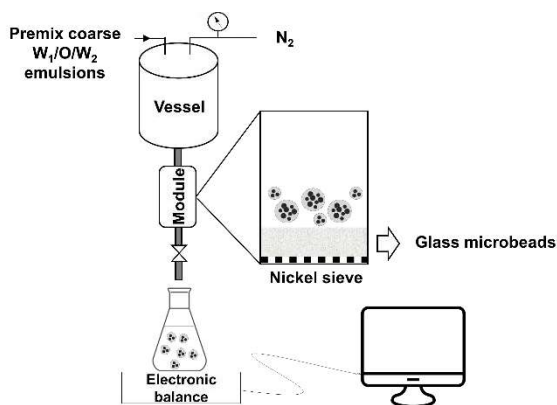


Figure 5.1. Schematic representation of experimental DMTS setup.

‘Blank’ emulsions were produced following an identical process except that the  $W_1$  phase consisted of a  $0.4 \text{ wt\%}$   $\text{NaCl}$  solution. The purpose of preparing blank emulsions is to eliminate the impact of proteins in the total polyphenol content quantification.

The DMTS module was disassembled after use, and nickel sieves and glass microbeads were reused after cleaning and drying following the cleaning protocol described in Chapter 2. Duplication was carried out for each formulation.

### 5.2.5 Environmental stress test

Freshly produced  $W_1/O/W_2$  emulsions were divided over several glass tubes that were tightly shut for further treatment at various environmental conditions. Samples were covered with aluminum foil to avoid light and stored at the required conditions depending on the environmental stress test performed. The stability of the emulsions was followed

using droplet size distribution, microstructure (microscopic images), visual appearance, zeta potential, and encapsulation efficiency.

### Temperature

The influence of temperature on emulsion stability was studied by storing the samples at -20 °C (in the freezer) for 24 h, at 4 °C (fridge) and 25 °C (room temperature) for 14 days, as well as holding the samples at 37 and 65 °C for 30 min and at 90 °C for 5, 15, 30, and 60 min individually on a dry bath heating block (FB15101, Fisher Scientific, UK). These latter three temperatures were chosen to represent the situation in the body, and during processing. Frozen samples were analyzed after thawing at room temperature. Samples maintained at 4 and 25 °C were analyzed after 1, 3, 7, and 14 days of storage. Samples subjected to heat treatment at 37, 65, and 90 °C were kept at room temperature for 24 h before analysis.

### pH

The influence of pH on emulsion stability was examined by adjusting the pH of the outer water phase of  $W_1/O/W_2$  emulsions to 1.5, 4.0, and 8.0 (pH deviations of 0.25) with 35-37% HCl or 1M NaOH. Samples were analyzed after storing them for 1, 7, and 14 days at room temperature.

### Osmotic stress

The influence of osmotic imbalance on emulsion stability was assessed from 10-fold water dilution of  $W_2$  fraction (leading to osmotic pressure  $\Pi_{W_1} > \Pi_{W_2}$ ) and addition of NaCl to  $W_2$  phase to create extra 50 or 250 mM salt concentration (resulting in osmotic pressure  $\Pi_{W_1} < \Pi_{W_2}$ ). Samples were stored at room temperature and analyzed after 1, 7, and 14 days of storage.

## 5.2.6 Characterization of emulsions

### Droplet size distribution

Droplet size distribution of  $W_1/O/W_2$  emulsions was measured after every emulsification cycle and during environmental stress tests by laser diffraction using Mastersizer 2000 (Malvern Instruments, UK). 0.4 wt% NaCl water solution was used as the continuous phase in Mastersizer Hydro 2000G accessory to disperse the emulsion at similar aqueous phase osmotic pressure. The particle reflective index and the dispersant reflective index were set to 1.480 and 1.330, respectively. Mean droplet size and droplet size dispersion were calculated and expressed as volume weighted mean diameter  $d_{4,3}$  (equation 5.2), and span  $\delta$  (equation 5.3), respectively.

$$d_{4,3} = \frac{\sum n_i D_i^4}{\sum n_i D_i^3} \quad \text{eq (5.2)}$$

Where  $n_i$  is the number of droplets, and  $D_i$  is the diameter of the  $i^{\text{th}}$  droplet.

$$\delta = \frac{d_{90}-d_{10}}{d_{50}} \quad \text{eq (5.3)}$$

Where  $d_x$  is the droplet diameter corresponding to x% volume of a cumulative droplet size distribution curve.

### Zeta potential

Zeta potential of freshly produced  $W_1/O/W_2$  emulsions and during environmental stress tests were measured using dynamic light scattering (Zetasizer Nano-ZS, Malvern Instruments, U.K.) in triplicate. The changes in zeta potential at altered pH values were also monitored over 14 days. The same values of reflective index of particle and dispersant as those indicated in section 5.2.6 were also applied here. Samples were diluted 200 times by deionized water.

### Encapsulation efficiency of polyphenols

Polyphenol encapsulation efficiency was deduced following the method previously described in Chapter 2. Blank  $W_1/O/W_2$  and  $W_1/O/W_2$  emulsions containing procyanidin-rich extract were centrifuged for 10 min at 825 g. Then, the  $W_2$  phase was carefully taken by needle and syringe, and total polyphenol concentration was analyzed based on Folin-Ciocalteu colorimetric method in triplicate. Briefly, 100  $\mu\text{L}$  of diluted sample and 100  $\mu\text{L}$  of Folin reagent were mixed with 2 mL of  $75 \text{ gL}^{-1} \text{ Na}_2\text{CO}_3$  solution and 2.8 mL of deionized water. After 1 h of incubation at room temperature in the dark, absorbance was measured at 750 nm by a UV-Vis spectrophotometer (Hach Lange DR5000, Hach Lange SLU, Spain). The concentration of polyphenol was calculated using a calibration curve with a known amount of gallic acid as standard and expressed as gram gallic acid equivalent per liter ( $\text{gGAE L}^{-1}$ ). The mass of polyphenols that remained encapsulated in  $W_1$  was expressed as polyphenol encapsulation efficiency (EE) by equation (5.4),

$$EE[\%] = \frac{m_{polyW_1}^0 - C_{polyW_2}(m_{W_1}^0 + m_{W_2}^0)}{m_{polyW_1}^0 - C_{polyW_2} m_{W_1}^0} \times 100 \quad \text{eq (5.4)}$$

where  $m_{polyW_1}^0$  is the initial polyphenol mass in the inner water phase ( $W_1$ ),  $C_{polyW_2}$  is the concentration of polyphenols in the outer water phase ( $W_2$ ),  $m_{W_1}^0$  is the initial mass of the inner water phase, and  $m_{W_2}^0$  is the initial mass of the outer water phase.

### Microstructure analysis

Laser scanning confocal microscope (NIKON model TE2000-E, the Netherlands) was used to observe the  $W_1/O/W_2$  emulsion structure and estimated droplet sizes.

### 5.2.7 Interaction of protein and polyphenols

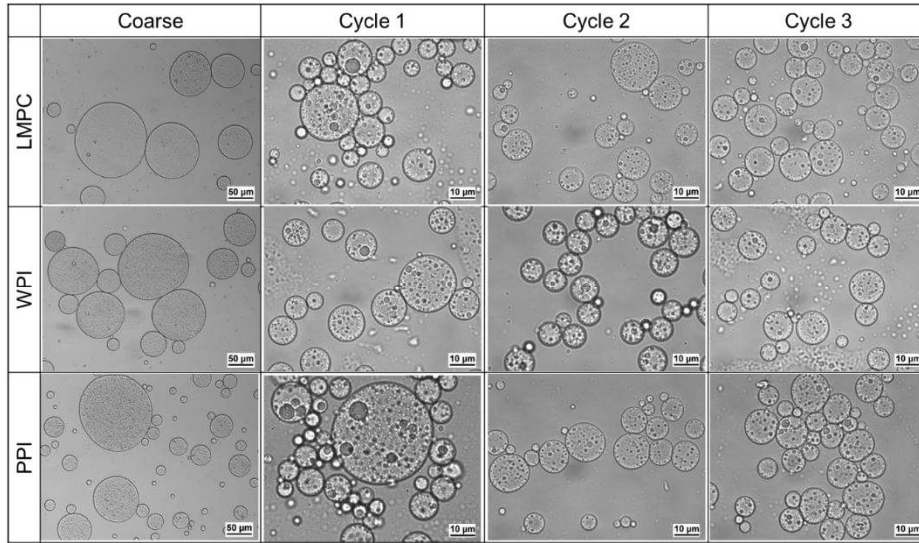
0.5 wt% WPI (0.4wt% NaCl) and 0.5% LMPC (0.06% NaCl) in 5 mM phosphate buffer (pH 7) solutions were used to assess the interaction with the procyanidin-rich extract (dissolved in a pH 7 phosphate buffer with 0.02 wt%  $Na_3N$ ) at concentrations ranging from 0 to 0.3%. The mixture was stirred, and the pH was adjusted in the range of 2.5 to 7.5 by adding 0.1 M NaOH or 0.1N HCl dropwise. The transmission of the solution was then measured by static multiple light scattering using Turbiscan Lab Expert (Formulation, France). The mixture was also centrifuged for 10 min at 3000 rpm to observe sediment formation. Duplicates were carried out for each polyphenol concentration.

## 5.3 Results and discussion

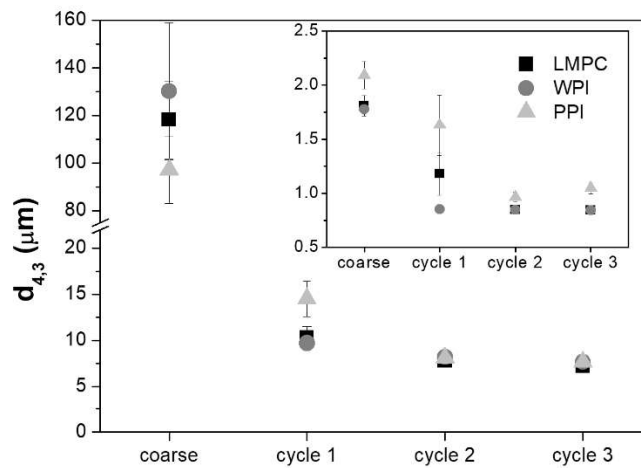
### 5.3.1. Production of $W_1/O/W_2$ emulsions stabilized with LMPC, WPI, and PPI

#### **Particle size distribution and transmembrane flux**

$W_1/O/W_2$  emulsions stabilized with three different emulsifiers, LMPC, WPI, and PPI, were produced following the procedure described in section 5.2.4. The microstructure of these emulsions is presented in Figure 5.2-A. It is clear from this figure that the  $W_1/O/W_2$  emulsions were successfully formed with all emulsifiers. The overall variations in  $d_{4,3}$  and span after emulsification cycles (Figure 5.2-B) followed the same trend for all the emulsions. Although coarse emulsions produced with different proteins resulted in differences in droplet size ( $d_{4,3} = 97.3\text{-}130.2 \mu\text{m}$ ), the DMTS system successfully refined them sharply to  $9.7 \pm 2.4 \mu\text{m}$  after the first emulsification cycle, and then to  $7.4 \pm 0.2 \mu\text{m}$  after the third cycle, regardless of the protein used. The span of WPI stabilized emulsions sharply decreased to 0.85 after the first cycle, while for LMPC and PPI emulsions the span reached this value after the second emulsification cycle. Therefore, the type of protein used to stabilize the oil- $W_2$  interface did not considerably affect the final droplet size distribution of the  $W_1/O/W_2$  emulsions after 3 emulsification cycles when using the DMTS system. The results obtained show, as previously reported by other authors, that it is possible to reduce coarse emulsions with a droplet size 2-3.5 times bigger than the interstitial void diameter of the glass microbeads layer to a value smaller than the interstitial void diameter (less than 50%)<sup>130</sup>. Moreover, the droplet size distribution obtained using LMPC, WPI and PPI is similar to the one reported by Sahin et al.<sup>144</sup> for the production of  $W_1/O/W_2$  emulsions stabilized with Tween 20 using the same emulsification technology with  $30 \mu\text{m}$  glass microbeads. Overall, LMPC has shown a comparable potential to stabilize  $W_1/O/W_2$  emulsions to WPI and PPI when using the low-energy membrane emulsification system.



(A)



(B)

Figure 5.2. (A) Microscopic images (scale bars on coarse emulsion indicate 50  $\mu\text{m}$ , and for the rest of cycles 10  $\mu\text{m}$ ) and (B)  $d_{4,3}$  and span of  $W_1/O/W_2$  emulsions stabilized with 1% LMPC, 1% WPI and 1% PPI as a function of emulsification cycle.

An important parameter to scale up the emulsification process is the transmembrane flux. Table 5.2 presents the values obtained during the three emulsification cycles and shows that the values (which are all high, especially when compared to regular membrane emulsification) and evolution are very similar for all three proteins. The lowest flux corresponds to the first emulsification cycle during which the highest droplet break-up occurs, and the energy is mostly invested in this process rather than to flow the emulsion through the DMTS system. During the second and third cycles, there is a higher flux since almost no droplet break-up occurs (Figure 5.2-B), and the pressure is mostly invested in

flowing the emulsion through the system. The fluxes reported in the literature using the same system differ from 0.5-1200  $\text{m}^3\text{m}^{-2}\text{h}^{-1}$ <sup>136,141</sup>. The differences in flux among the reported studies is expected, and not always comparable as they are related to various factors such as the composition of emulsion, DMTS setup (glass microbeads size and amount, nickel sieve size) and pressure applied. All in all, the flux values obtained with the three proteins are high and in the range of industrial interest.

### Encapsulation efficiency (EE)

Besides the ability of the proteins to stabilize the newly formed interfaces during the emulsification cycles, leading to a narrow droplet size distribution (Section 5.3.1), it is also important to focus on their ability to retain the bioactive compound in the  $W_1$  phase during the emulsification process. It can be seen from Table 5.2 that all the emulsions have similar EE, regardless of the protein used. For the coarse emulsions, the EEs reached as high as 86.1-89.8%, which reduced to 74.0-76.2% after the first emulsification cycle when major droplet break-up takes place, followed by a minor decrease (<2%) in the subsequent emulsification cycles. Emulsions stabilized with LMPC and WPI showed slightly higher values of EE than PPI for all the emulsification cycles. The evolution of EE obtained for the three proteins is similar to those reported for  $W_1/O/W_2$  emulsions produced by membrane emulsifications using DMTS<sup>141</sup> and regular membrane emulsification<sup>202,204,225</sup>.

Table 5.2. Transmembrane fluxes and encapsulation efficiencies of double emulsions stabilized with 1% LMPC, 1% WPI, and 1% PPI at each emulsification cycle.

	Flux ( $\text{m}^3\text{m}^{-2}\text{h}^{-1}$ )			EE (%)		
	LMPC	WPI	PPI	LMPC	WPI	PPI
Coarse	--	--	--	$87.3 \pm 1.4$	$89.8 \pm 0.1$	$86.1 \pm 2.2$
Cycle 1	$110.0 \pm 14.6$	$95.5 \pm 2.2$	$137.9 \pm 41.0$	$76.2 \pm 0.3$	$75.0 \pm 0.7$	$74.0 \pm 2.3$
Cycle 2	$392.2 \pm 23.0$	$377.1 \pm 6.1$	$389.5 \pm 48.3$	$75.2 \pm 0.8$	$74.4 \pm 1.2$	$72.8 \pm 1.7$
Cycle 3	$387.5 \pm 19.0$	$402.8 \pm 3.4$	$389.1 \pm 37.7$	$74.6 \pm 0.1$	$74.2 \pm 0.9$	$72.4 \pm 1.4$

### 5.3.2. Influence of environmental factors

In general, the stability of emulsions formulated with proteins is affected by heat, pH, high ionic strength, and protease activity<sup>303</sup>. Since our  $W_1/O/W_2$  emulsions may undergo different environmental conditions during processing, storage, and digestion, such as temperature, pH, and salt concentration, we studied changes in droplet size distribution, zeta potential, polyphenol release, and microstructure.

#### pH

To simulate the acidity of various food substrates (such as acidic soft drinks and neutral nutritional beverages) and the ingestion process (in mouth, stomach, and intestine), emulsions were incubated at various pH values (1.5, 4.0, and 8.0) at ambient temperature for 14 days and compared with emulsions at pH 6.5-7 (original pH).

Figure 5.3 shows the droplet size distribution of emulsions stabilized with LMPC, WPI, and PPI after 14 days of incubation at different pH values. At alkaline conditions (pH 8.0), all the emulsions show a similar droplet size distribution irrespective of the emulsifier used, close to the initial value of pH 6.5-7 for LMPC and WPI and even lower for PPI. The negative surface charge (see Figure 5.4) was stronger at pH 8, which promotes droplet stabilization by enhanced electrostatic repulsion. Also, at acidic conditions (pH 1.5), emulsions stabilized with WPI or LMPC were stable, while they presented aggregation at pH 4.0 resulting in increased size (which is related to floc formation). By contrast, the emulsions stabilized with PPI show significant aggregation at both pH 1.5 and 4.0 (inset images in Figure 5.5). The zeta potential as presented in Figure 5.5, is indicative of emulsion stability, with values exceeding 20 mV, either plus or minus, leading to stable systems, and this range coincides with the reported emulsion stability. Iso-electric point titrations of LMPC and PPI are shown in Figure 5.4, with clear differences at low pH.

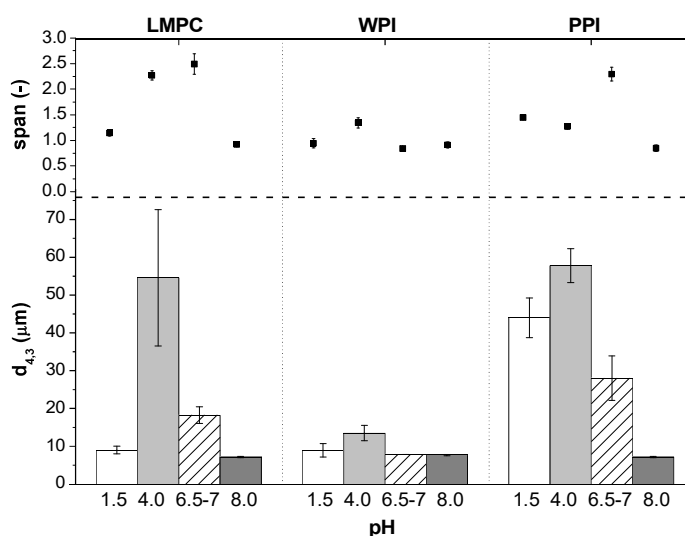


Figure 3. Droplet size distribution ( $d_{4,3}$  and span) of  $W_1/O/W_2$  emulsions stabilized with LMPC, WPI and PPI after 14 days of incubation at pH 1.5, 4.0, 6.5-7, and 8.0.

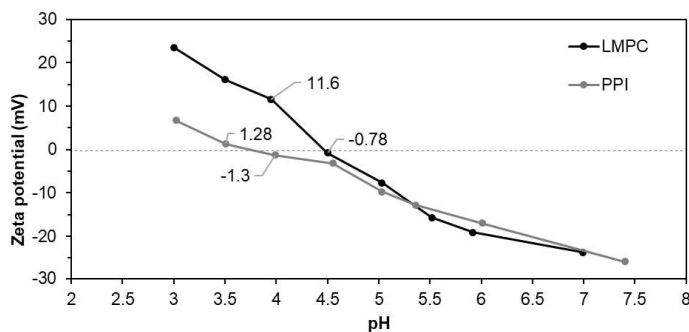


Figure 5.4. Zeta potential of LMPC and PPI solutions at pH range of 3.0-7.5.

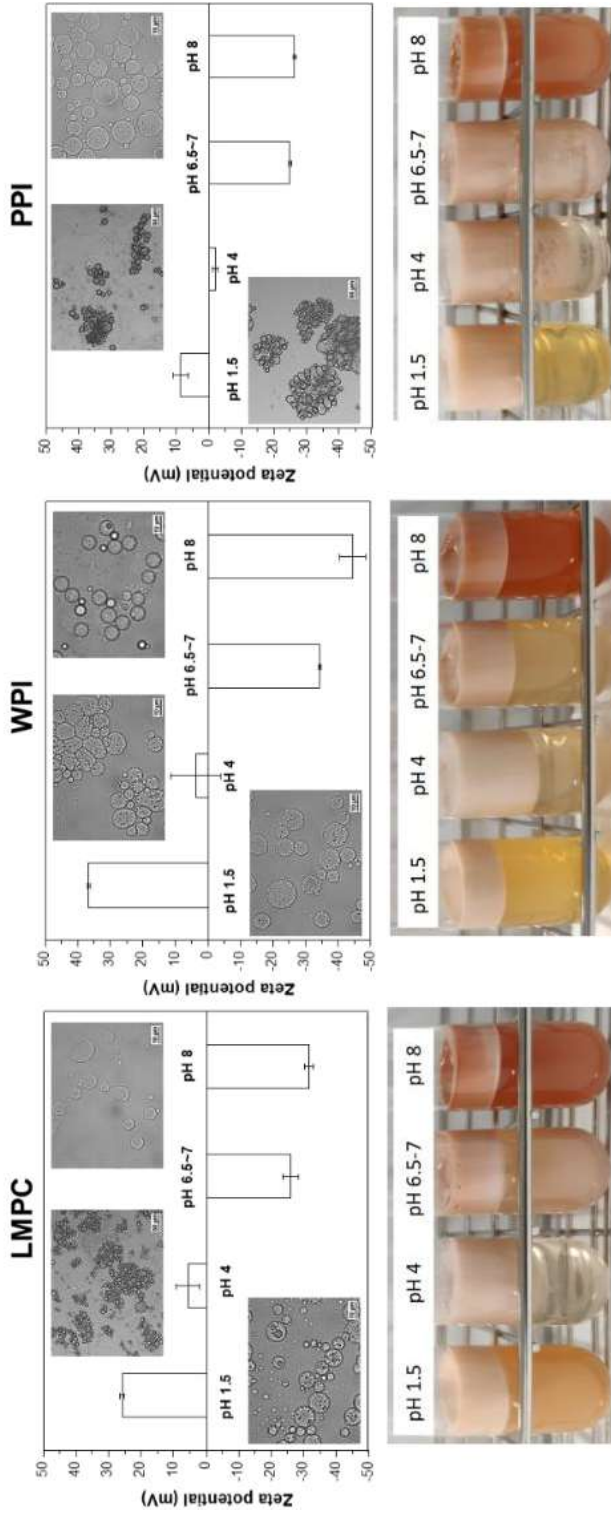


Figure 5.5. Effect of pH on zeta potential of W<sub>1</sub>/O/W<sub>2</sub> emulsions stabilized with LMPC, WPI and PPI after 14 days of incubation, and visual appearance of the emulsions. Insets show microstructure of the emulsions following adjustment to pH 1.5, 4.0, 6.5-7, and 8.0.

Similar pH stability of O/W emulsions stabilized with *T. molitor* protein extract was reported by<sup>82</sup>, and flocculation was observed at pH 4, and no significant changes at pH 2, 6, and 8, which is in line with our findings. Liang and Tang<sup>304</sup> observed that solubilized PPI at pH 3 showed better emulsifying properties than at neutral or basic pH for the production of soy oil-water emulsions, suggesting at acidic conditions pea protein forms a stronger and viscoelastic network. From the results in the present study, it can be concluded that PPI as we used it is not as efficient in stabilizing multiple emulsions as single emulsions at acidic pH, while LMPC and WPI show better performance.

To determine the total extent of polyphenol release also protein-polyphenol binding needed to be taken into account. It has been reported that proteins and polyphenols can form aggregates by both non-covalent bonding such as hydrogen bonding, hydrophobic bonding and van der Waals forces, and covalent binding interactions, which are affected by temperature, pH, salt concentration, and the presence of certain reagents<sup>58,59,305-307</sup>. From previous studies<sup>204,308</sup> it was clear that the interaction between the polyphenol and WPI in the  $W_2$  phase did not interfere with the polyphenol quantification method. A similar behavior was observed when analyzing EE in the emulsions stabilized with LMPC, WPI and PPI during the refining step with DMTS. In any of these cases, no increase in turbidity or presence of a precipitate in  $W_2$  was noted, which make us conclude that then no protein-polyphenol binding took place.

We first decided to investigate the effect of protein-polyphenol binding in aqueous solutions exposed to different pH, prior to exploring double emulsions. As Figure 5.6-A shows, the formation of insoluble protein-polyphenol complex was confirmed for WPI through the reduced transmission of WPI solution at a pH range of 3.5-5.5, leading to colored precipitate after centrifugation (Figure 5.6-C). Upon increasing the polyphenol concentration, the transmission was reduced further, and the amount of visible colored precipitate increased. For LMPC (Figure 5.6-B) the effect was even more pronounced, although it is good to point out that the protein by itself also showed severe aggregation in the pH range of 2.5-5.5. Comparing the transmission values of WPI and LMPC, Figure 5.6-A and B, respectively, we tentatively conclude that complex formation between the procyanidin-rich extract is more extensive and intensive for LMPC. Maybe even more importantly, it is clear from these results that the analysis of total polyphenol content in  $W_2$  could be compromised by the formation of protein-polyphenol complexes (especially within the pH range of 2.5-5.5), since it would only register polyphenols remaining in solution.

Polyphenol release can only be completely accounted for when no precipitate is formed, which is only the case at pH 1.5 and 8 for WPI. From Figure 5.7 it can be seen that at pH 1.5 there is a significant release of polyphenols during the first 24 h, that increases during the first week of storage, reaching the highest value after 14 days. The comparative values at pH 8 seem to be going down in time, possibly as a result of degradation under alkaline conditions as shown in the measurements presented in Figure 5.8, and also mentioned elsewhere<sup>309,310</sup>.

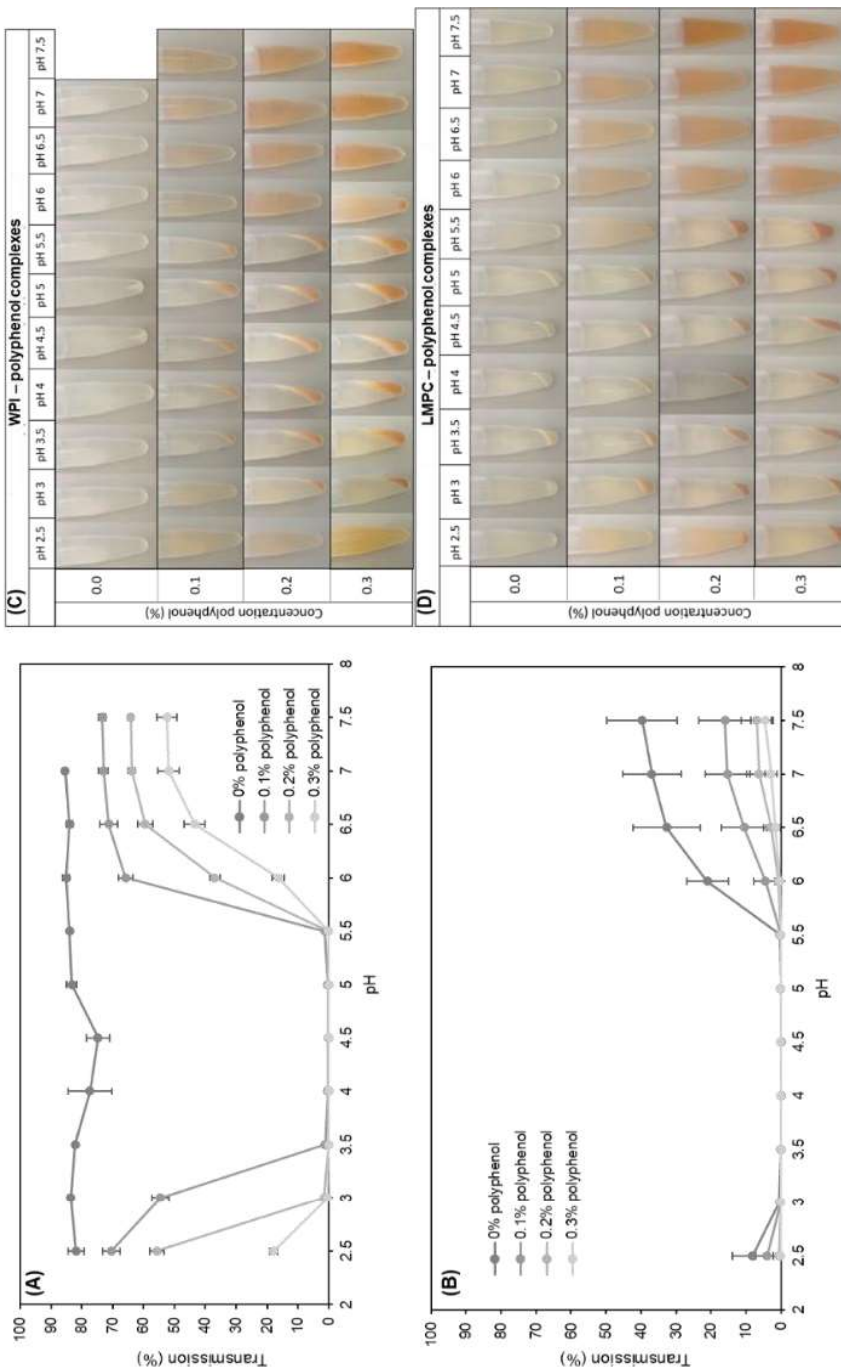


Figure 5.6. Transmission of (A) WPI and (B) LMPC solutions with polyphenol concentration at 0, 0.1, 0.2, and 0.3% versus pH range of 2.5 to 7.5, with attached visual observation of sediments after centrifugation (C) and (D).

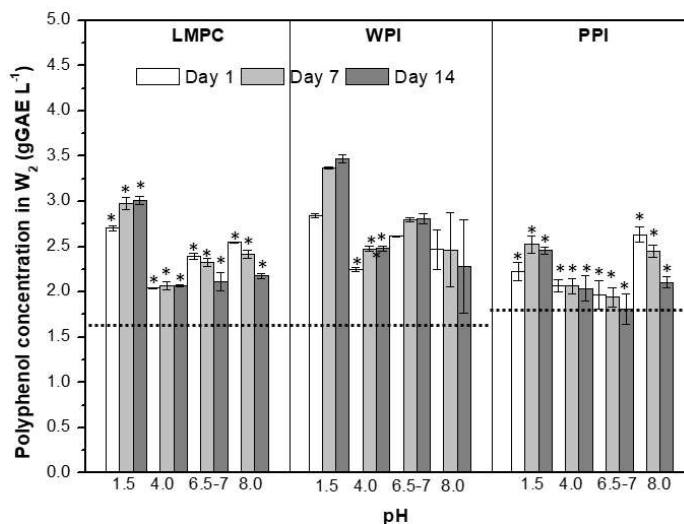


Figure 5.7. Polyphenol concentration in W<sub>2</sub> of emulsions stabilized with LMPC, WPI and PPI during a quiescent storage at pH 1.5, 4.0, 6.5-7, and 8.0 over 14 days at room temperature. Asterisk labels above the bars point out the appearance of a precipitate during polyphenol analysis. Dashed lines indicate the value in freshly produced emulsions.

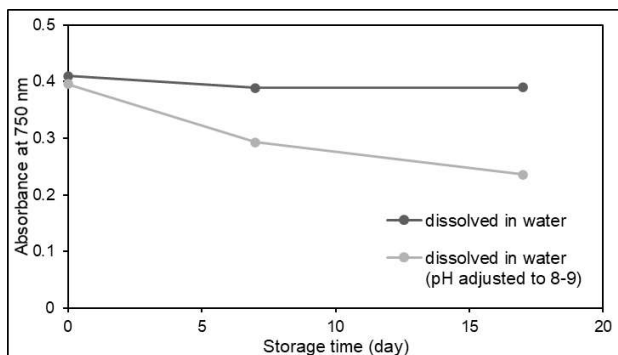


Figure 5.8. The variation of absorbance of polyphenols (Folin-Ciocalteu colorimetric method) from their solutions prepared in different media with storage time.

### Temperature

Next, the effect of temperature is investigated for conditions as they would occur during the production, storage, and utilization, e.g., freezing, cooling, pasteurization, sterilization, and ingestion of food products. The influence of storage temperature (-20, 4 and 25 °C) and heating (37, 65 and 90 °C) on microstructure, droplet size distribution, and polyphenol release in W<sub>1</sub>/O/W<sub>2</sub> emulsions was examined.

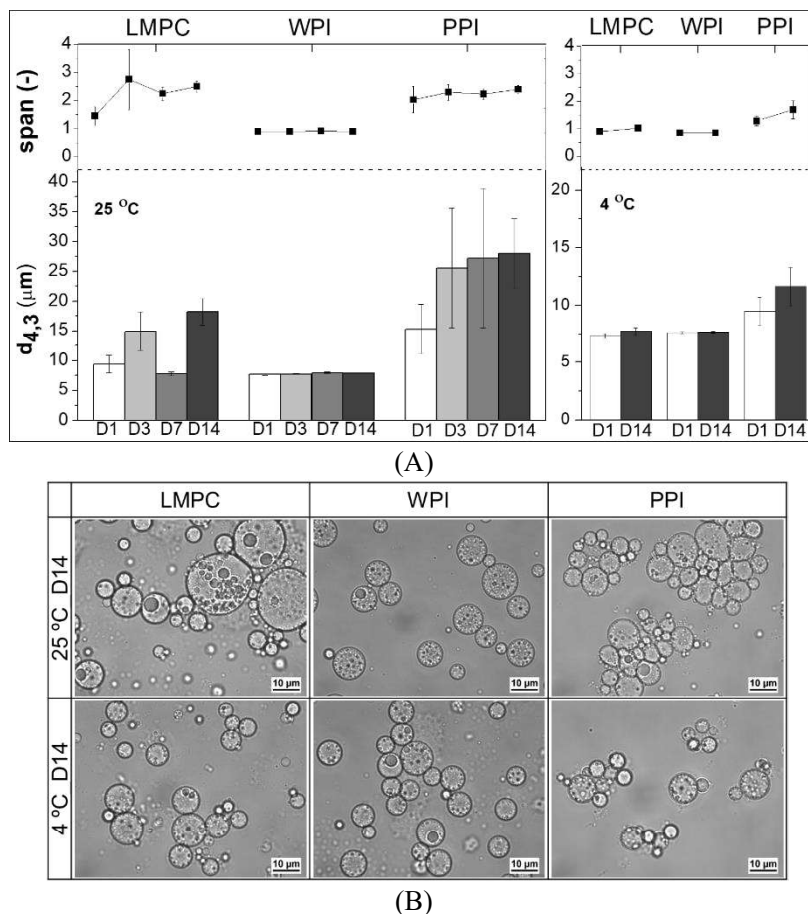


Figure 5.9. (A) Influence of storage temperature (25 and 4 °C) and storage time on droplet size distribution ( $d_{4,3}$  and span) of  $W_1/O/W_2$  emulsions stabilized with LMPC, WPI, and PPI. D1, D3, D7, and D14 correspond to storage time of 1, 3, 7, and 14 days. (B) Microstructure of emulsions after 14 days storage at 25 and 4 °C.

The stability of the three emulsions in terms of droplet size distribution presented large differences when stored at room temperature (25 °C) and under refrigeration (4 °C) (Figure 5.9-A) depending on the protein used to stabilize the  $O-W_2$  interphase. Emulsions stabilized with WPI did not show any changes in the droplet size distribution at 25 and 4 °C for two weeks, while the ones stabilized with LMPC or PPI showed an increase in size and span at 25°C (also as a result of flocculation), while having better stability when stored at 4°C. Compared to PPI, emulsions with LMPC are more stable in terms of droplet size distribution at both 25 and 4°C. From the emulsion microstructure images (Figure 5.9-B), the ‘increase in droplet size’ of LMPC and PPI stabilized emulsions seem to be caused by droplet flocculation/aggregation rather than coalescence. PPI stabilized emulsions started to flocculate immediately after production (Figure 5.2-A), with flocs easily redispersed during the droplet size distribution analysis in the Mastersizer. These effects are in line with results reported by Hinderink et al.<sup>54,56</sup> for low PPI concentration (<1%). All emulsions have considerable negative zeta potentials: PPI ( $-24.0 \pm 3.7$  mV),

followed by LMPC ( $-29.5 \pm 1.5$  mV), and WPI ( $-37.9 \pm 1.7$  mV). This implies that all emulsions should have considerable charge stabilization with the emulsions with the lowest charge being more susceptible to flocculation.

$W_1/O/W_2$  emulsions were also tested under simulated freezing storage temperature ( $-20$  °C) for 24 h and later analyzed at room temperature, i.e., one freeze-thaw process. From the results of droplet size distribution (Figure 5.10) and the microstructure (Figure 5.11), it is clear that all the samples were destabilized by coalescence and flocculation to a different extent, depending on the protein used in the emulsion formulation. Emulsions with WPI showed better freeze-thaw stability, maintaining a high-volume percentage of droplets with the initial droplet size and with a little population of bigger-sized droplets. LMPC and PPI emulsions showed an increase in the droplet size and a greater extent of coalescence as displayed in the microscopic images (Figure 5.11). Mao et al.<sup>174</sup> reported a similar observation on the droplet size change on whey protein stabilized O/W emulsions after the first freeze-thaw cycle, with droplet coalescence intensified with the increase in the number of freeze-thaw cycles.

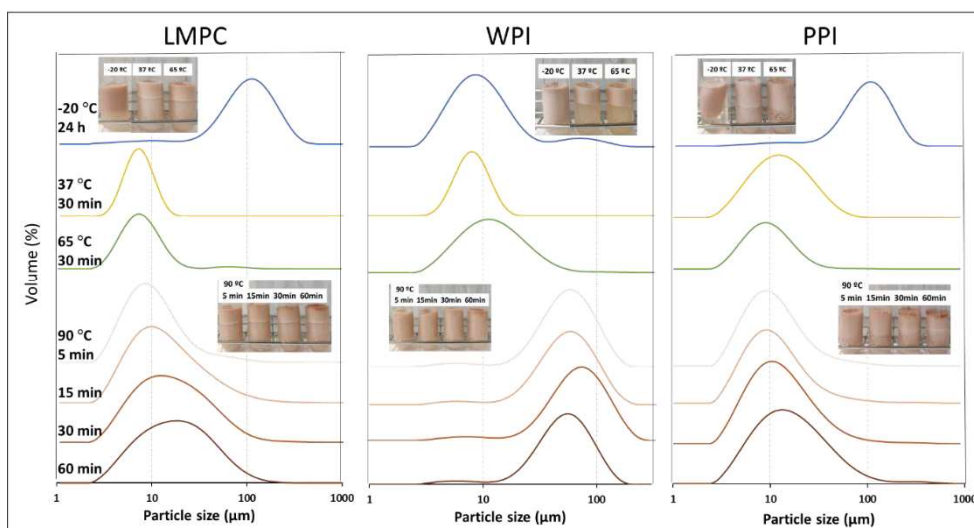


Figure 5.10. Droplet size distribution of  $W_1/O/W_2$  emulsions stabilized with LMPC, WPI, and PPI after simulated heat storage/treatment conditions ( $-20$ ,  $37$ ,  $65$ , and  $90$  °C), and visual appearance of the emulsions.

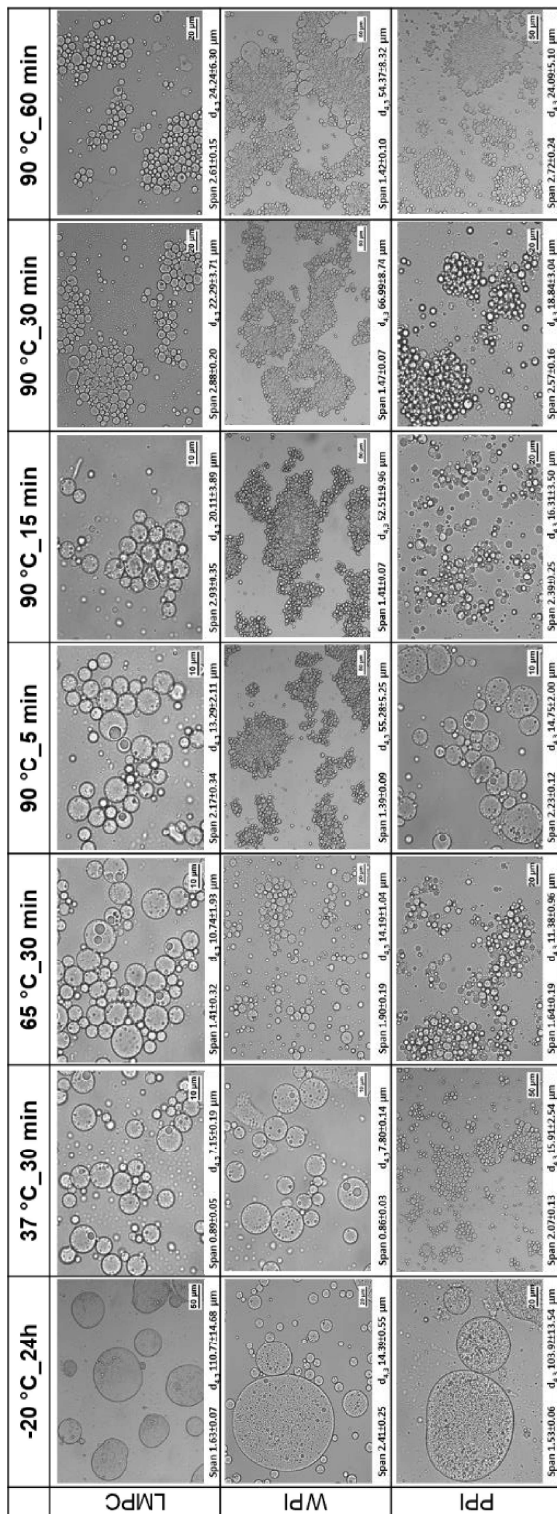


Figure 5.1.1. Microstructure of W<sub>1</sub>/O/W<sub>2</sub> emulsions stabilized with L MPC, W PI, and P PI after simulated heat storage/treatment conditions (-20, 37, 65, and 90 °C).

During the freezing process, oil droplets would concentrate in the unfrozen region and would be densely packed, while meanwhile, the ice crystals formed in the water phase could penetrate the oil globules and destroy the interfacial film, thus promoting droplet flocculation and coalescence during the thawing process<sup>311</sup>. Some studies on freeze-thaw stability of O/W and Pickering emulsions found a correlation between the type and thickness of the stabilizing agent<sup>174,312–314</sup>, as we also find here. In general, it is known that the thickness and viscoelasticity of the interfacial film layer determine the coalescence stability of a protein stabilized emulsion<sup>315</sup>, albeit not necessarily under cold conditions.  $\beta$ -lactoglobulin as one of the main components of whey protein gives interface viscoelastic characteristics due to a high 2-D packing density and strong protein-protein interactions<sup>316</sup>.

The  $W_1/O/W_2$  emulsions produced in this study are more complex since two interfaces ( $W_1/O$  and  $O/W_2$ ) have to remain stable simultaneously, and therefore various mechanisms can result in destabilization during the freeze-thaw process<sup>317</sup>. From the microstructure observation in the micrographs (Figure 5.11), some degree of coalescence of inner water droplets can be assumed and coalescence of the droplets seems to have happened, regardless of the protein used to stabilize the  $O/W_2$  interphase. Comparing the  $d_{4,3}$  for each emulsion after the freeze-thaw cycle, the  $W_1/O/W_2$  emulsions stabilized with WPI show a mean value about of 14  $\mu\text{m}$ , while for LMPC and PPI the values are 111 and 104  $\mu\text{m}$ , respectively (Figure 5.11). Moreover, using LMPC and PPI leads to a higher droplet aggregation as is evident from the clarified bottom aqueous phase (Figure 5.10). To improve the stability of LMPC emulsions at freezing conditions, the addition of a cryoprotectant is suggested to avoid protein denaturation, but this goes beyond the scope of the present study.

The emulsions were also exposed to temperatures relevant to digestion (37 °C), pasteurization (65 °C), and more severe temperature treatment at which protein denaturation takes place (90 °C). Before measuring droplet size distribution, the samples were mixed gently. Emulsions stabilized with WPI showed a decrease in stability with the increase of temperature (Figure 5.10), which can be linked to the denaturation of WPI. Droplet size distribution did not show any changes at 37 °C, but when the temperature increased to 65 and 90 °C (for 5 min),  $d_{4,3}$  increased to 14 and 55  $\mu\text{m}$ , respectively. The denaturation temperature of whey proteins is around 65-85 °C<sup>311</sup> therefore emulsion destabilization was expected to take place. From the microstructure, it can be seen that most of the aggregates consisted of oil globules ( $W_1/O$ ) having a similar size to the freshly produced  $W_1/O/W_2$  emulsions accompanied with a small part of coalesced droplets.

The emulsions stabilized with LMPC show similar stability to WPI emulsions at 37 and 65 °C and they seem less affected by heating at 90 °C than the ones with WPI. From the size distribution curve and the  $d_{4,3}$  values (Figures 5.10 and 5.11) and microstructures (Figure 5.11) at 90 °C it is clear that destabilization has taken place. Gould and Wolf<sup>82</sup> observed that 20% sunflower O/W emulsion stabilized by 0.44% *T. molitor* protein extract was stable during heat treatment at 60 and 70 °C, and the droplet aggregation

commenced and strengthened when heated up to 80 and 90 °C, which is in line with our findings.

Emulsions stabilized with PPI presented similar stability to LMPC during heating, even though for PPI a larger extent of droplet aggregation was observed at 37 °C, that increases with temperature (Figure 5.11). As observed in the microscopic images (Figure 5.11), droplets of PPI stabilized emulsions tend to form flocs or aggregates at 37 °C, which was not seen in emulsions stabilized with LMPC. We expect that the denaturation temperature for LMPC will be higher than that of WPI (65 °C)<sup>41</sup> and PPI (75-85 °C)<sup>294</sup>, and this translates into improved stability of the emulsions during short heat treatments at 80-90 °C.

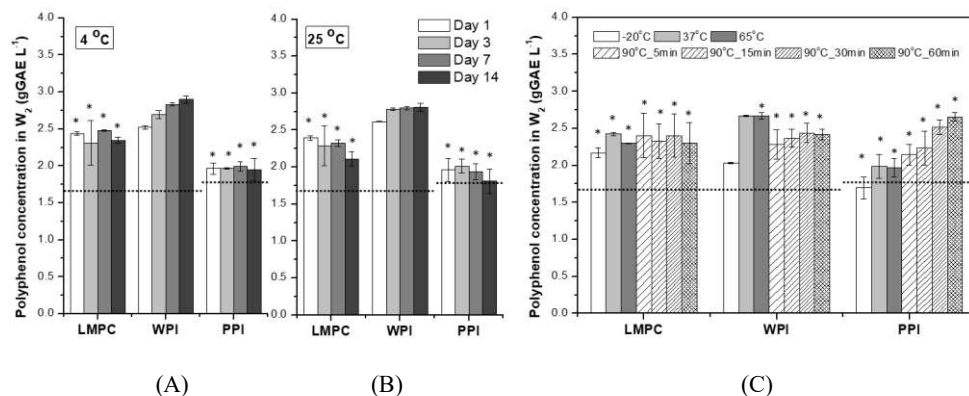


Figure 5.12. Polyphenol concentration in  $W_2$  of emulsions ( $C_{polyW_2}$ ) stabilized with LMPC, WPI and PPI during storage at 4 (A) and 25 °C (B) over 14 days, and (C) after subjected to different temperature stresses: -20 °C (24 h), 37°C (30 min), 65 °C (30 min) and 90 °C (5, 15, 30, and 60 min). Asterisk labels above the bars point out the appearance of a precipitate during polyphenol analysis. Dashed lines indicate the value in freshly produced emulsions.

Figure 5.12 shows the evolution of  $C_{polyW_2}$  for  $W_1/O/W_2$  emulsions during the temperature stress tests. First it is important to mention that the emulsion pH lies in the area (6.5-7) where the protein-polyphenol interaction is negligible for WPI and can be of significance depending on the polyphenol concentration for LMPC. The release of polyphenols to the  $W_2$  phase for emulsions stabilized with WPI show a considerable increase after one day of storage at 4 and 25 °C, that could be due to the concentration gradient between  $W_1$  and  $W_2$ . Considering that if all the polyphenol loaded into the  $W_1$  phase was released to the  $W_2$  phase, the concentration would be 6.2 g GAE L<sup>-1</sup>, it can be seen from Figure 5.12 that more than 50% of the loaded polyphenol is still encapsulated after 14 days at 4 and 25°C for WPI emulsions. For the higher temperature tests (65 and 90 °C), the presence of a precipitate hinders direct polyphenol quantification, which is also the case for the LMPC and PPI emulsions (Figure 5.12). Still, from the emulsion droplet size evolution during the different heat treatments (Figure 5.10) that is similar to the one obtained for WPI, we expect an overall retention of more than 50%.

## Osmotic stress

The influence of osmotic pressure differences on the stability of  $W_1/O/W_2$  emulsions was investigated through changes in droplet size distribution. The addition of salt and water to  $W_2$  led to an imbalance of osmotic pressure ( $\Pi$ ) between the two aqueous phases ( $W_1$  and  $W_2$ ), and the difference between  $W_2$  and  $W_1$  [ $\Delta(\Pi_{W_2}-\Pi_{W_1})$ ] corresponds to 0.46 MPa, 2.42 MPa and -0.54 MPa for the addition of salt concentration of 50 and 250 mM and 10-fold water dilution, respectively.

As can be seen in Figure 5.13,  $W_1/O/W_2$  emulsions stabilized with WPI maintained a rather constant droplet size distribution during 14 days of storage regardless of the changes in  $W_2$  phase, while from the color intensity change of the  $W_2$  phase (bottom part of tube) it is clear that polyphenol release increasingly takes place with storage time. For  $W_1/O/W_2$  emulsions stabilized with LMPC, during the first 7 days of storage no significant change in droplet size distribution was observed for the emulsion with the diluted  $W_2$  phase, after which some bigger droplets emerged, as seen from the microstructure images (Figure 14-A). For the PPI stabilized emulsions, dilution of the  $W_2$  phase changes the droplet size distribution, which is related to flocculation. The microstructure images (Figure 14) suggest a slight increase in the size of the inner water droplets because of the water efflux from  $W_2$  to  $W_1$  due to the imbalance of osmotic pressure.

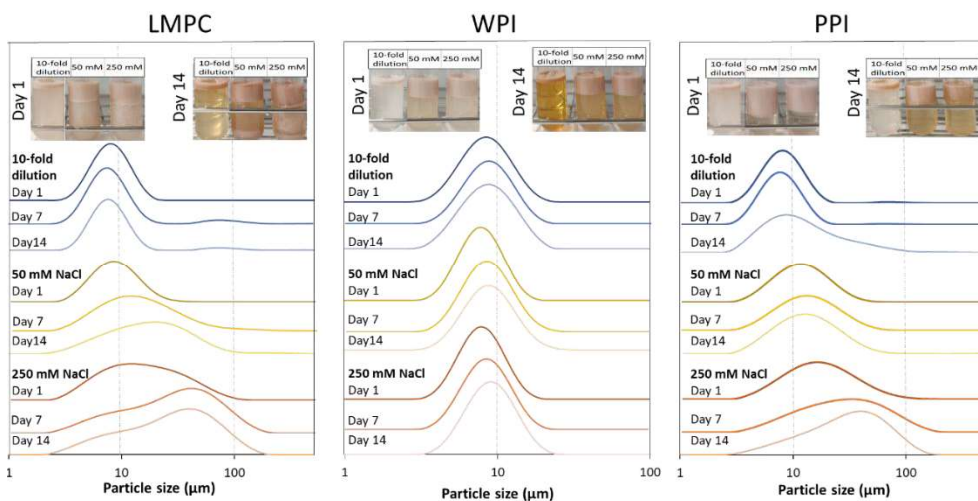
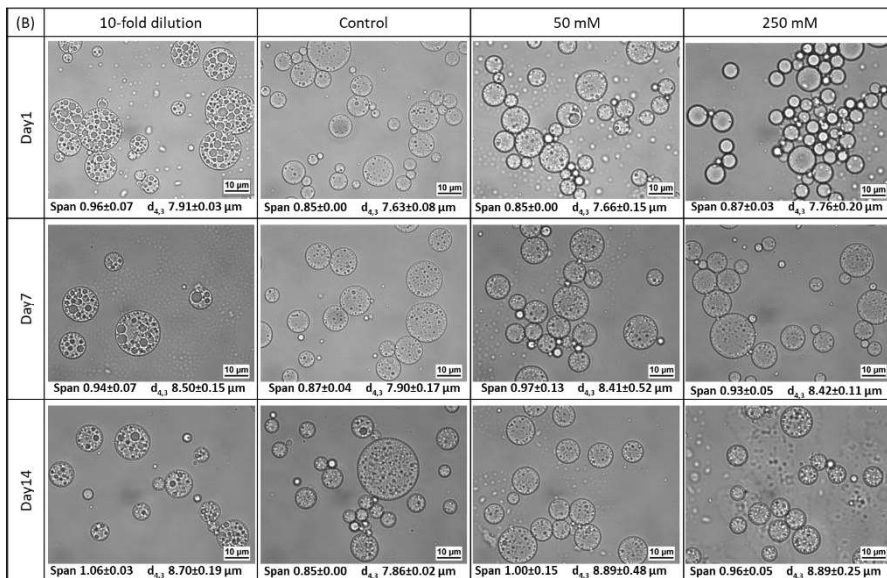
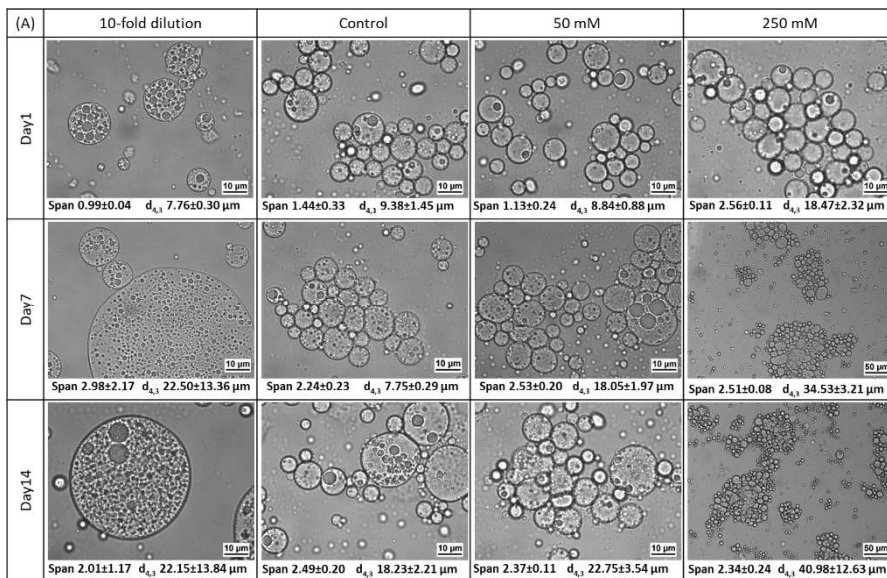


Figure 5.13. Droplet size distribution of  $W_1/O/W_2$  emulsions stabilized with LMPC, WPI and PPI after addition of NaCl (50 and 150 mM) and 10-fold of water dilution of  $W_2$  over a storage period of 14 days, inset images show the visual appearance of the emulsions after 1 and 14 days of storage.



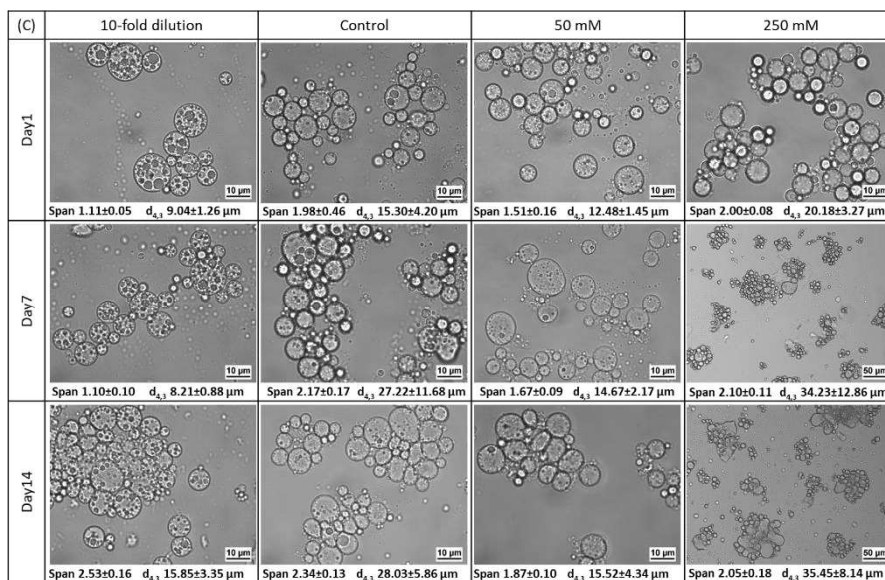


Figure 5.14. Microstructure of  $W_1/O/W_2$  emulsions stabilized with LMPC (A), WPI (B) and PPI (C) after addition of NaCl (50 and 150 mM) and 10-fold of water dilution of  $W_2$  during a storage period of 14 days.

Adding salt to any emulsion will influence charge effects responsible for emulsion stability<sup>318–320</sup>. In double emulsions, this can also induce water transfer between the two water phases. The addition of salt has an undoubted detrimental effect on the stability of  $W_1/O/W_2$  emulsions with LMPC and PPI, of which the internal water droplets most probably shrink over storage time and with amount of salt added. If all the inner water would be released to the outer phase, the resulting diameter would be 90% of the original emulsion droplet size, which cannot be distinguished by size measurement. There is a clear shift in droplet size toward bigger droplets/aggregates, while the polyphenol release is comparable to emulsions stabilized with WPI (visual observation). The most stable emulsions, under the range of salt concentration examined, would be the ones produced with WPI, followed by LMPC and PPI. The tested salt concentrations represent a suitable range as would be found in food products<sup>321</sup>, and the encapsulation systems can withstand these salt concentrations. There are no previous studies in the literature on the stability of multiple emulsions stabilized with insect proteins. The only reference is on the stability of sunflower O/W emulsions stabilized with *T. molitor* protein extract, that once produced were subjected to a NaCl concentration of 330 Mm<sup>82</sup> and remained stable.

To learn if water transport has any effects on the polyphenol release under the present experimental conditions, polyphenol concentration in  $W_2$  was measured after 1, 7 and 14 days of each osmotic stress test and plotted in Figure 5.15. For WPI stabilized emulsions it can be seen that the polyphenol concentration in  $W_2$  has a similar value (about 2.75 gGAE L<sup>-1</sup>) than the one obtained at 25 °C and neutral pH and is not affected by the presence of salt (Figure 5.15), therefore we can assume that more than 50% of the loaded polyphenols remain encapsulated under the osmotic stress conditions tested. For LMPC

and PPI emulsions, the presence of a precipitate hampers the polyphenol analysis. Moreover, it has been established (results not shown) that the salt present in  $W_2$  enhances complex formation between LMPC and polyphenols (Figure 5.15). Contrary to the temperature stress tests, emulsion stability for LMPC and PPI was more compromised by the salt addition in  $W_2$ , which could indicate that polyphenol release is higher than for WPI emulsions.

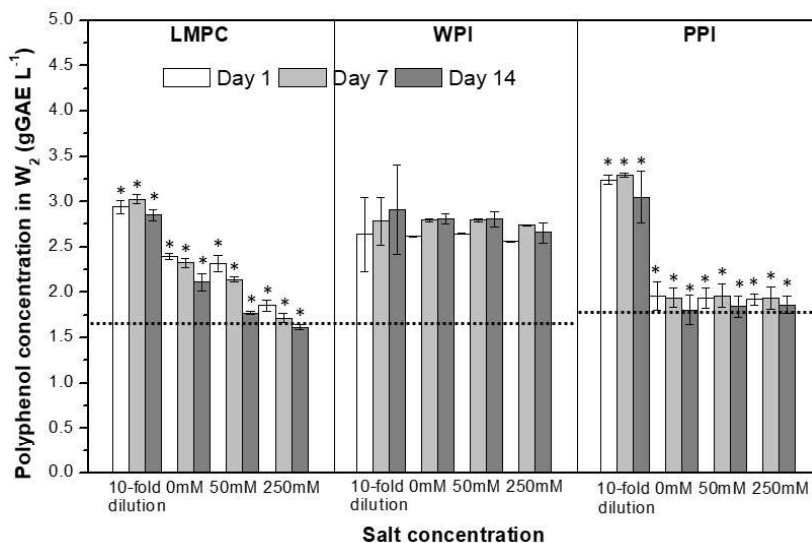


Figure 5.15. Polyphenol concentration in  $W_2$  of emulsions stabilized with LMPC, WPI and PPI during a quiescent storage of 14 days at room temperature. Emulsions were subjected to different conditions of 10-fold dilution by water, 0 (no extra addition of salt, kept at 25 °C), 50 and 250 mM salt addition. Asterisk labeled above the bars points out the appearance of a precipitate during the polyphenol analysis. Dashed lines indicate the value in freshly produced emulsions.

## 5.4 Conclusion

This study has proven the feasibility of using lesser mealworm protein concentrate to stabilize multiple emulsions to encapsulate a procyanidin-rich extract. The emulsions showed a droplet size distribution and stability at 4 and 25 °C comparable to emulsions produced with whey protein isolate. Moreover, the insect protein showed better performance to stabilize the multiple emulsions than a protein obtained from another sustainable source, such as pea protein. The interaction/complex formation between the LMPC and polyphenols is far more pronounced than for WPI, which may be instrumental in improving the chemical stability of such systems.

As for the stability under different environmental stresses (temperature, pH, and osmotic pressure imbalance) it was shown that all  $W_1/O/W_2$  emulsions were prone to droplet coalescence after a freeze (-20 °C) thaw cycle. At the highest temperatures tested (90 °C), the changes in droplet size distribution were less pronounced for  $W_1/O/W_2$  emulsions stabilized with LMPC than for WPI, pointing out a potential benefit of using this protein

in emulsions that need to undergo heat treatment. Within the pH range investigated, LMWC stabilized double emulsions behave comparably to their WPI stabilized counterparts  $W_1/O/W_2$  emulsions under acidic and alkaline conditions, and both outperform PPI. LMPC and PPI stabilized emulsions are less able to withstand osmotic pressure differences compared to WPI.

The results of this study show for the first time the use of an insect protein, LMPC, to stabilize multiple emulsions produced using a low-energy emulsification system to encapsulate a commercial polyphenol and open the door to future studies to investigate the incorporation of insect proteins in complex food formulations.



## Chapter 6

### Polyphenol loaded microcapsules from W/O/W emulsions stabilized with lesser mealworm (*Alphitobius diaperinus*) protein concentrate

#### **Abstract**

To preserve water-soluble bioactive compounds e.g., polyphenols, encapsulation is a trusted method. In the current paper, we start from water-in-oil-in-water ( $W_1/O/W_2$ ) emulsions, which can protect bio-actives from external environment influences (e.g., pH), while providing decent dispersibility and homogeneity of the aqueous medium. Whey protein isolate (WPI) is a conventional emulsifier for formulation of emulsions, and here we compare it with proteins from more sustainable sources. In this work, we use pea protein isolate (PPI) and lesser mealworm protein concentrate (LMPC) as alternatives to WPI, and use spray drying and freeze drying, to fabricate solid microcapsules with more than 85% of the procyanidin-rich extract retained in them. We also investigated reconstitution to  $W_1/O/W_2$  emulsions after rehydration, and found that spray-dried  $W_1/O/W_2$  emulsions stabilized by WPI returned most closely to their original droplet size, followed by LMPC and PPI. For freeze-dried emulsions, those stabilised with PPI displayed smaller average droplet size and uniformity followed by the ones stabilized with LMPC and PPI. In all cases, the formation and rehydration of microcapsules was successful, which indicates that the technical feasibility of insect protein and plant protein as alternative to animal protein in the production of solid microcapsules is high.

This chapter is intended for a submission as a short communication to the *Journal of Food Engineering*.



## 6.1 Introduction

Water-in-oil-in-water ( $W_1/O/W_2$ ) emulsions are widely applied as a means of encapsulation for protection and delivery of water-soluble bioactive compounds. To prolong their shelf-life, facilitate the use and dosage, and to reduce transport and storage the costs, these multiple emulsions are transformed into solid microcapsules by drying. Whey protein isolate (WPI) is a conventional protein emulsifier widely used in the formulation of  $W_1/O/W_2$  emulsions, and it has extensively been used in the formulation of solid microcapsules<sup>149,156,163</sup>. Because of their environmental impact, more sustainable protein sources, such as plant and insect proteins, need to be considered<sup>98,322</sup>. Soy protein and pea protein isolate (PPI) are most commonly reported<sup>48,315</sup>, and insect proteins are becoming more popular, but have not been reported in the production of solid microcapsules.

This study explores for the first time the use of a lesser mealworm (*Alphitobius diaperinus*) protein concentrate (LMPC) to stabilize procyanidin loaded  $W_1/O/W_2$  emulsions subsequently dried by spray drying or freeze drying. The ability to maintain the original droplet size distribution of the emulsion after rehydration has been studied and compared to WPI and PPI, as models for conventional and sustainable protein sources, respectively. The present study demonstrated that the production of solid microcapsules is feasible from  $W_1/O/W_2$  emulsion stabilized by pea protein and lesser mealworm protein, and also that rehydration is comparable, which shows that LMPC is a valid alternative.

## 6.2 Materials and methods

### 6.2.1 Materials

Table 6.1 presents the multiple emulsions prepared in this study, in which a commercial procyanidin-rich extract (Vitaflavan, DRT, France) with a total polyphenol content above 96% was incorporated in the internal water phase. The lipophilic emulsifier, polyglycerol polyricinoleate (PGPR, ref-4120 Palsgaard, Denmark), was dissolved in commercial sunflower oil (Borges S.A., Spain). As hydrophilic emulsifier, three proteins were used: whey protein isolate (WPI, BiPRO, lot no. JE 034-7-440-6, Davisco Foods International, Inc., Le Sueur, MN) with a reported protein content of 98.1% on dry basis, lesser mealworm protein concentrate (LMPC) extracted from insect powder BUFFALO'S (Kreca Ento-Food BV, the Netherlands), and pea protein isolate (PPI, Roquette, NUTRALYS, s85F, France) with a reported purity of 80-90%. To balance the osmotic pressure between the two aqueous phases, sodium chloride (NaCl, PanReac, Spain) was dissolved in the  $W_2$  phase, while sodium azide ( $Na_3N$ , Sigma-Aldrich, USA) was used to prevent microbial growth. To produce LMPC, the procedure described in section 6.2.2 was used.

Table 6.1. Formulation of  $W_1/O/W_2$  emulsions with the same composition for the  $W_1/O$  and different composition of the  $W_2$  phase.

Fraction	Phase	Composition	Medium
6 wt%	$W_1$	10 wt% procyanidin-rich extract	Deionized water
14 wt%	Oil	6 wt% PGPR	Crude sunflower oil
80 wt%	$W_2$	i. 1 wt% LMPC	5 mM phosphate buffer pH 7 (0.06 wt% NaCl, 0.02 wt% $Na_3N$ )
		ii. 1 % WPI	5 mM phosphate buffer pH 7 (0.4 wt% NaCl, 0.02 wt% $Na_3N$ )
		iii. 1 % PPI	5 mM phosphate buffer pH 7 (0.25 wt% NaCl, 0.02 wt% $Na_3N$ )

The WPI solution (2 wt%) was prepared by dissolving WPI powder in 5 mM phosphate buffer pH 7 (prepared with  $Na_2HPO_4 \cdot 2H_2O$ , Scharlau, Spain and  $NaH_2PO_4 \cdot H_2O$ , ACROS, Spain) stirring for 2 h at 400 rpm and kept in the fridge overnight. The LMPC and PPI solutions were also prepared by dissolving the protein powder in 5 mM phosphate buffer, and pH was adjusted to 7.0 every 30 min of stirring using 1M NaOH or 1N HCl. After two hours stirring, the solutions were transferred to the fridge where they were kept overnight. To quantify the protein concentration in the LMPC and PPI solutions, the Pierce™ BCA protein assay kit (Thermoscientific, USA) was used, and the results expressed as bovine serum albumin equivalent value (BSAE %, w/w). The concentrations of LMPC and PPI in Table 1 were obtained after dilution of the initial solution and are shown in % instead of BSAE % hereafter for simplicity.

Food grade maltodextrin (lot no. 219425, Pral, Barcelona) with a dextrose equivalent of 16.5–19.5 was added to the  $W_1/O/W_2$  emulsions as wall-building material for solid microcapsules before spray drying and freeze drying. Sodium carbonate (Panreac, Spain), gallic acid monohydrate (Panreac, Spain) and Folin-Ciocalteu's reagent (Panreac, Spain) were used for total polyphenol content (TPC) quantification.

The  $W_1/O/W_2$  emulsions were prepared by premix membrane emulsification, more specifically using a dynamic membrane module with 38  $\mu m$  glass micro-beads (Microspheres-nanospheres, USA) placed on top of a nickel sieve (Stork Verco, Erbeek, the Netherlands). Sodium hydroxide and ethanol (96%, Scharlab, Spain) were applied for cleaning of nickel sieve and silica beads, respectively.

### 6.2.2 Preparation of lesser mealworm protein concentrate (LMPC)

Defatting of the original lesser mealworm protein powder was carried out with 2-MeTHF<sup>268</sup>: the powder (50 g) was mixed with 250 mL of 2-MeTHF and magnetically stirred at 300 rpm for 1 h, left to stand for 20 min to allow that upper solvent layer to separate. The process was repeated 3 times in total by adding 250 mL of 2-MeTHF each time. The

remaining solvent in the powder was evaporated in the fume hood over 3 days. Next, protein extraction was carried out using the method of Gould & Wolf<sup>82</sup> with slight modifications. In short, dried defatted powder (30 g) was mixed with 150 mL 0.25M NaOH and stirred at 400 rpm for 1 h at 40 °C, followed by 15 min centrifugation at 4490 rpm to separate the supernatant. The pH of the supernatant was adjusted to 4.0-4.5 by adding HCl to precipitate the protein fraction. Further extractions following the same procedure were applied to the remaining pellet by adding 150 mL of 0.25 M NaOH. The protein from the 3 extractions was combined, centrifuged (15 min at 3750 rpm) and freeze dried (LYOQUEST-85 PLUS, Telstar, Spain) for 24 h at 0.2 mbar vacuum and plate temperature of 20 °C. The freeze-dried protein powders from several extractions were blended and stored in a desiccator until further use.

### 6.2.3 $W_1/O/W_2$ emulsions production

The  $W_1/O/W_2$  emulsions were produced following the same procedure as described in Chapter 2. In brief, the primary emulsion ( $W_1/O$ ) was produced by adding  $W_1$  phase (procyanidin solution) into sunflower oil with 6% PGPR under rotor-stator homogenization (Ultra Turrax T18 digital, IKA, Germany) for 5 min at 11000 rpm. This primary emulsion was then added into the  $W_2$  phase, that contains the dissolved protein, while stirring for 5 min at 1600 rpm to produce the coarse  $W_1/O/W_2$  emulsion (droplet size  $d_{3,2}$   $60.3 \pm 15.4$   $\mu\text{m}$  and span of  $1.9 \pm 0.2$ ). The coarse emulsion was refined by passing through the dynamic membrane module at 500 kPa for 3 times in total.

Blank samples for each formulation were prepared in the same way as that for the  $W_1/O/W_2$  emulsion but containing 0.4 wt% NaCl water solution instead of procyanidin-rich extract. Blanks were analysed in the same way as polyphenol loaded samples and the results enabled to eliminate potential masking effect of proteins, as mentioned in Chapter 5.

### 6.2.4 Solid microcapsules production

#### **Spray drying (SD)**

$W_1/O/W_2$  emulsions stabilized with different protein emulsifiers were gently mixed with a 75 wt% maltodextrin solution containing 0.02 wt%  $\text{Na}_3\text{N}$  at a mass ratio of 1:3 ( $W_1/O/W_2$  emulsion: maltodextrin solution). The mixture was then spray dried using a Büchi Mini Spray dryer B-290 (Flawil, Switzerland). Inlet temperature was set at 170 °C, and the outlet temperature was controlled at 92 °C ( $\pm 2$  °C). Nozzle pressure, feed flow rate and aspiration rate were set at 4.5 bar, 4 mLmin<sup>-1</sup> and 100% (35 m<sup>3</sup>h<sup>-1</sup>), respectively. Spray-dried powders were collected in a brown bottle filled with  $\text{N}_2$  and stored in a desiccator.

#### **Freeze drying (FD)**

The same mixtures as used for spray drying were put in petri dishes and freeze dried (0.2 mbar, 20 °C tray temperature) for 24 h. Then the samples were gently grinded with a mortar and pestle before storing in  $\text{N}_2$  filled brown bottles in a desiccator.

## Drying yield

The spray/freeze drying (SD/FD) yield was calculated based on the mass of solid microcapsules ( $m_{capsules}$ ) collected and the mass of total solids in inlet ( $m_{total\ inlet\ solids}$ ), calculated as eq 6.1.

$$Yield_{SD/FD} [\%] = \frac{m_{capsules}}{m_{total\ inlet\ solids}} \times 100 \quad \text{eq (6.1)}$$

## 6.2.5 Characterization of emulsions, solid microcapsules, and reconstituted emulsions

### Microstructure analysis

Laser scanning confocal microscope (NIKON model TE2000-E, The Netherlands) was used to observe the structure of freshly produced and reconstituted  $W_1/O/W_2$  emulsions. Environmental scanning electron microscope (FEI ESEM Quanta 600, Austria) was used to analyse the morphology of dried solid microcapsules.

### Water activity

Water activity ( $a_w$ ) of dried powders was measured using a hygrometer (Novasina IC-500 AW-LAB, Novasina) at room temperature. Each sample was measured in duplicate.

### Polyphenol quantification

For polyphenol quantification in the microcapsules the method described by Kanha et al.<sup>161</sup> was used with slight modification. A sample of solid microcapsules (0.1 g) was weighed in a glass tube, and dissolved in 1 mL deionized water by vigorously shaking (16000 rpm) using a vortex (Fisherbrand, Italy) for 30 seconds. 4 mL ethanol was added, and the sample was again vortexed for 30 seconds. Next, the tube was maintained in ultrasound water bath for 10 min to break the rehydrated emulsions, followed by 30-second vortexing, and a 10-minute ultrasound treatment, which was repeated twice. The thus obtained mixture was centrifuged at 4000 rpm for 5 min and the total polyphenol content (TPC) of the supernatant was measured using the Folin-Ciocalteu method, and expressed as gallic acid equivalent value. In brief, 100  $\mu$ L sample was added to 100  $\mu$ L Folin-Ciocalteu reagent and 1 mL of deionized water, and after 3 min 2 mL of 75 g/L  $Na_2CO_3$  and 1.8 mL of deionized water were added. Absorbance at 750 nm (DR5000, Hech, Germany) was measured after a 30-minute reaction at room temperature in the dark.

Surface polyphenol content (SPC) was quantified by mixing 0.1 g solid microcapsules with 5 mL ethanol absolute. The mixture was vortexed for 30 seconds, followed by centrifugation as described earlier.

The corresponding retention and encapsulation efficiency are calculated using equation 6.2 and 6.3, respectively.

$$RE (\%) = \frac{TPC}{Theoretical\ TPC} \times 100 \quad \text{eq (6.2)}$$

$$EE_m (\%) = \frac{TPC-SPC}{TPC} \times 100 \quad \text{eq (6.3)}$$

### Droplet size distribution

Droplet size distribution of freshly produced  $W_1/O/W_2$  emulsions in the presence of maltodextrin, and rehydrated  $W_1/O/W_2$  emulsions (in 0.4 wt% NaCl) were analysed using Mastersizer 2000 (Malvern Instruments, UK) by laser diffraction using 0.4 wt% NaCl as continuous phase to maintain the aqueous phase osmotic pressure. Particle and the dispersant reflective index were set to 1.480 and 1.330, respectively. Mean droplet size and droplet size dispersion were expressed as volume weighted mean diameter  $d_{4,3}$  (equation 6.4) and the span factor (equation 6.5), respectively.

$$d_{4,3} = \frac{\sum n_i D_i^4}{\sum n_i D_i^3} \quad \text{eq (6.4)}$$

$$\delta = \frac{d_{90}-d_{10}}{d_{50}} \quad \text{eq (6.5)}$$

$n_i$  is the number of droplets with diameter  $D_i$ ,  $d_x$  is the droplet diameter corresponding to  $x\%$  volume on a cumulative droplet size distribution curve.

## 6.3 Results and discussion

The  $W_1/O/W_2$  emulsions were produced successfully with all proteins, and more than 72% of procyanidin-rich extract was encapsulated (Table 6.2,  $EE_e$  values were calculated and referenced as described in Chapter 5). The next sections all related to microcapsules, obtained by spray or freeze drying.

Table 6.2. Droplet size distribution ( $d_{4,3}$  and span) and encapsulation efficiency ( $EE_e$ ) of procyanidin-rich extract in the refined (after 3 emulsification cycles)  $W_1/O/W_2$  emulsions stabilized with LMPC, WPI or PPI. Results are from Chapter 5.

Protein emulsifier	$d_{4,3}$ ( $\mu\text{m}$ )	Span (-)	$EE_e$ (%)
LMPC	$7.28 \pm 0.04$	$0.83 \pm 0.00$	$74.6 \pm 0.1$
WPI	$7.60 \pm 0.03$	$0.84 \pm 0.01$	$74.2 \pm 0.9$
PPI	$7.27 \pm 0.15$	$0.89 \pm 0.04$	$72.4 \pm 1.4$

### 6.3.1 Characterization

Irrespective to the emulsifier used, spray-dried capsules were spherical globules with smooth surfaces and very low agglomeration level (Figure 6.1-A), as reported for other spray-dried emulsions<sup>284,308,323</sup>. The capsules displayed a hollow core, and the shell thickness was about  $1.1 \pm 0.7 \mu\text{m}$  as shown in Figure 6.1-B. Freeze dried  $W_1/O/W_2$  emulsions (Figure 6.1-C and D), were more flake-like with irregular bumps and folds on the surface as observed for other freeze dried emulsions<sup>3,172,180</sup>. The diameter of the pores in freeze dried samples is  $\sim 6.0 \pm 0.9 \mu\text{m}$ . Most probably these cavities and pores are due to the formation of ice crystals and the later sublimation<sup>157,160,176,177</sup>.

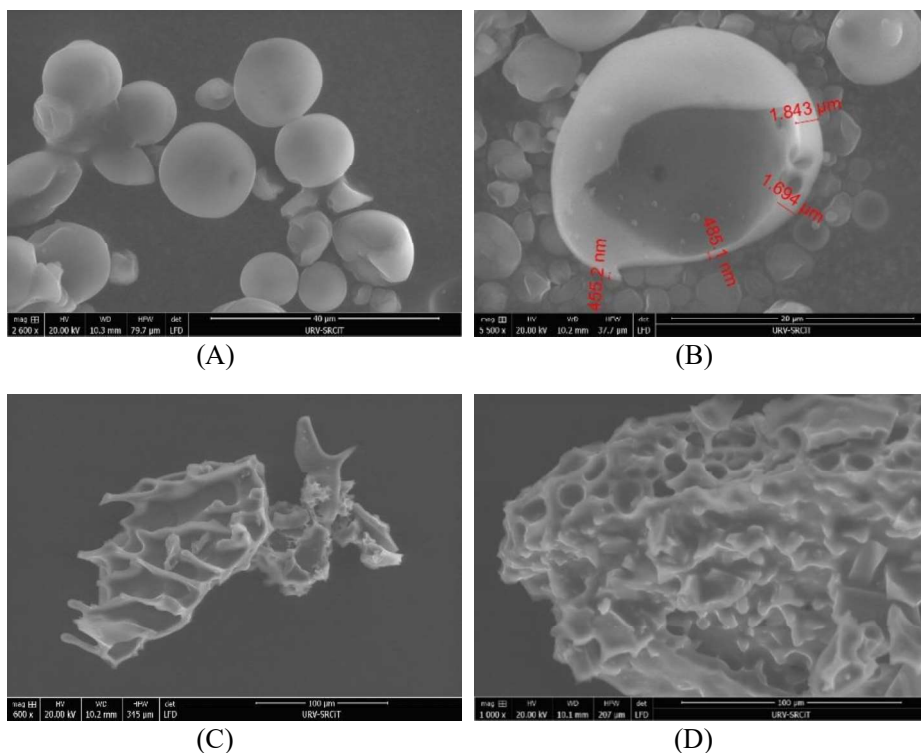


Figure 6.1. ESEM micro graphs of solid microcapsules from (A) spray dried  $W_1/O/W_2$  emulsions stabilized with LMPC, and (B) PPI (manually ruptured), freeze-dried  $W_1/O/W_2$  emulsions stabilized with (C) WPI, and (D) LMPC.

As described in Table 6.3, the yield of spray drying is much lower than for freeze drying as could be expected for lab-scale spray driers. All powders had  $a_w$  below 0.2, with freeze dried samples having slightly lower water activity ( $a_w$ ) than spray dried samples, which is in a safe range ( $a_w < 0.3$ ) for growth of microorganisms<sup>180</sup>. The total polyphenol content was rather similar for all samples, and that it is also the case for retention (>85%), and encapsulation efficiency, with the exception of freeze-dried PPI-stabilised emulsion. When comparing with Berendsen et al.<sup>149</sup> who also investigated whey protein stabilised  $W_1/O/W_2$  emulsions that were spray-dried, but prepared by SPG membrane emulsification, the values found in our work are typically twice as high.

Table 6.3. Characteristics of spray dried (SD) and freeze dried (FD) W<sub>1</sub>/O/W<sub>2</sub> emulsions stabilized with LMPC, WPI, and PPI.

	Yields (%)		a <sub>w</sub>		TPC (mg/g capsule)		RE (%)		EE <sub>c</sub> (%)	
	SD	FD	SD	FD	SD	FD	SD	FD	SD	FD
LMPC	25.8±2.6	93.4±0.1	0.10±0.01	0.08±0.00	9.2±0.2	9.2±0.1	87.7±1.3	87.9±1.2	71.1±0.4	60.7±0.5
WPI	35.5±6.6	92.7±0.5	0.11±0.00	0.08±0.01	9.3±0.7	10.0±0.2	89.9 ±6.4	96.2 ±1.9	70.2±2.2	70.0±0.6
PPI	18.67±3.4	93.6±0.3	0.17±0.04	0.07±0.01	9.0±0.2	8.9±0.4	87.0 ±1.5	85.2 ±3.5	63.4±0.6	37.8±0.4

### 6.3.2 Reconstituted emulsions

Figure 6.2 shows rehydrated solid microcapsules that all contained an internal water phase and had monomodal droplet size distribution, albeit that the  $d_{4,3}$  and span were higher as measured for the double emulsion prior to drying. Reconstituted emulsions from freeze dried powders had larger droplets compared to spray dried samples irrespective of the emulsifier used. This is not unexpected given the agglomerated nature of the freeze dried emulsions (See figure 6.1). When comparing the proteins, WPI-stabilised spray dried emulsion resembles the original emulsion most closely, followed by LMPC-stabilised spray dried emulsion. Largest droplets were found for WPI-stabilised freeze-dried emulsions. This may indicate that WPI is more sensitive to low temperature used during freeze drying, while PPI and LMPI-stabilised emulsions are much less sensitive. This shows that depending on the process applied, alternative proteins may deliver additional functionality to the product.

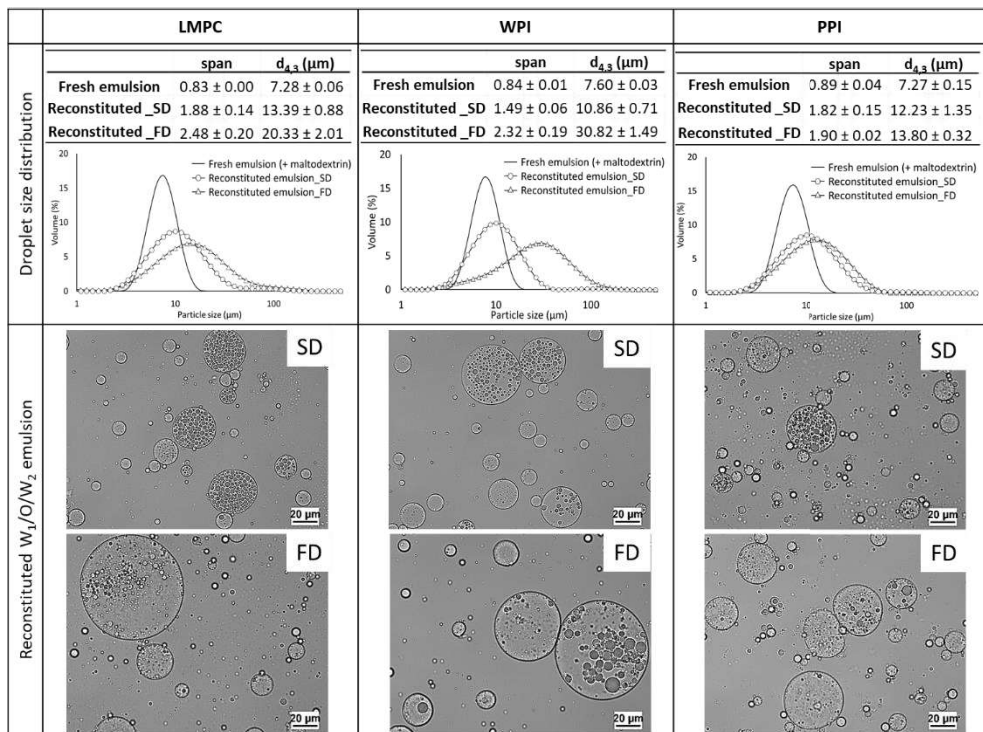


Figure 6.2. Droplet size distribution and microstructure of reconstituted  $W_1/O/W_2$  emulsions stabilized with LMPC, WPI and PPI from SD and FD.

### 6.4 Conclusion & future outlook

The drying method has great impact on the surface morphology of the formulated solid microcapsules. Spray drying formed smooth sphere shape capsules, while freeze-dried capsules had a flaky surface. All produced powders reconstituted into double emulsions upon rehydration, and depending on the drying method used the emulsion droplets were larger or smaller. WPI-stabilised spray-dried microcapsules are closest to their original

size, while the freeze-dried counterparts show largest droplets upon rehydration. The other two proteins show less pronounced differences, which is an important lead for adjustment of ingredients used for double emulsion formulation to warrant sufficient rehydration depending on the drying method use. In future work, the produced solid microcapsules will be assessed on *in vitro* bio-accessibility of polyphenols under simulated mouth, stomach and intestine conditions.



## Chapter 7 Conclusion



## 7.1 General conclusions

In this thesis, the feasibility of producing emulsion-based encapsulation systems stabilised with proteins from a sustainable source by a low-energy high-throughput technique is studied and discussed in detail. The use of dynamic membranes of tunable pore size (DMTS) throughout the entire study in the production of single (O/W) and multiple ( $W_1/O/W_2$ ) emulsions proves the capability and effectiveness of this technique. As for the sustainable protein sources, protein extracts from two insect species, black soldier fly (*H. illucens*) and lesser mealworm (*A. diaperinus*) have been successfully examined.

The single O/W emulsions targeted in this thesis are examples that incorporate sunflower oil or lemon oil as models for the most widely used oils in food applications. The sustainable protein sources selected to stabilize the O/W emulsions were black soldier fly protein concentrate (BSFPC) (1% and 2%) and lesser mealworm protein concentrate (LMPC) (1%), obtained by solubilisation of the insect meals at alkaline conditions followed by acid precipitation. BSFPC showed similar performance than whey protein isolate (WPI) to stabilize the sunflower oil emulsions when using premix emulsification with the DMTS system, regardless of the oil fraction and the protein concentration. For lemon oil emulsions, however, BSFPC successfully reduced droplet size distribution of emulsions with 20 to 40% oil fraction, while the ones produced with WPI for 40% oil fraction clearly showed an increase in the droplet size distribution from the third emulsification cycle onwards. This has been explained by the fact that lemon oil is partially soluble in water, leading to a reduction of the pH in the water phase close to the pI of WPI, therefore lowering its ability to stabilize the oil-water interface, while the stabilizing ability of BSFPC, with a lower pI than WPI, is less affected by the pH decrease. All the emulsions produced were relatively stable with a minor increase in the droplet size distribution over a week of storage at room temperature.

More complex emulsion-based encapsulation systems were studied in this thesis.  $W_1/O/W_2$  emulsions loaded with phenolic compounds from two different sources (carob pulp and grape seed) were produced using the DMTS system and stabilized with WPI, pea protein isolate (PPI) and LMPC. Premix emulsification with the DMTS enabled to generate polyphenol loaded stable emulsions regardless of the formulation. One of the most important factors that control  $W_1/O/W_2$  stability is to balance the osmolality between two aqueous phases, therefore, emulsion formulation was tailored depending on the polyphenol source. The carob pulp polyphenol, with an important amount of soluble solids (24.5 °Brix), lead to an osmolality of 1200 mOsmol/L in  $W_1$  that required the addition of 3.15 wt% NaCl and 28.2 wt% trehalose in the formulation of  $W_2$  phase with 1% WPI to balance the osmolality, achieving an encapsulation efficiency above 77% after 2 emulsification cycles. Similarly, different amounts of NaCl were incorporated in  $W_2$  phase for the encapsulation of the commercial polyphenol grape seed extract (Vitaflavan) depending on the protein used to stabilize the oil- $W_2$  interphase. Namely, 0.4 wt% for 1% WPI, 0.25 wt% for 1% PPI, and 0.06 wt% for 1% LMPC, reaching the encapsulation efficiency above 74% after 3 emulsification cycles regardless of the protein.

The stability of  $W_1/O/W_2$  emulsions with WPI, PPI, and LMPC was tested under several environmental conditions (temperature, pH, and osmotic pressure) to mimic processing, storage, and digestion conditions. The results show that all  $W_1/O/W_2$  emulsions were prone to droplet coalescence after a freeze (-20 °C) thaw cycle. At the highest temperatures tested (90 °C), the changes in droplet size distribution were less pronounced for  $W_1/O/W_2$  emulsions stabilized with LMPC than for WPI, pointing out a potential benefit of using this protein in emulsions that need to undergo heat treatment. Within the pH range investigated, LMPC stabilized double emulsions behave comparably to their WPI stabilized counterparts  $W_1/O/W_2$  emulsions under acidic and alkaline conditions, and both outperform PPI. LMPC and PPI stabilized emulsions are less able to withstand osmotic pressure differences compared to WPI. The interaction between polyphenols and LMPC was found to be much more pronounced than for WPI, which is thought to become relevant in improving the stability of such systems.

Since one of the key parameters in the scale-up of the emulsification systems is the productivity, the results of the thesis have proven that transmembrane fluxes obtained during emulsification are of industrial interest, with values between 120 and 600  $m^3m^{-2}h^{-1}$ , depending on the emulsion formulation and the pressure applied.

To integrate more sustainable fractionation strategies to insect meals processing, this thesis shows that greener solvents such as ethanol, iso-propanol, and 2-methyltetrahydrofuran are feasible for lesser mealworm meal defatting, resulting in similar extraction yields and lipid profile than the ones obtained with hexane. Moreover, the impact of the solvent in the techno-functional properties of the resulting protein fraction proved that LMPC remains the same regardless of the solvent used during defatting.

To increase the stability of the emulsion-based encapsulation systems and extend their shelf life, the production of solid microcapsules is highly recommended. This thesis has advanced in the assessment of insect proteins for the production of solid microcapsules, proving that LMPC performs similarly than WPI and PPI, regardless of the drying method selected (spray drying or freeze drying). The solid microcapsules from polyphenol loaded  $W_1/O/W_2$  emulsions stabilized with LMPC present the external structure typical from the microcapsules obtained by spray drying and freeze drying. Moreover, the  $W_1/O/W_2$  emulsion is recovered when rehydrated, with a similar increase in the droplet size distribution as it happens with WPI.

Based on the above, this thesis demonstrated a comprehensive approach of encapsulation of bioactive compounds using ingredients from sustainable sources, eco-friendly, and efficient methods. It provides useful information for the potential use of insect proteins and low-energy technologies for the production of emulsion-based encapsulation systems.

## 7.2 Future work

As a result of the knowledge gained in this thesis, the possible future work is outlined below.

- Advance the research to improve the fractionation of the insect powders, specifically to enhance solubility while maintaining the techno-functional properties. The use of ultrasound or microwave assisted extraction processes for both defatting and protein extraction are of interest. Moreover, to improve solubility and emulsifying properties of insect protein extract/concentrates, enzymatic hydrolysis is a promising solution to obtain active peptides.
- Broaden the knowledge of bioactive properties of insect proteins, specifically as anti-microbial, anti-inflammatory, antioxidant, and *in vitro* digestibility which will widen the applications of edible insect proteins in food, feed, pharmaceutical, and cosmetic industries.
- Harness the properties of certain insect fractions, such as lipids extracted from black soldier fly (*H. illucens*) that tend to be solid at room temperature, to produce solid-lipid microcapsules. Oil-soluble bioactive compounds such as vitamin E,  $\beta$ -carotenoid and some drugs for instance tocopherol nicotinate, teprenone and ethyl icosapentate can be incorporated into black soldier fly lipids to be encapsulated and to be utilized in lipid-based drug delivery systems. Further evaluation on the safety and risks in food and medical applications should be carried out.
- To have an overview of all the sustainable sourced proteins, a study on microalgae is promising. With the addition of the knowledge in protein derived from microalgae, especially on its techno-functional properties, a better and more comprehensive evaluation comparing plant, insect and microbial proteins which certainly will be helpful information to the future development.



## References

1. Tan, C. & McClements, D. J. Application of advanced emulsion technology in the food industry: A review and critical evaluation. *Foods* **10**, (2021).
2. Hu, M. & Russell, T. P. Polymers with advanced architectures as emulsifiers for multi-functional emulsions. *Mater. Chem. Front.* **5**, 1205–1220 (2021).
3. Lu, W., Maidannyk, V., Kelly, A. L. & Miao, S. Fabrication and characterization of highly re-dispersible dry emulsions. *Food Hydrocoll.* **102**, 105617 (2020).
4. Halmos, E. P., Mack, A. & Gibson, P. R. Review article: emulsifiers in the food supply and implications for gastrointestinal disease. *Aliment. Pharmacol. Ther.* **49**, 41–50 (2019).
5. Zhang, G. H. *et al.* Fabrication of hollow porous PLGA microspheres for controlled protein release and promotion of cell compatibility. *Chinese Chem. Lett.* **24**, 710–714 (2013).
6. Chen, M., Ouyang, H., Zhou, S., Li, J. & Ye, Y. PLGA-nanoparticle mediated delivery of anti-OX40 monoclonal antibody enhances anti-tumor cytotoxic T cell responses. *Cell. Immunol.* **287**, 91–99 (2014).
7. Kakran, M. & Antipina, M. N. Emulsion-based techniques for encapsulation in biomedicine, food and personal care. *Curr. Opin. Pharmacol.* **18**, 47–55 (2014).
8. Gupta, A., Eral, H. B., Hatton, T. A. & Doyle, P. S. Nanoemulsions: Formation, properties and applications. *Soft Matter* **12**, 2826–2841 (2016).
9. SONNEVILLEAUBRUN, O. Nanoemulsions: a new vehicle for skincare products. *Adv. Colloid Interface Sci.* **108–109**, 145–149 (2004).
10. Ajazuddin *et al.* Recent expansions in an emergent novel drug delivery technology: Emulgel. *J. Control. Release* **171**, 122–132 (2013).
11. Sakulku, U. *et al.* Characterization and mosquito repellent activity of citronella oil nanoemulsion. *Int. J. Pharm.* **372**, 105–111 (2009).
12. Beldengrün, Y. *et al.* Formation and stabilization of multiple water-in-water-in-water (W/W/W) emulsions. *Food Hydrocoll.* **102**, (2020).
13. Zarzar, L. D. *et al.* Dynamically reconfigurable complex emulsions via tunable interfacial tensions. *Nature* **518**, 520–524 (2015).
14. Li, B. *et al.* Synergistic effects of whey protein-polysaccharide complexes on the controlled release of lipid-soluble and water-soluble vitamins in W1/O/W2 double emulsion systems. *Int. J. Food Sci. Technol.* **47**, 248–254 (2012).
15. Choi, S. J., Decker, E. A. & McClements, D. J. Impact of iron encapsulation within the interior aqueous phase of water-in-oil-in-water emulsions on lipid

- oxidation. *Food Chem.* **116**, 271–276 (2009).
16. Lutz, R., Aserin, A., Wicker, L. & Garti, N. Release of electrolytes from W/O/W double emulsions stabilized by a soluble complex of modified pectin and whey protein isolate. *Colloids Surfaces B Biointerfaces* **74**, 178–185 (2009).
  17. MÁRQUEZ, A. L. & WAGNER, J. R. Rheology of double (w/o/w) emulsions prepared with soybean milk and fortified with calcium. *J. Texture Stud.* **41**, 651–671 (2010).
  18. Bonnet, M., Cansell, M., Placin, F., Anton, M. & Leal-Calderon, F. Impact of sodium caseinate concentration and location on magnesium release from multiple W/O/W emulsions. *Langmuir* **26**, 9250–9260 (2010).
  19. Saffarionpour, S. & Diosady, L. L. Multiple Emulsions for Enhanced Delivery of Vitamins and Iron Micronutrients and Their Application for Food Fortification. *Food Bioprocess Technol.* **14**, 587–625 (2021).
  20. Frank, K. *et al.* Stability of Anthocyanin-Rich W/O/W-Emulsions Designed for Intestinal Release in Gastrointestinal Environment. *J. Food Sci.* **77**, (2012).
  21. Shima, M., Matsuo, T., Yamashita, M. & Adachi, S. Protection of *Lactobacillus acidophilus* from bile salts in a model intestinal juice by incorporation into the inner-water phase of a W/O/W emulsion. *Food Hydrocoll.* **23**, 281–285 (2009).
  22. Lobato-Calleros, C. *et al.* Structural and textural characteristics of reduced-fat cheese-like products made from W1/O/W2 emulsions and skim milk. *LWT - Food Sci. Technol.* **41**, 1847–1856 (2008).
  23. Lobato-Calleros, C., Recillas-Mota, M. T., Espinosa-Solares, T., Alvarez-Ramirez, J. & Vernon-Carter, E. J. Low-Fat Stirred Yoghurts Made With Skim Milk and Multiple Emulsions. *J. Texture Stud.* **40**, 657–675 (2009).
  24. S, A. U. A., Premkumar, J. & Ranganathan, T. V. Emulsion and its applications in food processing : A review Emulsion and it ' s Applications in Food Processing – A Review. **4**, 241–248 (2017).
  25. Santana, R. C., Perrechil, F. A. & Cunha, R. L. High- and Low-Energy Emulsifications for Food Applications: A Focus on Process Parameters. *Food Eng. Rev.* **5**, 107–122 (2013).
  26. McClements, D. J. & Jafari, S. M. Improving emulsion formation, stability and performance using mixed emulsifiers: A review. *Adv. Colloid Interface Sci.* **251**, 55–79 (2018).
  27. Liu, Q., Huang, H., Chen, H., Lin, J. & Wang, Q. Food-grade nanoemulsions: Preparation, stability and application in encapsulation of bioactive compounds. *Molecules* **24**, 1–37 (2019).
  28. Griffin, W. C. Classification of Surface-Active Agents by HLB. *J. Soc. Cosmet. Chem.* **1**, 311–326 (1949).
  29. Piorkowski, D. T. & McClements, D. J. Beverage emulsions: Recent

- developments in formulation, production, and applications. *Food Hydrocoll.* **42**, 5–41 (2014).
30. Fang, Z. & Bhandari, B. Encapsulation of polyphenols – a review. *Trends Food Sci. Technol.* **21**, 510–523 (2010).
  31. Marcillo-Parra, V., Tupuna-Yerovi, D. S., González, Z. & Ruales, J. Encapsulation of bioactive compounds from fruit and vegetable by-products for food application – A review. *Trends Food Sci. Technol.* **116**, 11–23 (2021).
  32. Pichot, R., Spyropoulos, F. & Norton, I. T. O/W emulsions stabilised by both low molecular weight surfactants and colloidal particles: The effect of surfactant type and concentration. *J. Colloid Interface Sci.* **352**, 128–135 (2010).
  33. Lam, R. S. H. & Nickerson, M. T. Food proteins: A review on their emulsifying properties using a structure–function approach. *Food Chem.* **141**, 975–984 (2013).
  34. Kim, W., Wang, Y. & Selomulya, C. Dairy and plant proteins as natural food emulsifiers. *Trends Food Sci. Technol.* **105**, 261–272 (2020).
  35. Liceaga, A. M. Approaches for Utilizing Insect Protein for Human Consumption: Effect of Enzymatic Hydrolysis on Protein Quality and Functionality. *Ann. Entomol. Soc. Am.* **112**, 529–532 (2019).
  36. Nongonierma, A. B. & FitzGerald, R. J. Unlocking the biological potential of proteins from edible insects through enzymatic hydrolysis: A review. *Innov. Food Sci. Emerg. Technol.* **43**, 239–252 (2017).
  37. Nongonierma, A. B. & FitzGerald, R. J. Enhancing bioactive peptide release and identification using targeted enzymatic hydrolysis of milk proteins. *Anal. Bioanal. Chem.* **410**, 3407–3423 (2018).
  38. Sun, X. D. Enzymatic hydrolysis of soy proteins and the hydrolysates utilisation. *Int. J. Food Sci. Technol.* **46**, 2447–2459 (2011).
  39. Deeth, H. *Whey Proteins: An Overview*. *Whey Proteins* (Elsevier Inc., 2019). doi:10.1016/B978-0-12-812124-5.00001-1.
  40. Braun, K., Hanewald, A. & Vilgis, T. A. Milk emulsions: Structure and stability. *Foods* **8**, 1–16 (2019).
  41. Raikos, V. Effect of heat treatment on milk protein functionality at emulsion interfaces. A review. *Food Hydrocoll.* **24**, 259–265 (2010).
  42. Mei, L., McClements, D. J. & Decker, E. A. Lipid oxidation in emulsions as affected by charge status of antioxidants and emulsion droplets. *J. Agric. Food Chem.* **47**, 2267–2273 (1999).
  43. Tokle, T. & McClements, D. J. Physicochemical properties of lactoferrin stabilized oil-in-water emulsions: Effects of pH, salt and heating. *Food Hydrocoll.* **25**, 976–982 (2011).

44. Acevedo-Fani, A., Silva, H. D., Soliva-Fortuny, R., Martín-Belloso, O. & Vicente, A. A. Formation, stability and antioxidant activity of food-grade multilayer emulsions containing resveratrol. *Food Hydrocoll.* **71**, 207–215 (2017).
45. Teo, A. *et al.* Physicochemical properties of whey protein, lactoferrin and Tween 20 stabilised nanoemulsions: Effect of temperature, pH and salt. *Food Chem.* **197**, 297–306 (2016).
46. Schmitt, C., Aberkane, L. & Sanchez, C. Protein–polysaccharide complexes and coacervates. in *Handbook of Hydrocolloids* vol. 167 420–476 (Elsevier, 2009).
47. Stone, A. K., Nosworthy, M. G., Chiremba, C., House, J. D. & Nickerson, M. T. A comparative study of the functionality and protein quality of a variety of legume and cereal flours. *Cereal Chem.* **96**, 1159–1169 (2019).
48. Burger, T. G. & Zhang, Y. Recent progress in the utilization of pea protein as an emulsifier for food applications. *Trends Food Sci. Technol.* **86**, 25–33 (2019).
49. Peng, W. *et al.* Effects of heat treatment on the emulsifying properties of pea proteins. *Food Hydrocoll.* **52**, 301–310 (2016).
50. Chen, M. *et al.* Study on the emulsifying stability and interfacial adsorption of pea proteins. *Food Hydrocoll.* **88**, 247–255 (2019).
51. Sridharan, S., Meinders, M. B. J., Bitter, J. H. & Nikiforidis, C. V. On the Emulsifying Properties of Self-Assembled Pea Protein Particles. *Langmuir* **36**, 12221–12229 (2020).
52. Benjamin, O., Silcock, P., Beauchamp, J., Buettner, A. & Everett, D. W. Emulsifying properties of legume proteins compared to  $\beta$ -lactoglobulin and tween 20 and the volatile release from oil-in-water emulsions. *J. Food Sci.* **79**, E2014–E2022 (2014).
53. Tamm, F., Herbst, S., Brodkorb, A. & Drusch, S. Functional properties of pea protein hydrolysates in emulsions and spray-dried microcapsules. *Food Hydrocoll.* **58**, 204–214 (2016).
54. Hinderink, E. B. A., Kaade, W., Sagis, L., Schroën, K. & Berton-Carabin, C. C. Microfluidic investigation of the coalescence susceptibility of pea protein-stabilised emulsions: Effect of protein oxidation level. *Food Hydrocoll.* **102**, (2020).
55. Zhang, X. *et al.* Soy/whey protein isolates: interfacial properties and effects on the stability of oil-in-water emulsions. *J. Sci. Food Agric.* **101**, 262–271 (2021).
56. Hinderink, E. B. A., Münch, K., Sagis, L., Schroën, K. & Berton-Carabin, C. C. Synergistic stabilisation of emulsions by blends of dairy and soluble pea proteins: Contribution of the interfacial composition. *Food Hydrocoll.* **97**, 105206 (2019).
57. Ho, K. K. H. Y., Schroën, K., San Martín-González, M. F. & Berton-Carabin, C.

- C. Synergistic and antagonistic effects of plant and dairy protein blends on the physicochemical stability of lycopene-loaded emulsions. *Food Hydrocoll.* **81**, 180–190 (2018).
58. Dai, T. *et al.* Utilization of plant-based protein-polyphenol complexes to form and stabilize emulsions: Pea proteins and grape seed proanthocyanidins. *Food Chem.* **329**, (2020).
59. Dai, T. *et al.* Protein-polyphenol interactions enhance the antioxidant capacity of phenolics: Analysis of rice glutelin-procyanidin dimer interactions. *Food Funct.* **10**, 765–774 (2019).
60. Mintah, B. K. *et al.* Characterization of edible soldier fly protein and hydrolysate altered by multiple-frequency ultrasound: Structural, physical, and functional attributes. *Process Biochem.* **95**, 157–165 (2020).
61. Park, S. I., Kim, J. W. & Yoe, S. M. Purification and characterization of a novel antibacterial peptide from black soldier fly (*Hermetia illucens*) larvae. *Dev. Comp. Immunol.* **52**, 98–106 (2015).
62. Zarantoniello, M. *et al.* Black Soldier Fly (*Hermetia illucens*) reared on roasted coffee by-product and *Schizochytrium* sp. as a sustainable terrestrial ingredient for aquafeeds production. *Aquaculture* 734659 (2019)  
doi:10.1016/j.aquaculture.2019.734659.
63. Yi, L. *et al.* Extraction and characterisation of protein fractions from five insect species. *Food Chem.* **141**, 3341–3348 (2013).
64. Sousa, P., Borges, S. & Pintado, M. Enzymatic hydrolysis of insect: *Alphitobius diaperinus* towards the development of bioactive peptide hydrolysates. *Food Funct.* **11**, 3539–3548 (2020).
65. Zielińska, E., Karaś, M. & Baraniak, B. Comparison of functional properties of edible insects and protein preparations thereof. *LWT* **91**, 168–174 (2018).
66. Hall, F. G., Jones, O. G., O’Haire, M. E. & Liceaga, A. M. Functional properties of tropical banded cricket (*Gryllobates sigillatus*) protein hydrolysates. *Food Chem.* **224**, 414–422 (2017).
67. Ndiritu, A. K., Kinyuru, J. N., Kenji, G. M. & Gichuhi, P. N. Extraction technique influences the physico-chemical characteristics and functional properties of edible crickets (*Acheta domesticus*) protein concentrate. *J. Food Meas. Charact.* **11**, 2013–2021 (2017).
68. Mishyna, M., Martinez, J.-J. I., Chen, J. & Benjamin, O. Extraction, characterization and functional properties of soluble proteins from edible grasshopper (*Schistocerca gregaria*) and honey bee (*Apis mellifera*). *Food Res. Int.* **116**, 697–706 (2019).
69. Aguilar-Acosta, L. A., Serna-Saldivar, S. O., Rodríguez-Rodríguez, J., Escalante-Aburto, A. & Chuck-Hernández, C. Effect of ultrasound application on protein yield and fate of alkaloids during lupin alkaline extraction process.

*Biomolecules* **10**, (2020).

70. Soetemans, L., Uyttebroek, M., D'Hondt, E. & Bastiaens, L. Use of organic acids to improve fractionation of the black soldier fly larvae juice into lipid- and protein-enriched fractions. *Eur. Food Res. Technol.* **245**, 2257–2267 (2019).
71. Leni, G., Soetemans, L., Caligiani, A., Sforza, S. & Bastiaens, L. Degree of hydrolysis affects the techno-functional properties of lesser mealworm protein hydrolysates. *Foods* **9**, (2020).
72. R, S., Yadav, B. K. & Rawson, A. Optimization of protein extraction from yellow mealworm larvae. *Int. J. Chem. Stud.* **7**, 4577–4582 (2019).
73. Zhao, X., Vázquez-Gutiérrez, J. L., Johansson, D. P., Landberg, R. & Langton, M. Yellow mealworm protein for food purposes - Extraction and functional properties. *PLoS One* **11**, 1–17 (2016).
74. Jiang, Y. *et al.* Effects of salting-in/out-assisted extractions on structural, physicochemical and functional properties of *Tenebrio molitor* larvae protein isolates. *Food Chem.* **338**, 128158 (2021).
75. Wali, A. *et al.* Optimization of scorpion protein extraction and characterization of the proteins' functional properties. *Molecules* **24**, 1–16 (2019).
76. Purschke, B., Meinschmidt, P., Horn, C., Rieder, O. & Jäger, H. Improvement of techno-functional properties of edible insect protein from migratory locust by enzymatic hydrolysis. *Eur. Food Res. Technol.* **244**, 999–1013 (2018).
77. Yasumatsu, K. *et al.* Whipping and Emulsifying Properties of Soybean Products. *Agric. Biol. Chem.* **36**, 719–727 (1972).
78. Pearce, K. N. & Kinsella, J. E. Emulsifying properties of proteins: evaluation of a turbidimetric technique. *J. Agric. Food Chem.* **26**, 716–723 (1978).
79. Beuchat, L. R., Cherry, J. P. & Quinn, M. R. Physicochemical Properties of Peanut Flour as Affected by Proteolysis. *J. Agric. Food Chem.* **23**, 616–620 (1975).
80. Purschke, B. *et al.* Recovery of soluble proteins from migratory locust (*Locusta migratoria*) and characterisation of their compositional and techno-functional properties. *Food Res. Int.* **106**, 271–279 (2018).
81. Chatsuwan, N., Nalinanon, S., Puechkamut, Y., Lamsal, B. P. & Pinsiroadom, P. Characteristics, Functional Properties, and Antioxidant Activities of Water-Soluble Proteins Extracted from Grasshoppers, *Patanga succincta* and *Chondracris roseaprunner*. *J. Chem.* **2018**, (2018).
82. Gould, J. & Wolf, B. Interfacial and emulsifying properties of mealworm protein at the oil/water interface. *Food Hydrocoll.* **77**, 57–65 (2018).
83. Kim, T.-K. *et al.* Technical Functional Properties of Water- and Salt-soluble Proteins Extracted from Edible Insects. *Food Sci. Anim. Resour.* **39**, 643–654 (2019).

84. Kim, T. K. *et al.* Thermal stability and rheological properties of heat-induced gels prepared using edible insect proteins in a model system. *Lwt* **134**, 110270 (2020).
85. Bußler, S., Rumpold, B. A., Jander, E., Rawel, H. M. & Schlüter, O. K. Recovery and techno-functionality of flours and proteins from two edible insect species: Meal worm (*Tenebrio molitor*) and black soldier fly (*Hermetia illucens*) larvae. *Heliyon* **2**, (2016).
86. Jeong, M.-S., Lee, S.-D. & Cho, S.-J. Effect of Three Defatting Solvents on the Techno-Functional Properties of an Edible Insect (*Gryllus bimaculatus*) Protein Concentrate. *Molecules* **26**, 5307 (2021).
87. Adebowale, Y. A., Adebowale, K. O. & Oguntokun, M. O. Evaluation of nutritive properties of the large African cricket (*Gryllidae* sp). *Pak. J. Sci. Ind. Res.* **48**, 274–278 (2005).
88. Babiker, Hassan, Eltayeb, Osman, Elhassan, H. Solubility and Functional Properties of Boiled and Fried Sudanese Tree Locust Flour as a Function of NaCl concentration. *J. Food Technol.* **5**, 210–214 (2007).
89. Omotoso, O. T. An evaluation of the nutrients and some anti-nutrients in Silkworm, *Bombyxmori* L. (*Bombycidae*: *Lepidoptera*). *Jordan J. Biol. Sci.* **8**, 45–50 (2015).
90. Yang, A. *et al.* Enhancing protein to extremely high content in photosynthetic bacteria during biogas slurry treatment. *Bioresour. Technol.* **245**, 1277–1281 (2017).
91. Fasolin, L. H. *et al.* Emergent food proteins – Towards sustainability, health and innovation. *Food Res. Int.* **125**, 108586 (2019).
92. Zheng, C. *et al.* Characterization and emulsifying property of a novel bioemulsifier by *Aeribacillus pallidus* YM-1. *J. Appl. Microbiol.* **113**, 44–51 (2012).
93. Yamada, E. A. & Sgarbieri, V. C. Yeast (*Saccharomyces cerevisiae*) protein concentrate: Preparation, chemical composition, and nutritional and functional properties. *J. Agric. Food Chem.* **53**, 3931–3936 (2005).
94. Bertolo, A. P., Biz, A. P., Kempka, A. P., Rigo, E. & Cavalheiro, D. Yeast (*Saccharomyces cerevisiae*): evaluation of cellular disruption processes, chemical composition, functional properties and digestibility. *J. Food Sci. Technol.* **56**, 3697–3706 (2019).
95. Paraszkiwicz, K., Kanwal, A. & Długoński, J. Emulsifier production by steroid transforming filamentous fungus *Curvularia lunata*. Growth and product characterization. *J. Biotechnol.* **92**, 287–294 (2002).
96. Teuling, E., Schrama, J. W., Gruppen, H. & Wierenga, P. A. Characterizing emulsion properties of microalgal and cyanobacterial protein isolates. *Algal Res.* **39**, 101471 (2019).

97. United Nation. World population prospects 2019: Highlights (ST/ESA/SER.A/423).
98. FAO. *The future of food and agriculture - Trends and challenges*. Rome (2017).
99. Van Huis, A. *et al*. *Edible insects: future prospects for food and feed security*. Food and Agriculture Organization of the United Nations vol. 171 (2013).
100. DeFoliart, G. R. INSECTS AS FOOD: Why the Western Attitude Is Important. *Annu. Rev. Entomol.* **44**, 21–50 (1999).
101. Yen, A. L. Edible insects: Traditional knowledge or western phobia? *Entomol. Res.* **39**, 289–298 (2009).
102. Hartmann, C., Shi, J., Giusto, A. & Siegrist, M. The psychology of eating insects: A cross-cultural comparison between Germany and China. *Food Qual. Prefer.* **44**, 148–156 (2015).
103. Tan, H. S. G. *et al*. Insects as food: Exploring cultural exposure and individual experience as determinants of acceptance. *Food Qual. Prefer.* **42**, 78–89 (2015).
104. Schösler, H., Boer, J. de & Boersema, J. J. Can we cut out the meat of the dish? Constructing consumer-oriented pathways towards meat substitution. *Appetite* **58**, 39–47 (2012).
105. Balzan, S., Fasolato, L., Maniero, S. & Novelli, E. Edible insects and young adults in a north-east Italian city an exploratory study. *Br. Food J.* **118**, 318–326 (2016).
106. Duda, A., Adamczak, J., Chelminska, P., Juskiewicz, J. & Kowalczewski, P. Quality and nutritional/textural properties of durum wheat pasta enriched with cricket powder. *Foods* **8**, 1–10 (2019).
107. Hartmann, C. & Siegrist, M. Becoming an insectivore: Results of an experiment. *Food Qual. Prefer.* **51**, 118–122 (2016).
108. Osimani, A. *et al*. Bread enriched with cricket powder (*Acheta domesticus*): A technological, microbiological and nutritional evaluation. *Innov. Food Sci. Emerg. Technol.* **48**, 150–163 (2018).
109. Roncolini, A. *et al*. Protein fortification with mealworm (*Tenebrio molitor* L.) powder: Effect on textural, microbiological, nutritional and sensory features of bread. *PLoS One* **14**, 1–29 (2019).
110. Roncolini, A. *et al*. Lesser mealworm (*Alphitobius diaperinus*) powder as a novel baking ingredient for manufacturing high-protein, mineral-dense snacks. *Food Res. Int.* **131**, (2020).
111. Gordon, D. G. *The Eat-A-Bug Cookbook, Revised: 40 Ways to Cook Crickets, Grasshoppers, Ants, Water Bugs, Spiders, Centipedes, and Their Kin*. (Ten Speed Press, 2013).
112. Radia, S., Whippey, N. & Holmes, S. *Eat Grub: The Ultimate Insect Cookbook*.

- (Lumber Liquidators (LL), 2016).
113. Martin, D. *Edible: An adventure into the world of eating insects and the last great hope to save the planet*. (Houghton Mifflin Harcourt, 2014).
  114. Chen, X., Feng, Y., Zhang, H. & Chen, Z. *Review of the nutritive value of edible insects. Forest insects as food: human bite back* doi:10.1016/S0009-9260(03)00123-5.
  115. Raheem, D. *et al.* Entomophagy: Nutritional, ecological, safety and legislation aspects. *Food Res. Int.* **126**, 108672 (2019).
  116. Bosch, G., Zhang, S., Oonincx, D. G. A. B. & Hendriks, W. H. Protein quality of insects as potential ingredients for dog and cat foods. *J. Nutr. Sci.* **3**, 1–4 (2014).
  117. Van Krimpen, M., Bikker, P., Van der Meer, I., Van der Peet-Schwering, C. & Vereijken, J. Cultivation, processing and nutritional aspects for pigs and poultry of European protein sources as alternatives for imported soybean products. (2013).
  118. Gahukar, R. T. Entomophagy and human food security. *Int. J. Trop. Insect Sci.* **31**, 129–144 (2011).
  119. Dobermann, D., Swift, J. A. & Field, L. M. Opportunities and hurdles of edible insects for food and feed. *Nutr. Bull.* **42**, 293–308 (2017).
  120. Oonincx, D. G. A. B. & de Boer, I. J. M. Environmental Impact of the Production of Mealworms as a Protein Source for Humans - A Life Cycle Assessment. *PLoS One* **7**, 1–5 (2012).
  121. Baiano, A. Edible insects: An overview on nutritional characteristics, safety, farming, production technologies, regulatory framework, and socio-economic and ethical implications. *Trends Food Sci. Technol.* **100**, 35–50 (2020).
  122. Allergens), E. N. P. (EFSA P. on N. N. F. and F. *et al.* Safety of dried yellow mealworm (*Tenebrio molitor* larva) as a novel food pursuant to Regulation (EU) 2015/2283. *EFSA J.* **19**, 1–29 (2021).
  123. Allergens), E. N. P. (EFSA P. on N. N. F. and F. *et al.* Safety of frozen and dried formulations from whole house crickets (*Acheta domesticus*) as a Novel food pursuant to Regulation (EU) 2015/2283. *EFSA J.* **19**, (2021).
  124. Allergens), E. N. P. (EFSA P. on N. N. F. and F. *et al.* Safety of frozen and dried formulations from migratory locust (*Locusta migratoria*) as a Novel food pursuant to Regulation (EU) 2015/2283. *EFSA J.* **19**, (2021).
  125. Joscelyne, S. M. & Trägårdh, G. Membrane emulsification - A literature review. *J. Memb. Sci.* **169**, 107–117 (2000).
  126. Charcosset, C. *Preparation of nanomaterials for food applications using membrane emulsification and membrane mixing. Emulsions* (Elsevier Inc.,

- 2016). doi:10.1016/b978-0-12-804306-6.00002-7.
127. Nakashima, T., Shimizu, M. & Kukizaki, M. Membrane emulsification by microporous glass. *Inorg. Membr. ICIM2-91* **62**, 513–516 (1991).
  128. SUZUKI, K., SHUTO, I. & HAGURA, Y. Characteristics of the Membrane Emulsification Method Combined with Preliminary Emulsification for Preparing Corn Oil-in-Water Emulsions. *Food Sci. Technol. Int. Tokyo* **2**, 43–47 (1996).
  129. Piacentini, E., Giorno, L., Figoli, A. & Drioli, E. 3.13 Membrane Emulsification Advances and Perspectives. *Compr. Membr. Sci. Eng.* **3**, 331–356 (2017).
  130. Nazir, A., Schroën, K. & Boom, R. Premix emulsification: A review. *J. Memb. Sci.* **362**, 1–11 (2010).
  131. Nazir, A. & Vladislavljević, G. T. Droplet breakup mechanisms in premix membrane emulsification and related microfluidic channels. *Adv. Colloid Interface Sci.* **290**, (2021).
  132. Schroën, K., Ferrando, M., de Lamo-Castellví, S., Sahin, S. & Güell, C. Linking findings in microfluidics to membrane emulsification process design: The importance of wettability and component interactions with interfaces. *Membranes (Basel)*. **6**, (2016).
  133. van der Zwan, E. A., Schroën, C. G. P. H. & Boom, R. M. Premix membrane emulsification by using a packed layer of glass beads. *AIChE J.* **54**, 2190–2197 (2008).
  134. Nazir, A., Boom, R. M. & Schroën, K. Droplet break-up mechanism in premix emulsification using packed beds. *Chem. Eng. Sci.* **92**, 190–197 (2013).
  135. Sawalha, H., Sahin, S. & Schroën, K. Preparation of polylactide microcapsules at a high throughput with a packed-bed premix emulsification system. *J. Appl. Polym. Sci.* **133**, 3–9 (2016).
  136. Kaade, W. *et al.* Dynamic membranes of tunable pore size for lemon oil encapsulation. *LWT* **123**, 109090 (2020).
  137. Arkles, B. Hydrophobicity, hydrophilicity and silanes. *Paint Coatings Ind.* **22**, 114–135 (2006).
  138. Laouini, A., Charcosset, C., Fessi, H. & Schroen, K. Use of dynamic membranes for the preparation of vitamin E-loaded lipid particles: An alternative to prevent fouling observed in classical cross-flow emulsification. *Chem. Eng. J.* **236**, 498–505 (2014).
  139. Van Der Zwan, E., Schroën, K., Van Dijke, K. & Boom, R. Visualization of droplet break-up in pre-mix membrane emulsification using microfluidic devices. *Colloids Surfaces A Physicochem. Eng. Asp.* **277**, 223–229 (2006).
  140. Nazir, A., Boom, R. M. & Schroën, K. Influence of the emulsion formulation in premix emulsification using packed beds. *Chem. Eng. Sci.* **116**, 547–557 (2014).

141. Eisinaite, V., Juraite, D., Schroën, K. & Leskauskaite, D. Preparation of stable food-grade double emulsions with a hybrid premix membrane emulsification system. *Food Chem.* **206**, 59–66 (2016).
142. Ladjal-Ettoumi, Y. *et al.* Legume Protein Isolates for Stable Acidic Emulsions Prepared by Premix Membrane Emulsification. *Food Biophys.* **12**, 119–128 (2017).
143. Nazir, A., Maan, A. A., Sahin, S., Boom, R. M. & Schroën, K. Foam preparation at high-throughput using a novel packed bed system. *Food Bioprod. Process.* **94**, 561–564 (2015).
144. Sahin, S., Sawalha, H. & Schroën, K. High throughput production of double emulsions using packed bed premix emulsification. *Food Res. Int.* **66**, 78–85 (2014).
145. Ozkan, G., Franco, P., De Marco, I., Xiao, J. & Capanoglu, E. A review of microencapsulation methods for food antioxidants: Principles, advantages, drawbacks and applications. *Food Chem.* **272**, 494–506 (2019).
146. Ray, S., Raychaudhuri, U. & Chakraborty, R. An overview of encapsulation of active compounds used in food products by drying technology. *Food Biosci.* **13**, 76–83 (2016).
147. Su, Y. L. *et al.* Microencapsulation of Radix salvia miltiorrhiza nanoparticles by spray-drying. *Powder Technol.* (2008) doi:10.1016/j.powtec.2007.08.014.
148. Gharsallaoui, A. *et al.* Utilisation of pectin coating to enhance spray-dry stability of pea protein-stabilised oil-in-water emulsions. *Food Chem.* **122**, 447–454 (2010).
149. Berendsen, R., Güell, C. & Ferrando, M. Spray dried double emulsions containing procyanidin-rich extracts produced by premix membrane emulsification: Effect of interfacial composition. *Food Chem.* **178**, 251–258 (2015).
150. Sosa, N., Schebor, C. & Pérez, O. E. Encapsulation of citral in formulations containing sucrose or trehalose: Emulsions properties and stability. *Food Bioprod. Process.* **92**, 266–274 (2014).
151. Ramakrishnan, S., Ferrando, M., Aceña-Muñoz, L., De Lamo-Castellví, S. & Güell, C. Fish Oil Microcapsules from O/W Emulsions Produced by Premix Membrane Emulsification. *Food Bioprocess Technol.* **6**, 3088–3101 (2013).
152. Ramakrishnan, S. *et al.* Influence of Emulsification Technique and Wall Composition on Physicochemical Properties and Oxidative Stability of Fish Oil Microcapsules Produced by Spray Drying. *Food Bioprocess Technol.* **7**, 1959–1972 (2014).
153. Di Giorgio, L., Salgado, P. R. & Mauri, A. N. Encapsulation of fish oil in soybean protein particles by emulsification and spray drying. *Food Hydrocoll.* **87**, 891–901 (2019).

154. Guadarrama-Lezama, A. Y. *et al.* Preparation and characterization of non-aqueous extracts from chilli (*Capsicum annum* L.) and their microencapsulates obtained by spray-drying. *J. Food Eng.* **112**, 29–37 (2012).
155. Chen, J., Li, F., Li, Z., McClements, D. J. & Xiao, H. Encapsulation of carotenoids in emulsion-based delivery systems: Enhancement of  $\beta$ -carotene water-dispersibility and chemical stability. *Food Hydrocoll.* **69**, 49–55 (2017).
156. Toledo-Madrid, K., Gallardo-Velázquez, T. & Osorio-Revilla, G. Microencapsulation of purple cactus pear fruit (*Opuntia ficus indica*) extract by the combined method W/O/W double emulsion-spray drying and conventional spray drying: A comparative study. *Processes* **6**, 1–18 (2018).
157. Silva, E. K., Zobot, G. L. & Meireles, M. A. A. Ultrasound-assisted encapsulation of annatto seed oil: Retention and release of a bioactive compound with functional activities. *Food Res. Int.* **78**, 159–168 (2015).
158. Premi, M. & Sharma, H. K. Effect of different combinations of maltodextrin, gum arabic and whey protein concentrate on the encapsulation behavior and oxidative stability of spray dried drumstick (*Moringa oleifera*) oil. *Int. J. Biol. Macromol.* **105**, 1232–1240 (2017).
159. Castel, V., Rubiolo, A. C. & Carrara, C. R. Brea gum as wall material in the microencapsulation of corn oil by spray drying: Effect of inulin addition. *Food Res. Int.* **103**, 76–83 (2018).
160. El-Messery, T. M., Altuntas, U., Altin, G. & Özçelik, B. The effect of spray-drying and freeze-drying on encapsulation efficiency, in vitro bioaccessibility and oxidative stability of krill oil nanoemulsion system. *Food Hydrocoll.* **106**, (2020).
161. Kanha, N., Regenstein, J. M., Surawang, S., Pitchakarn, P. & Laokuldilok, T. Properties and kinetics of the in vitro release of anthocyanin-rich microcapsules produced through spray and freeze-drying complex coacervated double emulsions. *Food Chem.* **340**, 127950 (2021).
162. Maisuthisakul, P. & Gordon, M. H. Influence of polysaccharides and storage during processing on the properties of mango seed kernel extract (microencapsulation). *Food Chem.* **134**, 1453–1460 (2012).
163. Bušić, A. *et al.* The potential of combined emulsification and spray drying techniques for encapsulation of polyphenols from rosemary (*Rosmarinus officinalis* L.) leaves. *Food Technol. Biotechnol.* **56**, 494–505 (2018).
164. Assadpour, E. & Jafari, S. Spray drying of folic acid within nano-emulsions: Optimization by Taguchi approach. *Dry. Technol.* **35**, 1152–1160 (2017).
165. Esfanjani, A. F., Jafari, S. M., Assadpour, E. & Mohammadi, A. Nano-encapsulation of saffron extract through double-layered multiple emulsions of pectin and whey protein concentrate. *J. Food Eng.* **165**, 149–155 (2015).
166. Rodríguez-Huezo, M. E., Pedroza-Islas, R., Prado-Barragán, L. A., Beristain, C.

- I. & Vernon-Carter, E. J. Microencapsulation by Spray Drying of Multiple Emulsions Containing Carotenoids. *J. Food Sci.* **69**, 351–359 (2006).
167. Edris, A. & Bergnsthål, B. Encapsulation of orange oil in a spray dried double emulsion. *Nahrung/Food* **45**, 133–137 (2001).
168. Morais, A. R. D. V. *et al.* Freeze-drying of emulsified systems: A review. *Int. J. Pharm.* **503**, 102–114 (2016).
169. Mehyar, G. F., Al-Isamil, K. M., Al-Ghizzawi, H. M. & Holley, R. A. Stability of Cardamom (*Elettaria Cardamomum*) Essential Oil in Microcapsules Made of Whey Protein Isolate, Guar Gum, and Carrageenan. *J. Food Sci.* **79**, C1939–C1949 (2014).
170. Kaushik, V. & Roos, Y. H. Limonene encapsulation in freeze-drying of gum Arabic-sucrose-gelatin systems. *LWT - Food Sci. Technol.* **40**, 1381–1391 (2007).
171. No, J., Shin, M. & Mun, S. Preparation of functional rice cake by using  $\beta$ -carotene-loaded emulsion powder. *J. Food Sci. Technol.* **57**, 4514–4523 (2020).
172. Neves, I. C. O. *et al.* Effect of carrier oil on  $\alpha$ -tocopherol encapsulation in ora-pro-nobis (*Pereskia aculeata* Miller) mucilage-whey protein isolate microparticles. *Food Hydrocoll.* **105**, (2020).
173. Shaddel, R. *et al.* Double emulsion followed by complex coacervation as a promising method for protection of black raspberry anthocyanins. *Food Hydrocoll.* **77**, 803–816 (2018).
174. Mao, L., Roos, Y. H. & Miao, S. Effect of maltodextrins on the stability and release of volatile compounds of oil-in-water emulsions subjected to freeze-thaw treatment. *Food Hydrocoll.* **50**, 219–227 (2015).
175. De Aguiar, A. C., Silva, L. P. S., Alves De Rezende, C., Barbero, G. F. & Martinez, J. Encapsulation of pepper oleoresin by supercritical fluid extraction of emulsions. *J. Supercrit. Fluids* **112**, 37–43 (2016).
176. Carpenter, J., George, S. & Saharan, V. K. Curcumin Encapsulation in Multilayer Oil-in-Water Emulsion: Synthesis Using Ultrasonication and Studies on Stability and Antioxidant and Release Activities. *Langmuir* **35**, 10866–10876 (2019).
177. Fioramonti, S. A., Rubiolo, A. C. & Santiago, L. G. Characterisation of freeze-dried flaxseed oil microcapsules obtained by multilayer emulsions. *Powder Technol.* **319**, 238–244 (2017).
178. Orr, M. T. *et al.* Elimination of the cold-chain dependence of a nanoemulsion adjuvanted vaccine against tuberculosis by lyophilization. *J. Control. Release* **177**, 20–26 (2014).
179. Wang, T. *et al.* Preparation of submicron unilamellar liposomes by freeze-drying double emulsions. *Biochim. Biophys. Acta - Biomembr.* **1758**, 222–231

- (2006).
180. Eisinaité, V., Leskauskaitė, D., Pukalskienė, M. & Venskutonis, P. R. Freeze-drying of black chokeberry pomace extract-loaded double emulsions to obtain dispersible powders. *J. Food Sci.* **85**, 628–638 (2020).
  181. Wang, T., Wang, N., Li, T. & Deng, Y. Freeze drying of double emulsions to prepare topotecan-entrapping liposomes featuring controlled release. *Drug Dev. Ind. Pharm.* **34**, 427–433 (2008).
  182. Santos, M. G. *et al.* Coencapsulation of xylitol and menthol by double emulsion followed by complex coacervation and microcapsule application in chewing gum. *FRIN* **66**, 454–462 (2014).
  183. Choi, M. J. *et al.* Effect of cryoprotectant and freeze-drying process on the stability of W/O/W emulsions. *Dry. Technol.* **25**, 809–819 (2007).
  184. Emami, F., Vatanara, A., Park, E. J. & Na, D. H. Drying technologies for the stability and bioavailability of biopharmaceuticals. *Pharmaceutics* **10**, 1–22 (2018).
  185. Rababah, T. M. *et al.* Chemical, Functional and Sensory Properties of Carob Juice. *J. Food Qual.* **36**, 238–244 (2013).
  186. Abu Hafsa, S. H., Ibrahim, S. A. & Hassan, A. A. Carob pods (*Ceratonia siliqua* L.) improve growth performance, antioxidant status and caecal characteristics in growing rabbits. *J. Anim. Physiol. Anim. Nutr. (Berl)*. **101**, 1307–1315 (2017).
  187. Goulas, V., Stylos, E., Chatziathanasiadou, M., Mavromoustakos, T. & Tzakos, A. Functional Components of Carob Fruit: Linking the Chemical and Biological Space. *Int. J. Mol. Sci.* **17**, 1875 (2016).
  188. Román, L., González, A., Espina, T. & Gómez, M. Degree of roasting of carob flour affecting the properties of gluten-free cakes and cookies. *J. Food Sci. Technol.* **54**, 2094–2103 (2017).
  189. Tsatsaragkou, K. *et al.* Effect of Carob Flour Addition on the Rheological Properties of Gluten-Free Breads. *Food Bioprocess Technol.* **7**, 868–876 (2014).
  190. Sęczyk, Ł. *et al.* Effect of carob (*Ceratonia siliqua* L.) flour on the antioxidant potential, nutritional quality, and sensory characteristics of fortified durum wheat pasta. *Food Chem.* **194**, 637–642 (2016).
  191. Moreira, T. C. *et al.* Elaboration of yogurt with reduced level of lactose added of carob (*Ceratonia siliqua* L.). *LWT - Food Sci. Technol.* **76**, 326–329 (2017).
  192. Rached, I. *et al.* *Ceratonia siliqua* L. hydroethanolic extract obtained by ultrasonication: Antioxidant activity, phenolic compounds profile and effects in yogurts functionalized with their free and microencapsulated forms. *Food Funct.* **7**, 1319–1328 (2016).
  193. Almanasrah, M. *et al.* Selective recovery of phenolic compounds and carbohydrates from carob kibbles using water-based extraction. *Ind. Crops*

- Prod.* **70**, 443–450 (2015).
194. Nagy, E. Forward Osmosis. *Basic Equations Mass Transp. Through a Membr. Layer* 447–456 (2019) doi:10.1016/b978-0-12-813722-2.00017-0.
195. Long, Q. *et al.* Recent advance on draw solutes development in Forward osmosis. *Processes* **6**, 7–11 (2018).
196. Cath, T., Childress, A. & Elimelech, M. Forward osmosis: Principles, applications, and recent developments. *J. Memb. Sci.* **281**, 70–87 (2006).
197. Terefe, N. S. *et al.* Forward Osmosis. in *Innovative Food Processing Technologies* 177–205 (Elsevier, 2016). doi:10.1016/B978-0-08-100294-0.00007-9.
198. Sant’Anna, V. *et al.* Jaboticaba (*Myrciaria jaboticaba*) juice concentration by forward osmosis. *Sep. Sci. Technol.* **51**, 1708–1715 (2016).
199. Haupt, A. & Lerch, A. Forward Osmosis Application in Manufacturing Industries: A Short Review. *Membranes (Basel)*. **8**, 47 (2018).
200. Menchik, P. & Moraru, C. I. Nonthermal concentration of liquid foods by a combination of reverse osmosis and forward osmosis. Acid whey: A case study. *J. Food Eng.* **253**, 40–48 (2019).
201. Maknakhon, W. & Khongnakorn, W. Processing printing wastewater treatment by forward osmosis process. in *3rd Regional IWA Diffuse Pollution Conference “Innovation and Frontier Technology for Water Security and Scarcity”* (2018).
202. Berendsen, R., Güell, C. & Ferrando, M. A procyanidin-rich extract encapsulated in water-in-oil-in-water emulsions produced by premix membrane emulsification. *Food Hydrocoll.* **43**, 636–648 (2015).
203. Bamba, B. *et al.* Coencapsulation of Polyphenols and Anthocyanins from Blueberry Pomace by Double Emulsion Stabilized by Whey Proteins: Effect of Homogenization Parameters. *Molecules* **23**, 2525 (2018).
204. Estévez, M., Güell, C., De Lamo-Castellví, S. & Ferrando, M. Encapsulation of grape seed phenolic-rich extract within W/O/W emulsions stabilized with complexed biopolymers: Evaluation of their stability and release. *Food Chem.* **272**, 478–487 (2019).
205. Charcosset, C. Preparation of emulsions and particles by membrane emulsification for the food processing industry. *J. Food Eng.* **92**, 241–249 (2009).
206. Güell, C., Ferrando, M. & López, F. Monitoring and Visualizing Membrane-Based Processes. *Monit. Vis. Membr. Process.* 1–367 (2009) doi:10.1002/9783527622726.
207. Nazir, A., Schroën, K. & Boom, R. High-throughput premix membrane emulsification using nickel sieves having straight-through pores. *J. Memb. Sci.*

- 383**, 116–123 (2011).
208. Muschiolik, G. Multiple emulsions for food use. *Curr. Opin. Colloid Interface Sci.* **12**, 213–220 (2007).
209. AYAZ, F. A. *et al.* DETERMINATION OF CHEMICAL COMPOSITION OF ANATOLIAN CAROB POD ( CERATONIA SILIQUA L.): SUGARS, AMINO AND ORGANIC ACIDS, MINERALS AND PHENOLIC COMPOUNDS. *J. Food Qual.* **30**, 1040–1055 (2007).
210. Aziz, H. & Hicham, E. L. B. Optimization of Production of Carob Pulp Syrup from Different Populations of Moroccan Carob ( *Ceratonia siliqua* L . ). *Int. J. Emerg. Technol. Adv. Eng.* **4**, 855–863 (2014).
211. Muschiolik, G. & Dickinson, E. Double Emulsions Relevant to Food Systems: Preparation, Stability, and Applications. *Compr. Rev. Food Sci. Food Saf.* **16**, 532–555 (2017).
212. Kaade, W. *et al.* Low-energy high-throughput emulsification with nickel micro-sieves for essential oils encapsulation. *J. Food Eng.* **263**, 326–336 (2019).
213. Tolun, A., Altintas, Z. & Artik, N. Microencapsulation of grape polyphenols using maltodextrin and gum arabic as two alternative coating materials: Development and characterization. *J. Biotechnol.* **239**, 23–33 (2016).
214. Babu, B. R., Rastogi, N. K. & Raghavarao, K. S. M. S. Effect of process parameters on transmembrane flux during direct osmosis. *J. Memb. Sci.* **280**, 185–194 (2006).
215. Nayak, C. A. & Rastogi, N. K. Forward osmosis for the concentration of anthocyanin from *Garcinia indica* Choisy. *Sep. Purif. Technol.* **71**, 144–151 (2010).
216. Hameed, K. W. Concentration of Orange Juice Using Forward Osmosis Membrane Process. *Iraqi J. Chem. Pet. Eng.* **14**, 71–79 (2013).
217. Rodriguez-saona, L. E., Giusti, M. M., Durst, R. W. & Wrolstad, R. E. DEVELOPMENT AND PROCESS OPTIMIZATION OF RED RADISH CONCENTRATE EXTRACT AS POTENTIAL NATURAL RED COLORANT. *J. Food Process. Preserv.* **25**, 165–182 (2001).
218. Jampani, C. & Raghavarao, K. S. M. S. Process integration for purification and concentration of red cabbage (*Brassica oleracea* L.) anthocyanins. *Sep. Purif. Technol.* **141**, 10–16 (2015).
219. Nayak, C. A., Valluri, S. S. & Rastogi, N. K. Effect of high or low molecular weight of components of feed on transmembrane flux during forward osmosis. *J. Food Eng.* **106**, 48–52 (2011).
220. Gunathilake, K. D. P. P., Yu, L. J. & Rupasinghe, H. P. V. Reverse osmosis as a potential technique to improve antioxidant properties of fruit juices used for functional beverages. *Food Chem.* **148**, 335–341 (2014).

221. Kim, Y., Lee, S., Shon, H. K. & Hong, S. Organic fouling mechanisms in forward osmosis membrane process under elevated feed and draw solution temperatures. *Desalination* **355**, 169–177 (2015).
222. Nasar-Abbas, S. M. *et al.* Carob Kibble: A Bioactive-Rich Food Ingredient. *Compr. Rev. Food Sci. Food Saf.* **15**, 63–72 (2016).
223. Pawlik, A., Cox, P. W. & Norton, I. T. Food grade duplex emulsions designed and stabilised with different osmotic pressures. *J. Colloid Interface Sci.* **352**, 59–67 (2010).
224. Vladislavjević, G. T., Shimizu, M. & Nakashima, T. Preparation of monodisperse multiple emulsions at high production rates by multi-stage premix membrane emulsification. *J. Memb. Sci.* **244**, 97–106 (2004).
225. Vladislavjević, G. T., Shimizu, M. & Nakashima, T. Production of multiple emulsions for drug delivery systems by repeated SPG membrane homogenization: Influence of mean pore size, interfacial tension and continuous phase viscosity. *J. Memb. Sci.* **284**, 373–383 (2006).
226. Surh, J., Vladislavjević, G. T., Mun, S. & McClements, D. J. Preparation and Characterization of Water/Oil and Water/Oil/Water Emulsions Containing Biopolymer-Gelled Water Droplets. *J. Agric. Food Chem.* **55**, 175–184 (2007).
227. Ribeiro, H. S., Rico, L. G., Badolato, G. G. & Schubert, H. Production of O/W emulsions containing astaxanthin by repeated premix membrane emulsification. *J. Food Sci.* **70**, 117–123 (2005).
228. Simperler, A. *et al.* Glass transition temperature of glucose, sucrose, and trehalose: An experimental and in silico study. *J. Phys. Chem. B* **110**, 19678–19684 (2006).
229. Alexandratos, N. & Bruinsma, J. *WORLD AGRICULTURE TOWARDS 2030 / 2050 The 2012 Revision*. vol. ESA Workin (2012).
230. Charlton, A. J. *et al.* Exploring the chemical safety of fly larvae as a source of protein for animal feed. *J. Insects as Food Feed* **1**, 7–16 (2015).
231. Oonincx, D. G. A. B., Van Broekhoven, S., Van Huis, A. & Van Loon, J. J. A. Feed conversion, survival and development, and composition of four insect species on diets composed of food by-products. *PLoS One* **10**, 1–20 (2015).
232. Spranghers, T. *et al.* Nutritional composition of black soldier fly ( *Hermetia illucens* ) prepupae reared on different organic waste substrates. *J. Sci. Food Agric.* **97**, 2594–2600 (2017).
233. Zielińska, E., Baraniak, B., Karaś, M., Rybczyńska, K. & Jakubczyk, A. Selected species of edible insects as a source of nutrient composition. *Food Res. Int.* **77**, 460–466 (2015).
234. Amato, M. Insects as food: a cross-cultural comparison of consumers' intention and behaviour. 121 (2017).

235. Caligiani, A. *et al.* Composition of black soldier fly prepupae and systematic approaches for extraction and fractionation of proteins, lipids and chitin. *Food Res. Int.* **105**, 812–820 (2018).
236. Chou, T. H., Nugroho, D. S., Cheng, Y. S. & Chang, J. Y. Development and Characterization of Nano-emulsions Based on Oil Extracted from Black Soldier Fly Larvae. *Appl. Biochem. Biotechnol.* **191**, 331–345 (2020).
237. Kim, H., Setyabrata, D., Lee, Y. J., Jones, O. G. & Kim, Y. H. B. Pre-treated mealworm larvae and silkworm pupae as a novel protein ingredient in emulsion sausages. *Innov. Food Sci. Emerg. Technol.* **38**, 116–123 (2016).
238. Scholliers, J. *et al.* The effect of temperature on structure formation in three insect batters. *Food Res. Int.* **122**, 411–418 (2019).
239. Wang, Y.-S. & Shelomi, M. Review of Black Soldier Fly (*Hermetia illucens*) as Animal Feed and Human Food. *Foods* **6**, 91 (2017).
240. Ramos-Elorduy, J. *et al.* Nutritional Value of Edible Insects from the State of Oaxaca , Mexico. *J. Food Compos. Anal.* **157**, 142–157 (1997).
241. Lourenço, S. O. *et al.* Amino acid composition, protein content and calculation of nitrogen-to-protein conversion factors for 19 tropical seaweeds. *Phycol. Res.* **50**, 233–241 (2002).
242. Mellado-Carretero, J. *et al.* Rapid discrimination and classification of edible insect powders using ATR-FTIR spectroscopy combined with multivariate analysis. *J. Insects as Food Feed* **6**, 141–148 (2020).
243. Janssen, R. H., Vincken, J.-P. P., Van Den Broek, L. A. M. M., Fogliano, V. & Lakemond, C. M. M. Nitrogen-to-Protein Conversion Factors for Three Edible Insects: *Tenebrio molitor* , *Alphitobius diaperinus* , and *Hermetia illucens*. *J. Agric. Food Chem.* **65**, 2275–2278 (2017).
244. Oshimura, E. & Sakamoto, K. Amino acids, peptides, and proteins. *Cosmet. Sci. Technol. Theor. Princ. Appl.* 285–303 (2017) doi:10.1016/B978-0-12-802005-0.00019-7.
245. Burns, A., Olszowy, P. & Ciborowski, P. Biomolecules. in *Proteomic Profiling and Analytical Chemistry: The Crossroads: Second Edition* 7–24 (Elsevier Inc., 2016). doi:10.1016/B978-0-444-63688-1.00002-1.
246. Azagoh, C. *et al.* Extraction and physicochemical characterization of *Tenebrio molitor* proteins. *Food Res. Int.* **88**, 24–31 (2016).
247. Laroche, M. *et al.* Comparison of conventional and sustainable lipid extraction methods for the production of oil and protein isolate from edible insect meal. *Foods* **8**, (2019).
248. Young, V. R. & Pellett, P. L. Protein evaluation, amino acid scoring and the Food and Drug Administration’s proposed food labeling regulations. *J. Nutr.* **121**, 145–150 (1991).

249. Socrates, G. *Infrared and Raman Characteristic Group Frequencies Contents*. (Wiley, 2004).
250. Haque, M. A., Timilsena, Y. P. & Adhikari, B. Food Proteins, Structure, and Function. in *Reference Module in Food Science* 1–8 (Elsevier, 2016). doi:10.1016/B978-0-08-100596-5.03057-2.
251. Son, Y. J., Lee, J. C., Hwang, I. K., Nho, C. W. & Kim, S. H. Physicochemical properties of mealworm (*Tenebrio molitor*) powders manufactured by different industrial processes. *Lwt* **116**, 108514 (2019).
252. Chandra, S. Assessment of functional properties of different flours. *African J. Agric. Res.* **8**, 4849–4852 (2013).
253. McClements, D. J. & Gumus, C. E. Natural emulsifiers — Biosurfactants, phospholipids, biopolymers, and colloidal particles: Molecular and physicochemical basis of functional performance. *Adv. Colloid Interface Sci.* **234**, 3–26 (2016).
254. ONWULATA, C. I. MICROENCAPSULATION AND FUNCTIONAL BIOACTIVE FOODS. *J. Food Process. Preserv.* **37**, 510–532 (2013).
255. Rao, J. & McClements, D. J. Lemon oil solubilization in mixed surfactant solutions: Rationalizing microemulsion & nanoemulsion formation. *Food Hydrocoll.* **26**, 268–276 (2012).
256. Burt, S. Essential oils: Their antibacterial properties and potential applications in foods - A review. *Int. J. Food Microbiol.* **94**, 223–253 (2004).
257. Rao, J. & McClements, D. J. Impact of lemon oil composition on formation and stability of model food and beverage emulsions. *Food Chem.* **134**, 749–757 (2012).
258. Treesuwan, W., Neves, M. A., Uemura, K., Nakajima, M. & Kobayashi, I. Preparation characteristics of monodisperse oil-in-water emulsions by microchannel emulsification using different essential oils. *LWT - Food Sci. Technol.* **84**, 617–625 (2017).
259. González-Mas, M. C., Rambla, J. L., López-Gresa, M. P., Amparo Blázquez, M. & Granell, A. Volatile compounds in citrus essential oils: A comprehensive review. *Front. Plant Sci.* **10**, 1–18 (2019).
260. Cheong, M. W. *et al.* Characterisation of calamansi (*Citrus microcarpa*). Part I: Volatiles, aromatic profiles and phenolic acids in the peel. *Food Chem.* **134**, 686–695 (2012).
261. Diamante, L. M. & Lan, T. Absolute Viscosities of Vegetable Oils at Different Temperatures and Shear Rate Range of 64.5 to 4835 s<sup>-1</sup>. *J. Food Process.* **2014**, 1–6 (2014).
262. Trentin, A., Ferrando, M., López, F. & Güell, C. Premix membrane O/W emulsification: Effect of fouling when using BSA as emulsifier. *Desalination*

- 245, 388–395 (2009).
263. Surh, J., Jeong, Y. G. & Vladisavljević, G. T. On the preparation of lecithin-stabilized oil-in-water emulsions by multi-stage premix membrane emulsification. *J. Food Eng.* **89**, 164–170 (2008).
264. Zecca, E. Investigating the Role of Surface Hydrophobicity in Protein Aggregation. (2017).
265. Rumpold, B. A. & Schlüter, O. K. Nutritional composition and safety aspects of edible insects. *Mol. Nutr. Food Res.* **57**, 802–823 (2013).
266. Paul, A. *et al.* Insect fatty acids: A comparison of lipids from three Orthopterans and *Tenebrio molitor* L. larvae. *J. Asia. Pac. Entomol.* **20**, 337–340 (2017).
267. Tzompa-Sosa, D. A., Yi, L., van Valenberg, H. J. F., van Boekel, M. A. J. S. & Lakemond, C. M. M. Insect lipid profile: Aqueous versus organic solvent-based extraction methods. *Food Res. Int.* **62**, 1087–1094 (2014).
268. Ravi, H. K. *et al.* Alternative solvents for lipid extraction and their effect on protein quality in black soldier fly (*Hermetia illucens*) larvae. *J. Clean. Prod.* **238**, 117861 (2019).
269. Rapinel, V. *et al.* 2-methyloxolane (2-MeOx) as sustainable lipophilic solvent to substitute hexane for green extraction of natural products. Properties, applications, and perspectives. *Molecules* **25**, (2020).
270. Adámková, A., Kourimská, L., Borkovcová, M., Kulma, M. & Mlček, J. Nutritional values of edible Coleoptera (*Tenebrio molitor*, *Zophobas morio* and *Alphitobius diaperinus*) reared in the Czech Republic. *Potravinárstvo* **10**, 663–671 (2016).
271. Kumar, S. P. J. *et al.* Green solvents and technologies for oil extraction from oilseeds. *Chem. Cent. J.* **11**, 1–7 (2017).
272. Pace, V., Hoyos, P., Castoldi, L., Domínguez De María, P. & Alcántara, A. R. 2-Methyltetrahydrofuran (2-MeTHF): A biomass-derived solvent with broad application in organic chemistry. *ChemSusChem* **5**, 1369–1379 (2012).
273. Gehrmann, S. & Tenhumberg, N. Production and Use of Sustainable C2-C4 Alcohols – An Industrial Perspective. *Chemie-Ingenieur-Technik* **92**, 1444–1458 (2020).
274. Lavrenov, A. V., Saifulina, L. F., Buluchevskii, E. A. & Bogdanets, E. N. Propylene production technology: Today and tomorrow. *Catal. Ind.* **7**, 175–187 (2015).
275. Akpissan, R. *et al.* Protein Fractions and Functional Properties of Dried *Imbrasia oyemensis* Larvae Full-Fat and Defatted Flours. *Int. J. Biochem. Res. Rev.* **5**, 116–126 (2015).
276. Olkiewicz, M. *et al.* Effects of pre-treatments on the lipid extraction and biodiesel production from municipal WWTP sludge. *Fuel* **141**, 250–257 (2015).

277. Nakai, S. Measurement Of Protein Hydrophobicity. *Handb. Food Anal. Chem.* **1–2**, 301–313 (2005).
278. Alara, O. R., Abdurahman, N. H. & Ukaegbu, C. I. Extraction of phenolic compounds: A review. *Curr. Res. Food Sci.* **4**, 200–214 (2021).
279. Soetemans, L., Gianotten, N. & Bastiaens, L. Agri-food side-stream inclusion in the diet of alphitobius diaperinus. Part 2: Impact on larvae composition. *Insects* **11**, (2020).
280. Milićević, D. *et al.* The role of total fats, saturated/unsaturated fatty acids and cholesterol content in chicken meat as cardiovascular risk factors. *Lipids Health Dis.* **13**, 1–12 (2014).
281. Jantzen da Silva Lucas, A., Menegon de Oliveira, L., da Rocha, M. & Prentice, C. Edible insects: An alternative of nutritional, functional and bioactive compounds. *Food Chem.* **311**, 126022 (2020).
282. Li, H. & Chen, V. *Membrane Fouling and Cleaning in Food and Bioprocessing. Membrane Technology* (Elsevier Ltd, 2010). doi:10.1016/B978-1-85617-632-3.00010-0.
283. Güell, C., Ferrando, M., Trentin, A. & Schroën, K. Apparent interfacial tension effects in protein stabilized emulsions prepared with microstructured systems. *Membranes (Basel)*. **7**, 5–7 (2017).
284. Otálora, M. C., Carriazo, J. G., Iturriaga, L., Nazareno, M. A. & Osorio, C. Microencapsulation of betalains obtained from cactus fruit (*Opuntia ficus-indica*) by spray drying using cactus cladode mucilage and maltodextrin as encapsulating agents. *Food Chem.* **187**, 174–181 (2015).
285. Jiménez-Colmenero, F. Potential applications of multiple emulsions in the development of healthy and functional foods. *Food Res. Int.* **52**, 64–74 (2013).
286. Lu, W., Kelly, A. L. & Miao, S. Emulsion-based encapsulation and delivery systems for polyphenols. *Trends Food Sci. Technol.* **47**, 1–9 (2016).
287. Ballesteros, L. F., Ramirez, M. J., Orrego, C. E., Teixeira, J. A. & Mussatto, S. I. Encapsulation of antioxidant phenolic compounds extracted from spent coffee grounds by freeze-drying and spray-drying using different coating materials. *Food Chem.* **237**, 623–631 (2017).
288. Jolayemi, O. S., Stranges, N., Flamminii, F., Casiraghi, E. & Alamprese, C. Influence of Free and Encapsulated Olive Leaf Phenolic Extract on the Storage Stability of Single and Double Emulsion Salad Dressings. *Food Bioprocess Technol.* **14**, 93–105 (2021).
289. De Jesús Cenobio-Galindo, A. *et al.* Multiple emulsions with extracts of cactus pear added in a yogurt: Antioxidant activity, in vitro simulated digestion and shelf life. *Foods* **8**, (2019).
290. Huang, Y. & Zhou, W. Microencapsulation of anthocyanins through two-step

- emulsification and release characteristics during in vitro digestion. *Food Chem.* **278**, 357–363 (2019).
291. Aditya, N. P. *et al.* Co-delivery of hydrophobic curcumin and hydrophilic catechin by a water-in-oil-in-water double emulsion. *Food Chem.* **173**, 7–13 (2015).
292. Keršienė, M. *et al.* Development of a high-protein yoghurt-type product enriched with bioactive compounds for the elderly. *Lwt* **131**, 1–8 (2020).
293. Eisinaite, V., Juraite, D., Schroėn, K. & Leskauskaite, D. Food-grade double emulsions as effective fat replacers in meat systems. *J. Food Eng.* **213**, 54–59 (2017).
294. Lam, A. C. Y., Can Karaca, A., Tyler, R. T. & Nickerson, M. T. Pea protein isolates: Structure, extraction, and functionality. *Food Rev. Int.* **34**, 126–147 (2018).
295. Chang, C., Tu, S., Ghosh, S. & Nickerson, M. T. Effect of pH on the inter-relationships between the physicochemical, interfacial and emulsifying properties for pea, soy, lentil and canola protein isolates. *Food Res. Int.* **77**, 360–367 (2015).
296. Ladjal-Ettoumi, Y., Boudries, H., Chibane, M. & Romero, A. Pea, Chickpea and Lentil Protein Isolates: Physicochemical Characterization and Emulsifying Properties. *Food Biophys.* **11**, 43–51 (2016).
297. Xu, D. *et al.* The Stability, Microstructure, and Microrheological Properties of Monascus Pigment Double Emulsions Stabilized by Polyglycerol Polyricinoleate and Soybean Protein Isolate. *Front. Nutr.* **7**, 1–13 (2020).
298. Tamnak, S. *et al.* Encapsulation properties, release behavior and physicochemical characteristics of water-in-oil-in-water (W/O/W) emulsion stabilized with pectin-pea protein isolate conjugate and Tween 80. *Food Hydrocoll.* **61**, 599–608 (2016).
299. García-Segovia, P., Igual, M., Noguerol, A. T. & Martínez-Monzó, J. Use of insects and pea powder as alternative protein and mineral sources in extruded snacks. *Eur. Food Res. Technol.* **246**, 703–712 (2020).
300. Santiago, L. A., Fadel, O. M. & Tavares, G. M. How does the thermal-aggregation behavior of black cricket protein isolate affect its foaming and gelling properties? *Food Hydrocoll.* **110**, 106169 (2021).
301. de Matos, F. M., Novelli, P. K. & de Castro, R. J. S. Enzymatic hydrolysis of black cricket (*Gryllus assimilis*) proteins positively affects their antioxidant properties. *J. Food Sci.* **86**, 571–578 (2021).
302. Rivero-Pino, F., Guadix, A. & Guadix, E. M. Identification of novel dipeptidyl peptidase IV and  $\alpha$ -glucosidase inhibitory peptides from *Tenebrio molitor*. *Food Funct.* **12**, 873–880 (2021).

303. Ozturk, B. & McClements, D. J. Progress in natural emulsifiers for utilization in food emulsions. *Curr. Opin. Food Sci.* **7**, 1–6 (2016).
304. Liang, H. N. & Tang, C. H. PH-dependent emulsifying properties of pea [*Pisum sativum* (L.)] proteins. *Food Hydrocoll.* **33**, 309–319 (2013).
305. Czubinski, J. & Dwiecki, K. A review of methods used for investigation of protein–phenolic compound interactions. *Int. J. Food Sci. Technol.* **52**, 573–585 (2017).
306. Diaz, J. T., Foegeding, E. A. & Lila, M. A. Formulation of protein–polyphenol particles for applications in food systems. *Food Funct.* **11**, 5091–5104 (2020).
307. Seczyk, L., Swieca, M., Kapusta, I. & Gawlik-Dziki, U. Protein–phenolic interactions as a factor affecting the physicochemical properties of white bean proteins. *Molecules* **24**, 1–24 (2019).
308. Wang, J. *et al.* Low-energy membrane-based processes to concentrate and encapsulate polyphenols from carob pulp. *J. Food Eng.* **281**, 109996 (2020).
309. Friedman, M. & Jürgens, H. S. Effect of pH on the Stability of Plant Phenolic Compounds. *J. Agric. Food Chem.* **48**, 2101–2110 (2000).
310. Honda, S., Ishida, R., Hidaka, K. & Masuda, T. Stability of polyphenols under alkaline conditions and the formation of a xanthine oxidase inhibitor from gallic acid in a solution at pH 7.4. *Food Sci. Technol. Res.* **25**, 123–129 (2019).
311. Degner, B. M., Chung, C., Schlegel, V., Hutkins, R. & McClements, D. J. Factors influencing the freeze-thaw stability of emulsion-based foods. *Compr. Rev. Food Sci. Food Saf.* **13**, 98–113 (2014).
312. Zhu, X. F., Zhang, N., Lin, W. F. & Tang, C. H. Freeze-thaw stability of pickering emulsions stabilized by soy and whey protein particles. *Food Hydrocoll.* **69**, 173–184 (2017).
313. Palazolo, G. G., Sobral, P. A. & Wagner, J. R. Freeze-thaw stability of oil-in-water emulsions prepared with native and thermally-denatured soybean isolates. *Food Hydrocoll.* **25**, 398–409 (2011).
314. Cabezas, D. M., Pascual, G. N., Wagner, J. R. & Palazolo, G. G. Nanoparticles assembled from mixtures of whey protein isolate and soluble soybean polysaccharides. Structure, interfacial behavior and application on emulsions subjected to freeze-thawing. *Food Hydrocoll.* **95**, 445–453 (2019).
315. Tang, C.-H. Emulsifying properties of soy proteins: A critical review with emphasis on the role of conformational flexibility. *Crit. Rev. Food Sci. Nutr.* **57**, 2636–2679 (2017).
316. Dickinson, E. Double Emulsions Stabilized by Food Biopolymers. *Food Biophysics* (2011) doi:10.1007/s11483-010-9188-6.
317. Mun, S., Choi, Y., Park, K. H., Shim, J. Y. & Kim, Y. R. Influence of

- environmental stresses on the stability of W/O/W emulsions containing enzymatically modified starch. *Carbohydr. Polym.* **92**, 1503–1511 (2013).
318. Saral, Ö. *et al.* Apitherapy products enhance the recovery of CCL4-induced hepatic damages in rats. *Turkish J. Med. Sci.* **46**, 194–202 (2016).
319. Niu, F. *et al.* Synergistic effects of ovalbumin/gum arabic complexes on the stability of emulsions exposed to environmental stress. *Food Hydrocoll.* **47**, 14–20 (2015).
320. Hategekimana, J., Chamba, M. V. M., Shoemaker, C. F., Majeed, H. & Zhong, F. Vitamin E nanoemulsions by emulsion phase inversion: Effect of environmental stress and long-term storage on stability and degradation in different carrier oil types. *Colloids Surfaces A Physicochem. Eng. Asp.* **483**, 70–80 (2015).
321. He, F. J., Jenner, K. H. & Macgregor, G. A. WASH — World Action on Salt and Health. *Kidney Int.* **78**, 745–753 (2010).
322. Pimentel, D. Global warming, population growth, and natural resources for food production. *Soc. Nat. Resour.* **4**, 347–363 (1991).
323. Gallardo, G. *et al.* Microencapsulation of linseed oil by spray drying for functional food application. *Food Res. Int.* **52**, 473–482 (2013).

UNIVERSITAT ROVIRA I VIRGILI  
EMULSION-BASED ENCAPSULATION SYSTEMS STABILIZED WITH INSECT PROTEINS: PRODUCTION WITH  
PREMIX MICROPOROUS EMULSIFICATION  
Junjing Wang

UNIVERSITAT ROVIRA I VIRGILI  
EMULSION-BASED ENCAPSULATION SYSTEMS STABILIZED WITH INSECT PROTEINS: PRODUCTION WITH  
PREMIX MICROPOROUS EMULSIFICATION  
Junjing Wang

UNIVERSITAT ROVIRA I VIRGILI  
EMULSION-BASED ENCAPSULATION SYSTEMS STABILIZED WITH INSECT PROTEINS: PRODUCTION WITH  
PREMIX MICROPOROUS EMULSIFICATION  
Junjing Wang

UNIVERSITAT ROVIRA I VIRGILI  
EMULSION-BASED ENCAPSULATION SYSTEMS STABILIZED WITH INSECT PROTEINS: PRODUCTION WITH  
PREMIX MICROPOROUS EMULSIFICATION  
Junjing Wang



UNIVERSITAT  
ROVIRA i VIRGILI